THE
PHYSICAL REVIEW
A Journal of Experimental and Theoretical Physics Established by E. L. Nichols in 1893

VOL. 51, NO. 12 JUNE 15, 1937 SECOND SERIES

The Induced Radioactivity of Potassium

D. G. HURST* AND H. WALKE†
Radiation Laboratory, University of California, Berkeley, California
(Received May 3, 1937)

The paper reports a study of certain induced radioactivities associated with potassium. It is shown that the half-life of K^{42} is 12.4 ± 0.2 hours. In addition to the well-established deuteron and slow neutron reactions K^{42} is also formed by the reactions $Sc^{45}+n^1\rightarrow K^{42}+He^4$ and $Ca^{42}+n^1\rightarrow K^{42}+H^1$. This last appears to have a relatively small probability. No evidence was found for the reaction $Ca^{44}+H^2\rightarrow K^{42}+He^4$. Fast neutron irradiation of potassium yields active chlorine and A^{41} by the transmutations $K^{39 \text{ or } 41}+n^1\rightarrow Cl^{36 \text{ or } 38}+He^4$; $K^{41}+n^1\rightarrow A^{41}+H^1$. There was no indication of the presence of A^{39} in the activated samples. Alpha-particle bombardment of chlorine yields K^{38} according to the reaction $Cl^{35}+He^4\rightarrow K^{38}+n^1$. This isotope of potassium decays with a half-life of $7.7_6\pm0.1_8$ minutes, emitting positrons having a maximum energy of about 2 Mev and gamma-rays which may be annihilation radiation only. K^{38} is also obtained by deuteron bombardment of calcium thus: $Ca^{40}+H^2\rightarrow K^{38}+He^4$.

I. INTRODUCTION

BY irradiating potassium with slow neutrons Fermi and his co-workers[1] obtained an active substance which they showed by chemical tests was not isotopic with chlorine, argon or calcium, and which had a half-life of about 16 hours. Since the naturally occurring isotopes of potassium are

Mass Number	39	40	41
Abundance (percent)	93.4	0.01	6.6

the only radioactive isotope of potassium (excluding K^{40}) which can be formed by slow neutron capture is K^{42} which then decays by emitting electrons to form the stable Ca^{42}. Hence the period of 16 hours was assigned to this isotope. G. von Hevesy[2] obtained, by fast neutron activation of scandium, a radioactive isotope which decayed to half-value in 16 hours and which behaved chemically like sodium. This he supposed to be K^{42} produced from Sc^{45} by the emission of an alpha-particle after the absorption of the neutron.

Indications obtained by one of us[3] that the accepted value of 16 hours is incorrect led us to measure the half-life of K^{42}. It seemed worthwhile at the same time to search for other activities which one would expect to be associated with potassium. It is the purpose of the present paper to report our results.

The activating particles used in these investigations were deuterons, alpha-particles and neutrons produced in the Berkeley cyclotron[4] under conditions already described.[3] The activities were measured with quartz fiber electroscopes of the type developed by Lauritsen.

II. POTASSIUM (42)

(a) Period

The samples used in determining the period of K^{42} were prepared either by deuteron or slow

* 1851 Exhibition Scholar from McGill University, Montreal, Canada.
† Commonwealth Fund Fellow.
[1] Fermi, *et al.*, Proc. Roy. Soc. **A149**, 522 (1935).
[2] von Hevesy, Nature **135**, 96 (1935).
[3] Walke, Phys. Rev. **51**, 439 (1937).
[4] Lawrence and Cooksey, Phys. Rev. **50**, 1131 (1936).

neutron bombardment of potassium salts. The agreement between the results obtained by the two methods proves that the deuteron activation was due to the reaction

$$K^{41}+H^2 \rightarrow K^{42}+H^1. \quad (1)$$

After bombardment with 5.5 Mev deuterons the target material, either KCl or KF, was dissolved in water and potassium cobaltinitrite was precipitated. Fig. 1A shows the decay of the activity of such a precipitate. The decay of a sample of K_2CO_3 after irradiation with slow neutrons is shown in Fig. 1B. From such graphs we conclude that the half-life of K^{42} is 12.4 ± 0.2 hours. In a thick target the yield of K^{42} in reaction (1) is of the order 2×10^7 deuterons per active atom. A weak gamma-ray accompanies the decay.

The energy spectrum of the electrons has already been determined by Kurie, Richardson and Paxton.[5]

(b) The formation of K^{42} from scandium

Hevesy and Levi[6] have reported the formation of K^{42} according to the reaction:

$$Sc^{45}+n^1 \rightarrow K^{42}+He^4, \quad (2)$$

in which scandium is bombarded with fast neutrons. They activated a sample of scandium oxide with a radon-beryllium source and after dissolving the irradiated oxide in HCl added sodium chloride, which was subsequently recovered by evaporation and ignition after the precipitation of scandium as hydroxide by carbonate free ammonia. The sodium chloride was found to decay with a period of 16 hours, this being ascribed to the presence of K^{42}.

In the present experiments a sample consisting of two grams of Sc_2O_3 (which had been shown by deuteron activation to be free from potassium) was bombarded for several hours with fast neutrons. It was then dissolved in HCl and a little KCl was added followed by perchloric acid and ethyl alcohol. The precipitated potassium perchlorate was found to be active decaying to half-value in 12.4 ± 0.2 hours. The decay curve is shown in Fig. 1C. It is thus clear that the radioactive potassium isotope observed is K^{42} produced by reaction (2).

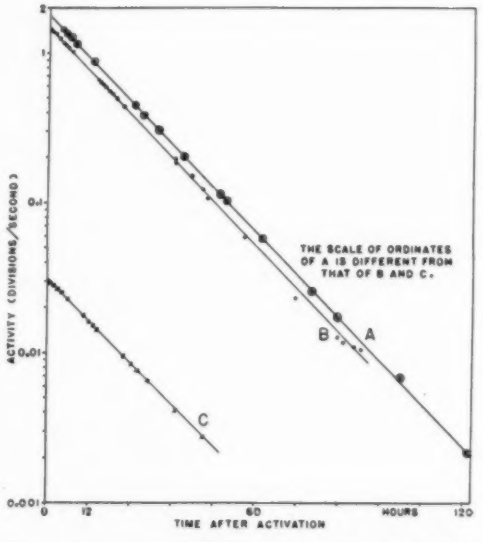

FIG. 1. Decay curves of K^{42} formed by different methods: (*A*) deuteron bombardment of potassium (as potassium fluoride); (*B*) slow neutron irradiation of potassium (as potassium carbonate); (*C*) fast neutron irradiation of scandium (as scandium oxide).

(c) The formation of K^{42} from calcium

Hevesy and Levi[7] have also reported the production of K^{42} by the transmutation:

$$Ca^{42}+n^1 \rightarrow K^{42}+H^1, \quad (3)$$

the half-life given being 16 hours.

In a previous repetition of their work[3] on calcium carbonate it was shown that the results obtained were consistent with the presence of a small amount of sodium or magnesium contamination as the weak activity observed decayed with the characteristic period of Na^{24}.

Recently, however, a very pure sample of calcium hydroxide, free from sodium and potassium, was strongly irradiated with fast neutrons for about ten hours. From the activated sample potassium was precipitated as perchlorate and was found to be weakly radioactive.

The experimental observations of its decay made during the first sixteen hours after separation from the calcium lie on a straight line with a half period of 12.5 hours. Measurements con-

[5] Kurie, Richardson and Paxton, Phys. Rev. **49**, 368 (1936).

[6] Hevesy and Levi, Det. Kgl. Danske Videnskabernes Selskab Math-Fysiske Meddelelser **14**, 5 (1936).

[7] Hevesy and Levi, Nature **135**, 580 (1935).

tinued for three days, however, disclosed the presence of a very weak long period of undetermined value, which may well be due to contamination or less probably to a heavier isotope of potassium. However, the earlier portion of the decay curve suggests the presence of K^{42} and it, therefore, appears not unlikely that reaction (3) has been detected.

III. Fast Neutron Irradiation of Potassium

Those reactions which might be expected to take place when potassium is bombarded with fast neutrons are, in addition to that in which K^{42} is formed, as follows:

$$K^{39,40,41}+n^1 \rightarrow A^{39,40,41}+H^1,$$
$$K^{39,40,41}+n^1 \rightarrow Cl^{36,37,38}+He^4.$$

Of the isotopes which could thus be produced A^{40} and Cl^{37} are stable; A^{41} has the half-life of 110 minutes;[8] A^{39} is absent from the mass spectrum of argon and hence is probably unstable; and either Cl^{36} or Cl^{38} has a half-period 37.5 minutes.[9] In the present experiments KF, K_2CO_3, KNO_3 and K metal were irradiated with fast neutrons. The KNO_3 was stated to have not more than 0.001 percent chlorine contamination. The decay curves of the activities show the presence of several periods, including that of K^{42}. Such a curve is shown in Fig. 2. After correcting for the activity due to K^{42} a composite curve is obtained. When there is sufficient residual activity as in the example shown, the later points can be considered to lie on a straight line of half-life 110 minutes corresponding to A^{41}. This activity can be then extrapolated to zero time and subtracted, and after this has been done the resulting points lie on a straight line of half-life 37.5 minutes.[10]

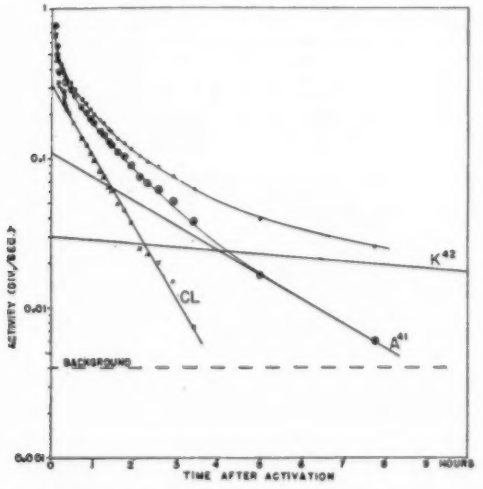

Fig. 2. The activity of potassium fluoride after irradiation with fast neutrons for 45 minutes. The sample was wrapped in cadmium and placed two or three cm behind the beryllium target, which was bombarded with about 15μa of deuterons. The original points are shown by dots. (Some of the early observations are omitted.) Observations later than any on the diagram enable the K^{42} line to be drawn. Subtraction of this from the original points yields the encircled points. Through the last two of these a line is drawn having a slope corresponding to a half-life of 110 minutes. This is subtracted and the resulting points are indicated by crosses. If these points are collinear the resolution is complete; and it will be seen that, except for the first few minutes (where, as explained in the text, the short period is due to O^{19} formed from the fluorine) they follow the line marked Cl which corresponds to a half-life of 37.5 minutes. Thus we may conclude that the total activity is due to K^{42}, A^{41} and active chlorine.

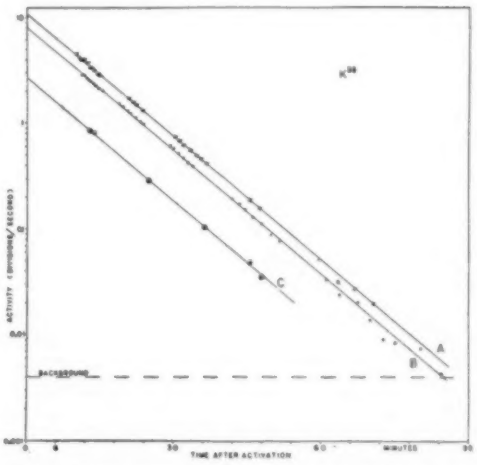

Fig. 3. Decay curves of K^{38}. *A* is the activity of potassium precipitated from lithium chloride after bombardment with 0.12μa of 11 Mev α-particles for 50 min. *B* is the activity of potassium precipitated from sodium chloride after bombardment with 0.1μa of 11 Mev α-particles for 50 min. *C* is the activity of potassium precipitated from lithium chloride after bombardment with 0.1μa of 11 Mev α-particles for 11 min.

In several cases part of the irradiated sample was dissolved in a dilute solution of potassium

[8] Snell, Phys. Rev. **49**, 555 (1936).

[9] Unpublished. Slow neutron activation of $PbCl_2$ and NH_4Cl.

[10] The short period in Fig. 2 is of the order 1 minute and is probably due to O^{19} formed from F^{19} in the reaction:

$$F^{19}+n^1 \rightarrow O^{19}+H^1.$$

The half-life of O^{19} is 40 sec. This short period was not found in K metal, K_2CO_3 or KNO_3.

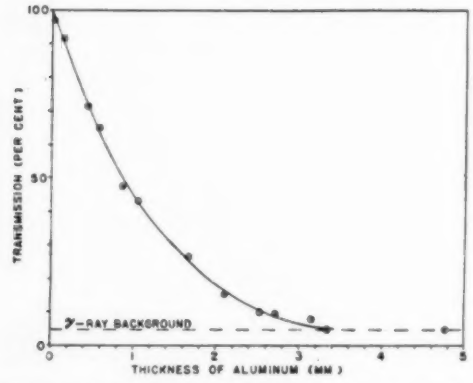

FIG. 4. Absorption in aluminum of the positrons from K^{38}. The upper limit is at 3.4 to 3.5 mm aluminum and corresponds to a maximum energy of 2 Mev.

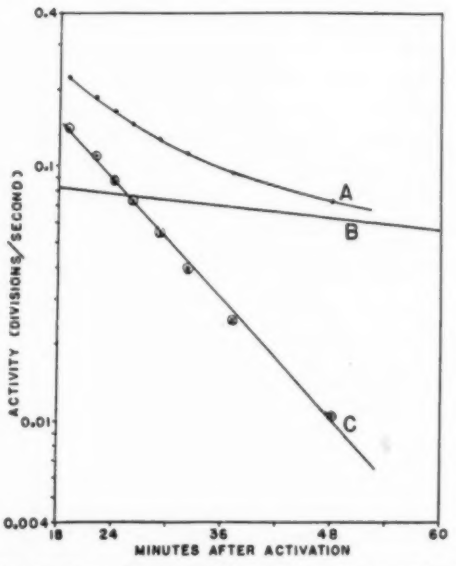

FIG. 5. Curve *A* is the activity of potassium perchlorate precipitated from a solution containing calcium which had been activated with deuterons. Some active scandium came down with the potassium and its activity, as obtained from later observations, is given by *B*. When the points of *A* are corrected by *B* the result is the line *C* corresponding to a half-life equal to that found for K^{38}; hence this isotope is produced by deuteron bombardment of calcium.

chloride and the chlorine was precipitated by the addition of silver nitrate. The activity of the silver chloride was found to decay with a single half-life of 37.5 minutes. The magnitude of the initial activity agreed with that of the 37.5 minute period found by resolving the composite curve. These results justify the statement that the chlorine isotope of period 37.5 minutes and A^{41} are produced by irradiating potassium with fast neutrons. There is no evidence of the formation of A^{39}. However, this isotope would not have been detected if it had a short or a very long half-life; nor could it have been observed if its period were nearly equal to one of the known periods of the composite decay curve. Madsen[11] was unable to detect active chlorine in potassium after irradiation with fast neutrons and suggested that this indicated that Cl^{38} is the known active chlorine isotope. In view of the present detection of A^{41} and active chlorine and the failure to observe A^{39}, it is clear that Madsen's argument, based on relative abundances, is not valid.

IV. POTASSIUM(38)

(a) Alpha-particle bombardment of chlorine

The usual alpha-particle reactions in which the bombarding particle is absorbed by a nucleus and a proton or neutron emitted suggest that K^{38} will be produced by bombarding chlorine with alpha-particles according to the reaction:

$$Cl^{35}+He^4 \rightarrow K^{38}+n^1; \quad K^{38} \rightarrow A^{38}+e^+$$

and that other argon and potassium isotopes formed will be stable. (We include K^{40} in this category.) Accordingly a search was made for this active potassium in lithium chloride bombarded with 11 Mev alpha-particles. After bombardment the lithium chloride was dissolved in a dilute solution of potassium chloride and the potassium was precipitated as potassium cobaltinitrite. The precipitate had a strong activity decaying to half-value in $7.7_5 \pm 0.1_5$ minutes as shown in Fig. 3. The particles emitted were positrons having a maximum energy as determined by Feather's rule from the thickness of aluminum required to stop them of 2 Mev. A gamma-ray was also present. The absorption curve in aluminum of the emitted radiations is shown in Fig. 4. Substitution of sodium chloride for the lithium chloride yielded the same isotope. The initial activity corresponds to 2×10^6 alpha-particles per active atom.

Pollard, Schultz and Brubaker[12] have observed the emission of neutrons from chlorine under

[11] Madsen, Nature **138**, 722 (1936).

[12] Pollard, Schultz and Brubaker, Phys. Rev. **51**, 140 (1937).

bombardment with alpha-particles from Ra C and Th C′. They ascribe these to the formation of K^{40} from Cl^{37} thus:

$$Cl^{37}+He^4\rightarrow K^{40}+n^1.$$

In view of the present results, however, it seems highly probable that they were detecting the formation of both K^{38} and K^{40}.

(b) The formation of K^{38} from calcium

In a previous paper[3] results obtained by one of us in a study of the radioactivities induced in calcium by deuteron bombardment were reported. It was noted that a weak activity was observed in the potassium fraction separated chemically from the irradiated metal. It was suggested that this might be due to contamination, though it was thought, in view of the fact that the half-period did not agree with that of any well-known contaminant, that it might be due to K^{38} formed thus:

$$Ca^{40}+H^2\rightarrow K^{38}+He^4;\quad K^{38}\rightarrow A^{38}+e^+.$$

Following the production of K^{38} by bombarding chlorine with alpha-particles, a search was made for this isotope in irradiated calcium. It has a sufficiently short half-life to have been unobservable in the previous experiments on account of the time needed for the chemical separation adopted.

Calcium metal was, therefore, bombarded with deuterons for half an hour and, following solution in HCl and the addition of inactive KCl, potassium was precipitated by means of perchloric acid and ethyl alcohol. In consequence the precipitate was contaminated with radioactive scandium.[5] However, on correcting for this it was found that K^{38} was present, the decay curve corresponding to a half-period of 7.6 ± 0.2 minutes. This curve is reproduced in Fig. 5.

The decay of this precipitate was measured until its corrected intensity was less than the natural leak of the electroscope, but no evidence was obtained of the 12.4 hour period of K^{42}. The expected reaction

$$Ca^{44}+H^2\rightarrow K^{42}+He^4;\quad K^{42}\rightarrow Ca^{42}+e^-$$

would thus appear to be rather improbable.

V. Conclusion

In conclusion we wish to thank the staff of the Radiation Laboratory for their cooperation, and especially Professor E. O. Lawrence for his interest and encouragement. The investigation has been aided by grants to the laboratory from the Research Corporation, the Chemical Foundation and the Josiah Macy, Jr. Foundation.

JUNE 15, 1937 PHYSICAL REVIEW VOLUME 51

The Disintegration of High Energy Protons

G. Nordheim, L. W. Nordheim,
Purdue University, Lafayette, Indiana

J. R. Oppenheimer and R. Serber
University of California, Berkeley, California

(Received March 22, 1937)

The coupling between light and heavy particles assumed in the Fermi theory of β-decay makes it possible for high energy protons in passing through matter to transfer a considerable fraction of their energy to electrons and neutrinos. If we suppose that this coupling is a maximum for relative energies of the light and heavy particles of the order $\hbar c/R$, with R the range of nuclear forces, and is small for much higher relative energies, the most important process which occurs, for sufficiently energetic protons, can be pictured as a sort of photodisintegration of the proton by the contracted Coulomb field of a passing nucleus, the proton changing into a neutron and emitting a positron and a neutrino. With a coupling of the type described, and of the magnitude required by the proton-neutron forces, processes involving more than one pair of light particles will be relatively rare. The cross section for the disintegration of a proton of energy E is found to be of the order

$$2\pi(\hbar/Mc)RZ^2\alpha^2\ln^2(E/Mc^2),$$

and is very small, even for heavy nuclei. The mean energy given to the positron per disintegration is of the order

$$2(\hbar c/R)(E/Mc^2)/\ln(E/Mc^2).$$

The positrons emitted in these disintegrations can account in order of magnitude for the incidence of showers observed under thick absorbers.

1. Some Consequences of the Fermi Coupling

UNTIL recently the only mechanisms known by which a proton could lose an appreciable fraction of its energy to electrons and γ-rays were elastic impacts of the proton with extranuclear electrons, and the relatively insignificant radiation emitted by the protons deflected in nuclear fields. The Fermi theory of β-decay provides a new mechanism for such energy transfer, because of the coupling assumed in this theory between the heavy particles (proton and neutron) and the electron-neutrino field. Owing to the weakness of the coupling necessary to explain the long lifetimes of the β-radioactive substances, this effect would be extremely small if one were to take over unmodified the coupling used in the theory of β-disintegration. However, a strong increase of the coupling with the energies of the particles concerned is suggested when one attempts an explanation of nuclear forces on the basis of Fermi's theory. The question of the consequences of this modified Fermi coupling for the behavior of heavy particles of high energy thus needs investigation.

An unambiguous answer to this question depends upon a satisfactory formulation of the problem of nuclear forces. The unsatisfactory character of present theories manifests itself in the occurrence of divergences in the method involved in their formulation, the method of successive approximations. This divergence of the method of successive approximations indicates that processes which from the point of view of this approximation are of high order, and which involve the cooperation of a large number of light particles, may be of dominant importance. The point of view adopted by Heisenberg[1] in his theory of showers would seem to be that this feature of the present inadequate field theory will also be characteristic of a correct theory, and that just those implications of present theory which would at first seem most subject to suspicion can have a qualitative validity.

Quite different from Heisenberg's suggestion is the more usual procedure of avoiding divergences by the formal device of reducing the coupling between heavy and light particles for high relative energies. In this way one can account for the finite range of nuclear forces by taking a coupling which becomes small for electrons and neutrinos whose de Broglie wave-length is smaller than this range ($\sim 2\times 10^{-13}$ cm). When the constants of the coupling are adjusted to give not only the range but the magnitude of nuclear forces, it turns out that even at its maximum the coupling is rather small, so that the probability of finding an electron-neutrino pair in the neighborhood of a heavy particle is less than one in ten, and the probability of finding many such pairs is negligible. In fact, if one applies the "Born approximation," and regards the coupling as small, the parameter which determines the relative magnitude of successive terms in this approximation is h/McR, where R is the range of nuclear forces.[2] This model is now so much modified as compared to that of Heisenberg that it no longer affords any explanation of showers.

This model makes it possible to give a quantitative estimate of the probability that a proton will disintegrate in its passage through matter into a neutron, a positron, and a neutrino, and of the magnitude of the energy loss to light particles for which the Fermi coupling is responsible. For very high energies such a disintegration of the proton will occur for quite distant impacts with atomic nuclei. These disintegrations may be thought of as a sort of photo-effect of the proton by the contracted Coulomb field of the passing nucleus. For sufficiently high energies these distant impacts, which are relatively easy to discuss, will contribute the dominant terms to the probability of proton disintegration.[3]

[1] W. Heisenberg, Zeits. f. Physik **101**, 533 (1936).

[2] Against the correctness of this formulation is the equality of the forces between proton and neutron and between proton and proton, since these appear in different orders in the Born approximation. It would seem that the electron-neutrino theory of nuclear forces could only very artificially be made to explain this equality, as well as the range and magnitude of the forces. The generalization of the β-transformation theory proposed by G. Gamow and E. Teller, Phys. Rev. **51**, 289 (1937), would give the same order of magnitude for the proton disintegration effect as derived in this paper.

[3] For the range of energies actually found in the cosmic rays, the probability of disintegration through a direct impact of the proton and nucleus may be expected, on the basis of our model, to have a magnitude comparable to that of the process we discuss for light elements, but to be considerably smaller for heavy ones. In comparing the results of our calculation with the observed incidence of sea level showers, it should not be forgotten that we have not taken these direct impacts into account, and that their contribution may be sensitive to the model assumed.

2. The Form of the Coupling

We investigate first the possibilities of formulating a modified and "cut-off" Fermi coupling convenient for the treatment both of nuclear forces and of high energy disintegrations.

The simplest form of the Fermi interaction energy is[4]

$$H_{PN}=G(mc^2)(\hbar/mc)^3\int(\psi_N^*\beta\varphi_e)(\varphi_\nu^*\beta\psi_P)d\tau, \quad (1)$$

which describes the transition of a proton, P, into a neutron, N, with the emission of a positron, e, and a neutrino, ν. Here the matrix β is the coefficient of the mass term in the Dirac equation written in its normal form, and the integrand is thus built up of the simplest scalars which can be formed from the Dirac wave functions of the heavy and light particles. G is a pure number which fixes the magnitude of the interaction. A coupling of the type (1) will lead to an interaction between a neutron and a proton which, to the second order in G, is represented by the Majorana potential $J(r)P^M$, given by

$$[J(r)P^M]_M=-\sum\{H_{NP}^{(1)}H_{PN}^{(2)}+H_{PN}^{(2)}H_{NP}^{(1)}\}/(\epsilon_e+\epsilon_\nu), \quad (2)$$

where the sum extends over all possible electron and neutrino states, with energies ϵ_e and ϵ_ν, respectively, and the upper indices (1), (2) distinguish the heavy particles.

It is well known, however, that the coupling (1), with G determined to give the correct order of magnitude for the lifetimes of the β-active nuclei ($G\sim10^{-12}$), gives the result that $J(r)$ is far too small for separations of the heavy particles of the order 10^{-13} cm, and is highly singular, behaving like r^{-5}, as $r\to0$. In order to obtain a potential of finite range and depth, and proper magnitude, without violating the facts of β-decay, it is necessary to modify (1) so that:

1. The order of magnitude of H_{PN} remains unchanged for energies of the light particles in the β-decay region ($<25\ mc^2$).

2. H_{PN} increases enormously for light particle energies of the order $\hbar c/R\sim137\ mc^2$.

3. $H_{PN}\to0$ for still higher light particle energies.

[4] The form of the spin dependence in (1) has been chosen because it gives Majorana forces.

To obtain such a dependence of (1) on the energies we could, for free particles, simply multiply the integrand by a suitable amplitude factor f, which is an invariant function of the four-vector momenta of all the particles. For arbitrary states the interaction could then be found by superposition of the individual Fourier components. Since $\hbar/R\ll Mc$ we can choose a coordinate system in which the heavy particle velocities are small. In this system our invariant, f, must reduce to an arbitrary function of the energies of electron and neutrino and of the angle between their directions of motion.

Thus our matrix element for the coupling becomes, in the rest system of the heavy particle (using plane waves for the electron and neutrino),

$$H_{PN}=G(mc^2)(\hbar/mc)^3\int(\psi_N^*\beta u)\times(w^*\beta\psi_P)f(\mathbf{p},\mathbf{q})\exp[(i/\hbar c)(\mathbf{p}-\mathbf{q})\cdot\mathbf{r}]d\tau, \quad (3)$$

where u and w are the Dirac amplitudes for the electron and neutrino wave functions, and $\mathbf{p}$ and $\mathbf{q}$ are c times their momenta.

For $J(r)$ we obtain from (2) and (3), after carrying out the summations over the spin variables in the usual way,[5]

$$J(r)=-\frac{G^2}{(mc^2)^4}\frac{1}{2(2\pi)^6}\int\frac{|f(\mathbf{p},\mathbf{q})|^2}{\epsilon_e+q}\exp[(i/\hbar c)(\mathbf{p}-\mathbf{q})\cdot\mathbf{r}]\times d\mathbf{p}d\mathbf{q},$$

where $\mathbf{r}=\mathbf{r}_1-\mathbf{r}_2$ is the distance between the two heavy particles. We can carry out the integrations over the directions of $\mathbf{p}$ and $\mathbf{q}$ if we make the assumption that there is no coupling between the directions of emission of the electron and neutrino. Neglecting the difference between p and ϵ_e, we find

$$J(r)=-\frac{G^2}{(mc^2)^4}\frac{1}{8\pi^4}\int\int\frac{|f(p,q)|^2}{p+q}\frac{\hbar c}{pr}\sin\frac{pr}{\hbar c}\times\frac{\hbar c}{qr}\sin\frac{qr}{\hbar c}p^2dpq^2dq. \quad (4)$$

The amplitude function $f(p, q)$ has to be adjusted so that (4) gives the right magnitude and range for the nuclear forces. The former will be given correctly when the energy of the first stationary state of the deuteron is ~0. Because

[5] In the first term of (2) (emission of an electron and an antineutrino by the neutron and their reabsorption by the proton) the summation is extended over all positive energy states of the electron and negative energy states of the neutrino, in the second term (emission of a positron and a neutrino by the proton and their reabsorption by the neutron) over all negative energy states of the electron and positive energy states of the neutrino. The density of electron and neutrino states in our units is $d\mathbf{p}d\mathbf{q}/(2\pi\hbar c)^6$.

of the short range, this condition is approximately satisfied when

$$\int_0^\infty J(r)rdr \sim -\hbar^2/M, \tag{5}$$

as Bethe has observed.[6] An alternative expression of this condition is the phase integral

$$\int_0^\infty [-MJ(r)]^{\frac{1}{2}}dr = \tfrac{1}{2}\pi\hbar. \tag{5a}$$

If we introduce (4) into (5) and reverse the order of integration, the integral over $a=r/\hbar c$ gives

$$\int_0^\infty a^{-1}da \sin ap \sin aq = -\tfrac{1}{2} \ln |p-q|/(p+q),$$

and the magnitude of G is determined by

$$\frac{1}{Mc^2}=\frac{G^2}{(mc^2)^4}\frac{1}{(2\pi)^4}\int\int\frac{|f(p,q)|^2}{p+q}\ln\frac{p+q}{|p-q|}pdpqdq. \tag{6}$$

The problem of finding a function f which satisfies the requirements 1, 2, and 3 has been studied by Camp,[7] and may be simply solved by taking

$$f(p,q)=(p+q)^{\frac{1}{2}}\exp[-(\alpha^2/2)|\mathbf{p}-\mathbf{q}|^2]\varphi(\mathbf{p}+\mathbf{q}),$$

which leads to the Gaussian potential

$$J(r)=-J_0e^{-r^2/(2a\hbar c)^2},$$

$$J_0=\frac{G^2}{(2mc^2)^4}\frac{\pi^{\frac{1}{2}}}{(2\pi)^6}\frac{1}{\hbar c\alpha^3}\int|\varphi(\mathbf{s})|^2d\mathbf{s}=\frac{\pi}{2Mc^2\alpha^2}$$

by (5a). When this coupling is applied to the problem of proton disintegration, it leads, because of the dependence of f on the angle between $\mathbf{p}$ and $\mathbf{q}$, to unnecessarily cumbersome integrals. Since it is unlikely that any real theoretical significance is to be attached to this f, we have chosen instead a form which is convenient for calculation, and which satisfies conditions 2 and 3:[8]

$$f(p,q)=(mc^2)^{-s}p^ne^{-p/A}q^{s-n}e^{-q/A}. \tag{7}$$

If in this formula s and n are adjusted ($s\sim 12$) to give a long enough life for the high energy β-emitters Li^8 and B^{12}, the potential $J(r)$ loses all resemblance to a simple trough, and shows marked oscillations. Since we can see that our results depend little on n and s, we shall choose, when it is necessary to fix them, the "compromise" values $s=4$, $n=2$. To the question of the effect of a dependence of f on the angle between $\mathbf{p}$ and $\mathbf{q}$, we shall return later.

One can show that with (7)

$$J(r)\rightarrow\begin{cases} r^{-(2s+5)}, & r\rightarrow\infty \\ \text{const}, & r\rightarrow 0. \end{cases}$$

The relation (6) becomes

$$G^2=\frac{2^{2s+6}\pi^4}{T_s(2s+2)!}\frac{m}{M}\left(\frac{2mc^2}{A}\right)^{2s+3}, \tag{8}$$

where T_s is a number of order unity, depending on the choice of s and n. For $s=2$, $n=1$, $T_s=0.77$, and for $s=4$, $n=2$, $T_s=0.70$. As a measure of the range we can use

$$R=2\int_0^\infty J(r)rdr/\int_0^\infty J(r)dr.$$

With $s=4$, $n=2$ we get $R=\frac{2}{3}\hbar c/p_0$, where $p_0=2A$ is the energy at which f has its maximum. As $R\sim 2.2\times 10^{-13}$ cm, we find in this case $p_0\sim 115\ mc^2$.

The choice (7) for f gives the simplest extrapolation of the form of interaction used in the theory of β-disintegration. Another form, which expresses the feature that f has a pronounced maximum, is the Gaussian function

$$f(p,q)=[(p+q)/mc^2]^{\frac{1}{2}}e^{-(p-p_0)^2/2\Delta^2}e^{-(q-p_0)^2/2\Delta^2}. \tag{9}$$

(9) can be considered as the limiting form of (7) for $n\sim\frac{1}{2}s\rightarrow\infty$, with the correspondence $p_0=nA$, $\Delta=n^{\frac{1}{2}}A$. The factor $[(p+q)/mc^2]^{\frac{1}{2}}$ is introduced to simplify the integration, which gives

$$J(r)=-\frac{G^2}{(mc^2)^5}\frac{\Delta^2p_0^4}{(2\pi)^3}\left(\frac{\hbar c}{p_0r}\right)^2\sin^2\frac{p_0r}{\hbar c}e^{-\Delta^2r^2/2(\hbar c)^2},$$

while the phase integral (5a) gives, for $\Delta\ll p$,

$$G^2=(2\pi)^3(m/M)(mc^2)^4/\Delta^2p_0^2. \tag{10}$$

3. Calculation of the Cross Section

The process of the disintegration of a high energy proton by the Coulomb field of a nucleus can be thought of, in the coordinate system in which the proton is initially at rest, as the emission by the proton of a positron and a neutrino, the positron then being deflected by the contracted Coulomb field of the passing

[6] Bethe and Bacher, Rev. Mod. Phys. **8**, 109 (1936).
[7] G. Camp, Phys. Rev. **51**, 1046 (1937).
[8] In the β-decay region this is equivalent to the general formulation of the coupling discussed by Uhlenbeck and Konopinski, Phys. Rev. **48**, 7 (1935).

nucleus.[9] From this formulation we can see that it is only when frequencies of the order p_0/h are important in this contracted field that the disintegration will be probable. In the whole of the calculation we shall confine ourselves to the case where the field is strongly contracted, where, therefore, the proton has a velocity, v, very close to that of light, and an energy large compared to its rest energy. We shall keep only the dominant terms in ξ and $\ln \xi$, where $\xi=1/(1-v^2/c^2)^{\frac{1}{2}}$.

One way which suggests itself for this calculation is the impact parameter method of v. Weizsäcker and Williams,[10] which replaces the contracted Coulomb field by a bundle of parallel γ-rays moving in the same direction as the nucleus. This method is valid if the momentum of the field normal to the direction of motion of the nucleus can be neglected compared to the transverse momenta of the wave packet representing the positron. As we shall see, in our problem values of the impact parameter for which this condition is not satisfied give an essential contribution to the cross section.

Instead, we shall make a Fourier analysis of the Coulomb field of the passing nucleus, without neglecting the transverse component of the propagation vector of the electromagnetic field. The field of a point charge Ze moving with velocity v in the z direction is given by

$$\varphi=Ze/[z^2+(x^2+y^2)/\xi^2]^{\frac{1}{2}},$$
$$A_z=(v/c)\varphi, \quad A_x=A_y=0.$$

Neglecting terms of order $1/\xi^2$, we find

$$\varphi=A_z=(Ze/2\pi^2\hbar c)\int \varphi(\mathbf{K})\, \exp\left[(i/\hbar c)(\mathbf{K}\cdot\mathbf{r}-kct)\right] d\mathbf{K}, \quad \varphi(\mathbf{K})=1/(g^2+k^2/\xi^2),$$

where the vector $\mathbf{k}$ is the component of $\mathbf{K}$ parallel to the z axis, and $\mathbf{g}$ is the component of $\mathbf{K}$ perpendicular to the z axis. By adding the gauge terms $\varphi'(\mathbf{K})=-\varphi(\mathbf{K})$, $\mathbf{A}'(\mathbf{K})=-(\mathbf{K}/k)\varphi(\mathbf{K})$ we obtain $\varphi=0$ and

$$\mathbf{A}=\int \mathbf{A}(\mathbf{K})\, \exp\left[(i/\hbar c)(\mathbf{K}\cdot\mathbf{r}-kct)\right] d\mathbf{K}/(2\pi\hbar c)^3, \quad \mathbf{A}(\mathbf{K})=-4\pi\hbar^2c^2Ze(\mathbf{g}/k)/(g^2+k^2/\xi^2). \tag{11}$$

The matrix element of the interaction energy, $H=e(\boldsymbol{\alpha}\cdot\mathbf{A})$, of an electron and the electromagnetic field (11), between a state of momentum $\mathbf{p}'/c$ and a negative energy state of momentum $-\mathbf{p}/c$, is

$$H_{p'p}=-4\pi\hbar^2c^2Z^2e^2(g/k)(u'^*\alpha_g u)/(g^2+k^2/\xi^2), \tag{12}$$

where $\mathbf{p}'+\mathbf{p}=\mathbf{K}$, and where we write s_g for the component of a vector $\mathbf{s}$ in the direction of $\mathbf{g}$.

For the transition from the initial state (proton with momentum $\mathbf{P}=0$) to the final state (neutron +positron+neutrino with respective momenta $\mathbf{N}$, $\mathbf{p}/c$, $\mathbf{q}/c$) through an intermediate state in which the electron has a momentum $\mathbf{p}'/c$, we obtain from (3) and (12), with the neglect of the kinetic energy of the heavy particle, the differential cross section

$$d\phi=\frac{2\pi}{\hbar c}(4\pi\hbar^2c^2)^2(mc^2)^2\left(\frac{\hbar}{mc}\right)^6 G^2Z^2e^4\frac{g^2}{k^2}\frac{|f(p',q)|^2}{(g^2+k^2/\xi^2)^2}\frac{d\mathbf{K}}{(2\pi\hbar c)^3}$$
$$\times d\rho_e d\rho_\nu \sum_w^2 |w^*\beta\psi_P|^2 \sum_{u,\psi_N}^2 \left|\sum_{u'}^4 \frac{(\psi_N^*\beta u')(u'^*\alpha_g u)}{E'-E_\nu}\right|^2,$$

with the density factors $d\rho_e=d\mathbf{p}/(2\pi\hbar c)^3$, $d\rho_\nu=q^2d\Omega_q/(2\pi\hbar c)^3$, $d\Omega_q$ the element of solid angle for the directions of emission of the neutrino, and ψ_P, ψ_N, the Dirac amplitudes for the heavy particle wave

[9] The two other processes, (1) the proton is first scattered by the nucleus into an intermediate state and then emits the light particles and (2) a β-transformation of the nucleus is induced by the Coulomb field of the passing proton, are much less important than the one discussed in the text.

[10] C. F. v. Weizsäcker, Zeits. f. Physik **88**, 612 (1934); E. J. Williams, Phys. Rev. **45**, 729 (1934), Danske Vid. Selsk. Math. Fys. **13**, 4 (1935).

functions. The momentum and energy relations are

$$\mathbf{p}+\mathbf{p}'=\mathbf{K}=\mathbf{k}+\mathbf{g},$$
$$\epsilon+q=k, \tag{13}$$
$$\epsilon=[p^2+(mc^2)^2]^{\frac{1}{2}}, \quad \epsilon'=[p'^2+(mc^2)^2]^{\frac{1}{2}}.$$

Carrying out the summation over the spin directions in the usual way, and integrating over the directions of emission of the neutrino and the azimuth of $\mathbf{g}$, we obtain for the cross section

$$\phi=\frac{G^2Z^2r_0^2}{4\pi^4(mc^2)^2}\int\frac{dk}{k}\int\frac{g^3dg}{(g^2+k^2/\xi^2)^2}\int\frac{q^2|f(p'q)|^2}{k(\epsilon'^2-q^2)^2}\frac{S}{\epsilon}d\mathbf{p}, \tag{14}$$

with

$$S=\epsilon(\epsilon'^2+q^2)-2(q-mc^2)[(\mathbf{p}\cdot\mathbf{p}')+(mc^2)^2+2p_0p_0']-mc^2(\epsilon'^2-q^2-2\epsilon q),$$

and $r_0=e^2/mc^2$.

The determining factors in (14) are the amplitude function f, which we assume to be large only for values of p' and q of the order $\hbar c/R$, and the resonance denominator (ϵ'^2-q^2). We introduce polar coordinates for $\mathbf{p}$, with θ the angle between $\mathbf{p}$ and z, and φ that between the $p-z$ and $g-z$ planes, and obtain from (13)

$$\epsilon'^2-q^2=p'^2-q^2+(mc^2)^2=g^2+2k\epsilon-2p(k\cos\theta+g\sin\theta\cos\varphi).$$

For $p\gg mc$, this becomes

$$g^2+(k/p)(mc^2)^2+2kp(1-\cos\theta)-2pg\sin\theta\cos\varphi, \tag{15}$$

and the minimum value of the resonance denominator is found to be

$$(1-p/k)\{g^2+(mc^2)^2/[(p/k)(1-p/k)]\}. \tag{16}$$

From (15) and (16) we see that the principal contribution comes from values of g small compared to k. This makes it possible to simplify S by retaining only the lowest power in g.

With the help of the relation

$$2(\mathbf{p}\cdot\mathbf{p}')=q^2+2\epsilon q-\epsilon'^2+2(mc^2)^2,$$

which follows from (13) for small g, we get for the leading term of S

$$S=(\epsilon'^2-q^2)(\epsilon+q-2mc^2)-4(mc^2)^2(q-mc^2). \tag{17}$$

On the other hand, the factor $g^3/(g^2+k^2/\xi^2)^2$ shows that only $g>k/\xi$ is effective. Therefore for $k/\xi>mc^2/[(p/k)(1-p/k)]^{\frac{1}{2}}$, i.e., not too large ξ, g will determine the magnitude of the resonance denominator and we can neglect all the mass terms and put $\epsilon=p$, $\epsilon'=p'$, obtaining

$$\phi=\frac{G^2Z^2r_0^2}{4\pi^4(mc^2)^2}\int_0^\infty\frac{dk}{k}\int_{k/\xi}^\infty\frac{dg}{g}I(g),$$
$$I(g)=\int\frac{q^2|f(p',q)|^2}{p(p'^2-q^2)}d\mathbf{p}. \tag{18}$$

If we had used the v. Weizsäcker-Williams method, introducing an impact parameter ρ, and replacing the field by an approximately equivalent light quantum field, g would not, of course, have appeared in the conservation laws (13), and thus the third integral in (14) would have been independent of g. Instead of (18) we should then have found

$$\phi\sim\frac{G^2Z^2r_0^2}{4\pi^4(mc^2)^2}\int\frac{dk}{k}\int^{\hbar c\xi/k}\frac{d\rho}{\rho}I(0). \tag{18a}$$

With the correlation $\rho\sim\hbar c/g$, this agrees with (18) for $g\ll 2mc^2$, the minimum value of $mc^2/[(p/k)(1-p/k)]^{\frac{1}{2}}$, or $\rho\gg\frac{1}{2}\hbar/mc$, since it follows from (16) that under these circumstances $I(g)\sim I(0)$. Since, however, values of g larger than $2\ mc^2$ contribute essentially to the result,

the introduction into (18a) of $\frac{1}{2}h/mc$ as a lower limit of the impact parameter would be wrong. The method of the impact parameter is inapplicable.

Owing to the resonance denominator only $p' \sim q$ will contribute to the dominant term in $\ln \xi$, and in (18) we can replace p' by q in $f(p', q)$ and integrate over the directions of $\mathbf{p}$,

$$\int d\mathbf{p}/p(p'^2-q^2) = \int Y p dp,$$

$$Y = \int_0^\pi \int_0^{2\pi} \frac{\sin\theta d\theta d\varphi}{g^2+2kp(1-\cos\theta)-2pg\sin\theta\cos\varphi} = 2\pi \int_0^\pi \frac{\sin\theta d\theta}{\{[g^2+2kp(1-\cos\theta)]^2-4p^2g^2\sin^2\theta\}^{\frac{1}{2}}}. \quad (19)$$

If we introduce $x=(1-\cos\theta)$ and replace $\sin^2\theta$ by $2x$ in the second term of the denominator, we get

$$Y \sim \begin{cases} (\pi/kp)\ln[4kp/g^2(1-p/k)], & g<g_{\max}=[4kp/(1-p/k)]^{\frac{1}{2}}, \\ 0, & g>g_{\max}. \end{cases}$$

The integration over g gives

$$\int_{k/\xi}^{g_{\max}} g^{-1}dg \ln[4kp/g^2(1-p/k)] = \ln^2[2\xi/(k/p-1)^{\frac{1}{2}}], \quad (20)$$

and (18) becomes, using $k=p+q$,

$$\phi = \frac{G^2Z^2r_0^2}{4\pi^3(mc^2)^2}\int_0^\infty q^2|f(q,q)|^2dq\int_0^\infty \frac{dp}{(p+q)^2}\ln^2\left[\frac{2\xi}{(k/p-1)^{\frac{1}{2}}}\right].$$

In the argument of the logarithm we may take $p\sim q\sim\frac{1}{2}k$, and we obtain for the dominant term in $\ln\xi$ in the cross section[11]

$$\phi = \frac{G^2Z^2r_0^2}{4\pi^3(mc^2)^2}\ln^2\xi\int_0^\infty q|f(q,q)|^2dq.$$

For large ξ the neglect of the mass term in the resonance denominator (ϵ'^2-q^2) is no longer allowed (although the mass dependent terms in (17) always give a negligible contribution). The only change introduced by the mass term will be that we have to replace (19) by

$$Y = 2\pi\int_0^2 \frac{dx}{\{[g^2+(k/p)(mc^2)^2+2kpx]^2-8p^2g^2x\}^{\frac{1}{2}}} \sim \begin{cases} \frac{\pi}{kp}\ln\frac{4kp}{(1-p/k)g^2+\frac{1}{2}(k/p)(mc^2)^2}, & g<g_{\max}, \\ 0, & g>g_{\max}, \end{cases}$$

where $g_{\max}$ is the value of g for which the argument of the logarithm is unity, and instead of (20) we will have

$$\int_{k/\xi}^{g_{\max}} \frac{dg}{g}\ln\frac{4kp}{\left(1-\frac{p}{k}\right)\left[g^2+\frac{1}{2}\frac{k}{p}\frac{(mc^2)^2}{(1-p/k)}\right]} \sim \begin{cases} \ln^2\frac{2\xi}{(k/p-1)^{\frac{1}{2}}}, & \frac{k}{\xi}<\kappa=\left[\frac{1}{2}\frac{k}{p}\frac{(mc^2)^2}{(1-p/k)}\right]^{\frac{1}{2}}, \\ \ln\frac{2^{\frac{1}{2}}p}{mc^2}\ln\frac{2^{\frac{1}{2}}\xi^2}{(1-p/k)}\frac{mc^2}{k}, & \frac{k}{\xi}>\kappa. \end{cases}$$

[11] In the order in which we are working the introduction of a nuclear radius $\sim R$ within which the fields (11) are incorrect will not affect our results.

In carrying out the integrations over p and q we may again in the argument of the logarithm put $p\sim q\sim\frac{1}{2}k$, and set $k\sim k_0=2q_0$, where q_0 is the value of q at the maximum of $q|f(q,q)|^2$. The dominant terms in the cross section are

$$\begin{aligned}\phi &= \phi_0 \ln^2 \xi, && \xi < k_0/mc^2,\\ \phi &= \phi_0 \ln (k_0/mc^2) \ln (\xi^2 mc^2/k_0), && \xi > k_0/mc^2,\\ \phi_0 &= \frac{G^2Z^2r_0^2}{4\pi^3(mc^2)^2}\int_0^\infty q|f(q,q)|^2 dq.\end{aligned} \tag{21}$$

We can also calculate, from (14), the energy distribution of the emitted positrons in the coordinate system in which the nucleus is at rest. If in the coordinate system in which the proton is initially at rest the positron is moving at an angle θ to the z axis, with energy ϵ and velocity u, it has in the rest system of the nucleus the energy

$$E=\xi\epsilon[1-(uv/c^2)\cos\theta]\sim\xi p(1-\cos\theta)=\xi px.$$

The energy distribution is obtained by introducing E as a new variable in place of x in (14), and reversing the order of integrations, leaving the integration over E till last. The cross section for emission of a positron in the energy range dE at E is thus

$$\phi(E)dE=\frac{G^2Z^2r_0^2}{2\pi^3(mc^2)^2}\frac{dE}{\xi}\int_0^\infty q^2|f(q,q)|^2dq\int_{E/2\xi}^\infty\frac{dp}{p+q}\int_{k/\xi}^\infty\frac{dg}{g}\frac{1}{\{[g^2+(k/p)(mc^2)^2+2kE/\xi]^2-8g^2pE/\xi\}^{\frac{1}{2}}}.$$

The integral over g gives approximately

$$\frac{\xi}{4kE}\ln\frac{2\xi E}{k(1-p/k)},\quad E>\frac{(mc^2)^2\xi}{2p},\quad \frac{k}{\xi},$$

and the cross section is found to be

$$\phi(E)dE=\tfrac{1}{2}\phi_0\frac{dE}{E}\ln\frac{\xi E}{k_0},\qquad \xi k_0>E>\frac{(mc^2)^2\xi}{k_0},\quad\frac{k_0}{\xi}. \tag{22}$$

For $E>\xi k_0$ the distribution falls off rapidly with E, the exact form of the high energy tail depending on the amplitude function f.[12]

For the total energy transmitted to the positrons per cm path, we obtain

$$W_e=N\int\phi(E)EdE\sim N\xi k_0\phi_0\ln\xi, \tag{23}$$

where N is the number of atoms per cm^3.

[12] In calculating the high energy tail it is not legitimate to replace $f(p',q)$ by $f(q,q)$. With the amplitude function (7), the cross section for high energies falls off exponentially.

The angular distribution of the neutrinos in the rest system of the proton will be uniform for any amplitude function which does not contain a constraint between the direction of emission of the positron and neutrino. The energy lost to neutrinos per cm path is thus

$$W_\nu=N\xi\bar{q}\phi,$$

$$\bar{q}=\int_0^\infty q^2|f(q,q)|^2dq\Big/\int_0^\infty q|f(q,q)|^2dq. \tag{24}$$

This is larger than W_e, because the positrons are ejected preferentially in the forward direction in the rest system of the proton, and therefore receive less energy. It is evident that the introduction of a constraint between the directions of the positron and neutrino could reduce W_ν to a value comparable to W_e.

4. Results and Discussion

Our final results for the cross section, energy distribution and energy losses for proton disintegration are contained in the expressions (21) to (24). We have now to evaluate ϕ_0, using the amplitude functions $f(p,q)$ discussed in §2.

From (7) we obtain

$$\phi_0=\frac{G^2Z^2r_0^2}{4\pi^3(mc^2)^{2s+2}}\int_0^\infty q^{2s+1}e^{-4q/A}dq$$

$$=\frac{Z^2r_0^2mc^2}{k_0}\frac{m}{M}\frac{4\pi(2s+1)}{T_s(2s+2)}=Z^2r_0^2\frac{mc^2}{k_0}t_s, \quad (25)$$

with $k_0=\frac{1}{2}(2s+1)A$, and the value of G^2 given in (8). Taking the numerical values for T_s from §2,

$$t_s=6.6\times10^{-3} \quad \text{for} \quad s=2, \quad n=1,$$

$$t_s=8.8\times10^{-3} \quad \text{for} \quad s=4, \quad n=2.$$

For $\bar{q}$, which appears in (24), we find

$$\bar{q}=(s+\tfrac{1}{2}s+1)k_0.$$

With $s=4$, $n=2$, $k_0\sim250\ mc^2$.

The Gaussian amplitude function (9) gives

$$\phi_0=\frac{G^2Z^2r_0^2}{2\pi^3(mc^2)^3}\int_0^\infty q^2e^{-2(q-p_0)^2/\Delta^2}dq$$

$$=(2\pi)^{\frac{1}{2}}Z^2r_0^2(mc^2/\Delta)(m/M) \quad (26)$$

for $\Delta\ll p_0$, with the help of (10). With the correspondence $\Delta\sim k_0/(2s)^{\frac{1}{2}}$, (26) gives practically the same results as (25). We see from (25) and (26) that the cross section does not depend sensitively on the details of the amplitude function.

The cross section is of the order of magnitude $2\pi r_0^2(Z^2/137)(m/M)\ln^2\xi$ and is therefore small even for large Z. As the main contribution comes from impact parameters of the order $\rho\leq\xi hc/k_0\sim\frac{1}{2}\xi r_0$ the probability of a disintegration for a single passage is very small, which is a necessary condition for the applicability of the Born approximation. The energy given to light particles per impact is, however, quite large, the mean energy lost to the positron being $\sim k_0\xi/\ln\xi$, or about $\frac{1}{2}$ billion volts for a 10 billion volt proton.

To obtain an idea of the total energy transmitted to the light particles, we compare (23) and (24) with the ordinary ionization losses which are given by

$$W_{\text{ion}}=2\pi NZr_0^2mc^2\ln(2\xi^2m^2c^4/Ry^2Z^2),$$

where $Ry=27$ ev.

TABLE I. *Numerical values for the energies transmitted to positrons and neutrinos, and the loss by ionization for a number of different energies in air (expressed in water equivalent) and in lead.*

	ξ	W_e Mev/cm	W_ν Mev/cm	W_{ion} Mev/cm	W_{ion} $E>100$ Mev Mev/cm	Distance per disintegration meters
Air (water equivalent)	10	0.017	0.022	1.7	0	320
	10^2	0.35	0.88	2.2	0.27	80
	10^3	5.2	19	2.7	0.61	36
Pb	10	1.8	2.3	12	0	3.0
	10^2	36	90	18	2.4	0.75
	10^3	540	2000	22	5.5	0.35

In Table I we give numerical values for the energies transmitted to positrons and neutrinos, and the loss by ionization, for a number of different energies in air (expressed in water equivalent) and in lead. The figures given are for $s=4$, $n=2$, but depend little on the particular values chosen.

We have already mentioned that the model which we have assumed for the Fermi coupling precludes its importance for cosmic ray showers. If, however, it be supposed that heavy particles constitute an essential part of the penetrating component of cosmic rays, then the proton (and neutron) disintegrations considered in this paper can provide a mechanism for transferring a considerable fraction of the proton's energy to a light particle, and thus for initiating showers at depths in matter to which no electrons or photons can penetrate. For in most of these disintegrations the positron will have a high enough energy to initiate a small shower.[13] In order to compare the effectiveness of these disintegrations with that of the energy transfer by direct impact with extranuclear electrons, we give in column 4 the energy lost per cm by such impacts to electrons of energy greater than 100 Mev.

In the last column of Table I we give the mean distance traveled by a proton per disintegration. This distance is of the right order of magnitude to account for the observed incidence of showers under great thicknesses (>10 cm) of Pb.

[13] A discussion of shower production by high energy electrons has been given by J. F. Carlson and J. R. Oppenheimer, Phys. Rev. **51**, 220 (1937) and by H. T. Bhabha and W. Heitler, Proc. Roy. Soc. **A159**, 432 (1937).

Heavy Particle Interactions from β-Decay Theory

GLEN D. CAMP
San Francisco, California

(Received April 15, 1937)

The small constant g of a Fermi type coupling is replaced by a function of the momenta of the light particles. A simple form of this function leads to a satisfactory phenomenological description of β-decay and proton-neutron interaction. The application of this function to the like-particle interactions, however, gives for them poorly defined ranges and magnitudes which are too small. The discrepancies seem to be intrinsic, so that this attempt to reconcile β-decay and heavy particle interactions has been abandoned.

I

IT is well known that the interactions between heavy particles, derived from Fermi type couplings designed to describe β-decay, are orders of magnitude too small. This is because the coupling must be very small to account for the observed decay constants.[1] However, the coupling need be small only for light particles of momenta $p_\beta \cong 25$,[2] since this is the highest momentum so far observed in β-decay. If suitable interactions are to come from this theory, the coupling must increase enormously for larger momenta and must then diminish so as to lead to a finite range $r_0 \backsimeq (137)^{-1}$, and to a finite magnitude. The maximum should presumably occur somewhere near $p_0 \backsimeq r_0^{-1} \backsimeq 137$.[3] Since p_0 is several times larger than p_β there appears to be a possibility of obtaining suitable interactions without affecting the rate of β-decay appreciably. This possibility was investigated in the hope that a formalism might emerge which would serve as a temporary method of making various calculations in a more uniform way than is possible at present and which might therefore be very useful until a more satisfactory method has been found.

As a convenient point of departure, a Fermi type coupling has been chosen, with matrix

$$(P_b; p|H|N_a; \pi)$$

$$= g_0 \int [u^*(P_b x)\varphi(\pi x)][\psi^*(px)u(N_a x)]d\mathbf{x} \quad (1)$$

corresponding to the destruction of a neutrino and neutron, states π and N_a, and the creation of an electron and proton, states p and P_b. The spin coupling of (1) leads to an attractive Majorana type exchange interaction between the neutron and proton. As is well known, any linear combination of Majorana and Heisenberg type interactions can be obtained, but the above simple form has been chosen because it simplifies the calculations. In the present discussion, we shall be concerned only with the range and order of magnitude of the interactions and these do not depend very much upon the form of spin coupling assumed.

Any coupling involving two light particles will have a matrix of the general structure of (1), and the most obvious alteration consists in replacing the small constant g_0 by an invariant function of the energy momentum four vectors of the light and heavy particles. Since such an assumption would lead to the occurrence of finite distance operators in the Lagrangian, it is not possible to put the resultant field equations into Hamiltonian form. This procedure therefore has meaning only within the framework of a method of successive approximations. Because of the smallness of m/Mr_0, it is possible, in treating nuclear forces, to choose a coordinate system in which the heavy particles may be treated nonrelativistically.[4] In this coordinate system, our invariant function reduces to a function of the energies of the light particles and the angle between their momenta,

$$(P_b; p|H|N_a; \pi)$$

$$= K(\mathbf{p}\pi) \int [u^*(P_b x)\varphi(\pi x)][\psi^*(px)u(N_a x)]d\mathbf{x}. \quad (1')$$

[1] Bethe and Bacher, Rev. Mod. Phys. **8**, 202 (1936).
[2] Units m, $\hbar/mc$, $\hbar/mc^2$ are used.
[3] Bethe and Bacher, reference 1, 203 (c).
[4] Nordheim, Nordheim, Oppenheimer and Serber, Phys. Rev. **51**, 1037 (1937).

This modification is of considerable generality and includes, for example, the KU-coupling as a special case.

The coupling (1′) must first of all avoid any outstanding conflict with β-decay. The decay probability calculated from (1′) differs from that calculated from (1) only in the replacement of the factor g_0^2 by the average, over the directions of $\mathbf{p}$ and $\boldsymbol{\pi}$, of $|K|^2$. By properly adjusting the details of K in the β-region, one can therefore obtain practically any desired distribution curves, and, independently, any formula for the dependence of the decay constant upon the maximum energy of the distribution. Since the β-region must contribute negligibly to the heavy particle interactions, and since the details of β-decay are not important to the present discussion, it is sufficient for the present purposes to require

$$|K(\mathbf{p}\boldsymbol{\pi})|^2 \eqsim g_0^2 \eqsim 10^{-24} \quad \text{in} \quad 0 \lesssim p,\ \pi \eqsim 25. \tag{2}$$

The proton-neutron interaction calculated from (1′) is, in lowest order,

$$(P, N; r) = -\tfrac{1}{2}(2\pi)^{-6} \times \int d\mathbf{p} d\boldsymbol{\pi} \exp\left(i(\boldsymbol{\pi}-\mathbf{p})\cdot\mathbf{r}\right) \frac{|K(\mathbf{p}\boldsymbol{\pi})|^2}{(\epsilon+\nu)}. \tag{3}$$

Various forms have been assumed for K, the simplest being the usual choice of a function which is approximately factorable in the momenta of the light particles,

$$K_1(p\pi) = (\epsilon+\nu)^{\frac{1}{2}} L(p) M(\pi). \tag{4}$$

This assumption factors (3) into a product of two integrals, and simple calculations then show that the imposition of the β-condition (2) necessarily leads to an interaction which is not of a good trough type, falling off too slowly beyond r_0 and thus having a poorly defined range. This is because the β-condition requires that low momenta be left out of L and M, and these are necessary for a sharp range. For example, ignoring the β-condition, one obtains from

$$L(p) = M(p) = L_0 e^{-r_0^2 p^2/4} \tag{5}$$

the sharp range

$$(P, N; r) = (P, N; 0) e^{-(r/r_0)^2}, \tag{6}$$

but then the imposition of the β-condition means that one must cut out practically all of (5) from $p=0$ up to $p \eqsim 25$. This changes (6) to a sum of terms having various ranges from r_0 up to $\sim(25)^{-1}$ and while the longer range terms are the smaller at $r=0$, they eventually predominate.

To avoid this difficulty, advantage was taken of the appearance of only the difference of momenta in the exponential of (3) by assuming K to be approximately factorable in the sum and difference of momenta,

$$K_2(\mathbf{p}\boldsymbol{\pi}) = (\epsilon+\nu)^{\frac{1}{2}} f(\mathbf{p}+\boldsymbol{\pi}) \exp\left(-r_0^2(\mathbf{p}-\boldsymbol{\pi})^2/8\right) \tag{7}$$

with f still to be determined. This assumption leaves f free to satisfy the β-condition, since one now obtains

$$(P, N; r) = (P, N; 0) e^{-(r/r_0)^2}, \tag{8}$$

$$(P, N; 0) = -\tfrac{1}{2}(2\pi)^{-6} \pi^{\frac{1}{2}} r_0^{-3} (\text{norm } f),$$

$$\text{with} \quad \text{norm } f = \int |f(\alpha)|^2 d\alpha \tag{9}$$

and the form of f is not involved. Using $r_0 \eqsim (137)^{-1}$, the depth (9) should be about 40 according to present ideas, and this requires

$$\text{norm } f \eqsim \tfrac{1}{3}, \tag{10}$$

whereas the β-condition restricts f according to

$$|f(\alpha)|^2 \eqsim (\epsilon+\nu)^{-1} \cdot 10^{-24} \quad \text{in} \quad 0 \lesssim \alpha \gtrsim 25 \tag{2′}$$

since the Gaussian factor in (7) is practically one in the β-region. Comparing this small value (2′) with (10), one sees that practically all of norm f comes from outside the β-region.

The foregoing results show that, so long as one considers only β-decay and proton-neutron interaction in lowest order, the coupling (1′), together with the kernel (7), leads to satisfactory results. Furthermore, these results do not impose any restrictions upon the form of f outside the β-region, but only determine its norm and its value inside the β-region. However, as soon as one considers the like-particle interactions, or the proton-neutron interaction in second order, difficulties appear in spite of the freedom available in the choice of f.

II

The like-particle interaction, in lowest order, contains two terms. One arises from sequences in

which both an electron and a neutrino are exchanged, whereas the other comes from sequences in which only an electron (or neutrino) is exchanged, each heavy particle reabsorbing the neutrino (or electron) which it emits. The double exchange term has the simpler structure, and will be discussed first,

$$|(P,P;r)_2| = |(N,N;r)_2| = (\tfrac{1}{2})^2(2\pi)^{-12}$$
$$\int d\mathbf{p}_1 d\boldsymbol{\pi}_1 d\mathbf{p}_2 d\boldsymbol{\pi}_2 \exp(\imath(\boldsymbol{\pi}_2-\mathbf{p}_2)\cdot\mathbf{r})$$
$$\times \exp(-\imath(\boldsymbol{\pi}_1-\mathbf{p}_1)\cdot\mathbf{r})\tfrac{3}{2}(\epsilon_1+\nu_1)^{-1}$$
$$\times \frac{|K(\mathbf{p}_1\boldsymbol{\pi}_1)|^2|K(\mathbf{p}_2\boldsymbol{\pi}_2)|^2}{(\epsilon_1+\nu_1)(\epsilon_2+\nu_2)}. \quad (11)$$

There is one consequence of (11) which does not depend upon the form of K, except for the assumption, needed in any case to make the magnitude of $(P, N; r)$ finite, that $p^2\pi^2|K(\mathbf{p}\boldsymbol{\pi})|^2$ has a maximum. Comparing (11) with (3), one has

$$|(P,P;r)_2| = \tfrac{3}{2}[(\epsilon_1+\nu_1)^{-1}]_{Av}(P,N;r)^2, \quad (11')$$

$$|(P,P;0)_2/(P,N;0)|$$
$$= \tfrac{3}{2}[(\epsilon_1+\nu_1)^{-1}{}_{r=0}]_{Av}|(P,N;0)|. \quad (12)$$

The factor $[(\epsilon_1+\nu_1)^{-1}]_{Av}$ is an average value of $(\epsilon_1+\nu_1)^{-1}$ and is therefore of order of magnitude of the value of this quantity at the maximum of $p^2\pi^2|K(\mathbf{p}\boldsymbol{\pi})|^2$. If the breadth of this maximum is very small compared to its "distance" from the origin, then $[(\epsilon_1+\nu_1)^{-1}]_{Av}$ is practically independent of r. It has been found that such a sharp maximum leads to a very long range for the single exchange term and is therefore an unsatisfactory assumption. However, we have seen by some simple calculations that even with a broad maximum, $[(\epsilon_1+\nu_2)^{-1}]_{Av}$ is a very slowly varying function of r and is, in fact, constant to within about 20 percent.

Since (11′) is practically proportional to the square of $(P, N; r)$, the double exchange term has a somewhat smaller range than that of the proton-neutron interaction, a result which is at least not seriously in disagreement with present ideas. On the other hand, the depth ratio (12) ought, from the experimental results of proton-proton scattering, to be greater than one, whereas it cannot be made larger than $\frac{3}{4}r_0|(P,N;0)| < \frac{1}{4}$. We shall see that the inclusion of the single exchange term cannot remove this difficulty. The single exchange term is more complicated than (11); for example, the factor $|K(\mathbf{p}_1\boldsymbol{\pi}_1)|^2|K(\mathbf{p}_2\boldsymbol{\pi}_2)|^2$ is replaced by $K^*(\mathbf{p}_1\boldsymbol{\pi}_2)K^*(\mathbf{p}_2\boldsymbol{\pi}_1)K(\mathbf{p}_1\boldsymbol{\pi}_1)K(\mathbf{p}_2\boldsymbol{\pi}_2)$. With this term, one meets a further difficulty, for here the elimination, by (2′), of the long wavelengths from the kernel K necessarily leads to long range forces, $\sim(25)^{-1}$, and the artifice of factorization introduced in (7) does not help.

The above results show that the satisfactory description of β-decay and heavy particle interactions imposes conflicting demands upon K. The conflicts appear only when one tries to include the like-particle interaction in the description, or the proton-neutron interaction in second order, and then takes two forms: Some of the interaction terms have poorly defined ranges, and the magnitude of the like-particle interactions are too small. These conclusions are in part based upon calculations made with the two kernels (4) and (7), and, so far as the magnitudes are concerned, the discrepancy is only about a factor of four. While it is therefore possible that some kernel not investigated would yield satisfactory results, we do not think that this is so, for one would expect[4] the second-order interactions to be smaller than the first by a factor of the order of $m/Mr_0 \simeq 1/13$. With $r_0 \simeq (137)^{-1}$, we have in fact been unable to find a K which gives for $|(P,P;0)_2| + |(P,P;0)_1|$ more than $\frac{1}{4}|(P,N;0)|$. As has been frequently pointed out, the experimental facts of nuclear stability suggest that like- and unlike-particle interactions, if they are to be understood at all upon this basis, should be obtained in the same order.[5]

The writer desires to express his appreciation to Professor F. Bloch, Professor J. R. Oppenheimer and Dr. R. Serber for their generous interest and valued advice.

[5] Gamow and Teller, Phys. Rev. **51**, 289 (1937).

The Signs of the Nuclear Magnetic Moments of Li^7, Rb^{85}, Rb^{87} and Cs^{133}*

S. MILLMAN** AND J. R. ZACHARIAS
Columbia University, New York, N. Y.

(Received April 22, 1937)

The atomic beam method of nonadiabatic transitions has been applied to the determination of the signs of the nuclear magnetic moments of Li^7, Rb^{85}, Rb^{87} and Cs^{133}. The experiments show that all of these signs are positive and therefore agree with results already known from h.f.s. determinations.

THE atomic beam method of nonadiabatic transitions as developed in this laboratory[1-3] has already been used to determine the signs of the nuclear magnetic moments of the proton, the deuteron, Na^{23} and K^{39}. We wish to report the further application of this method to determine the signs for Li^7, Rb^{85}, Rb^{87} and Cs^{133}.

METHOD

The angular momentum of an atom in a $^2S_{1/2}$ state with nuclear spin I can be characterized in a weak magnetic field by a total quantum number F with values $I+1/2$ and $I-1/2$, and a magnetic quantum number, m, which is the projection of F along the magnetic field direction. If the nuclear magnetic moment is positive, atoms in any of the $2I$ states having an F value of $I-1/2$ have, in strong magnetic field, a positive atomic moment; whereas of all the atoms with $F=I+1/2$, the fraction $(2I+1)/(2I+2)$ have negative atomic moment in strong field and $1/(2I+2)$ have positive moment. On the other hand if the nuclear moment is negative the situation is reversed and the atoms with $F=I-1/2$ have negative atomic moment in strong field. This provides the criterion for determining the sign of the nuclear moment.

The magnetic moment of an atom of any m value except $\pm(I+1/2)$ is a function of the magnetic field, and if $I>1/2$ there are always some states that have zero atomic moment for a definite value of the field. An atom in such a state is not deflected by the inhomogeneous field and a "zero moment peak" is produced in a curve which exhibits the variation of beam intensity with field at the position of zero deflection. With an apparatus of sufficient resolving power the intensity of this peak is made up of atoms of only two states, having the same m but different F. To separate one of these states from the other the field is set at a value sufficiently removed from the peak value to produce a split Stern-Gerlach pattern. A selector slit is then inserted to let atoms of one of these states through, and to obstruct the passage of the others. The selected atoms in passing through a nonadiabatic field can make transitions to states of different m value, but must retain their F quantum number. Therefore if an $I-1/2$ state is selected, transitions can take place only to states that have the same sign of atomic moment in strong field; whereas if an $I+1/2$ state is selected, transitions can take place to $2I$ states of the same sign and to one of the opposite sign. A subsequent strong field analysis enables one to tell whether the selected state has $F=I-1/2$ or $I+1/2$ and therefore to decide the sign of the nuclear moment.

APPARATUS

A schematic diagram of the apparatus is shown in Fig. 1 in which only the longitudinal dimensions are drawn to scale. The first field (75 cm long) is of the usual[4] two-wire type with the collimator slit in the center. The water flow in the wires (copper tubing 4.76 mm o.d.) is sufficient to allow a current of 1400 amperes without undue temperature rise. The transition field was taken from the apparatus used by Kellogg, Rabi and Zacharias[2] in their work on the proton and the deuteron. The second field is of the design used by Torrey.[3] It is placed in the apparatus so that the gradient of its field is in

* Reported at Atlantic City meeting of the American Physical Society, December, 1936.
** Barnard Fellow, Columbia University, 1936–37.
[1] Rabi, Phys. Rev. **49**, 324 (1936).
[2] Kellogg, Rabi and Zacharias, Phys. Rev. **50**, 472 (1936).
[3] Torrey, Phys. Rev. **51**, 501 (1937).
[4] Rabi, Kellogg and Zacharias, Phys. Rev. **46**, 157 (1934).

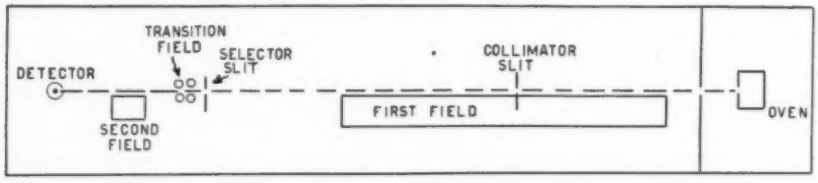

FIG. 1. Schematic diagram of apparatus.

the same direction as that of the first field. Thus atoms that have moment of the same sign in the two fields are deflected in the same direction. Refocusing of the beam is therefore obtained only if the moments of the atoms have different signs in the two fields. The selector slit is mounted on a ground joint and can be moved easily across the beam path. The total beam length is 155 cm.

PROCEDURE

The beam is detected and the current in the first field is varied until a "zero moment peak" is located. As has already been stated the intensity at the position of zero deflection is then made up of contributions from the two "zero moment" states only. We shall designate by the letter A the state that has a positive atomic moment for fields $H<H_0$ and a negative moment for $H>H_0$. The state that has a negative moment for $H<H_0$ we shall call B. It is necessary to separate the two states and to assign the correct F values to them. The current in the first field is now set at a value either higher or lower (8 percent to 25 percent) than H_0. A Stern-Gerlach pattern then shows two peaks about 0.2 mm apart. The tungsten filament detector is set on the positive moment peak (low number readings in our telemicroscope) and the selector slit is then inserted. With no current in the analyzing magnet the presence of the transition field is not noticeable. The current in the second field is now turned on and the detector is moved to analyze the resulting pattern. The gross features of the pattern depend on the F value of the state selected: If $F=I-1/2$ the pattern has only one peak and does not in any way depend on the magnitude of the transition field, since the strong analyzing field cannot differentiate between states of like sign even though the m values are different. On the other hand if $F=I+1/2$, the pattern has two peaks, the relative sizes of which depend on the magnitude of the transition field since transitions to both positive and negative states are possible and the transition probabilities depend on the field. This procedure is then repeated with the detector set on the negative moment peak of the Stern-Gerlach pattern.

RESULTS

Li^7

Li^7 has a nuclear spin of 3/2 and its zero moment peak occurs at 143 gauss.[5] Curve B of Fig. 2 shows the pattern obtained with the selector slit set to pass atoms with positive moment. As the magnitude of the first field is 176 gauss the curve represents a B state. Despite the presence of both the transition field and the analyzing field the pattern has only one peak. Furthermore, this situation is not altered by variations of the transition field, nor does the intensity of the peak vary. The F value of the B state is therefore $I-1/2$ and Li^7 has positive nuclear moment. This finding is corroborated by the data of curve A of Fig. 2 which shows the A state with two peaks.

The analyzed beam of curve B is found farther from the center than the selected beam because the second field produces deflection in the same direction as the first. Similarly, curve A shows one peak partially refocused and the other deflected away from the center position.

Rb^{85}

The nuclear spin of Rb^{85} is 5/2 and its two zero moment peaks[6] occur at 364 gauss and 728 gauss, respectively. The first field is set at 446 gauss and the selected beam on the positive moment side is a B state. Curve B of Fig. 3 shows

[5] Fox and Rabi, Phys. Rev. **48**, 746 (1935).
[6] Millman and Fox, Phys. Rev. **50**, 220 (1936).

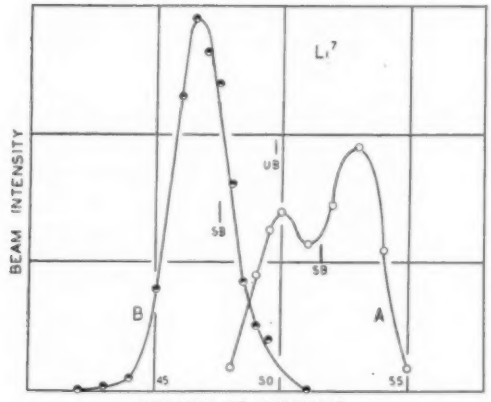

FIG. 2

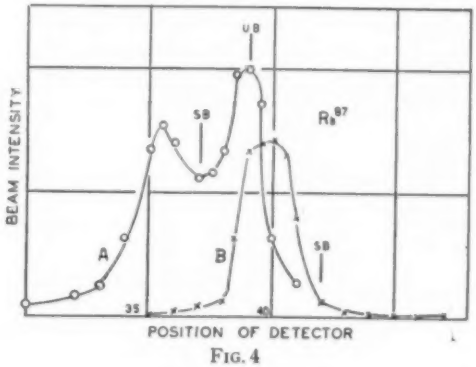

FIG. 4

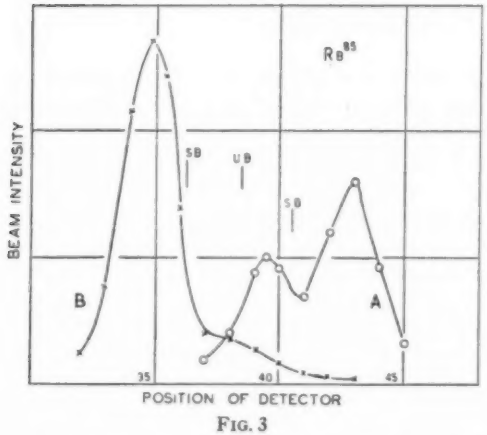

FIG. 3

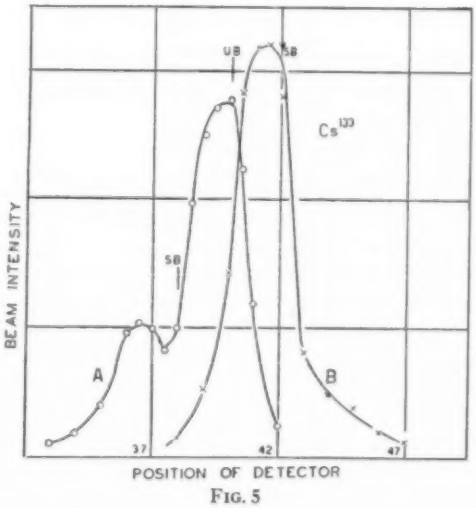

FIG. 5

FIGS. 2, 3, 4 AND 5. Second field analysis of selected beams. *UB* marks center of original undeflected beam. *SB* marks center of selected beam before second field is turned on. Position of detector read on telemicroscope; calibration—22 div. = 1 mm.

only one component for this B state indicating an F value of $I-1/2$ and a positive nuclear moment. The small unresolved peak at position 39 of the detector is due to contamination by some atoms of the A state of the second zero moment peak. Curve A of Fig. 3 shows the pattern for the A state of the first zero moment peak. The presence of two components indicates that the F value is $I+1/2$ and verifies the previous conclusion that the nuclear moment of Rb^{85} is positive.

Rb^{87}

Rb^{87} has a spin of 3/2 and its zero moment peak[6] occurs at 1230 gauss. Curve A of Fig. 4 shows the pattern obtained when positive moment atoms are selected. Due to the high current required for the zero moment peak it is more convenient to set the first field at a value less than H_0. The selected state is therefore an A state. The presence of two components indicates that its F value is $I+1/2$ and that the nuclear moment is positive. This is verified by the data of curve B of Fig. 4 for the selected B state.

Cs^{133}

Cs with nuclear spin of 7/2 has three zero moment peaks[7] at 825 gauss,[6] 1650 gauss and 2475 gauss, respectively. The first field is set at 655 gauss for the purpose of selecting the zero

[7] Cohen, Phys. Rev. **46**, 713 (1934).

moment states of the first peak. Curve *A* of Fig. 5 represents an *A* state and proves that the nuclear moment is positive. This is verified by the data of curve *B* of Fig. 5 for the selected *B* state.

The foregoing results are in agreement with the findings of the workers using the method of hyperfine structure.[8–10]

[8] Granath, Phys. Rev. **42**, 44 (1932).
[9] Kopfermann, Zeits. f. Physik **83**, 417 (1933).
[10] Granath and Stranathan, Phys. Rev. **48**, 726 (1935).

JUNE 15, 1937 PHYSICAL REVIEW VOLUME 51

The Radioactive Isotope of Rubidium

A. HEMMENDINGER AND W. R. SMYTHE
California Institute of Technology, Pasadena, California
(Received April 19, 1937)

By means of a high intensity mass spectrometer we have separated the isotopes of rubidium. Measurements of the radioactivity of the isotopic samples indicate that Rb^{87} is radioactive and that there is no other isotope with an appreciable activity compared to Rb^{87}.

INTRODUCTION

THE history of the radioactivity problem of rubidium is substantially the same as that of potassium, except that there is no record of an attempt to separate the isotopes of rubidium. The early work on the radioactivity of rubidium is recorded by St. Meyer and Schweidler,[1] and more recent data are collected in a paper by Klemperer.[2] There is some evidence that the beta-particles may lie in two bands. The known isotopes are at mass numbers 85 and 87. The best measurement of the abundance ratio is that of Brewer,[3] which gives $Rb^{85}/Rb^{87}=2.59$. Measurements of Nier[4] place an upper limit of the ratio Rb^{85}/Rb^{86} at 1/13,000 and of Rb^{85}/Rb^{88} at 1/22,000.

Klemperer[2] sets forth theoretical arguments for supposing the activity of rubidium to be due to a rare isotope at 86. v. Hevesy[5] also predicts a radioactive isotope at this point. Sitte[6] argues in favor of 87, as does Nier.[4] Quite recently Hahn, Strassmann and Walling,[7] and Mattauch,[8] have shown that the active isotope is Rb^{87}. Hahn and his collaborators separated the strontium from an old mineral rich in rubidium salts and found the strontium to be 99.7 percent pure Sr^{87}. Mattauch checked their measurements of atomic weight with mass spectroscopic data. This evidence is quite conclusive, but since our own measurements were very nearly completed when papers (7) and (8) appeared, we feel justified in presenting them here.

Using the same technique as in the determination of the radioactivity of potassium,[9] we have separated the isotopes of rubidium and measured their activities.

APPARATUS

The Rb^+ emitter was prepared in the same way as the K^+ emitter. For a single charge we used 150 g $Fe(NO_3)_3 \cdot 9H_2O$, 1.5 g RbCl and 1 g Al_2O_3. The fractional difference in atomic weight between the rubidium isotopes is less than half that between the potassium isotopes. To obtain equally accurate results with the former it is necessary therefore to improve the resolving power. Since the entire width of the peaks is due to lack of parallelism of the beam from the source due to the thermal velocity of the ions at right angles to the direction of acceleration, this can be accomplished in two ways, both of which were used. First, the magnet winding was increased from 890 to 2090 turns so that a current of 5 amperes saturated the magnetic circuit with a field of 4200

[1] St. Meyer and E. Schweidler, *Radioactivität* (B. G. Teubner, Berlin, 1927).
[2] O. Klemperer, Proc. Roy. Soc. **A148**, 638 (1935).
[3] A. K. Brewer, Phys. Rev. **49**, 867 (1936).
[4] A. O. Nier, Phys. Rev. **50**, 1041 (1936).
[5] G. v. Hevesy, Naturwiss. **23**, 583 (1935).
[6] K. Sitte, Zeits. f. Physik **96**, 593 (1935).
[7] O. Hahn, F. Strassmann and E. Walling, Naturwiss. **25**, 189 (1937).
[8] J. Mattauch, Naturwiss. **25**, 189 (1937).
[9] W. R. Smythe and A. Hemmendinger, Phys. Rev. **51**, 178 (1937).

gauss between the polepieces, which permitted an accelerating voltage of 4000 for Rb^+ ions. Second, the source was run as cold as possible, making the collecting currents smaller than used for potassium. Since Rb emits fifteen times as many beta-particles as potassium, the 2 mg samples collected in this way in a two-day run were adequate. The resolution maintained throughout is shown in Fig. 1. In this region the dispersion is 2.6 mm per mass unit. All isotopic samples were collected using a 2 mm focal plane slit.

Since the beta-particles from Rb have lower energies than those from potassium we replaced the 0.0245 mm aluminum cylinder of the Geiger-Müller counter by a cylinder of 0.013 mm aluminum foil. The counter had a steady background of approximately 1.5 per minute.

Measurements

In a preliminary set of measurements samples were collected at masses 84, 86, 87, 88, and 90. The first two samples were collected with very broad peaks before the full possibilities of running the source cold were realized and therefore could not be accurately compared with the last three which were collected at excellent resolving power. Before the first two could be repeated it was necessary to rebuild the counter because of an accident thus changing the relative positions of counter and collector and invalidating comparisons with subsequent measurements, except for the sample at 90, which showed no activity. These measurements all indicated, however, that the active isotope was near 87. To verify this we took the data shown in Table I. Samples 86 and 88 were collected with the resolution shown in Fig. 1. The 87 sample was collected on top of the 86 without opening the apparatus, by running the same source at a higher temperature, since it is evident that good resolving power is unnecessary for this sample.

TABLE I. *Beta-particle counts from separated isotopes of Rb.*

Collector Deposit	Counting Ratio R	Activity A	Specific Activity $a \times 10^4$
No deposit	1.10±0.05		
86, $Q=140$	1.22±0.06	0.12	8.7±5.7
87, $Q=196$	1.60±0.08	0.38	19.4±5.1
No deposit	0.96±0.04		
88, $Q=180$	1.22±0.06	0.26	14.4±3.9

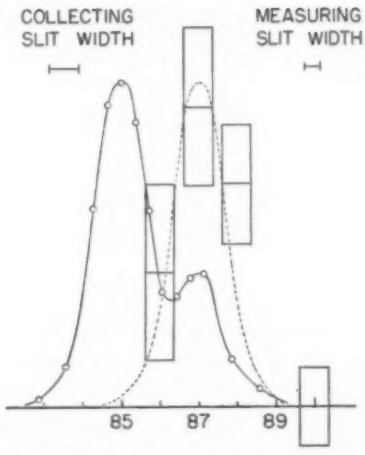

FIG. 1. The solid curve, giving the collecting current plotted against mass, is measured with a 2 mm slit and shows the resolution of the Rb isotopes. The long sides of the rectangles are the two edges of the collecting slit. The ordinates at the centers of the rectangles are proportional to the specific activities, and the lengths of the rectangles are twice the probable errors.

The size, Q, of each sample is given in microampere hours of collecting current measured at mass 85. The quotient, $A/Q=a$, where A is the activity defined in the paper on potassium,[9] is then a measure of the specific activity of a given isotope.

The specific activities are plotted in Fig. 1, showing the width and position of the collecting slit, as well as the probable error due to fluctuations in the counting data. The point from the preliminary measurements showing zero activity at 90 is included.

These measurements show that Rb^{87} is radioactive and that no other isotope of Rb has an appreciable activity compared to Rb^{87}.

We wish to acknowledge the assistance in the laboratory of Mr. Stephen Jennings.

The Effect of Temperature on the Intensity of Reflection of X-Rays from Zinc Crystals

E. O. WOLLAN*
Wayman Crow Hall of Physics, Washington University, St. Louis, Missouri

AND

G. G. HARVEY
George Eastman Laboratory of Physics, Massachusetts Institute of Technology, Cambridge, Massachusetts

(Received May 4, 1937)

Measurements have been made of the intensity of x-rays reflected from powdered zinc crystals at room temperature and at the temperature of liquid air. The atomic structure factors for the zinc atom at these temperatures are found to depend on the orientation of the particular plane from which the reflection of the x-rays takes place. Planes whose normals make small angles ψ with the c axis of the crystal give abnormally low values of the structure factor, while planes for which ψ is large give high values. From the measurements at the two temperatures the temperature factor for the various planes has been determined and with the aid of this factor the structure factor for the atom at rest has been calculated. The structure factor data for the atom at rest do not lie on a smooth curve as one might expect, but are also found to depend on the value of ψ. This indicates that the zinc atoms in the crystal do not possess spherical symmetry but are drawn out in the direction of the c axis. The average structure factor curve obtained experimentally has, however, been found to be in satisfactory agreement with a similar curve obtained from the theoretical charge distribution in the atom. The amplitude of thermal vibration of the atoms along various directions in the crystal has been determined. A comparison is made of the root mean square displacement as determined from the x-ray measurements with the average value obtained from specific heat data and a good agreement is found.

THE effect of temperature on the intensity of x-rays reflected from crystals has been studied by a number of investigators for the case of crystals of cubic symmetry. The theory for this case has been worked out by Debye and Waller and it has been found that the theory is in accord with experiment for temperatures up to about 400°Abs., above which the assumptions on which the theory is based are not valid.

In this paper a report is given of measurements of the intensity of reflection of x-rays from zinc crystals, how this depends on the temperature, and the conclusions which can be drawn from these measurements about the nature of the crystal and the atoms within the crystal.

In the case of zinc the Debye-Waller theory does not apply, since this theory was worked out for atoms of cubic symmetry. If zinc were an ordinary close packed hexagonal crystal, i.e., one having an axial ratio of 1.63, it is not unlikely that the Debye-Waller theory would have given an approximate explanation of the effect of temperature on the intensity of the reflected x-rays. However, zinc like cadmium differs considerably from the perfect close packed hexagonal structure in that the axial ratio is about 1.86 in place of the above-mentioned value. This value of the axial ratio means that the atoms are about 12 percent farther apart along the c axis than along a direction at right angles to this axis. This anisotropy of the crystal might lead one to expect that the amplitude of thermal vibration of the atoms is greater along the c axis than at right angles to it. One might also suppose that the atom itself is distorted, having a greater concentration of the outer electrons in one direction. If either or both of these effects are present, the measured values of the intensity of reflection of x-rays will be a function of the orientation with respect to the c axis of the particular plane which is reflecting the radiation, and in both cases the effect will be to decrease the intensity of reflection from planes whose normal makes a small angle with the c axis and increase the intensity for planes whose normal makes a large angle with this axis. Fortunately, however, any asymmetry of the atom will be noticed at small angles of scattering, while the effect of thermal vibration becomes larger as the angle of scattering increases.

A theoretical investigation of the effect of the anisotropy of the thermal vibrations on the intensity of reflection in zinc crystals has been

* This author was aided in part by a grant from the Rockefeller Foundation to Washington University for research in science.

made by Zener.[1] Measurements of the intensity of reflection of x-rays by zinc crystals at room temperature have already been made by Brindley,[2] while Jauncey and Bruce[3] have made measurements of the diffuse scattering of x-rays by zinc crystals. Both these experiments indicate that there is a considerable difference in the intensity of reflection from planes variously oriented with respect to the principal axis of the crystal.

However, only by measurements of the intensity of reflection at two or more temperatures can a quantitative relation between the intensity of reflection and the orientation of the reflecting planes be established, and it is primarily with this purpose in mind that this investigation has been carried out.

Experimental Procedure

In this work the photographic method of recording the intensities has been used. With this method the powdered crystal sample to be studied can be in the form of a very thin cylinder or in the form of a plate. The method of the cylinder has been used successfully by a number of investigators, but when the material to be studied is of large atomic weight the corrections for absorption become rather uncertain. The method of reflecting the x-rays from a flat plate of the powder has been used by Brindley and Spiers[4] and by Brentano[5] and has been discussed by them. It has the advantage of permitting a simple calculation of the absorption correction to be made and also on account of the Bragg focusing effect sharp lines are obtained with a wide incident beam and hence the exposure time is much reduced. This latter method was used in this work.

The sample of finely powdered zinc was prepared by subliming the zinc in a vacuum and collecting the condensed vapor. This zinc powder was held in a circular copper disk in which a depression about 1.5 cm in diameter by 1.5 mm in depth was turned out. This disk was held accurately in the center of the camera in contact with the inside cylinder of a metal Dewar flask which constituted the top of the camera. The inside of the Dewar was made of a very thin walled brass tube on the bottom of which was silver soldered a copper rod, half of which was accurately milled away on the lower end to form the sample holder. The inside was drilled out to allow the liquid air to come to about 1/8 inch from the back of the sample. The temperature of the sample was found to come immeasurably close to the temperature of liquid air. The flat surface of the sample holder allowed an x-ray mark to be made along a narrow strip on the edge of the film from which the angular setting of the sample with respect to the primary beam could be determined. This method gave values which agreed very well with the readings of a scale marked on the outside of the camera. The camera was evacuated with an ordinary fore pump and one filling of liquid air usually sufficed for each picture.

Measurements

From the microphotometer traces of the films the integrated intensity of reflections from the various planes was determined with the aid of intensity *vs.* blackening calibration marks on each film. A simple method of converting blackening into integrated intensities was used, and this will be described elsewhere. From the measured intensities one can determine the atomic structure factor with the aid of the well-known theory of reflection of x-rays from a flat plate of powder. In the notation used by Brindley the intensity I of the reflected x-rays is given by the expression

$$I = (\text{constant}) p S^2 f_T^2 \phi(\theta) A, \qquad (1)$$

where f_T is the atomic structure factor at the temperature T, S is the crystal structure factor which in the case of zinc is equal to 1, 2 and $\sqrt{3}$ for different reflecting planes, p is the multiplicity factor, $\phi(\theta) = (1+\cos^2 2\theta)/(\sin\theta \sin 2\theta)$ and $A = \sin(2\theta-\alpha)/(\sin(2\theta-\alpha)+\sin\alpha)$, where α is the angle between the incident beam and the plane face of the reflecting powder. This factor A takes account of the absorption of the x-rays in the powder sample. Since several values of α are

[1] C. Zener, Phys. Rev. **49**, 122 (1936).
[2] G. W. Brindley, Phil. Mag. **21**, 790 (1936).
[3] G. E. M. Jauncey and W. A. Bruce, Phys. Rev. **50**, 408 and 413 (1936).
[4] G. W. Brindley and F. W. Spiers, Proc. Phys. Soc. **46**, 841 (1934).
[5] J. C. M. Brentano, Proc. Phys. Soc. **47**, 932 (1935).

TABLE I. *Relative and absolute values of the structure factor at 295° Abs. and 85° Abs.*

				Room Temperature			Liquid-Air Temperature		
					rel.	Abs.		rel.	Abs.
Line	$\sin\theta/\lambda$	ψ^0	$pS^2\phi(\theta)$	I/A	f_{295}	f_{295}	I/A	f_{85}	f_{85}
0002	0.203	0	71.0	244	1.85	19.2	246	1.86	20.2
$10\bar{1}0$	0.217	90	45.3	223	2.22	23.0	218	2.20	22.8
$10\bar{1}1$	0.240	65.0	216.2	735	1.84	19.1	836	1.96	20.4
$10\bar{1}2$	0.297	47.0	43.0	111	1.61	16.6	119	1.67	17.4
$10\bar{1}3$	0.373	35.5	73.9	107	1.20	12.4			
				210	1.31	13.6	258	1.45	15.1
$11\bar{2}0$	0.376	90	48.3	103	1.46	15.1			
0004	0.405	0	13.8	13.7	1.00	10.3	22.0	1.26	13.1
$11\bar{2}2$	0.427	61.7	74.7	100	1.16	12.0	124	1.29	13.4
$20\bar{2}1$	0.446	76.9	52.5	78.2	1.22	12.6	92.0	1.32	13.7
$20\bar{2}3$	0.530	55.0	52.1	33.0	0.795	8.2	49.5	0.975	10.1
$10\bar{1}5$	0.551	23.2	56.6						
				52.3	0.630	6.5	96.0	0.850	8.8
$11\bar{2}4$	0.553	42.8	76.4						
$21\bar{3}1$	0.583	80.0	141.9	81.1	0.756	7.8	114	0.896	9.3
0006	0.608	0	20.4						
				30.0	0.608	6.3	49.0	0.765	8.0
$21\bar{3}2$	0.609	70.6	63.6						

used for each reflection it is convenient to tabulate the quantities I/A as representing the measured intensities. The experimental values of I/A are tabulated in the fifth column of Table I for the measurements at room temperature and in the eighth column of this table for the measurements at the temperature of liquid air. From these relative values of I/A relative values of f_T can be calculated with the aid of Eq. (1). In order that such values of the structure factor have any significance they must be put on an absolute basis. Since a direct evaluation of the absolute values is a difficult problem in itself it has become customary to accomplish the task by comparing the reflection from one or more planes of the substance under consideration with the reflections from some convenient planes of a crystal for which absolute measurements have already been made. This has been done with crystals of KCl and aluminum and Brindley has used these for standardizing the reflections from zinc. We have not repeated the work of Brindley in this respect but have accepted his absolute value for the reflection from the $11\bar{2}2$ plane as standard. He gives the experimental value of the structure factor for this plane and for copper $K\alpha$ radiation as 12.0. The absolute structure factors at room temperature which we obtain on the basis of this standard value are given in the sixth column of Table I.

In the case of some reflections two lines are unresolved and only the sum of the intensities is measured. In this case an average value of the structure factor $\bar{f}_T$ has been calculated. If the suffixes 1 and 2 indicate the two reflections, then the combined intensity is given by

$$I/A = \text{constant}\,[p_1 S_1^2 \phi_1(\theta) f_1^2 + p_2 S_2^2 \phi_2(\theta) f_2^2], \quad (2)$$

$$= \text{constant}\,[p_1 S_1^2 \phi_1(\theta) + p_2 S_2^2 \phi_2(\theta)]\bar{f}_T^2. \quad (3)$$

As is seen in what follows in the case of a crystal like zinc, it is generally not true that $f_1 = f_2 = \bar{f}_T$.

The relative values of the structure factor at liquid-air temperature are calculated in a similar manner as for room temperature from the measured values of I/A using Eq. (1). In order that these values can be compared with the absolute values at room temperature they must be standardized in terms of the room temperature data. This was accomplished in the following way. A sample containing a mixture of zinc powder and powdered magnesium oxide was used. Magnesium oxide has the advantage that it is readily obtainable in the form of a fine powder and also, due to its very high characteristic temperature, the effect of temperature on the intensity of reflection is very small. Any error which would be made in the calculation of its temperature factor from the values of the characteristic temperature are negligible. With this mixed sample, photographs were taken at room temperature and at the temperature of liquid air. The intensities of reflection for the 220 line of MgO were compared with those for the $10\bar{1}3$ and $11\bar{2}0$ pair for zinc. The result of this comparison gave the ratio of the intensity of the $10\bar{1}3$ and $11\bar{2}0$ pair at liquid-air temperature to the same pair at room temperature as 258/210 as indicated by the relative values of I/A for these lines in Table I. On the basis of this ratio of the intensities one obtains the following relation for the structure factor at the two temperatures.

$$[f(10\bar{1}3+11\bar{2}0)]_{T=85°K} = 1.11[f(10\bar{1}3+11\bar{2}0)]_{T=295°K}$$

and it is on the basis of this standardization that the absolute values of the structure factors for the temperature of liquid air are given in the last column in Table I.

Determination of the Temperature Factor

The atomic structure factor f_T which represents the amplitude of scattering by an atom in a crystal at temperature T is related to the structure factor f_0 for the atom at rest by the equation

$$f_T = f_0 e^{-M}, \tag{4}$$

where e^{-M} is commonly referred to as the Debye-Waller temperature factor. An expression for the exponent M was derived by Debye and Waller for the case of a cubic crystal of atoms of one kind and is given by the relation

$$M = \frac{6h^2T}{mk\Theta^2}\left(\phi(x)+\frac{x}{4}\right)\frac{\sin^2\theta}{\lambda^2}, \tag{5}$$

where m is the mass of the atom, Θ is the characteristic temperature of the crystal, $x=\Theta/T$ and $\phi(x)$ is the function which appears in the Debye theory of specific heats. The factor $(\phi(x)+x/4)$ which is referred to as the quantization factor does not differ much from unity when the temperature is larger than the characteristic temperature of the crystal. One sees then that for cubic crystals the exponent in the temperature factor is very nearly proportional to the temperature and to $\sin^2\theta/\lambda^2$.

Zener has investigated theoretically the effect of temperature on the intensity of reflection of x-rays from anisotropic crystals and gives an equation of the following form for the case of crystals like zinc or cadmium.

$$M = (a\cos^2\psi + b\sin^2\psi)\left(\phi(x)+\frac{x}{4}\right)\frac{\sin^2\theta}{\lambda^2}, \tag{6}$$

where a and b are constants and ψ is the angle which the normal to the reflecting plane makes with the c axis. If, as he indicated, a and b are linear functions of the temperature, we can factor out T and the equation can be written in the form

$$M = AT(B\cos^2\psi+1)Q(\sin^2\theta/\lambda^2), \tag{7}$$

where A and B are now constants independent of the temperature and Q has been written for the quantization factor which is, however, also a function of temperature, although its total effect is small.[6]

Since the intensity of reflection of x-rays is proportional to the square of the structure factor, we have from Eq. (4) that

$$I_1/I_2 = e^{-2(M_1-M_2)}, \tag{8}$$

where the subscripts 1 and 2 refer to the intensities and the temperature factors at two different temperatures. Hence we have

$$\log(I_2/I_1) = 2(M_1-M_2) \tag{9}$$

and substituting from Eq. (7) we can write

$$\frac{\log(I_2/I_1)}{(\sin\theta/\lambda)^2} = 2A(T_1Q_1-T_2Q_2)(B\cos^2\psi+1)$$
$$= 2AB(T_1Q_1-T_2Q_2)\cos^2\psi + 2A(T_1Q_1-T_2Q_2). \tag{10}$$

Hence we see that a plot of the quantity on the left side of this equation against $\cos^2\psi$ will make it possible to evaluate the constants A and B from the slope and the intercept of the curve if it turns out to be a straight line.

In Table II, column 5 are given the values of I_2/I_1 for the ratio of the intensities at the temperature of liquid air and at room temperature for a number of suitable reflecting planes, and with the aid of the other data in Table II the curve of Fig. 1 is obtained. Unfortunately one is restricted in the range of values of $\cos^2\psi$ by the fact that some of the most desirable values occur for lines which cannot be resolved. The point on the curve corresponding to the largest value of $\cos^2\psi$ is taken for one of these pairs but in this case the angle ψ for both lines is small. There is, however, a considerable difference in the values of $\cos^2\psi$ for the two lines constituting this pair but it is not believed that a very large uncertainty in the slope of the curve is introduced by using the intensity ratio for these lines at an average value of $\cos^2\psi$. The 0004 line was not included in this graph because it is a weak reflection and the accuracy of its measurement was not considered as good as for the other lines.

[6] It is likely that Q is also a function of the angle ψ, but since its total effect is small this refinement will be disregarded.

The slope of this curve has been taken equal to 1.57 and the intercept has been taken as 0.87. Room temperature was equal to 295° Abs. and the temperature of liquid air was 85° Abs. Taking the value of the characteristic temperature as determined by specific heat data $\Theta=235$ as representing an average value for the crystal, one finds that the quantization factor is given by $Q=1.018$ at 295° Abs. and 1.20 at 85° Abs. Using these data for evaluating the constants A and B we obtain the following values, $A=2.2$ and $B=1.8$. Substituting these values into Eq. (7), we obtain the experimentally determined temperature factor as

$$M=2.2\times10^{-3}T(1.8\cos^2\psi+1)Q(\sin^2\theta/\lambda^2). \quad (11)$$

The Atomic Structure Factor for the Zinc Atom at Rest

Using the value of M given by Eq. (11), the constants of which have been determined experimentally, we can now calculate the atomic structure factor for the atom at rest by using the relation $f_0=f_T e^{M_T}$. The values of M_T and e^{M_T} for room temperature and for the temperature of liquid air are tabulated in Table III for all the lines measured. For the lines which are not resolved each member of the pair will have its particular temperature factor and it is then necessary to define an average value which can be applied to the average structure factor at the temperature at which it was measured. This has been done in the following way. If we assume that the structure factor for the two lines is the same for the atom at rest, we have, acccording to Eq. (1) that the total intensity of the pair is given by

$$I/A=\text{constant}\quad[P_1e^{-2M_1}+P_2e^{-2M_2}]f_0^2, \quad (12)$$

Table II. *Ratio of intensities I_2/I_1 at 85° Abs. and 295° Abs.*

Line	$\frac{\sin^2\theta}{\lambda^2}$	ψ^0	$\cos^2\psi$	$\frac{I_2}{I_1}$	$\frac{\log(I_2/I_1)}{(\sin\theta/\lambda)^2}$
11$\bar{2}$2	0.182	61.7	0.224	1.24	1.18
20$\bar{2}$1	0.199	76.9	0.052	1.17	0.79
20$\bar{2}$3	0.280	55.0	0.328	1.49	1.42
10$\bar{1}$5	0.305	23.2	0.690	1.82	1.97
11$\bar{2}$4		42.8			
21$\bar{3}$1	0.340	80.0	0.030	1.40	0.99

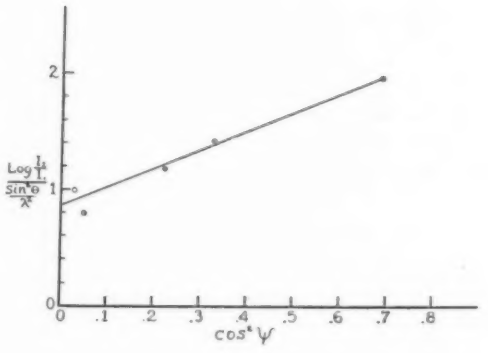

Fig. 1.

where P has been written in place of $pS^2\phi(\theta)$. We can also express this in terms of an average value of M by writing

$$I/A=\text{constant}\ [P_1+P_2]e^{-2M_{Av}}\cdot f_0^2. \quad (13)$$

These equations can now be solved for $e^{M_{Av}}$ and we obtain

$$e^{M_{Av}}=\left[\frac{P_1+P_2}{P_1e^{-2M_1}+P_2e^{-2M_2}}\right]^{\frac{1}{2}}. \quad (14)$$

The average values of the temperature factor which are listed in the table for the unresolved lines have been calculated in this way. A small error is introduced by calculating the averages in this way for lines having a small value of $\sin\theta/\lambda$ since, as we shall see, the structure factor for the atom at rest depends not only on $\sin\theta/\lambda$ but also to some extent on the value of ψ for the particular plane from which the reflection takes place. This will, however, only be appreciable for the first unresolved pair and since these have been resolved at room temperature, no appreciable inaccuracy will be introduced by this method of averaging.

The values of the structure factor for the atom at rest which we have determined by the application of the temperature factor are listed in columns eight and nine of Table III. These values will differ from the true atomic structure factor for the atom at rest by an additive quantity Δf_0 which arises from the fact that the copper $K\alpha$ radiation used in these measurements lies close to and on the long wave-length side of the K critical absorption limit for zinc. This has

the effect of changing the ordinate of the curve and need only be considered when a comparison with the theoretical values is made. For this reason, however, we have listed the values as f_0'.

A comparison of the f_0' values calculated from the room temperature data with those calculated from the measurements at the temperature of liquid air shows a satisfactory agreement, as should be expected. These values are also shown plotted together with the original values in Fig. 2. Since so many points are included in this figure, the average of the two sets of f_0' data have been replotted in Fig. 3. This shows very strikingly the fact that one does not get a single smooth structure factor curve for the atom at rest, as has been heretofore obtained with the isotropic crystals on which previous work has been done. The significance of this will be discussed below.

In order to make a comparison of the values of f_0' which we have obtained experimentally with those obtained from theory, we must take an average value of the experimental points, since the theoretical values are worked out for an isolated atom which lead to values lying on a smooth curve. The structure factors for the zinc atom have not as yet been calculated directly by the Hartree method of self-consistent fields but Brindley[2] has arrived at an f_0 curve for zinc which should be very approximately the same as that which one would obtain by a direct application of the Hartree method. The values which he obtains in this way for $f_0' \equiv f_0 - \Delta f_0$ where we take $\Delta f_0 = 2.2$ are shown in the first row of Table IV, and the corresponding values of f_0' which we have taken as representing a proper average of our experimental values are shown in the second row. The agreement between the theoretical and experimental values is as good as can be expected in view of uncertainties in the theoretical values as well as in the determination of the proper average experimental values.

The Asymmetry of the Zinc Atom

Let us return to a consideration of the atomic structure factors for the zinc atom at rest as plotted in Fig. 3. We have seen that the points do not fall on a single smooth curve but tend to separate as one goes to smaller values of sin θ/λ. Two limiting curves have been drawn in and it is apparent that the points having small values of ψ lie near the lower curve, those having large values of ψ lie near the upper curve, while points for which ψ has intermediate values lie in between. As was indicated in the introduction, this type of bifurcation, which becomes more pronounced toward small angles, is a definite indication that the zinc atom does not possess spherical symmetry.

From the nature of these data one is led to conclude that the electron atmosphere in a zinc atom is distorted so that the atom is more or less spheroidal in shape with the long axis directed along the c axis of the crystal. The rather large separation of the limiting curves at small values of sin θ/λ and the fact that this separation extends approximately to sin $\theta/\lambda = 0.6$ would indicate that several of the outer electrons in zinc are associated with the asymmetry.

The Amplitude of Thermal Vibration of the Zinc Atoms

The exponent M of the temperature factor is related to the mean square amplitude of thermal vibration of the atoms normal to the plane from which the x-rays are reflected by the equation

$$M = 8\pi^2 u_\psi^2 (\sin\theta/\lambda)^2, \qquad (15)$$

where u_ψ is the root mean square displacement of the atom in a direction which makes an angle ψ with the c axis of the crystal. This equation involves no assumption about the nature of the

Table III. *Temperature factor M and the structure factor f_0' for the atom at rest.*

Line	$\frac{\sin^2\theta}{\lambda^2}$	$\cos^2\psi$	M_{220}	$e^{M_{220}}$	M_{33}	$e^{M_{33}}$	f_0' $f_{220}e^{M_{220}}$	$f_{33}e^{M_{33}}$
0002	0.041	1.00	0.078	1.081	0.028	1.028	20.4	20.4
$10\bar{1}0$	0.047	0	0.031	1.031	0.011	1.011	23.6	23.0
$10\bar{1}1$	0.058	0.179	0.049	1.050	0.173	1.017	20.0	20.7
$10\bar{1}2$	0.088	0.466	0.107	1.116	0.038	1.039	18.5	18.1
$10\bar{1}3$	0.139	0.661	0.201	1.222	0.070	1.072	15.2	
				1.170		1.056	15.9	15.9
$11\bar{2}0$	0.141	0	0.092	1.096	0.033	1.034	16.5	
0004	0.164	1.00	0.313	1.368	0.111	1.117	14.1	14.6
$11\bar{2}2$	0.182	0.224	0.169	1.184	0.059	1.061	14.2	14.2
$20\bar{2}1$	0.199	0.052	0.145	1.156	0.052	1.053	14.5	14.4
$20\bar{2}3$	0.281	0.328	0.297	1.345	0.108	1.114	11.0	11.2
$10\bar{1}5$	0.304	0.842	0.503	1.655	0.178	1.195		
				1.55		1.17	10.1	10.3
$11\bar{2}4$	0.306	0.539	0.396	1.486	0.141	1.152		
$21\bar{3}1$	0.340	0.030	0.236	1.266	0.083	1.087	9.9	10.1
0006	0.370	1.00	0.680	1.97	0.240	1.272		
				1.43		1.13	9.0	9.0
$21\bar{3}2$	0.370	0.111	0.294	1.34	0.103	1.109		

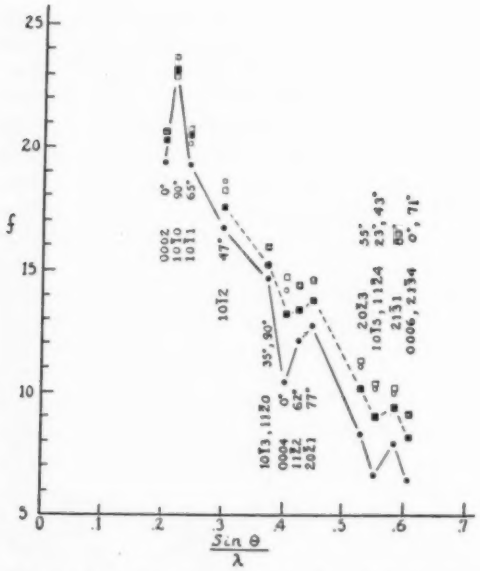

FIG. 2. The solid circles represent values of the structure factor as measured at room temperature, the solid squares represent the values at liquid-air temperature, while the open circles and squares represent the same quantities when respectively reduced to the atom at rest by means of the measured temperature factors. The values of the angles ψ in round numbers and the indices have been written in for each line. For the points at $\sin\theta/\lambda=0.3$ the average value is given for both temperatures, although this line was resolved at room temperature.

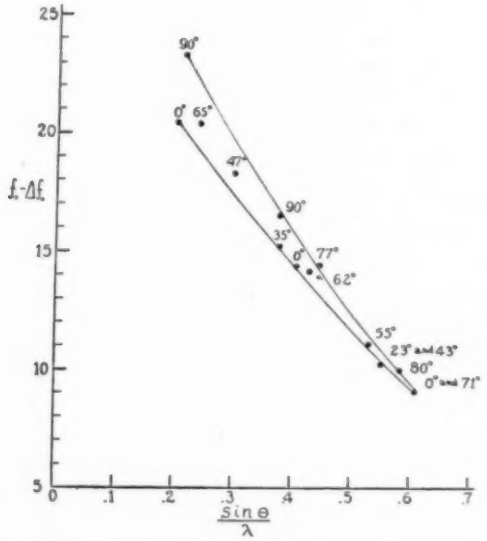

FIG. 3. This curve represents the average structure factor for the atom at rest less the dispersion correction. The two curves have been drawn in to indicate the effect of the asymmetry of the zinc atom.

vibrations. Hence with the aid of this equation and the experimentally determined relation for M, one can solve for u^2_ψ, obtaining

$$u^2_\psi=\frac{M}{8\pi^2(\sin\theta/\lambda)^2}=\frac{2.2\times T\times 10^{-3}}{8\pi^2}\times[1.8\cos^2\psi+1]Q. \quad (16)$$

Using this equation, we can now calculate the root mean square displacement of the atoms at any temperature T and along any direction in the crystal. When $\psi=0$, i.e., for vibrations parallel to the c axis of the crystal, we find at room temperature that $u_{\psi=0}=0.153$A. Likewise in a direction perpendicular to the c axis we find that $u_{\psi=90}=0.0913$A. We can similarly calculate this quantity for intermediate values of ψ and we then obtain the root mean square vibration as a function of the direction in the crystal, as shown graphically in Fig. 4.

THE CHARACTERISTIC TEMPERATURE OF ZINC

We have seen how the x-ray measurements lead to information about the atomic vibrations along the various directions in a zinc crystal. From measurements of the specific heat one also obtains information about the atomic vibrations, but in this case only an average value can be determined. It is of interest to compare the results from these two sources. Let us assume that the Debye-Waller theory gives an average value of the temperature factor for the zinc crystal. We can then combine Eq. (15) and Eq. (5) to get an average value of the mean square vibrations of the atoms in the crystal, and this gives

$$u^2=(3h^2T/4\pi^2mk\Theta^2)\cdot Q. \quad (17)$$

On solving this equation for Θ and substituting in the values of the constants for room tem-

TABLE IV. *Values of $f_0-\Delta f_0$, calculated and experimental.*

$\sin\theta/\lambda$	0.2	0.3	0.4	0.5	0.6
Theoretical Brindley	21.5	17.7	13.3	11.2	9.5
Average experimental	22.0	18.0	14.6	11.8	9.2

perature, we obtain

$$\Theta=\frac{260\times10^{-8}}{u}. \tag{18}$$

The value of Θ which we can calculate from this equation using an average experimental value of u can now be compared with the value of Θ obtained from measurements of the specific heat of zinc. Averaging the root mean square displacements over all values of ψ, one obtains the relation

$$u_{Av}=\frac{u_{\psi=0}+2u_{\psi=90}}{3} \tag{19}$$

and on substituting the numerical values at room temperature into this equation, we obtain $u_{Av}=0.112$A which average value is shown by the solid line in Fig. 4. This value when substituted into Eq. (18) gives us an average value of the characteristic temperature $\Theta_{Av}=232°$ Abs. The commonly accepted value obtained from specific heat measurements is $\Theta=235°$ Abs. and one sees that the agreement is good beyond all expectation.

It is also possible on the basis of Eq. (18) to define two other characteristic temperatures for a zinc crystal corresponding to vibrations along the principal axis and perpendicular to it. If we had a crystal in which the root mean square vibrations had the value $u_{\psi=0}=0.153$A the characteristic temperature of this crystal as determined by Eq. (18) would be $\Theta_{||}=170°$ Abs. and likewise if the value $u_{\psi=90}=0.0913$A were taken as the root mean square displacement, we would obtain a characteristic temperature $\Theta_{\perp}=285°$

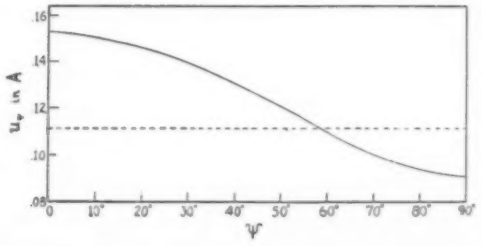

FIG. 4. The curve represents the dependence of thermal vibration on the direction in the crystal at room temperature. The value obtained from specific heat data is represented by the dotted line. This line also represents the measured values of u averaged over all values of ψ as accurately as it can be drawn on the curve.

Abs. By defining two characteristic temperatures for the crystal in this way we have not given the quantity any vector properties, but have merely associated two values with the two directions in the crystal.

One might stop here, but it should be pointed out that Grüneisen and Goens[7] in their measurements of the thermal expansion of zinc also obtain two values of the characteristic temperature along the two directions in the crystal. They give $\Theta_{||}=200°$ Abs. and $\Theta_{\perp}=320°$ Abs., values which are decidedly not in agreement with the results which we obtain, and at present no reason for this apparent discrepancy can be given.

One of us (G. G. H.) is indebted to Professor A. L. Hughes of Washington University for extending to him the use of the facilities of the Wayman Crow Laboratory during the summer of 1936.

[7] E. Grüneisen and E. Goens, Zeits. f. Physik **29**, 141 (1924).

Atomic Structure and Vibrations in Zinc Crystals

IV. Diffuse Scattering of X-Rays at Different Temperatures

G. E. M. JAUNCEY* AND W. A. BRUCE
Wayman Crow Hall of Physics, Washington University, St. Louis, Missouri

(Received May 3, 1937)

Further experiments have shown that in diffuse scattering experiments from single crystals of zinc the surfaces of the artificial crystals must be plane to 10^{-5} cm if the measurements are to be reliable. Methods of annealing and polishing the crystals are described in which this degree of planeness is obtained without producing a Beilby layer. The diffuse scattering was measured for orientations of 3° and 90° at a scattering angle of 30° at temperatures of 100°, 200°, 298°, 370°, 550°K. A method of obtaining the ratio of the mean square displacement parallel to that perpendicular to the principal axis is described. In this method there is no need to know the spectral distribution of the radiation used. Further discussion is deferred to paper VI.

1. INTRODUCTION

THE coherent part of the diffuse scattering of x-rays from a single crystal is given by

$$S_{\text{coh}} = (f^2/Z)(1-e^{-2M}), \qquad (1)$$

where, for the case of a hexagonal crystal like zinc, Zener[1] has derived the formula

$$M = (a\cos^2\psi + b\sin^2\psi)\cdot(\sin^2\tfrac{1}{2}\phi)/\lambda^2, \qquad (2)$$

where the orientation angle ψ is the angle that the line bisecting the angle between the forward direction of the scattered rays and the backward direction of the primary rays makes with the c axis of the specimen, T is the temperature of the crystal, and a/b is the ratio of the mean square thermal atomic displacement along the c axis to that perpendicular to this axis. In previous papers[2, 3] we have described the method of growing single crystals of zinc[4] and the measurement of the diffuse scattering of x-rays from these crystals. Our previous work was done on zinc at room temperature. We have now extended the measurement to crystals at temperatures 100°, 200°, 298°, 370° and 550°K. The melting point of zinc is 693°K. All the measurements were made at scattering angle of 30° and with the primary rays having the spectral distribution given by Fig. 1 of a previous paper.[3]

2. SURFACE IRREGULARITIES

The crystals in this experiment were grown in the way described in our previous work. We found, however, that these crystals which were simply taken from the mold, washed in 20 percent HCl, and mounted in the spectrometer, were giving slightly erratic results. Investigation with a 500 power direct illumination metallographic microscope showed that the crystals had small surface pits and irregularities of the order of 10^{-3} cm. By reference to Fig. 1 it is seen that the scattered ray BC has to pass through a thickness CD of zinc on its way to the ionization chamber. Obviously there will be less scattering from a surface such as that shown in Fig. 1 than from a perfectly flat surface. The effect of departure from a flat surface is very noticeable in the case of zinc, since the absorption coefficient of x-rays in this metal is such that 50 percent of the radiation is absorbed in a length of 0.007 cm. The absorption is one percent in a length of 10^{-5} cm. The crystals were therefore polished until irregularities of greater size than 10^{-5} cm had disappeared. Now it may be that the polishing and the handling of the crystal during polishing produce distortion and strain in the crystal.[5] The crystals were therefore annealed at

* The senior author was aided in part by a grant from the Rockefeller Foundation to Washington University for research in science.

[1] C. Zener, Phys. Rev. **49**, 122 (1936).

[2] G. E. M. Jauncey and W. A. Bruce, Phys. Rev. **50**, 408 (1936).

[3] G. E. M. Jauncey and W. A. Bruce, Phys. Rev. **50**, 413 (1936).

[4] The Horsehead Special zinc used in this work was kindly given to us by the New Jersey Zinc Company.

[5] See W. J. Poppy, Phys. Rev. **46**, 815 (1934); C. A. Cinnamon, Rev. Sci. Inst. **5**, 187 (1934); and C. F. Elam, *Distortions of Metal Crystals*, Chapters II and XIV.

200°C for 80 hours. It was found that some of the low angle (angle between the c axis and the normal to the polished surface) crystals recrystallize.[6] The new grains all formed on the polished surface and were all less than 0.01 cm deep. These recrystallized portions were removed by gentle polishing. In soft metals the polishing process leaves the surface somewhat altered. Electron diffraction pictures seem to indicate that polishing leaves an amorphous layer several hundred angstroms deep.[7] To remove this and any possible thin layer of distorted crystals the surfaces were etched with 4 percent HNO_3 in alcohol. Etching with HCl was found to be unsatisfactory because of pitting. It was found that these polished and annealed crystals gave a distinctly higher value of the scattering than the unpolished and unannealed crystals which we had previously used. In the case of crystals for which $\psi=0°$ the same value of the scattering was found for a polished and annealed surface of a crystal as for a virgin cleaved surface of a second crystal. The cleaved surface was produced at the temperature of liquid air. This cleaved surface was mirror-like and showed no irregularities, thus indicating that there were no macroscopic distortions and no optically mosaic structure. The fact that we found the same value for the two surfaces shows that the above treatment by polishing and annealing produces crystal surfaces which are perfect for the purposes of this investigation.

3. The Ratio of the Mean Square Displacements

In a previous paper[3] we introduced the quantity $(S\rho/\mu_1)_{\text{th}}$ defined by

$$(S\rho/\mu_1)_{\text{th}}=\int(S'\rho/\mu_1)Id\lambda\Big/\int Id\lambda, \qquad (3)$$

and

$$S'=\frac{f^2}{Z}-\frac{f^2}{Z}e^{-2M}+\frac{2K_\phi\mu_1[1-(1/Z)\Sigma E_r^2]}{K_0(\mu_1+\mu_2)(1+\alpha\ \text{vers}\ \phi)^3}, \qquad (4)$$

[6] See E. Schmitt and W. Boas, *Kristallplastizität*, Chapter VI, Section G.

[7] See the papers on the Beilby layer by Finch, Lees, Hopkins and others in the Discussion on the Structure of Metallic Coatings, Films and Surfaces, Trans. Faraday Soc., September 1935. See also F. Kirchner, Nature **129**, 545 (1932) and L. H. Germer, Phys. Rev. **43**, 724 (1933).

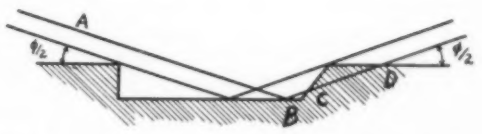

FIG. 1. A highly magnified pit shows the extra thickness of zinc CD an emerging ray BCD must traverse.

where the symbols have previously been defined.[3] There are three terms on the right side of (4). For a given scattering angle ϕ the first and third terms on the right side of (4) are functions of λ alone, whereas the second term, in virtue of (2), is a function of λ, ϕ, ψ and T. When the integration on the right side of (3) is carried out, we obtain

$$(S\rho/\mu_1)_{\text{th}}=G(\psi, T)+H, \qquad (5)$$

where H is a constant for a given spectral distribution and

$$G(\psi, T)=\int\frac{\rho}{\mu}\cdot\frac{f^2}{Z}\cdot e^{-2M}Id\lambda\Big/\int Id\lambda. \qquad (6)$$

For brevity we put $(S\rho/\mu_1)_{\text{th}}=X$. Then, if the scattering at a given angle ϕ is measured at ψ_1 and T_1 and at ψ_2 and T_2, we obtain

$$X_1-X_2=G(\psi_1, T_1)-G(\psi_2, T_2). \qquad (7)$$

Now, if the quantity on the left is made zero,

$$dG(\psi, T)=0. \qquad (8)$$

Writing M in the form

$$M=g(\psi, T)\cdot(\sin^2\tfrac{1}{2}\phi)/\lambda^2 \qquad (9)$$

we have from (6) and (8)

$$dg=0, \qquad (10)$$

whence

$$g(\psi, T)=\text{constant}. \qquad (11)$$

In virtue of (1) we therefore have

$$a\cos^2\psi+b\sin^2\psi=\text{constant}. \qquad (12)$$

Hence, if experimentally the scattering at ψ_1, T_1 equals the scattering at ψ_2, T_2 and the scattering angle is the same in both cases, we have from (12)

$$a(T_1)\cos^2\psi_1+b(T_1)\sin^2\psi_1 = a(T_2)\cos^2\psi_2+b(T_2)\sin^2\psi_2. \qquad (13)$$

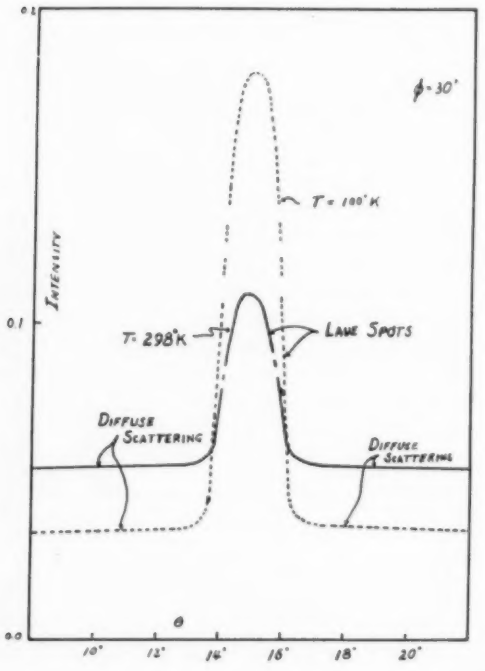

FIG. 2. Effect of temperature on intensities of diffuse scattering and on reflected x-rays. The intensity of the Laue spots are shown reduced by a factor of $\frac{1}{2}$ above the break in the curves.

Further, if experimentally we can make $\psi_1 = 0°$ and $\psi_2 = 90°$, we may write

$$a(T_1) = b(T_2). \tag{14}$$

We shall assume that a is related to the characteristic temperature $\Theta_{||}$ associated with displacements parallel to the c axis by the Debye formula

$$a(T) = (6h^2T/mk\Theta_{||}^2)Q(\Theta_{||}/T), \tag{15}$$

where Q is what Zener calls the quantization factor. We assume that a similar formula connects $b(T)$ with $\Theta_\perp$. Then if the Θ's do not vary with the temperature, it follows from (14) and (15) that

$$\Theta_\perp/\Theta_{||} = (T_1/T_2)^{\frac{1}{2}} \tag{16}$$

very nearly since the quantization factor Q is only slightly greater than unity for the temperatures used in our experiments. The ratio of the mean square displacements parallel and perpendicular to the c axis is therefore approximately given by

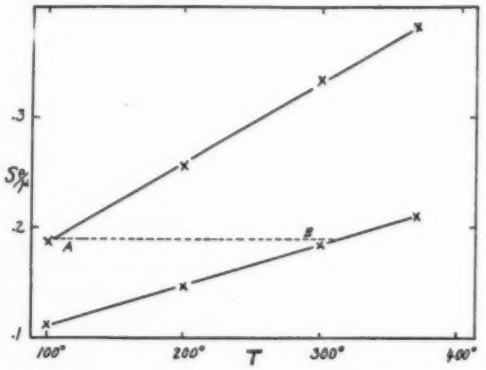

FIG. 3. The crosses represent experimental values, while the lines are merely average lines used in determining the ratio a/b.

$$a/b = \Theta_\perp^2/\Theta_{||}^2 = T_2/T_1. \tag{17}$$

It should be noted that the ratio a/b can thus be measured without a knowledge of the spectral distribution and that in this case just as good a measurement can be made with general radiation as with monochromatic rays.

4. EXPERIMENTAL RESULTS

The experimental method has been previously described.[3] Using this method, we obtained values of $(S\rho/\mu)_{\text{exp}}$ (defined in a previous paper[3]) at $T = 298°$ and 100°K which were some ten percent greater than the values reported previously.[3, 5] This increase is due to the removal of pits and other irregularities. In order to assure ourselves that this was the reason we made the following test: First, we determined the ratio of the scattering from a polished, annealed and etched 90° (i.e., $\psi = 90°$) crystal at $T = 298°$K to that at $T = 100°$K and obtained 1.63 for the

TABLE I. *Values of* $(S\rho/\mu)_{\text{exp}}$ *for zinc.* $\phi = 30°$.

T	$\psi = 3°$	90°
100°K	0.187	0.112
200	.255	.147
298	.333	.182
370	.382	.210
550	.403	—

[5] G. E. M. Jauncey and W. A. Bruce, Phys. Rev. **51**, 60 (1937).

ratio. Next we determined the ratio for an untreated crystal and obtained the value 1.62. These two values are equal within the experimental error even though the numerator and denominator of the ratio in the first case were about 10 percent larger than the numerator and denominator, respectively, in the second case. Similarly, we measured the ratio for two 0° crystals and obtained ratios of 1.66 and 1.68 for the treated and untreated crystals, respectively. Again, the ratios are equal within experimental error. By reference to Fig. 1, it is seen that the surface irregularities should produce no effect on the ratio of the scattering at two different temperatures. If the process of polishing, annealing and etching had produced distortion in the crystal lattice, it is likely that there would have been lack of agreement in the above ratios.

As a matter of interest we show two curves of $I(\phi, \theta)/u(\phi, \theta)$ (see a previous paper[2]) against θ for $\phi=30°$ and $\psi=0°$ in Fig. 2. The dotted curve is for $T=100°$K and the full curve is for $T=298°$K. It is seen that with increase of temperature the intensity of the Laue spot diminishes while the intensity of the diffuse scattering increases.

Our results are shown in Table I and in Fig. 3.

We now draw a horizontal line AB in Fig. 3. The ordinates of the points A and B indicate equal values of $(S\rho/\mu)_{exp}$. The temperature coordinates of these two points are 106° and 314°K. From (17) the value of a/b is therefore 2.96. This is the ratio of the mean square displacement in the direction of the c axis to that in a direction normal to this axis. It may be noted that this is considerably greater than the theoretical value 1.8 derived by Zener[1] from the elastic constants.

JUNE 15, 1937 PHYSICAL REVIEW VOLUME 51

Atomic Structure and Vibrations in Zinc Crystals

V. The Diffuse Scattering of X-Rays at Various Scattering Angles

W. A. Bruce and E. M. McNatt
Wayman Crow Hall of Physics, Washington University, St. Louis, Missouri

(Received May 3, 1937)

Former experimental results on the diffuse scattering of x-rays from single crystals of zinc at room temperature were not accurate enough to give certain evidence for the existence of asymmetry in the electron atmospheres of the zinc atoms. More exact and careful measurements of the diffuse scattering of x-rays at scattering angles ranging from $\phi=15°$ to $\phi=40°$ for the two orientation angles $\psi=14°$ and $\psi=90°$ are described. The results are discussed in paper VI.

1. Introduction

A RECENT experiment was performed in this laboratory[1] in which the diffuse scattering from single crystals of zinc was measured at values of ϕ, the angle of scattering, equal to 20°, 25°, 30°, 35°, and 40°. These results implied that the true atomic structure factor, f, is a function of ψ as well as $(\sin \frac{1}{2}\phi)/\lambda$. This must be due to asymmetry in the electron atmosphere of an atom in a zinc crystal. The data were not complete enough to make quantitative measurements of this asymmetry of the atomic structure factor.

[1] G. E. M. Jauncey and W. A. Bruce, Phys. Rev. **50**, 413 (1936).

2. Experimental Refinements

In the present experiment the diffuse scattering was measured at the same angles as before and also at $\phi=15°$. All of the measurements were made at room temperature. The expression for the experimental values is

$$(S\rho/\mu)_{exp}=\frac{4R^2Wm^2c^4}{ANZe^4(1+\cos^2\phi)}\cdot\frac{D(\phi,\theta)}{D_0u(\phi,\theta)}, \quad (1)$$

where $D(\phi, \theta)$, D_0 are the measured ionization currents[2] for the scattered and primary beams,

[2] For definition of terms and previous references, see G. E. M. Jauncey and W. A. Bruce, Phys. Rev. **50**, 408 (1936).

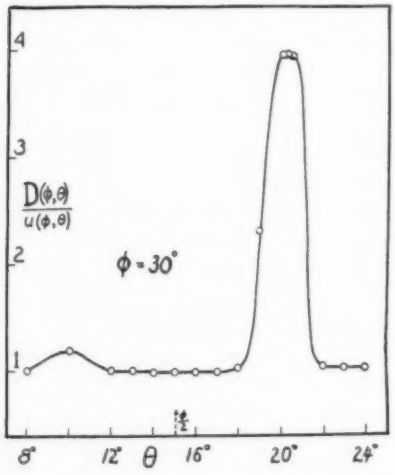

FIG. 1. Method of eliminating the Laue spot at $\theta=\phi/2$.

respectively, and

$$u(\phi, \theta)=\frac{2 \sin (\phi-\theta)}{\sin (\phi-\theta)+\sin \theta}. \qquad (2)$$

In an experiment where the angle of scattering is varied, the effects of surface pitting described in the fourth paper[3] of this series are particularly important, as is seen by reference to Fig. 1 of the fourth paper. Thus it is essential to have no irregularities more than 10^{-5} cm deep. A polished and annealed surface was used for $\psi=90°$ and a cleaved surface for $\psi=14°$.

The quantity given in (2) is very sensitive to changes of θ for small values of ϕ. Hence each experiment was done with the ionization chamber and crystal first on one side and then the other side of the primary beam. Thus small errors in lining up the crystal in its holder were eliminated.

For accurate work it is best to observe the scattering at $\phi/2=\theta$ or to observe it at symmetrical positions about the angle $\phi/2=\theta$ and interpolate for the point $\phi/2=\theta$. With the cleaved surface crystal this latter method is always used, but, where the polished face of a moulded casting is used, the Laue spot may, in general, occur at any angle. However, the minor axis may be controlled in the growth of a crystal as well as the major axis. Therefore a 90° crystal was grown so that a minor axis made an angle of about 5° with the normal to the face. This placed the $(20\bar{2}0)$ spot always a few degrees from $\theta=\phi/2$ and provided a wide region for diffuse scattering with its center at $\theta=\phi/2$. To see the advantage of this, compare our Fig. 1 with Fig. 3 in the second paper[2] of this series.

The quantity $D(\phi, \theta)$ of (1) was experimentally measured by observing the rate of deflection of the electrometer in the scattering position, Fig. 2, and subtracting the effect due to background as measured with the crystal in the background position, Fig. 2. In this position the drift of the electrometer registers the effect of cosmic rays, α-particles, etc., and the scattering from the air through which the primary beam passes. When the crystal is turned to the background position so that no scattering from the zinc gets into the chamber window, it cuts off the x-rays which are normally scattered from the column of air, indicated by the shaded area of Fig. 2. We therefore corrected for the scattering from the air in the space represented by the shaded area of Fig. 2.

At small angles it becomes necessary to correct for the height of the ionization chamber window and for the height of the primary beam. The effect of both heights is to make the average scattering angle greater than the angle as read on the spectrometer. Calculation showed that when the spectrometer was set at 10° the average scattering angle was about 11°. At settings of greater than 10° the discrepancy between the setting and the average scattering angle became

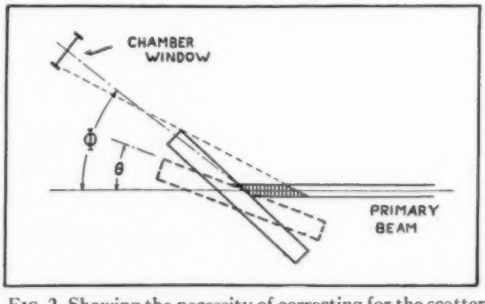

FIG. 2. Showing the necessity of correcting for the scattering from air. Full line rectangle-background position; broken line rectangle-scattering position.

TABLE I. *Values of* $(S\rho/\mu)_{exp}$ *at 298°K.*

ϕ	$\psi=90°$	14°
10	0.170	
15	.145	0.308
20	.169	.355
25	.183	.343
30	.183	.325
35	.171	.290
40	.160	.238

[3] G. E. M. Jauncey and W. A. Bruce, paper IV.

less than 1° and the scattering angle was taken as read on the spectrometer.

General radiation with a spectral distribution as shown in Fig. 1 of a previous paper[1] was used.

3. Experimental Results

The results are given in Table I and in Fig. 3. Owing to experimental difficulties, we were unable to obtain a value of $(S\rho/\mu)_{exp}$ at $\phi=10°$ with the $\psi=14°$ crystal. We obtained the value shown for $\phi=10°$ with the $\psi=90°$ crystal but we feel that due to experimental error the value is too large. However, the value shown was checked by a careful repetition of the experiment at this angle.

According to Zener[4] the diffuse scattering from the valence electrons at small angles falls off as the first power of the scattering angle rather than the second power as does the scattering from the core electrons. This theoretical prediction has been obtained independently by Debye.[5] Recently Scharwächter[6] has obtained results which confirm this theoretical prediction. For a light metal at small angles this effect is measurable, but for zinc it is within the limit of our experimental error and has a negligible effect upon our experimental results.

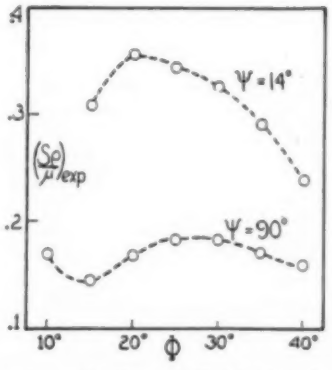

Fig. 3 Experimental values of $(S\rho/\mu)$ plotted against ϕ for $\psi=14°$ and $\psi=90°$.

Discussion of the results of this paper is deferred to the sixth paper of this series.

The authors wish to thank Professor G. E. M. Jauncey for his suggestion of this problem and his aid in refinement of the experimental method.

[4] C. Zener, Phys. Rev. **48**, 573 (1935).
[5] P. Debye, Physik. Zeits. **38**, 161 (1937).
[6] W. Scharwächter, Physik. Zeits. **38**, 165 (1937).

JUNE 15, 1937 PHYSICAL REVIEW VOLUME 51

Atomic Structure and Vibrations in Zinc Crystals

VI. Determination of Electron Asymmetry and the Two Principal Characteristic Temperatures

G. E. M. Jauncey* and W. A. Bruce
Wayman Crow Hall of Physics, Washington University, St. Louis, Missouri

(Received May 3, 1937)

The results reported in papers by Brindley, Miller and the two previous papers of this issue of the *Physical Review* are discussed. The results show that the true atomic structure factor f (the effect of atomic vibrations having been removed) is a function of the orientation angle ψ out to $(\sin\frac{1}{2}\phi)/\lambda=0.6$. It is shown how the f values may be obtained for two values of ψ from diffuse scattering measurements alone at room temperature. The f curves for $\psi=14°$ and 90° coincide for $(\sin\frac{1}{2}\phi)/\lambda$ between 0.6 and 1.0. At 0.6 the curves fork. Correcting Miller's F values ($\lambda=0.71$A) for atomic vibrations and Brindley's F values ($\lambda=1.54$A) for atomic vibrations and dispersion, f points are obtained which mostly fall between or on the f curves for $\psi=14°$ (this is practically the same as the f curve for $\psi=0°$) and $\psi=90°$. It is shown that the difference between the two f curves is due to a reasonable asymmetry in the spatial distribution function of the valence electrons. The ΔF's between Miller's and Brindley's F values are corrected for atomic vibrations, and the resultant Δf's are all equal within experimental error. The average $\Delta f=2.35$ in good agreement with the quantum mechanical $\Delta f=2.36$. The characteristic temperatures associated with vibrations parallel and perpendicular to the principal axis have been found. The characteristic temperature for parallel vibrations decreases while that for perpendicular vibrations remains almost constant with rise of temperature in agreement with Zener's theory. The average characteristic temperature for vibrations in all directions is just slightly greater than the characteristic temperature for specific heat in agreement with Zener's theory. The decrease of the characteristic temperature with temperature appears to begin when the root mean square displacement exceeds about 0.13A.

* The senior author was aided in part by a grant from the Rockefeller Foundation to Washington University for research in science.

1. Effect of Orientation on the Structure Factor

IN a group of three papers appearing in the September 1, 1936 issue of the *Physical Review*, the evidence for the anisotropy of the atomic vibrations of zinc crystals was discussed. We shall refer to these papers[1] as I, II, and III. As pointed out by Brindley[2] the large intensity of the $(10\bar{1}0)$ reflection of Cu $K\alpha$ x-rays from powdered zinc relative to the intensity of the (0002) reflection indicates that not only is there anisotropy in the thermal vibrations of the atoms of a zinc crystal but also the electron atmospheres of the atoms are distorted. However, Brindley was reluctant to accept this explanation of the abnormally high F value for the $(10\bar{1}0)$ reflection. He preferred to ascribe the abnormality to an impurity. In this laboratory Miller and Foster, using Mo $K\alpha$ rays instead of Cu $K\alpha$ rays, confirmed Brindley's result, and also Brindley found a similar result for the $(10\bar{1}0)$ reflection of Cu $K\alpha$ rays from powdered cadmium.[3] The possibility of impurity seems to be ruled out.

According to Zener[4] the effect of the thermal vibrations may be removed from the structure factor F so as to obtain the true atomic structure f by means of

$$f = Fe^{M}, \tag{1}$$

where for hexagonal crystals like zinc

$$M = (a\cos^2\psi + b\sin^2\psi)\cdot\frac{\sin^2(\frac{1}{2}\phi)}{\lambda^2}, \tag{2}$$

ϕ is the angle of scattering and ψ is the orientation angle.

We pointed out in paper I that the f values calculated from Miller and Foster's F values for the (0002), $(10\bar{1}0)$ and $(10\bar{1}1)$ reflections indicate that when f values are plotted against $(\sin\frac{1}{2}\phi)/\lambda$ the f point for the $(10\bar{1}1)$ reflection falls between the curves which may be imagined as respectively passing through the f points for the (0002) and $(10\bar{1}0)$ reflections. This means that one way of showing the existence of asymmetry in the electron atmospheres of the atoms in zinc crystals is to correct the structure factors for thermal vibration and to plot the resulting f values against $(\sin\frac{1}{2}\phi)/\lambda$. If there is asymmetry, the f points will in general fall between two f curves, one for $\psi=0°$ and the other for $\psi=90°$. Such a tendency has recently been found by Miller[5] for Mo $K\alpha$ rays reflected from powdered zinc. The dependence of f on the orientation must result from the spatial distribution of the outer electrons being a function of the direction. Since probably only the two valence electrons are involved in this asymmetry and since the contribution of the valence electrons to f becomes small at large values of $(\sin\frac{1}{2}\phi)/\lambda$, the dependence of f upon ψ must vanish at a certain value of $(\sin\frac{1}{2}\phi)/\lambda$. The f curves for $\psi=0°$ and $\psi=90°$ will coincide for values of $(\sin\frac{1}{2}\phi)/\lambda$ greater than this value but will be separate at values less than this value. It was expected that the place of forking of the curves would be at a value of $(\sin\frac{1}{2}\phi)/\lambda$ somewhat greater than 0.240 since this is the value for the $(10\bar{1}0)$ reflection. One surprising result found by Miller[5] was the low F value for the (0004) reflection. Although, owing to the difficulty of making accurate measurements on this very weak reflection, Miller's value of $F(0004)=10.6$ is not to be considered as accurate within ± 1.0, yet even if the value 11.6 is taken and the f value calculated, this f value is still low compared to the f values for the reflections on either side of this reflection. The (0004) reflection is for $\psi=0°$ and occurs at $(\sin\frac{1}{2}\phi)/\lambda=0.406$. Hence the separation of the f curves for $\psi=0°$ and $\psi=90°$ is considerable at $(\sin\frac{1}{2}\phi)/\lambda=0.406$. It seems very likely that the separation continues at least as far out as $(\sin\frac{1}{2}\phi)/\lambda=0.6$.

In the preceding two papers, IV and V, appearing in this issue of the *Physical Review*, further measurements on the diffuse scattering from single crystals of zinc are described. The results of experiments on diffuse scattering of x-rays at various angles of scattering for orientation angles $\psi=14°$ and $\psi=90°$ are shown as circles in Fig. 1. The measurements were made with the crystals at room temperature. The

[1] I. G. E. M. Jauncey and W. A. Bruce, Phys. Rev. **50**, 408 (1936); II. G. E. M. Jauncey and W. A. Bruce, Phys. Rev. **50**, 413 (1936); III. R. D. Miller and E. S. Foster, Phys. Rev. **50**, 417 (1936).
[2] G. W. Brindley, Phil. Mag. **21**, 790 (1936).
[3] G. W. Brindley, Proc. Leeds Phil. Soc. **3**, 200 (1936).
[4] C. Zener, Phys. Rev. **49**, 122 (1936).
[5] R. D. Miller, Phys. Rev. **51**, 959 (1937).

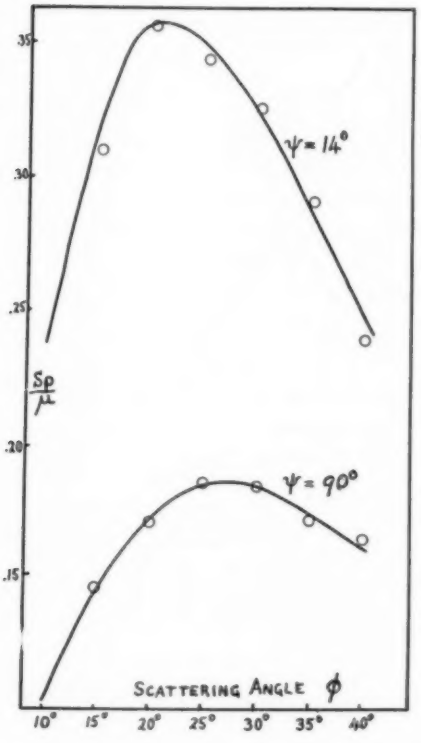

FIG. 1. The experimental values of $(S\rho/\mu)$ are shown in the circles. The curves are obtained from the theoretical equations using the f's given in Table IV and $g=2.27\cos^2\psi+0.64\sin^2\psi$.

spectral distribution of the energy in the primary x-rays is shown in Fig. 2. We shall show that from the values given in Table I, paper V or shown in Fig. 1 we can obtain values of a and b in Zener's formula for M and also f values for $\psi=14°$ and $\psi=90°$.

Because the largest angle of scattering is 40°, we shall neglect the effect of the Compton change of wave-length on the incoherent part of the diffuse scattering. From (9) and (10) of paper II we have

$$(S\rho/\mu)_{exp}=\int(S_{coh}+S_{inc})\cdot(\rho/\mu)Id\lambda, \qquad (3)$$

where

$$S_{coh}=f^2(1-e^{-2M})/Z, \qquad (4)$$

$$S_{inc}=1-(1/Z)\Sigma E_r^2 \qquad (5)$$

and the spectral distribution $I(\lambda)$ is normalized

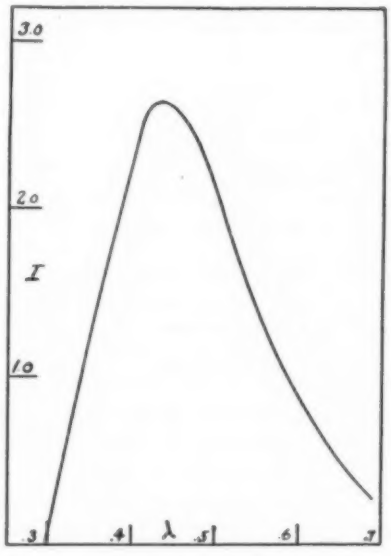

FIG. 2. Spectral distribution curve for the x-rays falling upon the crystal.

so that

$$\int Id\lambda=1. \qquad (6)$$

We may consider the quantity on the left as an experimental quantity whose value is calculated by means of (8) of paper II. We shall show later that S_{inc} is very insensitive to the value of the orientation angle ψ and we shall therefore assume that S_{inc} is independent of ψ. The values of ΣE_r^2 for zinc shown in Table I are interpolated from a table given by Compton and Allison.[6] From Table I and Fig. 2 we have calculated Table II. Subtracting these from the corresponding values in Table I of paper V, we obtain Table III.

For a first approximation we shall assume that the primary rays consist of monochromatic rays of $\lambda=0.44$A (half-value absorption in aluminum). This assumption gives fairly good results so long as the calculations are made for the scattering at angles greater than the angles at which the humps of the respective curves occur in Fig. 1. The values of $(\sin\frac{1}{2}\phi)/\lambda$ are then 0.6 and 0.78 for

[6] A. H. Compton and S. K. Allison, *X-Rays in Theory and Experiment*, p. 782.

30° and 40° respectively. At a given angle of scattering

$$\frac{S_{\text{coh}}(\psi=\psi_1)}{S_{\text{coh}}(\psi=\psi_2)}=\frac{1-e^{-2g_1x^2}}{1-e^{-2g_2x^2}}, \tag{7}$$

where $x=(\sin\frac{1}{2}\phi)/\lambda$ and

$$g=a\cos^2\psi+b\sin^2\psi. \tag{8}$$

Then from the values of the ratio $S_{\text{coh}}(14°)/S_{\text{coh}}(90°)$ at $\phi=30°$ and $\phi=40°$ we obtain two equations containing the two unknowns g_1 and g_2. From these two values of g, values of a and b are obtained by means of (8). The μ/ρ for $\lambda=0.44$A in zinc is 14.5 g^{-1} and we calculate values of S_{coh} from the values given in Table III. Knowing a and b we then calculate f values and plot a curve of f against $(\sin\frac{1}{2}\phi)/\lambda$. Using this f curve, the spectral distribution curve, and the values of a and b we have found values of

$$\int(S_{\text{coh}}\rho/\mu)Id\lambda \tag{9}$$

graphically. These values differ slightly from the values shown in Table III. Then by successive approximations it is possible to find values of a and b and of f that will make the values of (9) fit best with the values of Table III. We finally obtained

$$a=2.27\text{A}^2 \quad \text{and} \quad b=0.64\text{A}^2$$

and the f values shown in Table IV. The graphs of these f values are shown in Fig. 3. Using these values together with the values of a and b given above, we have plotted the curves in Fig. 1. Since we have been able to make the curves pass very nearly through the experimental points, we have a considerable degree of confidence in the values of a and b and in the f values of Table IV. Two f curves—one for $\psi=14°$ and the other for $\psi=90°$—are definitely required for values of $(\sin\frac{1}{2}\phi)/\lambda$ not greater than 0.6, the fork occurring at this value.

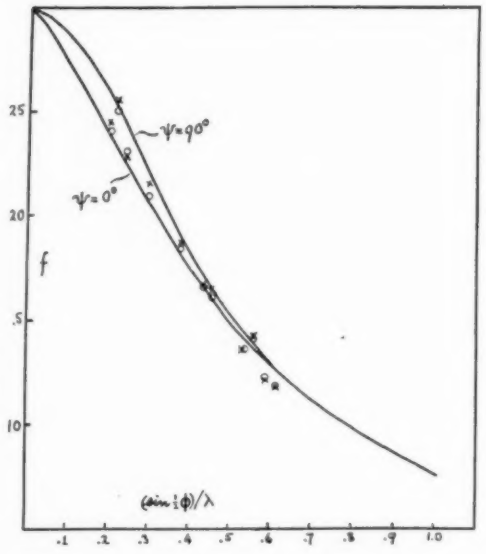

FIG. 3. The f curves are obtained from diffuse scattering experiments and the points are f values obtained from powder crystal F values through the formula $f=Fe^M$.

It should be noted that a and b and the f values have been determined by diffuse scattering measurements at room temperature for two orientation angles at various scattering angles. We have however, assumed the quantum mechanical values of S_{inc} and the absence of any effect due to electron asymmetry at $\phi=30°$. Still we need not make this latter assumption since if for instance we assume no asymmetry effects beyond $\phi=25°$ we are unable to obtain curves which pass so nearly through the experimental points as do the curves of Fig. 1.

TABLE I. *Values of* ΣE_r^2 *for zinc.*

$(\sin\frac{1}{2}\phi)/\lambda$	ΣE_r^2	$(\sin\frac{1}{2}\phi)/\lambda$	ΣE_r^2
0.0	30	0.6	9.4
.1	24.8	.7	7.3
.2	19.0	.8	6.3
.3	14.7	.9	6.2
.4	12.5	1.0	5.2
.5	10.4	1.1	4.2

TABLE II. *Values of* $f(S_{\text{inc}}\rho/\mu)Id\lambda$.

10°	15°	20°	25°	30°	35°	40°
0.025	0.034	0.039	0.044	0.047	0.050	0.058

TABLE III. *Values of* $f(S_{\text{coh}}\rho/\mu)Id\lambda$.

ψ \ ϕ	15°	20°	25°	30°	35°	40°
14°	0.274	0.316	0.299	0.278	0.240	0.180
90°	0.111	0.130	0.137	0.136	0.121	0.102

2. Comparison with Powdered Crystal Results

The circles in Fig. 3 represent the f values calculated from Miller's F values when the above values of a and b are used in M, while the crosses represent the values of $(f+2.36)$ where f has been calculated from Brindley's F values in a similar way. The addition of 2.36 is due to dispersion. The f points fall very well between the $\psi=0°$ (more correctly the $\psi=14°$ curve but the difference between the $\psi=0°$ and $\psi=14°$ curves must be small) and the $\psi=90°$ curve. Only at the larger values of $(\sin\frac{1}{2}\phi)/\lambda$ do the f points fall outside the area between the two curves but owing to the method of approximation used some disagreement might be expected at the larger angles. However, we feel that the small disagreement may be due to error in the F values.

Although the accuracy is not very great it is interesting to calculate the difference Δf between Brindley's and Miller's f values from the difference ΔF between their F values by means of

$$\Delta f=\Delta F\cdot e^{M} \tag{10}$$

and the above values of a and b. The Δf values are given in Table V, from which it is seen that Δf has values which scatter about the average value 2.35. The amount of departure from the average value is in no case greater than that due to experimental error in ΔF. The results support the view that Δf is constant with respect to $(\sin\frac{1}{2}\phi)/\lambda$ as quantum mechanics requires that it should be according to Hönl.[7] The average Δf is 2.35. The quantum-mechanical value for Δf when $\lambda(\text{Mo } K\alpha)=0.71\text{A}$, $\lambda(\text{Cu } K\alpha)=1.54\text{A}$ and Zn $K=1.28\text{A}$ is 2.36. This agreement indicates that the values of a and b have been well chosen.

3. The Two Principal Characteristic Temperatures

We next consider the results reported in paper IV. The diffuse scattering was measured at a scattering angle $\phi=30°$ in all cases. The values of $(S\rho/\mu)_{\text{exp}}$ for $\psi=3°$ and 90° and for $T=100°$, 200°, 298°, 370°K are given in Table I of paper IV. Using the f values given in Table IV and the spectral distribution given in Fig. 2, we have calculated a and b for each temperature. These values are shown in Table VI. The quantity a is related to the characteristic temperature $\Theta_{||}$ associated with displacements parallel to the c axis by the Debye formula

$$a=\frac{6h^2T}{mk\Theta_{||}^2}Q\left(\frac{\Theta_{||}}{T}\right), \tag{11}$$

where Q is what Zener calls the quantization factor. A similar formula connects b with $\Theta_{\perp}$. The values of the two characteristic temperatures are shown in Table VI. It is to be noted that, excepting at low temperatures, $\Theta_{||}$ falls with rise of temperature. This is exactly the same effect that James and Firth[8] working with NaCl, and James and Brindley[9] working with KCl, have observed at temperatures from 600° to 900°. This deviation from a constant characteristic temperature can be explained by assuming that the Debye model is no longer valid because the very large atomic vibrations introduce third and fourth order terms into the expression for the potential energy. This approach has been investigated by Waller[10] but even for simple cubic crystals the problem is so complicated that no quantitative results are available. On the other hand, Zener and Bilinsky,[11] using the Debye model, have found that (11) is valid provided that the characteristic temperature is itself considered to be a function of tem-

Table IV. *Structure factors for zinc.*

$(\sin\frac{1}{2}\phi)/\lambda$	0.0	0.1	0.2	0.3	0.4	0.5	0.6	0.8	1.0
$\psi=14°$	30.0	27.3	23.8	20.5	17.3	14.7	12.8	9.8	7.6
$\psi=90°$	30.0	28.7	25.9	21.8	18.2	15.2			

Table V. *Effect of dispersion.*

Reflection	ΔF	Δf	Reflection	ΔF	Δf
0002	2.2	2.4	2021	1.8	2.1
1010	1.9	2.1	2023	2.2	2.1
1011	2.6	2.7	1015	1.3	2.2
1012	1.9	2.2	1124		
1013	2.3	2.7	2131	2.1	2.7
1120			0006	1.55	2.4
1122	1.9	2.3	2132		

[7] H. Hönl, Zeits. f. Physik **84**, 1 (1933).

[8] R. W. James and E. M. Firth, Proc. Roy. Soc. **A117**, 62 (1928).

[9] R. W. James and G. W. Brindley, Proc. Roy. Soc. **A121**, 155 (1928).

[10] I. Waller, Ann. d. Physik **83**, 153 (1927).

[11] C. Zener and S. Bilinsky, Phys. Rev. **50**, 101 (1936).

TABLE VI. *Calculated values of a, b, and the characteristic temperatures.*

T	a	b	a/b	$\Theta_{\|\|}$	$\Theta_{\perp}$	$(2\Theta_{\perp}+\Theta_{\|\|})/3$
100°K	0.68A²	0.26A²	2.6	169°K	281°K	244°K
200	1.25	.44	2.8	170	290°	250°K
298	2.36	.64	3.7	150	290°	243°K
370	3.80	.84	4.5	130	276°	227°K
550	6.20			122		

perature. Zener and Bilinsky give the formula

$$\Theta(T)=\Theta(0)e^{-KH(T)}, \tag{12}$$

where $\Theta(0)$ is the characteristic temperature obtained by means of the Debye specific heat formula from C_v measured at low temperatures and $KH(T)$ is a quantity depending upon the thermal expansion coefficient and the compressibility of the crystal. Let us write M in the form $g\cdot(\sin^2\frac{1}{2}\phi)/\lambda^2$. From the curves given by Zener and Bilinsky it is seen that the characteristic temperature for KCl or NaCl is constant for the range $g=0$ to $g=1.0$, but decreases for values of g greater than 1.0. By reference to our Table VI, it is seen that $\Theta_{||}$ begins to decrease when $a>1.25$. Our a corresponds to the g for KCl or NaCl. So our results for the vibrations parallel to the c axis of a zinc crystal are in qualitative agreement with the results for KCl and NaCl. Next we may point out that no approach to this problem through higher terms in the potential energy could predict a lower value of $\Theta_{\perp}$ at 100°K than at 200°K. Zener has called it to our attention that this effect may be due to the change in the sign of the linear thermal expansion coefficient for a direction perpendicular to the c axis of a zinc crystal[12] which occurs in the region of 100°K.

For the purpose of calculating the specific heat of a hexagonal crystal it is necessary to use an average characteristic temperature given by

$$\Theta_h=(2\Theta_{\perp}+\Theta_{||})/3. \tag{13}$$

Values of this average are given in Table VI. It is interesting to note that Θ_h for room temperature is 243°K. The Θ which is used for specific heat purposes is 235°K. According to Zener and Bilinsky the Θ for x-rays should be somewhat larger than that for specific heat. In the case of cubic crystals with a Poisson ratio of 0.25, the Θ for x-rays should be 2.5 percent greater than the Θ for specific heat. Our result for the hexagonal crystal zinc is thus in qualitative agreement with Zener and Bilinsky's theoretical prediction.

According to Zener[4] the ratio a/b should be 1.8. It is interesting to note that our value of a/b is considerably greater than this at all temperatures.

In paper IV we described how the ratio a/b could be measured without a knowledge of the spectral distribution $I(\lambda)$. The value found was 2.96. Strictly speaking, the method used in paper IV is only applicable when a/b is independent of the temperature, and this is so when $\Theta(T)$ may be taken as equal to $\Theta(0)$ and the quantization factor is nearly unity. But, when a is greater than 1.25A² or the root mean square displacement parallel to the c axis is greater than 0.126A, $\Theta(T)$ falls below $\Theta(0)$ and the method begins to fail. Since the temperatures used in the method were 106° and 314°K, the method really gives a value which is between the true value of a/b for 106° and a/b for 314° and this it does as seen by reference to Table VI.

It should be noted that the method of diffuse scattering has a distinct advantage over other methods in that the characteristic temperatures $\Theta_{||}$ and $\Theta_{\perp}$ can be measured at a single temperature T. Some methods give the average characteristic temperatures between two temperatures. The reason for this is that the diffuse scattering can be measured at the same scattering angle and the same temperature for two values of ψ. We thus obtain two equations containing a and b and we can solve for these two quantities. However, the diffuse scattering measurements must be made at a scattering angle large enough to be beyond the effect of the structure asymmetry of the valence electrons. In powdered crystal work each reflection is for a fixed value of ψ and ϕ and the experimenter must take what nature gives him; whereas in the case of diffuse scattering the experimenter can arrange the ϕ's and ψ's at will, taking care only to evade the Laue spots.

[12] In the derivation of M by Debye and Waller and by Zener and Jauncey, no account was taken of the effect the change in the separation of the lattice due to thermal expansion has on the mean square displacement.

4. Asymmetry of the Electron Atmosphere

The two valence electrons may be considered as having a spatial distribution something like that of the electron of a hydrogen atom. According to quantum mechanics the probability of a hydrogen electron being in a volume element dv at a distance r from the nucleus is

$$(1/\pi a^3)e^{-2r/\gamma}dv,$$

where γ is the radius of the first Bohr orbit in hydrogen. From this it follows that the structure factors for the hydrogen electron are given by

$$E=1/(1+4\pi^2\gamma^2x^2)^2, \qquad (14)$$

where $x=(\sin\frac{1}{2}\phi)/\lambda$. In order to introduce asymmetry we shall suppose that γ^2 in (14) is replaced by

$$p^2\cos^2\psi+q^2\sin^2\psi. \qquad (15)$$

We shall represent E for a given value of x and ψ by $E(x, \psi)$. Using the values

$$p=0.7\text{A} \quad \text{and} \quad q=0.3\text{A}$$

we have calculated values of $2\delta E$, where $\delta E=E(x, 90°)-E(x, 0°)$. These values are shown in Table VII. The δf values in this table are values of $f(x, 90°)-f(x, 14°)$ which are obtained from Table IV. It is probable that $f(x, 14°)$ is very nearly equal to $f(x, 0°)$. There is no attempt in Table VII to show that $\delta f=2\delta E$, but merely to show that a valence electron asymmetry designated by the above values of p and q does have an effect out to $(\sin\frac{1}{2}\phi)/\lambda=0.6$ and that the effect of the asymmetry is of the proper order. Further, the values $p=0.7$A and $q=0.3$A are not unreasonable in view of the fact that γ for the hydrogen atom in (14) is 0.53A. A more accurate agreement between $2\delta E$ and δf can probably be obtained by using another formula than (14) for E and another way than (15) of taking care of the asymmetry. However, the δf at $(\sin\frac{1}{2}\phi)/\lambda=0.2$ is so large, being apparently larger than 2, that perhaps the asymmetry extends to electrons beneath the valence electrons.

Table VII.

$(\sin\frac{1}{2}\phi)/\lambda$	$2\delta E$	δf
0.1	0.46	1.4
.2	.90	2.1
.3	.88	1.3
.4	.70	0.9
.5	.48	.5
.6	.17	.0

In Section 1 of this paper we said that S_{inc} was insensitive to change of ψ. At $(\sin\frac{1}{2}\phi)/\lambda=0.3$, we have $\Sigma E_r^2=14.7$ from Table I. If we take the two valence electrons to be hydrogen-like, we have E for each of these equal to 0.25. The ΣE_r^2 for the core electrons is therefore $14.7-2\times0.25^2=14.57$. Now $E(0.3, 90°)=0.57$ and $E(0.3, 0°)=0.13$. Hence, including the valence electrons, we have $\Sigma E_r^2(0.3, 0°)=14.65+2\times0.13^2=14.68$ and $\Sigma E_r^2(0.3, 90°)=14.65+2\times0.57^2=15.3$. Hence

$$S_{\text{inc}}(0.3, 0°)-S_{\text{inc}}(0.3, 90°)=0.02.$$

Now the experimental value of $S_{\text{coh}}+S_{\text{inc}}$ for $(\sin\frac{1}{2}\phi)/\lambda=0.3$ and $\psi=90°$ is 2.1. The change in S_{inc} due to going from $\psi=0°$ to $\psi=90°$ is thus one percent of the experimental value of S. The error introduced into our theoretical calculations by not taking account of the change in S_{inc} due to a change in ψ is therefore no greater than our experimental error, which is about 1 or 2 percent.

Rotation of Water Molecules in Carbon Disulfide Solution

E. L. KINSEY AND J. W. ELLIS
University of California at Los Angeles, California
(Received February 8, 1937)

The absorption spectrum of water dissolved in carbon disulfide is investigated for the combination bands whose centers for the vapor lie at 1.135, 1.379 and 1.875μ by means of a recording quartz spectrograph with a slit width adjusted to 0.003μ, and for the band lying in the 3μ region by means of a Hilger rocksalt spectrometer with a slit width adjusted to 0.04μ. Percent transmission curves for the combination bands show vapor-like absorption the minima of which fall in the position of vapor minima analyzed by Mecke into P and Q branches. If a correlation is made between the bands of the solution and vapor on the basis of the absence of a vapor-to-solution shift, then for each band the P branch is strong, the Q branch is weak and the R branch is absent. If the correlation is made so that bands in the solution are regarded as shifted toward longer wave-lengths, it is found that (1) the branches of any one band are shifted by the same amount on a wave number scale, (2) that the shift varies from band to band (the shifts lie between 76 and 156 cm^{-1}), and (3) that Q branches are strongest, R branches are weak, and in every case the P branch is absent. Under either correlation the structure in each band indicates that the molecule in the solution is freely rotating. Reasons for expecting it to do so are discussed. In the 3μ region a doublet is found in the solution of components at 2.80 and 2.65μ, the center of which coincides with a shoulder in the liquid absorption band.

FRUITFUL investigations have been made lately on the state of the water molecule in liquid water. From the x-ray diffraction patterns of liquids, and from such discussions as those of Bernal and Fowler,[1] Pauling,[2] and Debye,[3] one is led to conceive a liquid as a quasi-crystalline state in which the molecules undergo rotational oscillations and, under certain conditions, freely rotate.

Debye has shown that in liquid water the conditions for free rotation are not met. Large lattice interactions occur to prevent it, and these broaden and shift the centers of the liquid absorption bands in the infrared, and produce the diffuse Raman bands which are so characteristic of liquid water. It has been shown, however, that these interactions can be reduced by dissolving water in suitable solvents. The Raman bands of water sharpen, and the infrared absorption bands sharpen and shift toward their vapor positions, in the spectra of mixtures of water and nitric acid.[4]

The electric moment of water dissolved in benzene has a value which is not very different from its value in the vapor state, so that in this case interactions not only between water molecules but between water and benzene molecules are not large. The question arises therefore whether in solutions, at least of nonpolar solvents, the interactions are sufficiently reduced to allow free rotation to occur. This point has been investigated by studying the infrared absorption of water dissolved in carbon disulfide.

MEASUREMENTS AND RESULTS

The absorption of a cell one-meter long of carbon disulfide saturated with water was studied in the region 1.0–2.5μ by means of the self-recording quartz spectrograph of the laboratory, with its slit width adjusted to correspond to about 0.003μ. The accuracy of the wave-length measurements given later is of this order. Carbon disulfide was chosen as the solvent because of the relatively high solubility of water in it—0.1 percent by weight between 0° and 40° (*International Critical Tables*), and because of its freedom from obscuring bands of its own in the region studied. The solubility in benzene is reported as about half of this value at room temperature, and in carbon tetrachloride as about one-tenth.[5] Four of the original records are shown in Fig. 1, where the ordinates are galvanometer deflections and the abscissae wave-lengths in μ.

The absorption of one meter of carbon disulfide saturated with distilled water at room temperature is shown by curve A; the spectral dis-

[1] Bernal and Fowler, J. Chem. Phys. **1**, 515 (1933).
[2] L. Pauling, Phys. Rev. **36**, 430 (1930).
[3] P. Debye, Physik. Zeits. **35**, 100 and 193 (1935).
[4] Kinsey and Ellis, Phys. Rev. **36**, 603 (1930).
[5] Rosenbaum and Walton, J. Am. Chem. Soc. **52**, 3568 (1930).

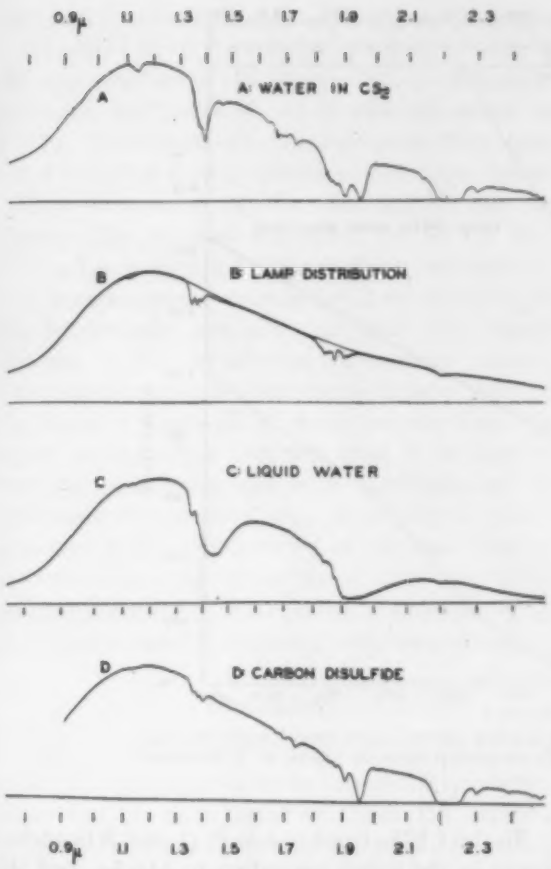

FIG. 1. Automatically recorded transmission curves. *A*, 1 meter of saturated solution of water in CS_2. *B*, Lamp distribution, showing atmospheric water vapor bands. *C*, 0.25 mm of liquid water. *D*, 1 meter of freshly distilled and dried CS_2. In *A* and *D* water vapor bands are greatly reduced because of insertion of the long absorption cell.

tribution of the source and the absorption of water vapor in the light path of the spectrograph by *B*; the absorption of liquid water in a cell 0.25 mm thick by *C*; and the absorption of Eimer and Amend carbon disulfide without water by *D*. The latter sample was distilled over phosphorous pentoxide to remove the water that was found to be present in all the commercial samples. Inspection of the four curves at the 1.379μ band shows the presence of a trace of the water band in the distilled sample, as well as the extent to which the band deepens after the carbon disulfide is saturated with water.

These results show, as previous brief reports of this work pointed out, the characteristic sharpening and shifting toward short wave-lengths of the liquid bands which occur when water is

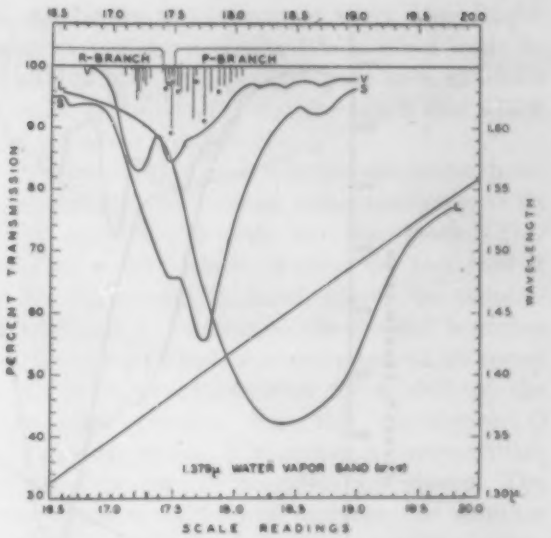

FIG. 2. 1.4μ region. Percent transmission scale reading curves; wave-length scale reading dispersion curve. *V*, vapor band with Mecke's rotational analysis above it. *S*, solution band. *L*, liquid band.

dissolved in carbon disulfide.[6] Values of the percent transmissions for the vapor, liquid, and solution states were obtained in the usual way and are plotted against the plate scale readings in Figs. 2, 3, and 4. The dispersion curve of the instrument is given in each figure with wave-length values plotted as ordinates on the right. The vapor curve, *V*, was obtained by using the extrapolated portion of the spectral distribution curve as a background—extrapolated through the three vapor bands at 1.135, 1.379, and 1.875μ as shown in curve *B*, Fig. 1.

The percent transmission curves for the 1.379μ and 1.875μ bands (Figs. 2 and 3) show clearly that there is structure in the solution absorption, and suggest that it is caused by rotation. The individual lines as given by Mecke[7] in his analysis of the water vapor spectrum are shown at the top of the figures by lines of lengths proportional to intensities. Black dots mark strong lines which do not appear in the classification, but whose wave-lengths and intensities have been measured by Plyler[8] and others. In the 1.379μ band, the classified lines, according to Mecke, form *P* and *R* branches which appear as the three minima in the vapor curve. The first,

[6] Kinsey and Ellis, Phys. Rev. **49**, 105 and 209 (1936
[7] R. Mecke, Zeits. f. Physik **81**, 313 (1933).
[8] E. K. Plyler, Phys. Rev. **39**, 77 (1936).

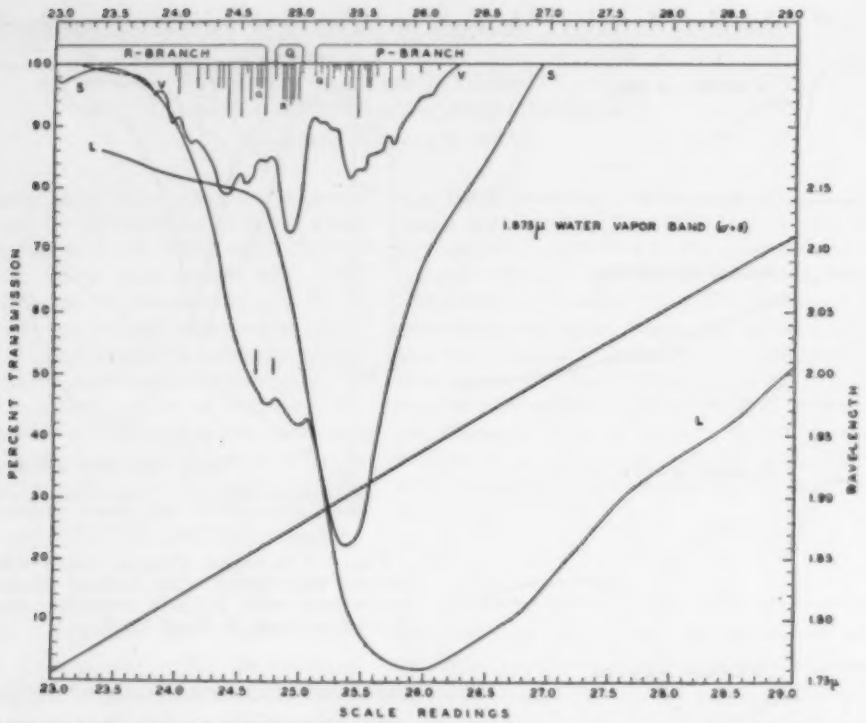

FIG. 3. 1.9μ region. Percent transmission scale reading curves; wave-length scale reading dispersion curve. *V*, vapor band with Mecke's rotational analysis above it. *S*, solution band. *L*, liquid band.

a broad band at about 1.405μ, and part of the second at 1.380μ, form the *P* branch, and the third at 1.360μ forms the *R* branch. The second minimum at 1.380μ falls in the midst of the unclassified lines. It forms the remainder of the *P* branch, and possibly a *Q* branch also, to which some of the unclassified lines belong. Only two minima occur in the solution spectrum, one at 1.400μ and the other at 1.383μ. Each one coincides, within the errors of measurement, with strong unclassified lines and lines of the *P* branch, and lies exactly under a minimum of the observed vapor curve. A minimum corresponding to the *R* branch, however, is absent, or is so weak that it fails to appear on the rapidly rising short wave-length side of the *P* branch.

The band stretching from 1.425 to 1.485μ (scale readings 18.10–18.90), so far as we know, has not been analyzed, but here again a long wave-length component which appears in the vapor at 1.468μ appears in the solution at the same position, whereas short wave-length components are absent. It is probably the combination band $\sigma+2\delta$.

In the 1.875μ band $(\sigma+\delta)$ *P*, *Q*, and *R* branches occur in the vapor according to Mecke, and the minima corresponding to these may be seen in the vapor curve of Fig. 2. In the solution three minima occur. The strongest, at 1.900μ, lies exactly under a vapor minimum and falls among the strongest lines of the *P* branch. Two weaker bands appear at 1.876μ and 1.861μ. The first of these coincides with a set of the strongest lines of the *Q* branch, whereas the second falls under a less pronounced vapor minimum corresponding to a region of overlapping *Q* and *R* branches. Its center falls at the position of a strong line of the *R* branch and between two fairly strong lines of the *Q* branch, which are shown with their appropriate intensities just above the short wave-length solution minimum in Fig. 3. There is no solution minimum coinciding with the strongest part of the *R* branch.

In the 1.135μ band $(\sigma+\pi+\delta)$ the transmission minimum of the solution falls at 1.145μ which is exactly in the midst of a group of lines classified by Mecke as a *P* branch (not shown in the figure). The vapor minimum corresponding to this is

just perceptible in Fig. 4. The Q branch in the vapor curve is very weak (too weak to be seen in the reproduction of the figure), but the R branch is strong and corresponds to the minimum at 1.125μ. There is no solution minimum that coincides with the R or Q branch of the vapor band.

The absorption of the solution in the 3μ region (Fig. 5) was examined for us by Mr. Waldo Lyon with a Hilger rocksalt instrument. The measurements were difficult to obtain with the instrument available, so that only small sections of the absorption curves are shown. They show not only the characteristic shift of the band toward short wave-lengths from its liquid position but indicate that it is double. The slit width for curve B corresponded to 0.05μ and for curve C was decreased to correspond to 0.04μ. The centers of the two minima in the solution spectrum lie at 2.65 and 2.80μ and are accurate to about 0.04μ. The shoulder in the liquid curve falls between these two values.

Discussion

Two alternative correlations of the vapor and solution bands appear to be reasonable. A correlation can be made based on either the absence or the presence of a shift in the positions of the vibrational centers of the solution bands with respect to those of the vapor.

If it is assumed that no shift occurs (or one less than 15–20 cm^{-1}), an assumption which is in agreement with the fact that seven minima in four combination bands of the solution spectrum coincide with minima in the vapor spectrum, it follows from the behavior of the 1.379 and 1.135μ bands that intensities are altered in such a way that in the solution P branches are strong, Q branches are weak, and R branches are absent. If this be the case, then the short wave-length solution minimum of the 1.875μ band must be identified with the two Q branch lines at which it falls, and not with the R branch line which also occurs at this position.

A correlation of each solution minimum, however, with the first strong vapor minimum on its short wave-length side can be made. This assumes a shift which, despite the fact that it varies from band to band, meets the requirement that it is the same for the Q and R branches within a given band, a requirement which seems to be a necessary criterion for a shift of the vibrational centers. For this correlation Q branches are strong, R branches are intermediate in intensity, and P branches are absent. The wave number differences between the solution spectrum and vapor spectrum minima correlated in this way are 103 and 122 cm^{-1} for the 1.379μ band (an agreement within the error of measurement), 71, 76, and 76 cm^{-1}, respectively, for the Q and the two R branch minima of the 1.875μ band, and 156 cm^{-1} for the minimum of the 1.135μ band.

For the 3μ region a similar ambiguity in identification is encountered. The two vapor centers of the σ and π fundamentals are given by Mecke as 2.67μ and 2.80μ, the latter being optically inactive or very weak in the vapor. For the 2.67μ band the P, Q, and R branches form minima in the vapor at about 2.76, 2.67, and 2.59μ, respectively. The question whether

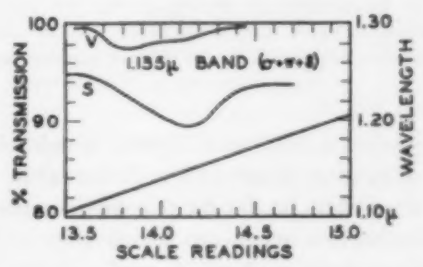

FIG. 4. 1.1μ region. Percent transmission scale reading curves; wave-length scale reading dispersion curve. V, vapor band. S, solution band.

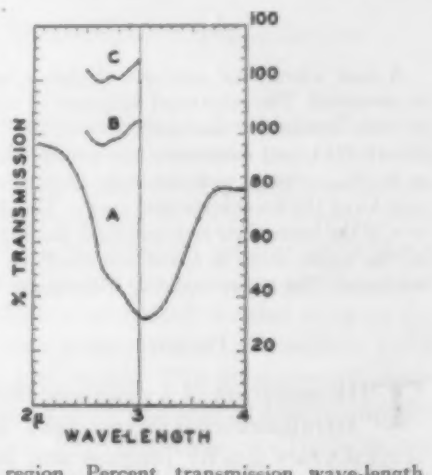

FIG. 5. 3μ region. Percent transmission wave-length curves. A, 0.01 mm of liquid water. B, 18 cm of saturated solution of water in CS_2. C, same as B, but with slits narrowed.

the two minima in the solution spectrum at 2.65 and 2.80μ should be identified with the centers of the σ and π bands, the latter occurring through a breakdown of selection rules in the solution, cannot be settled at present. A significant fact is the agreement of the position of the shoulder in the liquid curve with the center of the solution doublet. It suggests that the minimum in the liquid on the long wave-length side of the solution band is caused by polymer or lattice couplings and that in the liquid free molecules still exist in sufficient numbers to produce their own type of absorption without appreciable shift with respect to their absorption in solution.

The question of the existence of line structure in the solution spectrum also cannot be answered with the present resolving power. The fact that some structure which appears in the vapor in the 1.875μ band seems to be absent in the solution spectrum makes it likely that line structure is wiped out by the broadening of the vibrational centers caused by the perturbing effects of the carbon disulfide molecules. Broadening of the order of 10–20 cm^{-1}, the distance between individual lines, would be sufficient to wipe out such structure.

The structure which the bands of the solution spectrum show indicates that regardless of which of the two suggested correlations turns out to be the correct one rotation of the molecules in the solution occurs. The occurrence of free rotation under these conditions can be predicted on the basis of the work of Debye. Debye[3] has calculated that in liquid water a molecule must possess an energy of 10 kT before it can rotate 90° in the field of its neighbors. If his method is applied to the water molecule in benzene, the case for which its electric moment is known, the energy E that it must possess before it can turn through 90° is approximately kT. This follows from Debye's equations, $y=E/kT$, and $R(y)=1-L^2(y)$, where $L(y)$ is Langevin's function, and $R(y)$ is the ratio of the molar polarization of the molecule in solution (64 cm^3) to that of the free molecule (71 cm^3). Since the dipole behavior of water in carbon disulfide seems likely to differ little from its behavior in benzene, this criterion shows that free rotation will very probably occur.

JUNE 15, 1937 PHYSICAL REVIEW VOLUME 51

The Structure of the α and β Band Systems of SiF

EUGENE H. EYSTER
California Institute of Technology, Pasadena, California
(Received February 18, 1937)

A new vibrational analysis of the α system of SiF is presented. The rotational structure of the (0, 0) band of this system is analyzed, giving $B_0''=0.5795$ and $B_0'=0.5743$, and confirming the nature of the transition to be $^2\Pi_{reg.}\rightarrow{}^2\Pi_{reg.}$, with the upper state extremely near to case b and the lower state near case a. The doublet separation in the lower state is determined, but the spin doubling in the upper state is found too small to be accurately evaluated. The A type doubling is discussed. The rotational structure of the (0, 0) band of the β system is also analyzed, and the transition confirmed to be of the type $^2\Sigma\rightarrow{}^2\Pi_{reg.}$, the $^2\Pi$ state being the lower state in the α system. For the $^2\Sigma$ state $B_0=0.622$ is obtained, being less accurate than the values for the other two states because of experimental difficulties encountered in photographing this band. The spin doubling in the $^2\Sigma$ state is discussed, and the constants of the known electronic states of SiF are summarized.

Introduction

THE spectrum of a discharge through silicon tetrafluoride gas was carefully photographed several years ago by Johnson and Jenkins,[1] who discovered a large number of strong bands in the region between 2100 and 7000A, in addition to the blue system observed by Porlezza[2] in 1911. They were able to divide this entire spectrum into five band systems, to which they assigned the designations α, β, γ, δ, and ϵ. Vibrational

[1] Johnson and Jenkins, Proc. Roy. Soc. **A116**, 327 (1927).

[2] Porlezza, Rend. Acad. Linc. **20**, 488 (1911); also **33**, 283 (1924).

analyses of the α and β systems were proposed, and a rotational analysis of the strong band at 4368A, called the (0, 0) band of the former, attempted. Their results led them, however, to rather improbable conclusions concerning the emitter of the spectrum. It was subsequently shown in this laboratory, by Badger and Blair,[3] that the band at 4368A was of a more complex nature than had been supposed from the apparently simple structure at its origin. A new interpretation of the original band head data was recently given by Asundi and Samuel,[4] who proposed vibrational analyses for the α, β, and γ systems, attributing the first to a $^2\Pi \rightarrow {}^2\Pi$, and each of the latter to a $^2\Sigma \rightarrow {}^2\Pi$ transition. While their analyses of the β and γ systems are satisfactory, that of the α system not only appears incompatible with the observed band intensities, but also gives as the ratio A/B for the upper state, which must be very near to case b because of the strong satellite branches, the value 48, which is certainly many times too large.

In the following report is presented a new interpretation of these data which removes the two above objections, and also rotational analyses of the (0, 0) bands of both the α and β systems.

Experimental

For all of the photographs employed in this investigation, the spectrum was excited by a discharge through silicon tetrafluoride gas, in essentially the manner described by Johnson and Jenkins. The excellent set of high dispersion plates of the α system obtained in this laboratory by Dr. C. M. Blair, who has kindly placed them at my disposal, were taken in the third order of a 21-foot concave grating, where the dispersion was 0.78 A/mm. The bands appeared with such great intensity that a small air-cooled Pyrex discharge tube with aluminum electrodes provided an adequate source. Exposures were of the order of one to two hours. The lines were relatively sharp, and all could be easily measured directly under the comparator with respect to standard iron lines in the third order.

The β system was photographed by the author in the fourth order of the same grating, obtaining a dispersion of 0.58 A/mm. A filter consisting of a saturated solution of very pure nickel sulfate was found effective in separating this order from the third, which contained some of the bands of the much stronger α system. A 5 mm layer completely removed the region of the spectrum between 3600 and 4300A, but was very transparent in the ultraviolet. The low intensity of the β system, the high dispersion, and the poor reflecting power of the grating in this region of the spectrum made adequate exposures difficult to obtain. A large Pyrex discharge tube with a quartz window and massive aluminum electrodes was used. It was completely water cooled, and run on the secondary of a 5 kva General Electric transformer. The silicon tetrafluoride was pumped continuously through the tube at about 1 mm pressure, and the voltage in the primary adjusted to give maximum intensity. The most satisfactory plates were exposed for fifty hours, but even then much of the structure was difficult or impossible to measure directly under the comparator. Consequently most of the lines were measured on enlarged microphotometer curves, using as references the strong lines of the Q branches, which were directly measurable on the plates with respect to iron lines in the third order. Test measurements of a number of standard iron lines photographed in the second and third orders have disclosed no systematic error arising from the use of the method of coincidences with this grating.

The Structure of the α System

Vibrational analysis

Careful consideration of the high dispersion plates of the α system reveals that all strong heads may be grouped in pairs of approximately equal intensity, separated by an interval very nearly equal to the doublet separation in the β system. Each strong head is, in addition, accompanied by an apparently weaker head on the high frequency side, so that a complete band consists of four heads. The strongest of these bands, which includes the head at 4368A, appears to be the (0, 0) band of the system. The principal sequence can be traced to the (8, 8) band, and the first four bands of the (1, 0) sequence are clearly visible, though many times weaker than the

[3] Badger and Blair, Phys. Rev. **47**, 881 (1935).
[4] Asundi and Samuel, Proc. Ind. Acad. Sci. **3**, 346 (1936).

former. The (0, 1) and (5, 5) bands are both rather weak and seem to be in almost perfect coincidence, but some of the higher members of the (0, 1) sequence are observed, separated from the overlapping bands of the principal sequence. A few bands of the (0, 2) sequence are also present, but too weak to have been accurately measured. This analysis of the data of Johnson and Jenkins is presented in Table I.

Comparison of the $\Delta G''(v)$ values obtained from the strong heads with those obtained by Asundi and Samuel from the Q heads of the β system shows satisfactory agreement, and indicates that these two systems do indeed possess a common lower state. Since band heads, instead of origins, have been used, differences are to be expected, but these should decrease for higher values of v, since the heads appear to draw in toward the origins in ascending each sequence, approaching rather rapidly some nearly constant separation. Such is seen to be the case. From the $\Delta G'(v)$ values the vibrational constants of the upper state may be determined, and when most weight is given those differences for which v is

TABLE I. *Vibrational analysis of the α system of SiF.*

v' \ v''	0	1	2	3	4	5	6	7	8	
0	22958.4 22886.2 22780.1 22718.3	—— 22040.1 —— 21878.2	—— —— —— 21037							687.7
1	23613 23573.9 23448.4 23411.6	22789.4 22729.9 22613.4 22565.9	—— 21900 —— ——	—— —— —— 20911						676.5
2		23440.1 23404.3 23772.4 23242.4	22610.7 22568.1 22442.8 22405.4	—— —— —— 21577	—— 20930 —— 20761					659.0
3			23256.1 23226.7 23090.1 23065.0	22434.2 22399.1 22267.4 22236.9	21622 21577 21456 21413	—— 20733 —— 20611				642
4				23066.3 23041.7 22901.3 ——	22252.8 22222.9 22086.4 22061.0	—— 21413 —— 21252	—— 20611 —— 20448			627
5						—— 22040.1 —— 21878.2	—— —— —— ——	—— —— —— 20421		
6							—— 21851.5 —— 21689	—— —— —— ——	—— —— —— 20112	
7								—— 21655 —— 21497	—— —— —— ——	
8									—— 21456 —— ——	↑
	845.3	836.0	827.9	817.4	809.5	803 (α system)	←	Means of first		
	847.3	838.2	828.0	817.7	811.5	800.8 (β system)		differences		

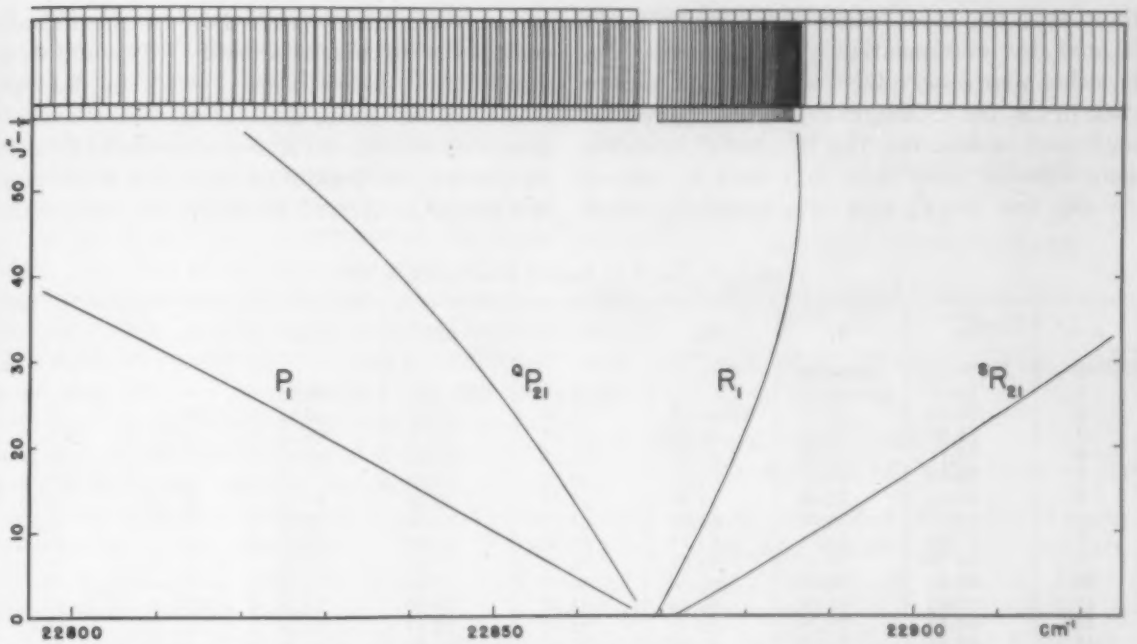

FIG. 1. The lines, disposition of branches, and Fortrat diagram of the high frequency sub-band of the (0, 0) band of the α system. The two unmarked lines near the origin are the first two lines of the weak Q_1 branch.

large, the results should be rather reliable. The best values obtained by this method are:

$$\omega_e = 710.9 \text{ cm}^{-1}, \qquad x_e\omega_e = 8.6 \text{ cm}^{-1}.$$

These results at once imply certain conclusions concerning the electronic states involved in the α system. Since the lower state seems certainly to be $^2\Pi$, the absence of strong Q branches at the origin of the (0, 0) band means that the upper state must also be $^2\Pi$. But the approximate equality of the doublet separations in the α and β systems suggests that this $^2\Pi$ state is very near to case b, under which circumstances branches violating the Σ selection rule, as observed in the ultraviolet spectrum of O_2^+ by Stevens,[5] are to be expected. Each band would then include four head forming branches, as observed in the α system. Since $\omega_e'' - \omega_e'$ is nearly equal to the doublet separation in the lower $^2\Pi$ state, overlapping of bands is so complete that the rotational analysis has been of necessity limited to the (0, 0) band.

Rotational analysis

The analysis of the (0,0) band of the α system, whose four heads occur at 4354, 4368, 4388, and 4400A, was begun on the assumption that it arose from a transition between states of the type described above. In the most general case, such a band is divided into two twelve-branch sub-bands, separated by a frequency equal approximately to the magnetic coupling constant, A''. The high frequency sub-band includes the $^SR_{21}$, R_1, $^RQ_{21}$, Q_1, $^QP_{21}$, and P_1 branches, and the low frequency component the R_2, $^QR_{12}$, Q_2, $^PQ_{12}$, P_2, and $^OP_{12}$ branches, each of which is itself a double branch because of the Λ type doubling of the rotational levels. Actually, however, the latter is small, and the resulting four Q branches are not only weak, but also coalesce with their P and R branch neighbors when the spin doubling in the upper state is small, which proves to be the case in this system. Hence each sub-band consists essentially of four branches, whose arrangement is shown in Fig. 1 for the high frequency component of the (0, 0) band. The appearance of the other sub-band is very similar to that shown, with the positions of regular and satellite branches interchanged.

The lines of the $^SR_{21}$ and R_2 branches, which occupy analogous positions in the two sub-bands, were completely free from overlapping beyond

[5] Stevens, Phys. Rev. 32, 1292 (1931).

their first ten lines, which were hence easily located by extrapolation. The R_1 and ${}^{Q}R_{12}$ branches were observable from their first lines to their heads, but in neither case could the returning branch be detected. The ${}^{Q}P_{21}$ and P_2 branches were followed from their first lines to beyond $J=60\frac{1}{2}$, but the P_1 and ${}^{O}P_{12}$ branches, whose spacings are about twice those of the former, coincided with them at around $J=19\frac{1}{2}$, and were impossible to follow below $J=15\frac{1}{2}$. In the high frequency sub-band, these coincidences were so good that the P_{21} and R_1 branches were mistaken by Johnson and Jenkins for the P and R branches of a simple $\Sigma\rightarrow\Sigma$ band. Since the first lines of the

TABLE II. *The (0, 0) band of the α system of SiF.*

$J-\frac{1}{2}$	${}^{S}R_{21}$	R_1	${}^{Q}P_{21}$	P_1	R_2	${}^{Q}R_{12}$	P_2	${}^{O}P_{12}$
0	22871.33	22869.24						
1	73.08	69.77		22866.64	22712.38	22709.13		22705.96
2	74.82	70.36	22866.89	64.80	14.07	09.64	22706.32	04.09
3	76.55	70.89	66.30	62.97	15.75	10.14	05.48	02.22
4	78.27	71.44	65.70	61.15	17.41	10.63	04.77	00.36
5	79.98	71.97	65.11	59.33	19.05	11.11	04.13	698.47
6	81.68	72.49	64.50	57.57	20.68	11.57	03.46	96.65
7	83.37	72.99	63.88	55.77	22.30	12.02	02.82	94.80
8	85.05	73.54	63.25	54.06	23.90	12.48	02.10	93.00
9	86.70	74.05	62.62	52.25	25.48	12.97	01.38	91.16
10	88.40	74.57	62.00	50.47	27.05	13.33	00.64	89.23
11	90.05	75.04	61.33	48.63	28.60	13.73	699.94	87.32
12	91.70	75.55	60.70	46.89	30.13	14.13	99.17	85.47
13	93.30	76.02	60.03	45.06	31.65	14.54	98.39	83.58
14	94.95	76.50	59.38	43.24	33.13	14.91	97.58	81.65
15	96.54	76.97	58.69	41.39	34.63	15.25	96.78	79.67
16	98.16	77.43	58.03	39.58	36.09	15.55	95.95	77.70
17	99.76	77.91	57.35	37.77	37.54	15.82	95.10	75.68
18	901.32	78.34	56.65	35.90	38.96	16.13	94.24	73.69
19	02.89	78.77	55.93	34.01	40.35	16.40	93.37	71.66
20	04.49	79.21	55.22	32.19	41.77	16.67	92.49	69.66
21	06.05	79.59	54.53	30.34	43.15	16.94	91.63	67.60
22	07.59	80.02	53.80	28.38	44.51	17.13	90.70	65.55
23	09.12	80.43	53.06	26.59	45.87	17.38	89.76	63.44
24	10.66	80.80	52.29	24.66	47.17	17.57	88.80	61.40
25	12.19	81.18	51.54	22.78	48.48		87.81	59.27
26	13.68	81.61	50.77	20.86	49.75		86.83	57.10
27	15.17	81.96	49.97	18.94	51.01		85.86	54.96
28	16.65	82.33	49.18	17.02	52.27		84.84	52.83
29	18.12	82.69	48.39	15.10	53.49		83.80	50.63
30	19.59	83.03	47.57	13.07	54.68		82.73	48.47
31	21.02	83.33	46.77	11.18	55.88		81.63	46.25
32	22.43	83.65	45.93	09.22	57.06		80.54	44.03
33	23.86	83.91	45.09	07.25	58.17	head	79.44	41.76
34	25.25	84.18	44.22	05.25	59.27	18.38	78.31	39.48
35	26.64	84.39	43.34	03.26	60.38		77.15	37.21
36	28.00	84.62	42.47	01.11	61.43		75.96	34.93
37	29.35	84.90	41.60	799.18	62.47		74.76	32.57
38	30.69	85.06	40.68	97.16	63.49		73.52	30.21
39	31.97	85.27	39.75	95.11	64.50		72.30	27.86
40	33.31		38.82	93.05	65.44		71.06	25.49
41	34.54		37.86	90.98	66.41		69.75	23.11
42	35.81		36.87	88.87	67.34		68.45	20.63
43	37.13		35.91	86.78	68.18		67.12	18.18
44	38.30		34.91	84.63	69.10		65.81	15.70
45	39.47		33.85	82.51	69.91		64.40	13.27
46	40.66	head	32.82	80.36	70.74		62.97	10.74
47	41.78	86.22	31.79	78.15	71.51		61.54	08.11
48	42.97		30.70	76.02	72.32		60.09	05.33
49	44.05		29.63	73.83	72.97		58.63	
50	45.12		28.51	71.55	73.65		57.15	
51	46.15		27.33	69.34	74.35		55.58	
52	47.23		26.21	67.08	74.96		53.99	
53	48.22		25.00	64.76	75.59		52.42	
54	49.17		23.77	62.29	76.19		50.81	

Also the lines $Q_1(\frac{1}{2})=22867.47$ and $Q_1(1\frac{1}{2})=22868.04$. ${}^{P}Q_{12}(1\frac{1}{2})$ was too confused to be measured.

R_1, ${}^QR_{12}$, ${}^QP_{21}$, and P_2 branches were visible, their numberings were determined at once. The first lines, and hence the numberings, of the extrapolated ${}^SR_{21}$ and R_2 branches were then chosen to provide the correct number of missing lines. The numbering and the frequency of the lower lines of the two remaining branches were determined by means of the term differences in the upper state. The ${}^RQ_{21}$ and Q_1 branches were found to have coalesced with the R_1 and ${}^QP_{21}$ branches, but since the Q_1 branch begins with $J=\frac{1}{2}$ and the ${}^QP_{21}$ with $J=2\frac{1}{2}$, the first two lines of the former were observed, and proved to be of the expected low intensity. In the other sub-band an analogous situation occurs, the first line of the ${}^PQ_{12}$ branch being observable, since it begins with $J=1\frac{1}{2}$, while the P_2 branch begins with $J=2\frac{1}{2}$. All of the lines below $J=55\frac{1}{2}$ are listed in Table II, the measurements being made in all cases to the center of the Λ doublets.

The rotational terms of the upper and lower states may be expressed by the following equations, which follow immediately from the application to the ${}^2\Pi$ state of the general expressions for case a and case b molecular multiplets,[6] assuming the Λ doubling negligible in the upper state, and including all functions independent of J, K, and Σ as the quantity T_0, which will hence be constant for any one band:

$$\begin{aligned}
T_1'(K)&=T_0'+f(K,+\tfrac{1}{2})+B_v'K(K+1)\\
&\quad+D_v'K^2(K+1)^2+\cdots,\\
T_2'(K)&=T_0'+f(K,-\tfrac{1}{2})+B_v'K(K+1)\\
&\quad+D_v'K^2(K+1)^2+\cdots,\\
T_1''(J)&=T_0''-A''/2-B_{v1}''^*/4+\phi_i(-\tfrac{1}{2},J)\\
&\quad+B_{v1}''^*J(J+1)+D_{v1}''^*J^2(J+1)^2+\cdots,\\
T_2''(J)&=T_0''+A''/2-9B_{v2}''^*/4+\phi_i(+\tfrac{1}{2},J)\\
&\quad+B_{v2}''^*J(J+1)+D_{v2}''^*J^2(J+1)^2+\cdots.
\end{aligned}\tag{1}$$

The constants of the lower state marked with asterisks are introduced to allow for a tendency toward case b. They are given, according to the theory of Hill and Van Vleck,[6] by the following expression, for a ${}^2\Pi$ state:

$$B_v^*=B_v(1\pm B_v/A).\tag{2}$$

The value of B_{v2}^* is given by the upper, and of B_{v1}^* by the lower sign.

Aside from the Λ doubling, the term differences are given by the relations:

$$\begin{aligned}
\Delta_2T_1'(J)&=R_1(J)-P_1(J)\\
&={}^QR_{12}(J)-{}^QP_{12}(J),\\
\Delta_2T_2'(J)&=R_2(J)-P_2(J)\\
&={}^SR_{21}(J)-{}^QP_{21}(J),\\
\Delta_2T_1''(J)&=R_1(J-1)-P_1(J+1)\\
&={}^SR_{21}(J-1)-{}^QP_{21}(J+1),\\
\Delta_2T_2''(J)&=R_2(J-1)-P_2(J+1)\\
&={}^QR_{12}(J-1)-{}^OP_{12}(J+1).
\end{aligned}\tag{3}$$

Eqs. (1) show that, if the small quantities $\Delta_2f(K, J-K)$ be neglected:

$$\begin{aligned}
\Delta_2T_1'/2(2K+1)&=\Delta_2T_2'/2(2K+1)\\
&=B_v'+2D_v'(K^2+K+1)+\cdots.
\end{aligned}\tag{4}$$

Hence when the left side of (4) is plotted against $(K+\frac{1}{2})^2$, a straight line of slope $2D_v'$ and intercept $B_v'+\frac{3}{2}D_v'$ should be obtained. Such a graphical treatment of the term differences obtained from the ${}^SR_{21}$, ${}^QP_{21}$, R_2, and P_2 branches enabled B_0' to be evaluated within an uncertainty of ±0.0001 cm^{-1}, and D_0' within limits of about ±1.5 percent. Exactly analogous expressions in terms of J apply to the lower state, and the constants were found in the same manner, with comparable results. The values so determined are as follows:

$$\begin{aligned}
B_0''&=0.5795\text{ cm}^{-1}, & D_0''&=-1.12\times10^{-6}\text{ cm}^{-1},\\
B_0'&=0.5743\text{ cm}^{-1}, & D_0'&=-1.59\times10^{-6}\text{ cm}^{-1}.
\end{aligned}$$

The value of A'' was determined by the following relation, obtained from Eqs. (1) by neglecting the term $\phi_i(\Sigma, J)$:

$$\begin{aligned}
A''+(B_{01}''^*-9B_{02}''^*)/4&={}^QP_{21}(J)\\
&\quad-P_2(J)-J(J+1)(B_{02}''^*-B_{01}''^*)+\cdots.
\end{aligned}\tag{5}$$

The right-hand expression was found to be constant within the experimental error, when evaluated for the first twelve lines of the two branches, and gave the average value of 160.83 cm^{-1}. Hence, with Eq. (5), the value of A'' may be obtained, and is found to be $+161.99$ cm^{-1}, making A''/B_0'' equal to $+279.53$. The latter indicates that the lower ${}^2\Pi$ state is, as was assumed, intermediate between case a and case b, but much closer to the former.

The intensity of the satellites, the doublet separation in the α system, and the coalescence of branches already remarked indicate that the

[6] Mulliken, Rev. Mod. Phys. **2**, 105, 114 (1930).

upper $^2\Pi$ state is very near to case b. It would hence be anticipated[7] that the spin doublet separation be given by the expression:

$$\Delta f(K)=[A'/K(K+1)+\gamma_i](K+\tfrac{1}{2}), \quad (6)$$

where the value of γ_i is different for the c and d sub-levels.[8] Since γ_i is almost negligibly small in this case, and since, moreover, the Λ doublets are unresolved at low values of J, it may be replaced by an average value $\gamma_{av.}$, in the calculation of A'. With this assumption, Eq. (6), combined with Eqs. (1), gives the expression:

$$[{}^qR_{12}(J)-P_2(J+1)]/(J+1)-2B_{02}''^* -4J^2D_{02}''^*=A'/(J+\tfrac{1}{2})(J+\tfrac{3}{2})+\gamma_{av}. \quad (7)$$

An analogous equation applies in the other sub-band. The left-hand expression in (7) plotted against $1/(J+\frac{1}{2})(J+\frac{3}{2})$ should give a straight line of slope A' and intercept $\gamma_{av.}$. When actually attempted, it was found that these quantities were of the order of magnitude of the experimental errors, so that no unique line was determined. It can only be stated that A' is surely positive, and probably less than 0.10 cm^{-1}. This means that A'/B_0' is about 0.17, and that the upper state is as close to case b as the $^2\Pi$ state of BeH.[9]

The origins of the two sub-bands cannot be precisely determined without exact values of A' and γ_i, but the following values, obtained from the R_1 and P_2 branches are probably quite accurate:

$$\nu_{01}=T_0'-T_0''+A''/2+B_{01}''^*/4=22868.50 \text{ cm}^{-1},$$
$$\nu_{02}=T_0'-T_0''-A''/2+9B_{02}''^*/4 =22707.70 \text{ cm}^{-1}.$$

The P_2 and ${}^qP_{21}$ branches can be followed out to very high values of J, where the Λ doublets are well resolved. Between $J=35\frac{1}{2}$ and $70\frac{1}{2}$, the doubling in the $^2\Pi_i$ state is well represented by the expected relation:[10]

$$\phi_c(J)-\phi_d(J)=a(J+1/2). \quad (8)$$

The constant a is found to be 0.0067 cm^{-1}. The doubling in the $^2\Pi_{ii}$ state is less accurately observable because of the overlapping (1, 1) band, but beyond $J=40\frac{1}{2}$ it is of about the same order of magnitude, but increasing more rapidly and nonlinearly with $J+1/2$. This behavior of the Λ doublets indicates that they arise almost entirely from doubling of the rotational levels of the case a $^2\Pi$ state.

[7] Mulliken and Christy, Phys. Rev. **38**, 87 (1931).
[8] Mulliken, Rev. Mod. Phys. **2**, 108, 110 (1930).
[9] Watson and Parker, Phys. Rev. **37**, 167 (1931).
[10] Mulliken, Rev. Mod. Phys. **3**, 113 (1931).

The Structure of the β System

Vibrational structure

Asundi and Samuel's analysis of the band head data attributes the β system to a $^2\Sigma\rightarrow{}^2\Pi$ transition, but the constants of Johnson and Jenkins have been but slightly altered, since the doublet separation was found to be very nearly equal to $\omega_e'-\omega_e''$. The resulting superposition is remarkably accurate in the bands near the origin of the system, measurable separations commencing only in the weaker (2, 0), (0, 2), and (0, 3) sequences, where the extra heads were supposed by Johnson and Jenkins to arise from a vibrational isotope effect. Of course the isotopic displacement coefficient failed to agree with any calculated from masses of silicon isotopes. Careful investigation of heavily exposed photographs of this system taken on a quartz Littrow spectrograph giving a dispersion of 3.7A/mm in the vicinity of 2900A showed no evidence of true isotopic heads.

Because of the coincidence remarked above, only the low frequency sub-band of the first band of each sequence would be expected to be free from complete overlapping. Fortunately, however, the Franck-Condon diagram for the system is a narrow parabola, the only member of the principal sequence appearing with appreciable intensity being the (0, 0) band itself. Beside being confused by this superposition, the (0, 1) and (1, 0) bands were too weak after 50 hours exposure to permit analysis, which consequently was limited to the (0, 0) band.

Rotational analysis

The (0, 0) band, whose heads occur at 2880, 2881, 2893, and 2894A, would be expected to consist of six regular and two satellite branches, if the spin doubling in the $^2\Sigma$ state were small. Such is found to be the case, though measurable spin doublets are observed in the higher members of the Q_1 branch. Of the six regular branches, three are head forming, while the fourth head of the complete band is formed by one of the satellites. All six main branches are observed, but only the head forming ${}^qP_{12}$ satellite is found, and its individual lines, despite their favorable

location, were not measurable. The ${}^{s}R_{21}$ branch is presumably hidden by the stronger regular branches. The observed intensity relations among these branches confirm Asundi and Samuel's conclusion that the β system arises from a ${}^{2}\Sigma \rightarrow {}^{2}\Pi$ transition.

Because of the low total intensity, of which, moreover, less than half is divided among the P and R branches, the latter were hidden at low values of J by the strong Q branches, while all of the branches of the low frequency sub-band were lost when they overlapped the P_1 head of the second sub-band. The latter branch, moreover, could not be followed through the strong Q_1 head. It was therefore necessary to number the lines in an indirect manner. Only one method of numbering gave both the same term differences in the upper state, given by Eqs. (3), and also a reasonable value of D_0'. The term differences in the lower state were then found in agreement with those obtained from the α system. The Q branches were numbered by the approximate relation

$$R(J)-Q(J)=Q(J+1)-P(J-1). \qquad (9)$$

TABLE III. *The (0, 0) band of the β system of SiF.*

$J-\frac{1}{2}$	P_1	Q_1	R_1	${}^{s}P_{12}$	P_2	Q_2	R_2
0							
1						34559.91	
2	head	head		head	head	60.78	
3	34702.43	34717.39		34559.98	34556.47	61.76	
4						62.76	
5						63.81	
6						64.99	
7						66.22	
8		18.04				67.54	
9		18.47				69.61	
10		18.94				70.51	
11		19.54				72.18	
12		20.23				73.85	
13		——				75.69	
14		——				77.62	
15		——	34740.86			79.63	
16		22.85	43.15		61.16	81.63	
17		23.83	45.65		62.15	83.79	
18		24.97	48.12		63.04	85.98	
19		26.26	50.61		64.10	88.32	
20		27.57	53.18		65.41	90.83	34618.71
21		29.05	55.88		66.62	93.39	22.51
22		30.60	58.71		68.04	95.98	26.37
23		32.23	61.22		69.41	98.60	30.46
24	03.35	33.94	64.07		70.93	601.37	34.46
25	03.92	35.82	67.24		72.68	04.28	38.41
26	04.52	37.70	70.17		74.34	07.31	42.54
27	05.18	39.71	73.32		76.04	10.33	46.78
28	05.96	41.84	76.68		77.90	13.71	51.10
29	06.90	44.11	80.04		79.94	17.56	55.49
30	07.82	46.38	83.54		82.09	20.14	60.11
31	08.84	48.76	86.95		84.16	23.57	64.80
32	09.97	51.18	90.50		86.40	27.10	69.53
33	11.16	53.95	94.10		88.83	30.67	74.56
34	12.63	56.56	98.13		91.17	34.30	79.12
35	14.17	59.39	802.00		93.76	38.09	
36	15.78	62.24	05.78		96.36	41.93	
37		65.16	09.80		98.99	45.87	
38		68.33	14.09		601.77	49.86	
39		71.50	18.36		04.63	53.96	
40		74.88	22.68		07.65	58.07	
41		78.04	27.23		11.04	62.46	
42		81.39	32.31		14.26	66.78	
43		85.02	37.03		17.51	70.07	
44		88.57	41.95		20.72	75.75	
45		92.36	47.06		24.34		
46		96.11	52.12				
47		800.12	57.25				
48		04.21	62.45				
49		08.25	67.42				
50		12.47	72.77				

TABLE IV. *Constants of the SiF molecule.*

STATE	$T_e+G(0)$ (cm^{-1})	$T_e+G(0)$ (volts)	ω_e (cm^{-1})	$x_e\omega_e$ (cm^{-1})	B_0 (cm^{-1})	r_0 (A)
$C^2\Sigma$	39531.5[1]	4.877[1]	891.7[1]	6.2[1]		
$B^2\Sigma$	34717.39	4.283	1011.2[1]	4.8[1]	0.662	1.54
$A^2\Pi_{reg.}$	22868.50	2.821	710.9	8.6	0.5743	1.606
	160.83	0.020				
$X^2\Pi_{reg.}$	0	0	856.7[1]	4.7[1]	0.5795	1.599

[1] Asundi and Samuel, Proc. Ind. Acad. Sci. **3**, 346 (1936).

An independent numbering was also possible, since when the first differences are plotted against J, they extrapolate to $-B_{01}''^*$ at $J=-1/2$, for the Q_1, and to $+B_{02}''^*$ at $J=-3/2$, for the Q_2 branch. The two numberings were found identical, though it seems impossible to obtain the Λ doubling in the $^2\Pi$ state by the usual combinations with the Q branches. This is probably to be expected from the small magnitude of the doubling, and the extreme difficulties and certain errors involved in the measurements of the lines. The frequencies and numbering of the lines are shown in Table III.

B_0' was determined by the graphical method already described, but since so few combinations were available, the slope of the line was determined independently by Kratzer's relation

$$D_e=-4B_e^3/\omega_e^2. \tag{10}$$

From the slope so obtained, B_0' was found to be equal to 0.622 cm^{-1}.

From the separations of the Q_1 and $^RP_{21}$ branches, which are measurable beyond $J=50\frac{1}{2}$, the value of the spin doubling coefficient γ was found to be approximately 0.011 cm^{-1}.

CONCLUSION

It is felt that the present analysis establishes with reasonable certainty the nature of three of the electronic states of the SiF molecule, while Asundi and Samuel's vibrational analysis of the γ system suggests the nature of a fourth state to be $^2\Sigma$, though it could scarcely be distinguished with certainty from a close $^2\Delta$ without further investigation. The known constants of these four states are collected in Table IV, where the upper state of the γ system is designated $C^2\Sigma$, in accordance with the conclusions of Asundi and Samuel.

The $A^2\Pi$ state of this molecule has proved to be a most unusual and interesting one. The occurrence of nearly pure case b coupling in the $^2\Pi$ state of so heavy a molecule is itself unique, and the (0, 0) band of the α system, with its visible origin and strong satellite branches, provides an excellent example of the rotational structure of a $^2\Pi$ (case b)$\rightarrow{}^2\Pi$ (case a) band. In addition, this state appears to constitute a genuine exception to such empirical relations as Badger's rule[11] between r_e and ω_e, for while r_e is very nearly the same in the two states, ω_e differs by 145.8 cm^{-1}. Of course, such empirical rules mean only that a fairly consistent relationship has been found to exist between the position of the minimum in the potential functions of ordinary molecules and the value of the second derivative at that point, while their failure in any particular case signifies a deviation of its potential function from the usual type. The $^1\Pi$ state of AlH, for example, is obviously unusual in possessing a dissociation energy of only 0.26 ev, and ω_e is observed to be about 600 cm^{-1} lower than calculated from r_e. Though the extreme case b coupling in the $A^2\Pi$ state of SiF is extraordinary, there exists no obvious correlation between it and the low value of ω_e, for the latter shows no trend away from the normal in the $^2\Pi_u$ state of O_2^+, which approaches case b, nor in the nearly pure case $b^2\Pi$ states of CH or BeH. Since there exist no extended vibrational progressions in the α system, little can be definitely stated concerning the magnitude of the dissociation energy for the $A^2\Pi$ state, and the nature of the potential function at points far from the equilibrium position. It does, however, appear that the two $^2\Pi$ states are derived from the same electronic states of the silicon and fluorine atoms, and should be analogous to the $^2\Pi$ states of O_2^+.

The author is pleased to express his appreciation to Professor R. M. Badger, at whose suggestion this investigation was undertaken, for his encouragement and assistance in its completion, as well as to Dr. C. M. Blair, to whom he is especially indebted for the photographs of the α system, and measurements of several of the branches of its (0, 0) band.

[11] R.M. Badger, J. Chem. Phys. **3**, 710 (1935).

The Spectra of K III, Ca IV, and Sc V,[1] and their Relation to the Spectra of Other Ions in the Isoelectronic Sequence Cl I to Mn IX

P. Gerald Kruger and L. W. Phillips
Department of Physics, University of Illinois, Urbana, Illinois

(Received April 29, 1937)

The successful excitation of highly ionized scandium atoms has enabled the classification of Sc V multiplets which arise from transitions between $3s^23p^5\ ^2P^0$ and $3s3p^6\ ^2S$; $3s^23p^44s\ ^{4,2}P$, ^2D, ^2S. Spectrograms of scandium and calcium have been taken with a twenty-one foot grazing incidence vacuum spectrograph. The large dispersion and resolution of this instrument enabled the above transitions to be identified in Ca IV also. The identification of these multiplets supplies spectroscopic data necessary to complete the study of the isoelectronic regularities in the sequence.

IN chlorine-like ions, the ground state electron configuration $3s^23p^5$ gives rise to a $^2P^0$ term which is inverted. The first excited state is the $^2S_{1/2}$ from the $3s3p^6$ configuration. Still higher lie the terms $^{4,2}P$, ^2D and ^2S from the $3s^23p^44s$ configuration. All of these higher terms combine with the ground state $^2P^0$ to give intense multiplets which are characteristic of the ions in this sequence.

Previously S. G. Weissberg and P. G. Kruger[2] reported the $3s^23p^5\ ^2P^0-3s^23p^44s\ ^2P$ multiplet in Ti VI and suggested a classification of the same multiplet in Ca IV using lines taken from Ekefors'[3] data. At the same time two strong lines were picked as the strongest lines in the corresponding multiplet in Mn IX. A year later in another report[4] the same authors reported the P^0-P multiplet in V VII, Cr VIII and Mn IX and showed that their previous[2] choice for the Mn IX multiplet was incorrect. In the second report[4] the $3s^23p^5\ ^2P^0-3s3p^6\ ^2S$ multiplet in Ti VI, V VII, Cr VIII and Mn IX was also given. This confirmed the new choice of the PP^0 multiplet in Mn IX.

Recently B. Edlén[5] has confirmed all of the previous work[2, 4] and has extended the sequence to Fe X and Co XI. He has also found the $3s^23p^5\ ^2P^0-3s^23p^44s\ ^2D$, ^2S multiplet lines and part of the $^2P^0-^4P$ multiplet from the same configurations.

In this sequence the spectra of Ca IV and Sc V have been very hard to classify. This is true for two reasons. The region where Ca IV is found is very densely populated with lines so that the previous measurements of Ekefors[3] were inadequate as far as resolution is concerned. Moreover scandium is very hard to excite and a satisfactory spectrum was obtained only after trying many different kinds of electrodes. It is the purpose of this paper to present the results of the study of Ca IV and Sc V.

Spectrograms of calcium were taken with a twenty-one foot grazing incidence vacuum spectrograph.[6] The electrodes in this case consisted of a pure copper electrode at negative potential and a positive (grounded) electrode of pure metallic calcium in a copper shell. The power for excitation was supplied by a four-tube kenetron bridge which gave a peak potential of 100 kv and charged a bank of condensers (0.2 mf capacity) which was connected across the vacuum spark gap. Approximately 6000 sparks gave a very good calcium spectrogram.

The most satisfactory scandium electrodes were made by packing a mixture of four parts of scandium oxide and one part boron oxide into a copper (Al) shell electrode and then heating the electrode until the mixture hardened so that the spark would not blow the powder out of the copper shell. Fifteen thousand sparks gave a good scandium spectrogram.

The measurement of our calcium spectrograms showed that only one line (ν297,128 cm^{-1}) of the previously suggested[2] $^2P^0\ ^2P$ multiplet was correct. Two new lines (ν295,047 cm^{-1} and 300,249 cm^{-1}) not in Ekefors'[3] data were found to fit

[1] Some of these data have been reported by L. W. Phillips and P. G. Kruger, Bull. Am. Phys. Soc. Washington Meeting **12**, 28 (1937).
[2] S. G. Weissberg and P. G. Kruger, Phys. Rev. **47**, 798 (1935).
[3] Ekefors, Inaugural Dissertation, *Verlagsbuchhandlung*, (Julius Springer, Berlin, 1931).
[4] S. G. Weissberg and P. G. Kruger, Phys. Rev. **49**, 872 (1936).
[5] B. Edlén, Zeits. f. Physik **104**, 407 (1937).
[6] P. G. Kruger, Rev. Sci. Inst. **4**, 128 (1933).

TABLE I. *Newly classified lines and term values in K III, Ca IV and Sc V of the chlorine sequence.*

		$3s3p^6$	$3s^23p^44s$							
		$^2S_{1/2}$	$^4P_{1/2}(^3P)$	$^4P_{3/2}(^3P)$	$^4P_{1/2}(^3P)$	$^2P_{3/2}(^3P)$	$^2P_{1/2}(^3P)$	$^2D_{3/2}(^1D)$	$^2D_{1/2}(^1D)$	$^2S_{1/2}(^1S)$
	Term Values							225,980	226,341	246,012
K III								(2) 442.518	(5) 441.812	(6) 406.484
$3s^23p^5\ ^2P^0_{3/2}$	0							225,980	226,341	246,012
								(5) 446.830		(8) 410.102
$3s^23p^5\ ^2P^0_{1/2}$	2165							223,799		243,842
	Term Values	152,440	291,373	293,011	294,291	298,175	300,249	314,079	314,373	337,207
Ca IV		(12)* 655.996	(6) 343.203	(15) 341.284	(5) 339.800	(25) 335.374	(2) 333.057	(4) 318.392	(15) 318.093	(5) 296.554
$3s^23p^5\ ^2P^0_{3/2}$	0	152,440	291,373	293,011	294,291	298,175	300,249	314,079	314,373	337,207
		(10)* 669.721		(6) 344.958	(8) 343.444	(5) 338.929	(15) 336.555	(10) 321.593		(4) 299.315
$3s^23p^5\ ^2P^0_{1/2}$	3124	149,316		289,890	291,168	295,047	297,128	310,952		334,096
	Term Values	174,410	387,508	388,857	391,575	395,496	398,437	410,114	410,043	437,503
Sc V		(8) 573.362	(1.5) 258.059	(3) 257.164	(1) 255.379	(15) 252.847	(7) 250.981	(1) 243.835	(12) 243.877	(2) 228.570
$3s^23p^5\ ^2P^0_{3/2}$	0	174,410	387,508	388,857	391,575	395,496	398,437	410,114	410,043	437,503
		(5) 587.938		(1) 260.054	(2) 258.238	(3) 255.646	(10) 253.738	(11) 246.435		(2) 230.852
$3s^23p^5\ ^2P^0_{1/2}$	4328	170,086		384,535	387,240	391,166	394,107	405,786		433,178

* Identified by Bowen, Phys. Rev. **31**, 498 (1928).

the off diagonal lines and the line ν298,201 cm^{-1} previously used was found to be double and resolved into two components (ν298,175 cm^{-1} and 298,205 cm^{-1}) in the second order. These data lead to the classifications given in Table I. Lines from the transitions $3s^23p^44s\,^4P, {}^2D, {}^2S - 3s^23p^5\,^2P^0$ have also been identified, and are given in the same table. Two lines at ν337,207 cm^{-1} and ν334,096 cm^{-1}, previously classified by Ram[7] as $3s^23p^5\ ^2P^0_{3/2,\,1/2} - 3s^23p^43d(^1S)^2D_{3/2}$ have been reclassified as $3s^23p^5\ ^2P^0_{3/2,\,1/2} - 3p^23p^44s(^1S)^2S_{1/2}$. This necessitates a corresponding change in Ram's classification of the two lines ν246,012 cm^{-1} and ν243,842 cm^{-1} in K III. In addition to these two lines, three other lines taken from Ekefors'[3] K III data have been identified as $3s^23p^5\ ^2P^0_{3/2,\,1/2} - 3s^23p^44s(^1D)^2D_{3/2,\,5/2}$. Constant second difference graphs (Fig. 1) and $\Delta\nu^2P^0$ frequency differences support these classifications.

[7] Ram, Ind. J. Phys. **8**, 163 (1933).

The approximate positions of the lines due to transitions from the $3s^23p^44s$ configuration to the ground state of Sc V were predicted by means of constant second difference displacement graphs, shown in Fig. 1. The identification of the lines is unambiguous, due to the relatively few lines in

TABLE II. *Radiated frequencies with constant first differences.*

Ion	$3s^23p^5\ ^2P_{1/2} - 3s3p^6\ ^2S_{1/2}$	Δ_1	$3s^23p^5\ ^2P_{3/2} - 3s3p^6\ ^2S_{1/2}$	Δ_1
A II	107,290	21,155	108,722	21,887
K III	128,445	20,871	130,609	21,831
Ca IV	149,316	20,770	152,440	21,970
Sc V	170,086	20,714	174,410	22,215
Ti VI	190,800	20,704	196,625	22,536
V VII	211,504	20,672	219,161	22,962
Cr VIII	232,176	20,539	242,123	23,168
Mn IX	252,715		265,291	

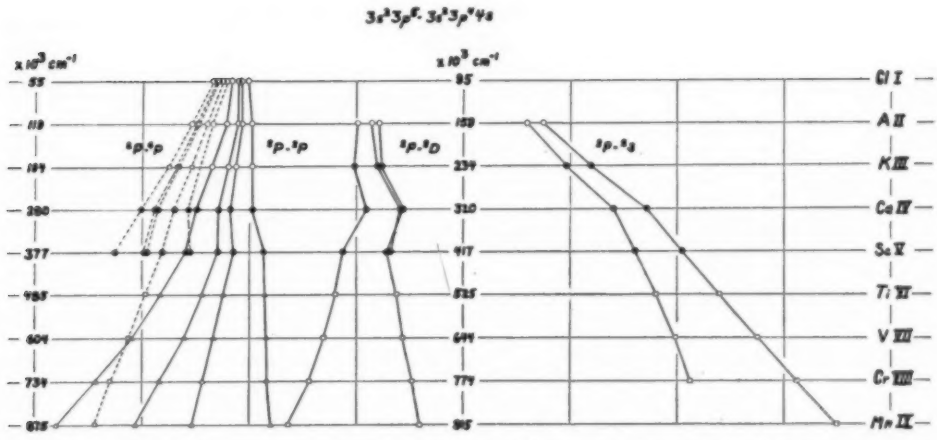

FIG. 1. Displaced frequency diagram; constant second difference 11,000 cm^{-1}. Open circles, data from Bacher and Goudsmit, "Atomic Energy States." Triangles, Weissberg and Kruger. Squares, Edlén. Filled circles, newly identified lines.

the region and the excellent agreement among the values obtained for the ground state separation from the various multiplets. The $3s^23p^44s$-$(^1D)^2D$ term, which is normal in A II, K III and Ca IV, is found to be inverted in Sc V, as it is in succeeding ions of the sequence. An average value of 4328 cm^{-1} is obtained for the separation of the ground state.

The $3s^23p^5\,^2P^0_{3/2,\,1/2} - 3s3p^6\,^2S_{1/2}$ transition has also been identified in Sc V. Table II gives the radiated frequencies and first differences for this transition in all ions of the sequence and shows how well this transition follows the irregular doublet law. These data are shown by the graph in Fig. 2.

Table III gives the radiated frequencies, and first and second differences for the $^2P^0_{3/2} - {}^2P_{3/2}$ transition. The second differences are reasonably constant except for a discontinuity at scandium. This is the first such irregularity that has been found when using graphs like those of Fig. 1 as a guide to aid in the identification of multiplets.

TABLE III. *Radiated frequencies with first and second differences.*

Ion	$3s^23p^5\,^2P^0_{3/2} - 3s^23p^44s\,^2P_{3/2}$	Δ_1	Δ_2
Cl I	74,222		
		64,022	
A II	138,244		10,456
		74,478	
K III	212,722		11,075
		85,553	
Ca IV	298,175		11,668
		97,221	
Sc V	395,496		9,881
		107,102	
Ti VI	502,598		10,952
		118,054	
V VII	620,652		10,886
		128,940	
Cr VIII	749,592		11,037
		139,977	
Mn IX	889,569		

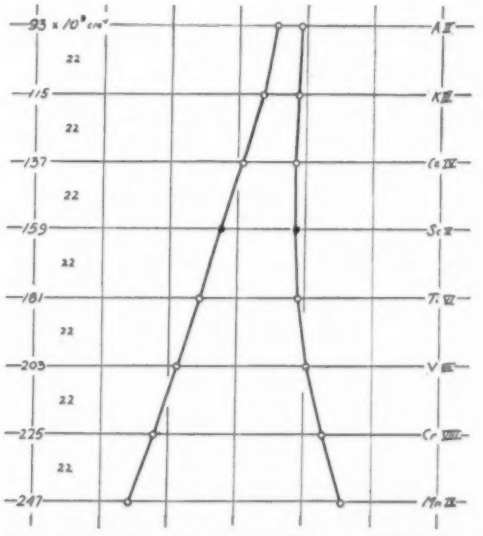

FIG. 2. Displaced frequency diagram $3s^23p^5\,^2P_{3/2,\,1/2} - 3s3p^6\,^2S_{1/2}$. Horizontal scale, 1 div. = 4000 cm^{-1}. Vertical scale, constant first difference is 22,000 cm^{-1}.

The Spectra of Sc IV,* Ti V, Mn VIII and Fe IX in the Isoelectronic Sequence A I to Fe IX

P. GERALD KRUGER, S. G. WEISSBERG AND L. W. PHILLIPS
Department of Physics, University of Illinois, Urbana, Illinois

(Received April 29, 1937)

The successful excitation of scandium in a vacuum hot spark has enabled the completion of the spectroscopic data in the isoelectronic sequence A I to Fe IX and has led to the identification of radiation connecting the higher terms with the ground state ($^1S_0$) in all ions up to and including Fe IX.

IN a previous report[1] the radiation $3p^6\,{}^1S_0 - 3p^5 5s\,{}^3P_1{}^0$, $^1P_1{}^0$ for various ions in this sequence was reported. Since then the spectrum of scandium has been strongly excited and thus it is possible to fill the gaps in the previous report due to a lack of scandium data at that time. At the same time additional data have been obtained in Ti V, Mn VIII and Fe IX.

Newly identified lines are given in Table I. In order to correlate the new data with those previously presented, displaced frequency graphs for ions of the sequence are given in Figs. 1 and 2 and the corresponding data in Tables II and III.

In Table IV are listed the series limits calculated from two members of the $3p^6\,{}^1S_0 - 3p^5 ms\,{}^1P_1{}^0$ series (designated by $L(^1P_1{}^0)$), and the limits $L(^3P_1{}^0)$ calculated from the first two members of the $3p^6\,{}^1S_0 - 3p^5 ms\,{}^3P_1{}^0$ series. A comparison between the difference $L(^1P_1{}^0) - L(^3P_1{}^0)$ and the known $^2P_{3/2,\,1/2}$ splitting in the chlorine-like ions is shown in columns 4 and 5.

Tables V and VI give the revised term values and ionization potentials for all ions of the sequence.

TABLE I. *Newly identified lines in argon-like ions.*

Ions	Relative Intensities	λ(A)	ν(cm⁻¹)	Transitions
Sc IV	6	298.027	335540	$3p^6\,{}^1S_0 - 3p^5 4s\,{}^3P_1{}^0$
	8	293.260	340994	$3p^6\,{}^1S_0 - 3p^5 4s\,{}^1P_1{}^0$
	3	217.187	460432	$3p^6\,{}^1S_0 - 3p^5 5s\,{}^3P_1{}^0$
	2	215.317	464432	$3p^6\,{}^1S_0 - 3p^5 5s\,{}^1P_1{}^0$
Ti V	6	164.450	608088	$3p^6\,{}^1S_0 - 3p^5 5s\,{}^3P_1{}^0$
	5	163.140	612970	$3p^6\,{}^1S_0 - 3p^5 5s\,{}^1P_1{}^0$
Mn VIII	10	124.055	806094	$3p^6\,{}^1S_0 - 3p^5 4s\,{}^3P_1{}^0$
	15	122.168	818544	$3p^6\,{}^1S_0 - 3p^5 4s\,{}^1P_1{}^0$
Fe IX	6	105.236	950245	$3p^6\,{}^1S_0 - 3p^5 4s\,{}^3P_1{}^0$
	8	103.580	965437	$3p^6\,{}^1S_0 - 3p^5 4s\,{}^1P_1{}^0$

TABLE II. *Radiated frequencies with first and second differences. First series members.*

Ion	$3p^6\,{}^1S_0 - 3p^5 4s\,{}^3P_1{}^0$			$3p^6\,{}^1S_0 - 3p^5 4s\,{}^1P_1{}^0$		
A I	93743			95392		
		69494			71070	
K II	163237		11196	166462		10161
		80690	10923		81231	
Ca III	243927			247693		12070
		91613	9723		93301	
Sc IV	335540			340994		9485
		101336	11088		102786	
Ti V	436876			443780		11087
		112424	10608		113873	
V VI	549300			557653		10919
		123032	10730		124792	
Cr VII	672332			682445		11307
		133762	10389		136099	
Mn VIII	806094			818544		10794
		144151			146893	
Fe IX	950245			965437		

TABLE III. *Radiated frequencies with first and second differences. Second series members.*

Ion	$3p^6\,{}^1S_0 - 3p^5 5s\,{}^3P_1{}^0$			$3p^6\,{}^1S_0 - 3p^5 5s\,{}^1P_1{}^0$		
A I	113635			114965		
		99358			100054	
K II	212993		16229	215019		16325
		115587	16265		116379	
Ca III	328580			331398		16655
		131852	15804		133034	
Sc IV	460432			464432		15504
		147656	16015		148538	
Ti V	608088			612970		17417
		163671	15680		165955	
V VI	771759			778925		15460
		179351	(15039)		181415	
Cr VII	951110			960340		(17245)
		(194390)			(198660)	
Mn VIII	(1145500)			(1159000)		

TABLE IV. *Series limits calculated from two members of each series.*

Ion	$L(^1P_1{}^0)$ (cm⁻¹)	$L(^3P_1{}^0)$ (cm⁻¹)	$L(^1P_1{}^0) - L(^3P_1{}^0)$ (cm⁻¹)	$\Delta\,{}^2P_{3/2,\,1/2}$ (cm⁻¹)
A I	128,854	127,398	1456	1432
K II	258,234	256,776	1458	2165
Ca III	415,568	413,267	2301	3124
Sc IV	599,413	596,295	3118	4328
Ti V	809,040	805,465	3575	5825
V VI	1,046,420	1,040,090	6330	7657
Cr VII	1,308,280	1,299,700	8580	9944
Mn VIII		(1,585,000)		
Fe IX		(1,893,000)		

* Some of these data have been reported by L. W. Phillips and P. G. Kruger. Bull. Am. Phys. Soc. Washington Meeting **12**, 28 (1937).

[1] P. G. Kruger and S. G. Weissberg, Phys. Rev. **48**, 659 (1935).

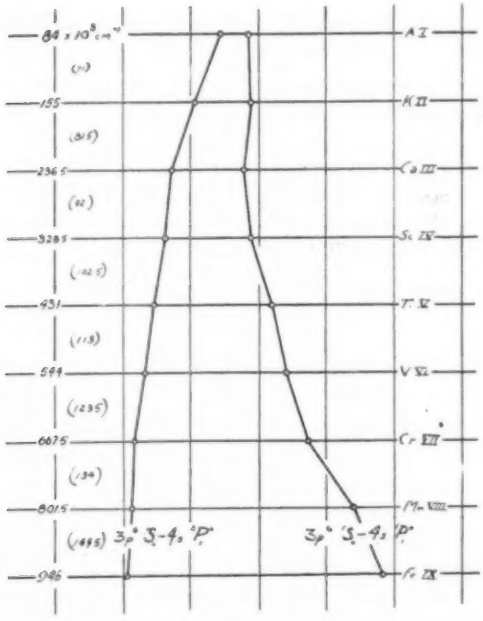

FIG. 1. Displaced frequency diagram. First series members $3p^6\ ^1S_0 - 3p^5 4s\ ^3P_1^0$, $^1P_1^0$. Horizontal scale, 1 div. = 4000 cm^{-1}. Vertical scale, constant second difference is 10500 cm^{-1}.

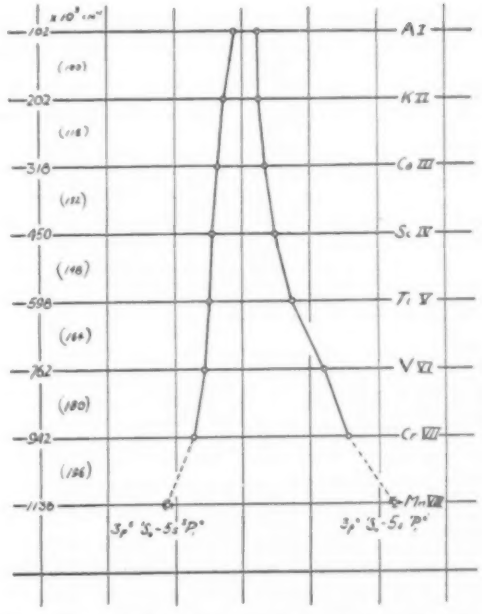

FIG. 2. Displaced frequency diagram. Second series members $3p^6\ ^1S_0 - 3p^5 4s\ ^3P_1^0$, $^1P_1^0$. Horizontal scale, 1 div. = 4000 cm^{-1}. Vertical scale, constant second difference is 16000 cm^{-1}.

TABLE V. *Term values.*

Ion	$3p^6\ ^1S_0$ (cm^{-1})	$3p^5 4s\ ^3P_1^0$ (cm^{-1})	$3p^5 4s\ ^1P_1^0$ (cm^{-1})	$3p^5 5s\ ^3P_1^0$ (cm^{-1})	$3p^5 5s\ ^1P_1^0$ (cm^{-1})
A I	127103.8	33360.86	31711.62	13468.4	12138.4
K II	256637	93400	90176	43644	41618
Ca III	413127	169200	165434	84547	81729
Sc IV	596295	260755	255301	135863	131863
Ti V	805465	368589	361685	197377	192485
V VI	1040090	490790	482437	268331	261165
Cr VII	1299700	627368	617256	348590	338360
Mn VIII	(1585000)	(778906)	(766456)	(439500)	(426000)
Fe IX	(1893000)	(942755)	(927563)	(538000)	

TABLE VI. *Ionization potentials.*

Ion	Ionization Potential (volts)	First Difference (volts)	Second Difference (volts)
A I	15.69	15.98	3.35
K II	31.67	19.33	3.3
Ca III	51.0	22.6	3.2
Sc IV	73.6	25.8	3.1
Ti V	99.4	28.9	3.1
V VI	128.3	32.0	(3)
Cr VII	160.3	(35)	(3)
Mn VIII	(195.5)	(38)	
Fe IX	(233.5)		

The Rankine Magnetic Balance and the Magnetic Susceptibility of H_2O, HDO and D_2O

HAIG P. ISKENDERIAN
Columbia University, New York, N. Y.
(Received March 31, 1937)

Details are given of the construction of a Rankine magnetic balance which realizes the full theoretical sensitivity of this type of instrument. The volume magnetic susceptibilities of stated mixtures of light and heavy water relative to that of ordinary water are reported, and from these data the relative mass susceptibilities of HDO and D_2O are deduced. The mass susceptibility of H_2O is assumed to be -0.7200×10^{-6}, in terms of which that of HDO is -0.6807×10^{-6} and of D_2O is -0.6466×10^{-6}.

IN 1933 Professor A. O. Rankine described in principle a novel form of magnetic balance whose nature and high theoretical sensitivity suggested its eminent fitness as an instrument to measure the relative magnetic susceptibilities of feebly magnetic substances.[1] Rankine later constructed a balance embodying these principles, but this instrument failed to function with the requisite sensitivity, chiefly because of ferromagnetic impurity in some of the structural materials.[2]

The present paper contains a description of a Rankine balance which realizes the full theoretical sensitivity of this type of instrument. The balance has been used to measure the diamagnetic susceptibilities of mixtures of light and heavy water with an accuracy of about 0.06 percent, and the results of these measurements form a second part of this report.

THE RANKINE MAGNETIC BALANCE

If a bar magnet stands parallel to the plane surface of a magnetizable medium the induced polarity on the surface exerts a force on the magnet, which is an attraction if the substance is paramagnetic and a repulsion if it is diamagnetic, and which depends in magnitude on the magnetic susceptibility of the material. If, now, the magnet is mounted, with its axis vertical, at one end of a horizontal beam supported by a vertical torsion fiber, this force will produce a torque about the fiber axis and the beam will rotate. The relative magnetic susceptibilities of different materials can be deduced theoretically from the magnitudes of such rotations, or, preferably, from the relative magnitudes of small nonuniform magnetic fields which, acting on the magnet, return it to a fiducial position close to the surface.

The theoretical sensitivity of such an instrument is very high, but is completely vitiated in practice by the fact that neither the earth's magnetic field nor the horizontal component of the magnet's moment can be nearly enough annulled to reduce the consequent residual directive torque on the beam to a value comparable with that exerted by a fine suspension fiber. In the Rankine balance the theoretical sensitivity is in large measure regained by the simple expedient of suspending the magnet from the beam on a torsion fiber of the same nature as that which supports the beam itself. It is apparent that with such an arrangement the control exerted by extraneous magnetic fields which are uniform over the magnet can operate at worst to halve the sensitivity. In fact, it can readily be shown[3] that the effective torsional coefficient, τ, of the instrument is given by the expression

$$\tau=\tau'+[(1/\tau'')+(1/\mu' H)]^{-1},$$

in which τ is the ratio of the torque on the beam due to the force between specimen and magnet, to the resulting angular displacement, τ' and τ'' are the torsional coefficients of the two fibers, respectively, μ' is the horizontal magnetic moment, and H is the extraneous uniform horizontal magnetic field. The present values of these constants are $\tau'=3\times10^{-4}$ dyne cm/radian, $\tau''=3\times10^{-5}$ dyne cm/radian, $\mu'=0.3$ e.m.u. and

[1] Rankine, Proc. Phys. Soc. **46**, 1 (1934).
[2] Rankine, Proc. Phys. Soc. **46**, 391 (1934).
[3] Rankine, reference 1, p. 11.

$H=0.16$ oersted, so that the term in $\mu' H$ is negligible in comparison with the others.

The foregoing considerations apply only when the extraneous field is uniform over the magnet. A nonuniform field exerts on the magnet a force, and on the beam a directive couple, of the same nature as, and possibly much larger than, that which it is desired to observe. In the presence of such forces the balance may be difficult, if not impossible, to use, and its sensitivity may be materially impaired. However, nonuniform fields can readily be eliminated by removing ferromagnetic bodies from the neighborhood of the instrument, and in particular *by constructing the balance of materials which contain no ferromagnetic impurity*. The latter specification is by far the most important item in the design of a successful instrument.

Fig. 1 is a schematic diagram of the magnetic balance here to be described. The base is a circular disk of OFHC copper 21.5 cm in diameter, and is provided with three leveling screws. The cell *S* into which the specimen fluid is admitted is blown of Pyrex glass and is approximately 5 mm thick by 20 mm wide by 50 mm high. An entrance tube is provided at the bottom and an exit tube at the top.

The magnet *DE* is a right circular cylinder of 36 percent cobalt steel, 3 mm in diameter and 25 mm long. Its pole strength is 36 e.m.u. and its weight 1.5 g. A Duralumin hook pointed with tungsten is firmly attached to the top of the magnet in such position that the point of the hook lies on the prolongation of the cylinder axis. This point rests on a jewel set in the inner side of a Duralumin ring. The ring, with the magnet pendant below it, is supported in a vertical plane by a quartz fiber affixed with shellac to a pin attached to it at the top.

The fiber *CD* which supports the magnet is 22 cm long and is affixed with shellac to one end of a horizontal Duralumin beam *BC*, at the other end of which is a counterweight *W*. The beam is about 0.6 mm thick by 6 cm long, and the center of support is located 2 cm from the end which carries the magnet. A small mirror, and a hook similar to that which supported the magnet are attached to the beam at this point. The beam is suspended in the same manner as the magnet by a quartz fiber *AB* 28 cm long affixed at its upper end to a torsion head.

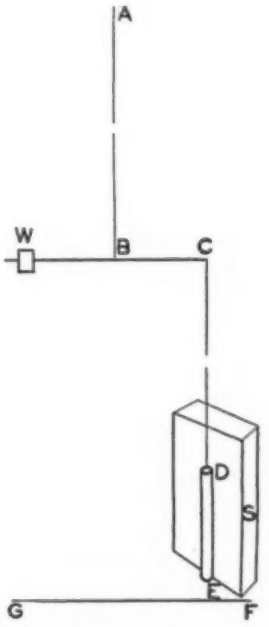

FIG. 1. Schematic diagram of the Rankine magnetic balance. *AB* and *CD*, quartz fibers; *BC*, Duralumin beam; *W*, counterpoise; *DE*, permanent magnet; *S*, specimen tube; *GF*, copper conductor.

The torsion head is supported by three vertical Pyrex glass rods located at the vertices of an equilateral triangle 8.8 cm on edge. The rods are cemented at each end with glycol cement into OFHC copper bushings. This cement has been found to be both efficacious and free from ferromagnetic impurity. It is made by cooking a mixture of one gram molecular weight each of glycol and phthallic anhydride at 200°C for 2 hours, after which it is poured a little at a time into cold water.

A vertical screw on the torsion head permits the height of the entire suspended system to be so adjusted that the bottom of the magnet is about 0.5 mm from the copper base plate. The field of the eddy currents induced in the plate by the magnet when in motion effectively damps any oscillation of the system. When not in use the system can be lowered so that the beam rests on the top of a centrally located vertical glass rod.

Two insulated conductors are mounted be-

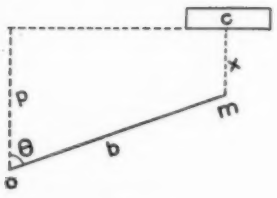

FIG. 2.

neath the base plate so as to lie in the plane of the beam when in use. The field of a current in one of these serves to establish the fiducial position of the magnet and to return it thereto against the magnetic force exerted by the contents of the cell. This position is such that the surface of the magnet is about 3 mm from that of the cell, and is indicated by a light beam reflected from the mirror to a scale about 4 meters distant. The field of a current in the other conductor is used when needed as an additional control on the motion of the suspended system.

The apparatus is enclosed in a bell jar, which rests on the copper base plate, and is further protected against fluctuations in temperature by mounting it in a Celotex box covered with hair felt. The bell jar is evacuated when measurements are made.

The factors which determine the sensitivity of the balance can readily be deduced from Fig. 2, in which C denotes the cell, viewed from above, m a pole of the magnet, b the length of the beam between m and the (fixed) point of support at O, p the perpendicular from O to the plane of the cell, and x the distance from m to the cell. The force exerted upon m by the magnetic material in the cell is, approximately,[4] $\pi m^2\kappa/2x^2$, provided the volume susceptibility, κ, is small in comparison with unity. Accordingly, the equilibrium condition for the beam is

$$T_0+T+\frac{\pi m^2\kappa b\sin\theta}{2x^2}+\tau(\theta+\theta_0)=0, \qquad (1)$$

in which T_0 denotes the torque on the beam due to extraneous fields and to the magnetization of the cell by the magnet, T that due to the current in the conductor, θ the angle between p and b, and θ_0 an unknown angular twist of the suspension fiber. It follows from this equation that if T_0 and T are held constant, then

$$\frac{\Delta\kappa}{\Delta\theta}=\frac{x^2}{\pi m^2 b\sin\theta}\left[\frac{2b\sin^2\theta-x\cos\theta}{x^3}\pi m^2 b\kappa-2\tau\right].$$

The optimum value of θ, i.e., the optimum orientation of the cell, is that which makes this expression a minimum for fixed values of b and x. However, accidental disturbances incident to the present arrangements do not warrant an effort to obtain greater sensitivity than that afforded by the orientation for which $\theta=90°$. Under these circumstances the second term in the brackets is negligible in comparison with the first, and the theoretical uncertainty in κ is given by the formula $\Delta\kappa=(2b\kappa/x)\Delta\theta$, where $\Delta\theta$ is the uncertainty in θ. It follows that, with the present balance, an uncertainty of the order 10^{-10} may be expected in the measurement of susceptibilities of the order 10^{-6}. The observed precision measure of κ agrees with this estimate.

The experimental procedure for measuring the volume susceptibility, κ_x, of a specimen liquid relative to the susceptibility, κ_s, of a standard liquid is as follows:

The bell jar and cell are evacuated and the current, i_0, is noted which maintains the magnet in the fiducial position with respect to the cell. The equilibrium condition for the beam may then be written in the form

$$T_0+ci_0+\tau\theta_0=0, \qquad (2)$$

where c is a constant whose value depends on the moment of the magnet and its position relative to the current.

Next the cell is filled with the standard liquid, and the current, i_s, is noted which maintains the magnet in its former position. The equilibrium condition is

$$T_0+f\kappa_s+ci_s+\tau\theta_0=0, \qquad (3)$$

TABLE I. *Comparison of data on benzene-nitrobenzene mixtures, obtained with the manometric and Rankine balances.*

C	$\kappa\times10^6$ Manometric balance	Rankine balance
0.1086	0.6062	0.6070
.2296	.6074	.6077
.3356	.6083	.6078
.8821	.6115	.6125

[4] Mason and Weaver, *The Electromagnetic Field*, p. 149.

where f is a constant whose value depends on the pole strength of the magnet and its position with respect to the cell. It follows from Eqs. (2) and (3) that

$$f\kappa_s = c(i_s - i_0). \tag{4}$$

Lastly, the cell is filled with the specimen liquid, and the fiducial current, i_x, again noted. The equation corresponding to Eq. (4) is $f\kappa_x = c(i_x - i_0)$ and it follows that

$$\kappa_x/\kappa_s = (i_x - i_0)/(i_s - i_0). \tag{5}$$

The currents, which are a few milliamperes, are measured with a L and N type K potentiometer. The standard liquid used throughout the present measurements was water, the volume susceptibility of which at the temperature of measurement, namely 21.3°C, was assumed to be -0.7186×10^{-6}.

An initial test of the Rankine balance showed its performance to be thoroughly satisfactory. Susceptibility measurements made with this instrument were in excellent accord with others made on the same substances with a Wills-Boeker manometric balance.[5] The specimen materials were mixtures of nitrobenzene in benzene. Typical data are given in Table I, in which the first column indicates the concentration by weight of nitrobenzene in benzene, the second, the volume susceptibility of the mixture as measured by Seely with the manometric balance,[6] and the third, the corresponding value obtained with the Rankine balance. The temperature at which the measurements were made was 21.8°C.

Another inference can be drawn from the concordance of these results. In the manometric balance the specimen material is placed in a field of approximately 15,000 oersteds, while in the Rankine balance it is subjected to a field of only about 100 oersteds. It appears, therefore, that the susceptibilities of the mixtures relative to water are independent of field strength over this range.

TABLE II. *The magnetic susceptibility of mixtures of H_2O, HDO and D_2O.*

f	ρ_f	κ/κ_w	$-\kappa\times10^6$	$-\chi\times10^6$
0	0.9979	1.	0.7186	0.7200
0.2	1.0195	0.9985	.7175	.7039
.4	1.0410	.9976	.7168	.6887
.6	1.0626	.9962	.7159	.6737
.8	1.0842	.9956	.7154	.6599
1.0	1.1058	.9949	.7149	.6466

[5] Wills and Boeker, Phys. Rev. **42**, 687 (1932).
[6] Seely, Phys. Rev. **49**, 812 (1936).

Experimental Results

The results of the observations on mixtures of light and heavy water are given in Table II. The first column gives the molar concentration of "heavy water," i.e., the ratio of the number of D atoms to the number of D plus H atoms in the mixture. The corresponding densities, shown in the second column, are calculated for the temperature 21.3°C with the formula[7]

$$\rho_f = 0.9979 + 0.1079f. \tag{6}$$

The third column contains the observed ratios of the volume susceptibilities of the mixtures to that of H_2O. The volume susceptibilities shown in the fourth column are calculated from these ratios and the value $\kappa_w = -0.7186\times10^{-6}$. The last column gives the mass susceptibilities of the mixtures, and is calculated from the data of the second and fourth columns with the formula $\chi = \kappa/\rho$.

The mass susceptibility of the constituent, HDO, of the mixtures can be computed from the observed mass susceptibility of any one mixture, on the assumption that the constituent susceptibilities are additive. The value thus obtained can then be used to *calculate* the susceptibilities of the remaining mixtures, and so the validity of this assumption can be tested. The equilibrium equation involved is $H_2O + D_2O \rightleftharpoons 2HDO$. The equilibrium constant of this reaction has been measured by Topley and Eyring.[8] Thus

$$(N_{12})^2/N_{11}N_{22} = 3.26, \tag{7}$$

where N_{11}, N_{12}, N_{22} are the molar concentrations of H_2O, HDO and D_2O, respectively. Additional relations between the N's are

$$\left.\begin{aligned} N_{22} + \tfrac{1}{2}N_{12} &= f, \\ \text{and} \qquad N_{11} + N_{12} + N_{22} &= 1. \end{aligned}\right\} \tag{8}$$

The additivity law may be written in the form

$$m\chi = m_{11}\chi_{11} + m_{12}\chi_{12} + m_{22}\chi_{22}, \tag{9}$$

where $m = m_{11} + m_{12} + m_{22}$,

$$m_{r_0}/m = W_{r_0}N_{r_0}/(W_{11}N_{11} + W_{12}N_{12} + W_{22}N_{22}), \tag{10}$$

[7] Lewis and Luten, J. Am. Chem. Soc. **55**, 5061 (1933); Taylor and Selwood, J. Am. Chem. Soc. **56**, 998 (1934).
[8] Topley and Eyring, J. Chem. Phys. **2**, 217 (1934).

and W_{rs} denotes the molecular weight of the constituent. The N's corresponding to a given f are calculated with Eqs. (7) and (8), the mass ratios with Eq. (10), and, finally, χ_{12} with Eq. (9). The values of W_{rs} adopted in the present calculation are $W_{11}=18.015$, $W_{12}=19.021$ and $W_{22}=20.027$.

The calculated value of χ_{HDO} corresponding to $f=0.2$ is -0.6807×10^{-6}. When this value is substituted in Eq. (9) the calculated mass susceptibilities of the remaining three mixtures are $\chi_{0.4}=-0.6885$, $\chi_{0.6}=-0.6739$, and $\chi_{0.8}=-0.6600$, all $\times10^{-6}$. These agree with the observed data of Table II with a maximum discrepancy of 2 in the fourth figure.

The present value of the molar susceptibility, χW, of D_2O is $-12.95\pm0.01\times10^{-6}$ compared with the value -12.97×10^{-6} for H_2O. Other investigators have obtained the values 12.90,[9] 12.76,[10] and 12.96 ± 0.02,[11] all $\times-10^{-6}$. It should be noted that the difference of amount 0.02×10^{-6} here found between the molar susceptibilities of H_2O and D_2O rests upon the adoption of the value 1.1058 for the density of D_2O at 21.3°C. An earlier measurement of this quantity by Lewis and Luten[12] yielded the value 1.1035, and the molar susceptibility of D_2O calculated from the present data with this figure is -12.97×10^{-6}. The experimental verification of the additivity law subsists whichever value is chosen.

In conclusion the writer gratefully acknowledges his indebtedness to Dr. W. B. Ellwood, of the Bell Telephone Laboratories, for his assistance in securing the magnet; to Dr. H. C. Urey, who supplied the mixtures of H_2O and D_2O; to Dean G. B. Pegram, in whose home in New York City this research was conducted; and to Dr. A. P. Wills, who suggested the problem and followed the progress of the work with helpful counsel and encouragement.

[9] Selwood and Frost, J. Am. Chem. Soc. **55**, 4335 (1933).
[10] Cabrera and Fahlenbrach, Naturwiss. **22**, 417 (1934).
[11] J. H. Cruickshank, Nature **268**, 135 (1935).
[12] Lewis and Luten, reference 7.

JUNE 15, 1937 PHYSICAL REVIEW VOLUME 51

The Piezodielectric Effect and Electrostriction in Anisotropic or Isotropic Media

HAROLD OSTERBERG AND JOHN W. COOKSON
Department of Physics, University of Wisconsin, Madison, Wisconsin

(Received February 4, 1937)

A phenomenological theory of the piezodielectric effect in homogeneous isotropic or anisotropic solids is presented. This theory rests upon the assumption that the changes in the dielectric constants ϵ_{ij} are linear in the six components of applied mechanical stress. It is shown that 36 piezodielectric moduli are required for a complete description of the piezodielectric effect. The number of independent moduli is two in isotropic solids, eight in alpha-quartz and tourmaline, and twelve in Rochelle salt. The matrices for the piezodielectric and piezooptical moduli are identical in all crystal classes which we have considered. The term electrostriction is applied to the case in which the components of strain are quadratic functions of the applied electrical field. The character of electrostriction in any solid is predicted by considering the piezodielectric effect together with the first and second laws of thermodynamics. The relation of electrostriction to the piezodielectric effect is very similar to the relation of the converse piezoelectric effect to the direct piezoelectric effect. The equations for the components of "electrostrictive strain" in isotropic solids and alpha-quartz are given in detail. General expressions for "electrostrictive stress" are derived. The equations of motion of a perfectly elastic, piezoelectric and electrostrictive solid which is subjected to mechanical and electrical fields are then stated. From considerations of crystalline symmetry and Neumann's hypothesis it can be seen that every solid may exhibit electrostriction whereas relatively few solids are piezoelectric.

1. THE THEORY OF THE PIEZODIELECTRIC EFFECT

THE term *piezodielectric effect* is here applied to those changes in the dielectric constants ϵ_{ij} of a homogeneous solid which result from the application of mechanical stress. The following considerations are limited to the case in which the changes are linear in the applied stress. Direct experimental evidence for this linearity has been recently obtained by A. H. Scott.[1]

Let the x, y and z components of the electric

[1] A. H. Scott, Nat. Bur. Stand. J. Research **15**, 13 (1935).

field intensity E and of the electric induction D be denoted respectively by E_1, E_2, E_3 and D_1, D_2, D_3. The dielectric constants ϵ_{ij} in the initial or the unstrained state are now defined by the relations

$$D_i=\sum_{j=1}^{3}\epsilon_{ij}E_j, \quad i=1, 2, 3, \tag{1}$$

in which it can be shown that

$$\epsilon_{ij}=\epsilon_{ji}. \tag{2}$$

The change which is brought about in ϵ_{ij} by the application of stress is denoted by e_{ij}. It is assumed that the dielectric constants in the stressed state are $\epsilon_{ij}+e_{ij}$, in which

$$e_{ij}=\sum_{k=1}^{6}g_{ijk}X_k \tag{3}$$

or

$$e_{ij}=\sum_{k=1}^{6}b_{ijk}x_k, \tag{4}$$

where X_k and x_k are, respectively, the components of mechanical stress and strain after the notation of Goranson.[2]

From arguments similar to those used to show that $\epsilon_{ij}=\epsilon_{ji}$ it can be shown that in the stressed state $\epsilon_{ij}+e_{ij}=\epsilon_{ji}+e_{ji}$. Hence

$$e_{ij}=e_{ji}$$

and

$$g_{ijk}=g_{jik}. \tag{5}$$

Since i or $j=1$, 2, 3, and $k=1$, $2\cdots6$, 36 constants g_{ijk} or b_{ijk} are thus required to describe the piezodielectric effect in crystalline media. The constants g_{ijk} are called the *piezodielectric moduli*. These are by assumption independent of X_k. They are in general a function of the temperature. In nonisothermal processes Eq. (3) is more general when written in the form

$$e_{ij}=\sum_{k=1}^{6}\int_0^{X_k}g_{ijk}dX_k, \tag{6}$$

where the initial state is unstressed.

The electrostatic energy E per unit volume of an anisotropic solid is usually assumed to be[3] given by

$$2E=\sum_{i=1}^{3}\sum_{j=1}^{3}\epsilon_{ij}E_iE_j=\sum_{j=1}^{3}D_jE_j. \tag{7}$$

It is here assumed that the electrostatic energy ξ per unit volume in the strained state is likewise given by

$$2\xi=\sum_{i=1}^{3}\sum_{j=1}^{3}(\epsilon_{ij}+e_{ij})E_iE_j. \tag{8}$$

Let ϕ represent the change in the electrostatic energy per unit volume due to the piezodielectric effect. Then,

$$2\phi=2\xi-2E=\sum_{i=1}^{3}\sum_{j=1}^{3}e_{ij}E_iE_j. \tag{9}$$

When ϕ is referred to the crystallographic axes, it can be shown[4] that for most of the crystalline groups $\epsilon_{ij}=0$, when $i\neq j$.

ϕ may be written in terms of the components of stress by substituting for e_{ij} in (9) the corresponding values given by (3). Thus

$$2\phi=\sum_{k=1}^{6}X_k\sum_{i=1}^{3}\sum_{j=1}^{3}g_{ijk}E_iE_j. \tag{10}$$

In a given crystalline group the number of independent moduli which are different from zero can be reduced from considerations of crystalline symmetry and Neumann's hypothesis.[5] This reduction can be made by means of an energy method through the energy function ϕ. A primed Cartesian coordinate system is related to the unprimed, rectangular crystallographic axes by a set of linear transformations which correspond to rotation through an angle θ about an axis or to reflection across a plane. Thus with respect to the primed system

$$2\phi'=\sum_{k=1}^{6}X_k'\sum_{i=1}^{3}\sum_{j=1}^{3}g'_{ijk}E_i'E_j'. \tag{11}$$

When the linear transformations

$$X_k'=F_k(X_p, \theta) \quad \text{and} \quad E_s'=G_s(E_r, \theta) \tag{12}$$

are substituted into (11), ϕ' becomes an explicit function of X_k, E_m, E_n and θ. Let the value of θ or

[2] R. W. Goranson, *Thermodynamic Relations* (1930).
[3] Voigt, *Lehrbuch der Kristallphysik* (1910), p. 413
[4] Reference 3, p. 414.
[5] Love, *Mathematical Theory of Elasticity* (1920), p. 155.

the nature of the reflections correspond to a "covering operation."[6] Since the energy ϕ is invariant with respect to the coordinate system, the necessary equations for determining the number of independent piezodielectric moduli are obtained by equating the coefficients of $E_m E_n$ in (10) to the corresponding coefficients in ϕ'. This is similar to the manner in which the elastic constants are reduced by Love.[7]

The reduction to the number of independent piezodielectric moduli has been carried out in the above manner by the writers for (1) the isotropic case and for those crystals which in Voigt's[8] notation possess the symmetry (2) $A_x^3 A_z^2$ (alpha-quartz), (3) $A_x^3 E_x$ (tourmaline), (4) $A_x^2 A_z^2$ (Rochelle salt), and (5) $A_x^2 E_z$. The following matrices state the relations which were found to exist among the piezodielectric moduli. For the sake of ready comparison of these matrices with those which are already known to exist for the piezooptical effect, the writers have reduced g_{ijk} to a second-order tensor by means of the convention $g_{ijk}=g_{hk}$ (h and $k=1, 2\cdots 6$) in which the integers h, i and j are related by the scheme

$$\begin{array}{cccccccccc} h & 1 & 2 & 3 & 4 & 4 & 5 & 5 & 6 & 6 \\ i & 1 & 2 & 3 & 3 & 2 & 3 & 1 & 2 & 1 \\ j & 1 & 2 & 3 & 2 & 3 & 1 & 3 & 1 & 2. \end{array} \qquad (13)$$

Thus, for example, $g_{32k}=g_{23k}=g_{4k}$. With this convention (2) and (3) are conveniently written in the form

$$\epsilon_{ij}=\epsilon_h \qquad (14)$$

and

$$e_{ij}=e_h=\sum_{k=1}^{6} g_{hk}X_k, \quad h=1, 2\cdots 6. \qquad (15)$$

When the elements g_{hk} of these matrices are known from physical measurements, the piezodielectric effect is calculated by means of Eqs. (13) and (15).

Isotropic case:

$$\|g_{hk}\|=\begin{Vmatrix} g_{11} & g_{12} & g_{12} & 0 & 0 & 0 \\ g_{12} & g_{11} & g_{12} & 0 & 0 & 0 \\ g_{12} & g_{12} & g_{11} & 0 & 0 & 0 \\ 0 & 0 & 0 & 0 & 0 & 0 \\ 0 & 0 & 0 & 0 & 0 & 0 \\ 0 & 0 & 0 & 0 & 0 & 0 \end{Vmatrix}. \qquad (16)$$

[6] Reference 5, p. 150.
[7] Reference 5, p. 153.
[8] Reference 3, p. 97.

$A_x^3 A_z^2$ and $A_x^3 E_x$:

$$\|g_{hk}\|=\begin{Vmatrix} g_{11} & g_{12} & g_{13} & g_{14} & 0 & 0 \\ g_{12} & g_{11} & g_{13} & -g_{14} & 0 & 0 \\ g_{31} & g_{31} & g_{33} & 0 & 0 & 0 \\ g_{41} & -g_{41} & 0 & g_{44} & 0 & 0 \\ 0 & 0 & 0 & 0 & g_{44} & 2g_{41} \\ 0 & 0 & 0 & 0 & g_{14} & (g_{11}-g_{12}) \end{Vmatrix}. \qquad (17)$$

$A_x^2 A_z^2$ and $A_x^2 E_x$:

$$\|g_{hk}\|=\begin{Vmatrix} g_{11} & g_{12} & g_{13} & 0 & 0 & 0 \\ g_{21} & g_{22} & g_{23} & 0 & 0 & 0 \\ g_{31} & g_{32} & g_{33} & 0 & 0 & 0 \\ 0 & 0 & 0 & g_{44} & 0 & 0 \\ 0 & 0 & 0 & 0 & g_{55} & 0 \\ 0 & 0 & 0 & 0 & 0 & g_{66} \end{Vmatrix}. \qquad (18)$$

A phenomenological theory of the *piezooptical effect* has been studied by Pockels,[9] Günther[10] and Szivessy.[11] The reduction of the piezooptical moduli q_{ij} was made by the so-called geometrical method since a suitable energy function was not available. It will be observed that the matrices[12] for the piezooptical and the piezodielectric moduli are identical in form. This may be expected since the indices of refraction are closely related to the dielectric constants. To predict the piezodielectric effect in the remaining 27 crystal classes not considered in (16), (17) or (18) one may thus employ the known piezooptical matrices. It is, however, preferable to determine the piezodielectric constants by the energy method of Eqs. (11) or (12) since the writers do not present proof that the energy and geometrical methods necessarily lead to identical matrices for all crystal classes.

The writers have not succeeded in finding the relations which exist between the piezooptical and the piezodielectric moduli. A knowledge of these relations would enable one to determine the piezodielectric moduli from measurements upon the piezooptical effect as well as from measurements upon the piezodielectric effect and electrostriction.

[9] F. Pockels, *Lehrbuch der Kristalloptik* (1906), p. 498.
[10] N. Günther, Ann. d. Physik **405**, 783 (1932).
[11] G. Szivessy, *Handbuch der Physik*, Vol. 21 (1929), p. 832.
[12] Compare (16), (17) and (18) with matrices found in reference 11, p. 841.

2. Electrostriction

When solids are subjected to electric fields, they suffer deformations in which the components of strain may be linear and quadratic in the x, y and z components of the applied field. The case in which the components of strain are linear functions of the components of the electric field is known as the converse piezoelectric effect.[13] The term *electrostriction* is here applied to the case in which the strain components are *quadratic* functions of the applied field. A phenomenological theory of electrostriction does not appear to have been developed. It will be shown that electrostriction is related to the piezodielectric effect in a manner similar to that in which the converse piezoelectric effect is related to the direct piezoelectric effect. If the piezodielectric effect and electrostriction are thus assumed to exist, the energy function ϕ together with the first and second laws of thermodynamics may be used to predict the nature of electrostriction in any medium from its piezodielectric properties.

When a body is subjected to mechanical stress or to electrical fields, the resulting physical changes depend upon the thermodynamical conditions under which these changes take place. We suppose that during the change a quantity of heat dQ crosses the boundary of the small volume element under consideration and that mechanical work dW is done by the volume element. So long as energy transfers are limited to mechanical work and heat, the corresponding change in the intrinsic energy u is

$$du=dQ-dW, \tag{19}$$

in which it will be understood that du, dQ and dW are referred to some path. If the volume element possesses a piezodielectric effect, energy may appear in the electrostatic form. For the purpose of the following argument only the piezodielectric portion of the electrostatic energy need be considered. Consequently, over any path

$$du=dQ-dW+d\phi. \tag{20}$$

If the change is assumed to be reversible, Eq. (20) can be written in the form

$$du=TdS+\sum_{k=1}^{6} X_k dx_k+\tfrac{1}{2}\sum_{i=1}^{3} E_i dD_i, \tag{21}$$

where S is the entropy and T is the Kelvin temperature. This potential function u is suitable for discussing the adiabatic case $dS=0$.

It is convenient to define the potential function

$$\zeta\equiv u-TS-\sum_{k=1}^{6} X_k x_k. \tag{22}$$

$$\text{Thus}\quad d\zeta=-SdT-\sum_{k=1}^{6} x_k dX_k+\tfrac{1}{2}\sum_{i=1}^{3} E_i dD_i. \tag{23}$$

The thermodynamic state is usually determined by three variables (v, p, T) or (x_k, X_k, T) for which there is assumed the existence of a function

$$F(x_k, X_k, T)=0. \tag{24}$$

The state of piezodielectric substances depends also upon E_i or D_i. We assume, after (24), the existence of a function

$$G(x_k, X_k, T, E_i)=0. \tag{25}$$

Any three of the four variables in this equation may be taken as independent. Let T, X_k and E_i be chosen as independent variables. The portion of D_i which is due to the piezodielectric effect is

$$D_i=\sum_{j=1}^{3}\sum_{k=1}^{6} g_{ijk}X_k E_j. \tag{26}$$

$$\therefore\quad dD_i=\sum_{j=1}^{3}\sum_{k=1}^{6}\left[g_{ijk}(E_j dX_k+X_k dE_j)+(\partial g_{ijk}/\partial T)X_k E_j dT\right]. \tag{27}$$

By substituting (27) into (23), it is found that in isothermal processes ($dT=0$)

$$d\zeta=\sum_{k=1}^{6}(-x_k+\tfrac{1}{2}\sum_{i=1}^{3}\sum_{m=1}^{3} g_{imk}E_i E_m)dX_k+\tfrac{1}{2}\sum_{n=1}^{6}\sum_{i=1}^{3}\sum_{j=1}^{3} g_{ijn}E_i X_n dE_j. \tag{28}$$

Since ζ is exact $\left(\text{or provided } \dfrac{\partial^2\zeta}{\partial X_k\partial E_i}=\dfrac{\partial^2\zeta}{\partial E_j\partial X_k}\right)$,

[13] See reference 3, p. 817.

$$\frac{\partial}{\partial E_j}(-x_k+\tfrac{1}{2}\sum_{i=1}^{3}\sum_{m=1}^{3}g_{imk}E_iE_m)=\tfrac{1}{2}\frac{\partial}{\partial X_k}\sum_{n=1}^{6}\sum_{i=1}^{3}g_{ijn}X_nE_i. \quad (29)$$

$$\therefore \quad -\frac{\partial x_k}{\partial E_j}+\sum_{i=1}^{3}g_{ijk}E_i=\tfrac{1}{2}\sum_{i=1}^{3}g_{ijk}E_i$$

or

$$\frac{\partial x_k}{\partial E_j}=\tfrac{1}{2}\sum_{i=1}^{3}g_{ijk}E_i,$$

$$k=1, 2\cdots 6; \quad j=1, 2, 3. \quad (30)$$

In carrying out the partial derivatives of (29), it should be remembered that $g_{imk}=g_{mik}$.

Suppose that the components of strain are linear in X_n and quadratic in E_i and E_j such that

$$x_k=\sum_{n=1}^{6}s_{kn}X_n+\sum_{i=1}^{3}\sum_{j=1}^{3}a_{ijk}E_iE_j \quad (31)$$

where s_{kn} are the elastic moduli. If the electrostrictive effect exists, a comparison of (30) and (31) shows that the coefficients a_{ijk} are related in the isothermal case to the piezodielectric moduli according to the law

$$a_{ijk}=\tfrac{1}{2}g_{ijk}. \quad (32)$$

In the absence of mechanical stress ($X_n=0$)

$$x_k=\tfrac{1}{2}\sum_{i=1}^{3}\sum_{j=1}^{3}g_{ijk}E_iE_j \quad (k=1, 2, \cdots 6). \quad (33)$$

These components of strain x_k will be called the components of "electrostrictive strain."

It will be seen from the above argument that although g_{ijk} remain fixed during an isothermal process, they depend upon the temperature at which the process takes place. Adiabatic processes are more complicated theoretically than isothermal processes since the temperature (and hence in general g_{ijk}) is variable in the adiabatic case. The theory of adiabatic processes is not included in this paper, but it may be observed that provided g_{ijk} are sufficiently slow functions of T or provided T remains sensibly constant during adiabatic processes, the corresponding components of electrostrictive strain may be computed with considerable accuracy from (33).

An examination of (3) and (33) shows that in any solid a large piezodielectric effect is associated with large components of electrostrictive strain. Further, the piezodielectric moduli may be measured either from the piezodielectric effect or from electrostriction. It seems likely that these moduli can be measured with greater ease and accuracy from the piezodielectric effect since small changes of capacity are more easily measured than the deflections due to electrostriction. When the relations between the piezooptical and the piezodielectric moduli become known, a third method becomes available for measuring the piezodielectric moduli.

The components of electrostrictive strain in the isotropic solid are

$$\begin{aligned}2x_1&=g_{11}E_1^2+g_{12}(E_2^2+E_3^2);\\ 2x_2&=g_{11}E_2^2+g_{12}(E_1^2+E_3^2);\\ 2x_3&=g_{11}E_3^2+g_{12}(E_1^2+E_2^2);\\ x_4&=x_5=x_6=0.\end{aligned} \quad (34)$$

Electrostriction cannot, therefore, give rise to the shear components of strain in isotropic substances. In alpha-quartz and tourmaline

$$\begin{aligned}2x_1&=g_{11}E_1^2+g_{12}E_2^2+g_{41}E_3^2+2g_{41}E_2E_3;\\ 2x_2&=g_{12}E_1^2+g_{11}E_2^2+g_{31}E_3^2-2g_{41}E_2E_3;\\ 2x_3&=g_{13}(E_1^2+E_2^2)+g_{33}E_3^2;\\ 2x_4&=g_{14}(E_1^2-E_2^2)+2g_{44}E_2E_3;\\ 2x_5&=2g_{14}E_1E_2+2g_{44}E_1E_3;\\ 2x_6&=2(g_{11}-g_{12})E_1E_2+4g_{41}E_1E_3.\end{aligned} \quad (35)$$

In these solids the shear components of electrostrictive strain are not zero. It will be noted that the strain components involve cross products of the components of the electric field. The terms in these cross products change sign when the sign of one member E_s is reversed. This aspect of electrostriction does not appear to have been considered or tested.

Reversibility has been assumed in the theory leading to (33). Consequently (33) does not accurately apply to viscoelastic solids of the type discussed by J. H. C. Thompson.[14] Rochelle salt is sufficiently viscoelastic that (33) can be expected to apply only after the components of electrostrictive strain have reached equilibrium with the impressed electric field. These components lag varying fields and thus give rise to hysteresis.

[14] J. H. C. Thompson, Phil. Trans. Roy. Soc. London **231**, 358 (1932–33).

3. The Elastic, Piezoelectric, Electrostrictive Solid

The components of strain in a perfectly elastic solid which is piezoelectric and electrostrictive will be considered briefly. In this solid the components of strain are increased by the components which originate from the converse piezoelectric effect. Hence for this solid Eq. (31) assumes the form

$$x_k=\sum_{n=1}^{6} s_{kn}X_n+\tfrac{1}{2}\sum_{i=1}^{3}\sum_{j=1}^{3} g_{ijk}E_iE_j+\sum_{i=1}^{3} d_{ik}E_i, \quad (36)$$

where d_{ik} are the piezoelectric moduli.

4. The Equations of Motion

When a body is not in equilibrium with a system of mechanical and "electrostrictive stresses," the series of states through which it passes is described by the equations of motion and the boundary conditions. When only the mechanical stresses are present, the equations of motion are[15]

$$\begin{aligned}
&\frac{\partial X_1}{\partial x}+\frac{\partial X_6}{\partial y}+\frac{\partial X_5}{\partial z}+\rho X=\rho\frac{\partial^2 u}{\partial t^2};\\
&\frac{\partial X_6}{\partial x}+\frac{\partial X_2}{\partial y}+\frac{\partial X_4}{\partial z}+\rho Y=\rho\frac{\partial^2 v}{\partial t^2};\\
&\frac{\partial X_5}{\partial x}+\frac{\partial X_4}{\partial y}+\frac{\partial X_3}{\partial z}+\rho Z=\rho\frac{\partial^2 w}{\partial t^2}.
\end{aligned} \quad (37)$$

If (4) is substituted into (9)

$$2\phi=\sum_{k=1}^{6} x_k\sum_{i=1}^{3}\sum_{j=1}^{3} b_{ijk}E_iE_j, \quad (38)$$

in which b_{ijk} are the "piezodielectric constants." These are connected with the piezodielectric moduli by the relations

$$b_{ijm}=\sum_{k=1}^{6} g_{ijk}c_{km}, \quad (39)$$

where c_{km} are the elastic constants.

[15] Reference 5, p. 85.

With the aid of (38) the thermodynamic potential ζ may be expressed using x_k, E_j and T as independent variables. Following a method similar to that leading to (33), one can show that

$$X_k=\tfrac{1}{2}\sum_{j=1}^{3}\sum_{i=1}^{3} b_{ijk}E_iE_j \quad (k=1, 2\cdots 6), \quad (40)$$

wherein X_k are components of "electrostrictive stress," i.e., those components of mechanical stress which would bring about a state of strain identical with that produced by electrostriction.

Let R_k denote the sum of the mechanical, electrostrictive, and piezoelectric stresses, i.e., let

$$R_k=X_k+\tfrac{1}{2}\sum_{j=1}^{3}\sum_{i=1}^{3} b_{ijk}E_iE_j+\sum_{i=1}^{3} e_{ik}E_i, \quad (41)$$

where e_{ik} are the piezoelectric constants in the notation of Voigt. The equations of motion in elastic, piezoelectric and electrostrictive media are now obtained by replacing the purely mechanical stresses X_k in (37) by R_k from (41). The solution of the equations of motion and an appropriate set of boundary conditions determines the instantaneous states through which the medium passes.

The boundary conditions may specify the X, Y and Z[16] components of surface traction across a plane element of normal ν at the boundary of the medium. The components X_ν, Y_ν, and Z_ν, of the surface traction are

$$\begin{aligned}
X_\nu&=R_1\cos(x\nu)+R_6\cos(y\nu)+R_5\cos(z\nu);\\
Y_\nu&=R_6\cos(x\nu)+R_2\cos(y\nu)+R_4\cos(z\nu);\\
Z_\nu&=R_5\cos(x\nu)+R_4\cos(y\nu)+R_3\cos(z\nu).
\end{aligned} \quad (42)$$

The above equations of motion and boundary conditions are accurate only in the isothermal case, but when the effects of the adiabatic temperature changes are negligibly small, the adiabatic case can be solved in the first approximation as an isothermal problem.

The senior writer is indebted to the Wisconsin Alumni Research Foundation whose financial assistance made possible the time spent by him on this work.

[16] Reference 5, p. 78.

LETTERS TO THE EDITOR

Prompt publication of brief reports of important discoveries in physics may be secured by addressing them to this department. Closing dates for this department are, for the first issue of the month, the eighteenth of the preceding month, for the second issue, the third of the month. Because of the late closing dates for the section no proof can be shown to authors. The Board of Editors does not hold itself responsible for the opinions expressed by the correspondents.

Communications should not in general exceed 600 words in length.

Artificial Radioactivity Produced by Alpha-Particles

We have found that Co, Cu, and Ni become strongly radioactive when bombarded with about 0.05 microamperes of 7 Mev alpha-particles. The relative initial intensities of the activities, corrected to infinite bombarding time, are in the ratio Co : Cu : Ni = 100 : 15 : 22. The following identifications are suggested for the radioelements formed.

Co: The half-life of the activity has been measured with some care (Fig. 1) by means of a Lauritsen type electroscope; it is 9.65±0.07 minutes. The emitted particles have been found to be positrons by deflection in a magnetic field. Since Co has only one abundant isotope, Co^{59}, it is suggested that this radioelement is Cu^{62}, formed in the reaction Co^{59} (α, n) Cu^{62}. Heyn[1] and Pool, Cork and Thornton[2] have attributed an activity found by them to be induced in Cu by fast neutrons to Cu^{62}, the reaction being Cu^{63} $(n, 2n)$ Cu^{62}. The half-lives given are 10.5±0.5 min.[1] and 10 min.[2] Bothe and Gentner[3] have found an activity of half-life about 11 minutes produced in Cu by bombardment with 17 Mev gamma-radiation; this they have attributed to Cu^{62}, formed by the reaction Cu^{63} (γ, n) Cu^{62}. The present result provides independent confirmation of the assignment of the radioactivity made by the above-mentioned authors, the difference in half-lives probably being too small to be significant.

Cu: The half-life of the positron emitting radioelement formed in the alpha-particle bombardment of Cu is 59±1 minutes. The possible radioelements formed are Ga^{66} and Ga^{68}. Since Bothe and Gentner[3] have found that an activity of 60 minutes is produced in Ga by gamma-ray bombardment, which they have attributed to Ga^{69} formed by Ga^{69} (γ, n) Ga^{68}, it seems reasonable to suppose that the activity we observe is due to Ga^{68}. The reaction involved here is then Cu^{65} (α, n) Ga^{68}.

Ni: While one would expect, in analogy with the two foregoing reactions, that the 38 minute radioelement attributed by Bothe and Gentner[3] to Zn^{63} would be formed in the bombardment of Ni with alpha-particles, this activity, if present, is so weak as to have escaped detection. The strong activity found decays with the hitherto unknown period (Fig. 2) of 3.25±0.05 hours, positrons being

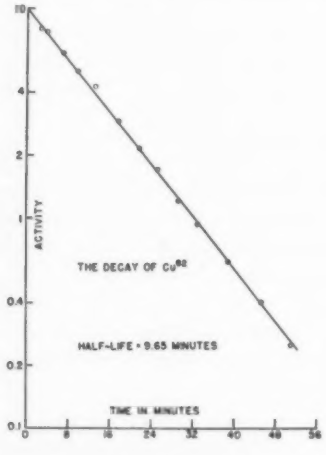

FIG. 1. The decay of Cu^{62}.

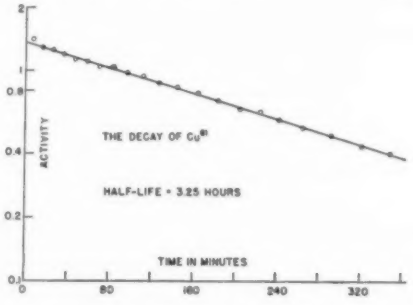

FIG. 2. The decay of Cu^{61}.

emitted. Chemical experiments identify the activity as due to an isotope of Cu. Since isotopes of Cu, stable and radioactive, are known for all mass numbers from 62 to 66, inclusive, we assign this activity to Cu^{61}, formed from Ni by the reaction Ni^{58} (α, p) Cu^{61}. Ni is believed to be the heaviest element in which the (α, p) reaction has been so far observed.

We are indebted to our colleagues, Drs. M. G. White and M. C. Henderson, who have been chiefly responsible for the construction of the cyclotron with which these results were obtained.

LOUIS N. RIDENOUR
W. J. HENDERSON

Palmer Physical Laboratory,
Princeton University,
Princeton, N. J.,
May 27, 1937.

[1] Heyn, Nature **138**, 723 (1936) and Physica **4**, 160 (1937).
[2] Pool, Cork, and Thornton, Phys. Rev. **51**, 890 (1937).
[3] Bothe and Gentner, Naturwiss. **25**, 90 (1937) and **25**, 191 (1937).

Radioactive Alpha-Particles from Li^7+H^2

From their disintegration experiments with the separated isotopes of lithium, Rumbaugh and Hafstad[1] concluded that the energy difference of the normal states of Li^8 and Be^8 had a minimum value 3 to 4 Mev greater than the maximum energy of the beta-rays which are produced when Li^7 is bombarded by deuterons and which Crane, Delsasso, Fowler and Lauritsen[2] had attributed to Li^8. This discrepancy could be accounted for by assuming the nucleus resulting from the beta-disintegration to be an excited configuration[3] of Be^8 and the possibility was presented of observing the disintegration of this nucleus into two alpha-particles. We have looked for and found alpha-particle radioactivity when lithium is bombarded by deuterons. This radioactivity has in the meantime been reported by Lewis, Burcham and Chang.[4]

A target of lithium metal placed within a well inside a cloud chamber was bombarded by 850 kv peak deuterons. A grid allowing the observation of particles making an angle of $90°\pm5°$ with the incident deuterons was covered by a thin Al foil of 4 mm air equivalent stopping power. The target was bombarded for 1.8 seconds during each cycle and the cloud chamber expanded 0.2 seconds after the end of the bombardment. Gas-vapor mixtures of stopping powers 0.05, 0.10, 0.13, 0.16, 0.25, 0.50 and 1.00 were employed to secure the numbers distribution of the particles over various portions of the range. The lowest stopping powers were secured by using He as the chamber gas and water as the vapor, and were checked by measurement of the known ranges of He^4 and He^3 from Li^6+H^1.

The complete distribution in range curve secured in this manner is shown in Fig. 1. The large spread in range of the radioactive alpha-particle distribution is evident. No certain evidence was found for any line-structure in the curve. The distribution in energy of the alpha-particles has a maximum at 1.3 Mev and falls sharply to less than half the maximum at 1.0 Mev. The width at half-maximum of this distribution corrected for straggling and target spreading is very close to 0.5 Mev. The high energy portion of the distribution decreases rapidly with increasing energy but extends to at least 6.0 Mev. The average energy of the alpha-particles is 2.0 Mev.

The reactions proposed to account for the observed beta- and alpha-activity and the energy relation governing the experimentally determinable quantities are as follows:

$$Li^7+H^2\rightarrow Li^8+H^1+Q$$
$$Li^8\rightarrow Be^{8*}+e^-+E_0$$
$$Be^{8*}\rightarrow 2He^4+T$$
$$Q+E_0+T=15.6\pm0.2 \text{ Mev.}$$

Rumbaugh and Hafstad[1] have shown that the range of protons accompanying the formation of Li^8 is probably less than 8 cm so that $Q<1.8$ Mev and the observation that the beta-activity requires a bombarding energy of 500 kv establishes that $Q>-0.5$ Mev. We have shown[2] that E_0 extends up to at least 10 Mev and that the average kinetic energy of the beta-rays is 3.9 Mev. If the reactions proposed above are correct, then several points are of especial interest in connection with the observed alpha-particle distribution.

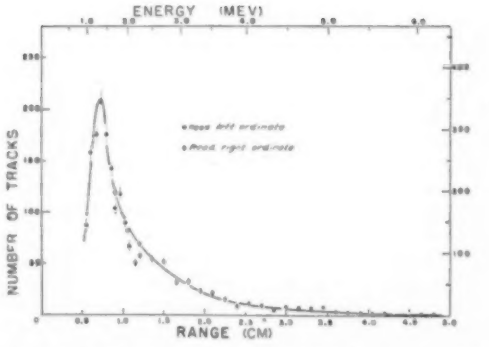

FIG. 1. Distribution in range of the radioactive alpha-particles from Li^7+H^2. The solid points were secured with stopping powers of 0.05 to 0.16 and when the left ordinate is read indicate the number of tracks counted in 0.06 cm intervals of normal range. The circles were secured with stopping powers of 0.25 to 1.0 and when the right ordinate is read indicate the number of tracks counted in 0.15 cm intervals. The two sets of data have been fitted together at 1 cm normal range.

(1) As has been previously pointed out[1, 3] a rigid selection rule must forbid the beta-neutrino transition from Li^8 to the normal state of Be^8 which suggests that the angular momentum of normal Li^8 and normal Be^8 must differ by at least two units.

(2) A straightforward application of Fermi's theory of beta-decay would require that the probability of disintegration of Li^8 contain a factor $(W_m-T)^7$ where W_m is the excess energy of the Li^8 nucleus over two alpha-particles and where $\gamma\sim5$ on Fermi's interaction ansatz and $\gamma\sim7$ on on the Konopinski-Uhlenbeck ansatz. This factor in conjunction with the Gamow penetration factor governing the behavior of low energy alpha-particles will essentially account for the observed shape of the curve below 3 Mev provided that Be^8 has no stationary state of appropriate angular momentum below 2 Mev excitation. Because of the factor $(W_m-T)^7$ we would expect from this fewer long range particles than are observed. Feenberg and Phillips[5] have suggested that triplet states of Be^8 may account for these high energy particles; the relatively large contribution of these states may be understood in terms of their long lifetimes.

(3) The observed beta-spectrum must no longer be looked upon as a transition with a single maximum energy end point. An additional asymmetry will be introduced into the spectrum but definite conclusions cannot be drawn until the possibility of gamma-ray emission has been investigated.

W. A. FOWLER
C. C. LAURITSEN

W. K. Kellogg Radiation Laboratory,
California Institute of Technology,
Pasadena, California,
May 7, 1937.

[1] Rumbaugh and Hafstad, Phys. Rev. **50**, 681 (1936).
[2] Crane, Delsasso, Fowler and Lauritsen, Phys. Rev. **47**, 971 (1935).
[3] Wigner and Breit, Phys. Rev. **50**, 1191 (1936).
[4] Lewis, Burcham and Chang, Nature **139**, 24 (1937).
[5] Feenberg and Phillips, Phys. Rev. **51**, 597 (1937).

On the Origin of Cosmic Rays

The accumulating evidence that a major part of the cosmic rays comes from beyond the Milky Way suggests a renewed examination of the consequences of Lemaitre's hypothesis of their origin as a part of the explosion of the primeval concentration of matter from which the present world system has developed. This hypothesis deserves renewed attention also because of the support given by Hubble's recent observations[1] to this particular model of the Friedmann universe.

The difficulty of obtaining any satisfactory alternative explanation of the origin of cosmic rays is becoming more and more apparent. The measurements by Millikan and Regener of the ionization by cosmic rays from high altitudes down to depths where they are completely absorbed have shown that the cosmic rays bring to the earth about the same amount of heat as does starlight. But, as these authors have noted, the earth, being within a local star cluster which is itself a part of a major galaxy, receives much more than a fair sample of the heat radiated by stars. If the cosmic rays come from beyond the Milky Way, at a really typical place in intergalactic space the density of cosmic-ray energy would be of the order of 10^2 times as great as that of starlight. It is thus apparent that either the source of the rays must be a radiator which is very powerful compared with stars as a source of light, or the cosmic rays once emitted must be retained by the metagalactic system instead of being lost as is starlight.

None of the attempts to interpret cosmic rays as arising from stellar electric or magnetic fields would seem adequate to deliver energy in the required amounts. If the electromotive forces are due to the motion of the stars in the magnetic fields of the star system, the maximum energy that could thus be supplied would be that of the kinetic energy of the stars which form the system. Even such a kinetic energy as that of the sun as a part of the galactic rotation is small compared with the energy radiated by the sun as light in 10^9 years. Likewise, if we consider the electric field between concentric clouds of matter surrounding an exploding nova, the work done by these clouds in pulling ions from the interior cannot be greater than the kinetic energy of the clouds themselves. Also, if these clouds are driven by radiation pressure, the work done by this radiation is necessarily much less than the energy of the radiation itself, whence the radiation emitted must be of much greater energy than the electric particles that may arise as a secondary consequence. Similar considerations make the other hypotheses of this type also difficult to defend.

Although nuclear processes occurring in interstellar space might result in an adequate total energy, it appears that such processes are inadequate to account for the great energies of the individual cosmic-ray particles. Latitude effect studies show that the average energy of the primary particles is of the order of 10^{10} electron volts, whereas burst studies indicate occasional rays with energies as great as 10^{12} ev. Since the mass of a hydrogen atom is equivalent to only 10^9 ev, this means that even nuclear sources are inadequate as an origin for cosmic rays.

A primeval explosion of the type imagined by Lemaitre could supply the necessary amount of total and individual energy for the cosmic rays, if merely because no limit is assigned to the amount of energy available, and no specific mechanism is postulated for the ejection of the individual particles.

If only gravitational fields are effective in bending the paths of the particles, the cosmic rays which we observe in our galaxy must have come out of the primeval explosion with our neighboring galaxies, while particles originating in our galaxy are permanently lost to us, but may be observed on the extra-galactic nebulae around us. This picture would immediately explain the isotropic origin of the cosmic rays as observed in our galaxy. For in a homogeneous isotropic universe of relativistic cosmology, an observer on any nebula (or galaxy) would observe the same phenomenon of expansion of other nebulae around him. Hence, we should expect an isotropic type of cosmic-ray phenomenon to be observed not only by us but also by observers situated on any other nebula in space (condition of homogeneity).

This hypothesis leads, however, to a serious difficulty regarding the composition of the rays. From such a violent cataclysm we should expect particles of all types to be ejected—if electrons, then certainly photons, and presumably also protons, alpha-particles and ions of all types. Our cosmic-ray studies have, however, revealed in the primary cosmic rays only positive and negative electrons and electrical particles of higher mass (the more penetrating component), which may be either protons or the "heavy electrons" recently suggested by Street and Stephenson. According to present evidence, few if any photons, neutrons or alpha-particles seem to enter the earth as cosmic rays.

Is it possible that electrically-charged rays emitted by the initial explosion may be deflected by stellar or galactic magnetic fields just as a cosmic-ray electron is deflected by the earth's magnetic field? If so, those particles which would be most probably retained by the metagalactic system would be those with the highest ratio of e/m, i.e., in order, electrons, protons, etc., whereas all neutral rays might be forever lost.

If the magnetic fields of the earth and sun are typical, a strong deflection of a cosmic-ray particle on traversing a galaxy would be an event of low probability. Thus the cosmic rays should not acquire any considerable part of the motion of the star streams through which they pass, and their spatial distribution should remain sensibly isotropic. Since most of their time would thus be spent in intergalactic space, however, such cosmic-ray electrons should be subject to the same "red-shift" decay of energy as would photons. If this is true, the energies of the cosmic rays now striking the earth must be much less than those of the rays in the early history of the earth.

A. H. Compton
University of Chicago

P. Y. Chou
National Tsing Hua University,
Peiping.
May 28, 1937

[1] E. Hubble, Astrophys. J. **84**, 270 and 517 (1936).

Determination of the Shower Producing Efficiency of Cosmic-Ray Particles

The approximate agreement of the Bethe-Heitler theory with observations on electrons[1] adds to the importance of determining the shower producing capacity of those rays which are recorded in a conventional counter telescope. For this purpose we counted coincidences between two layers of very thin walled Geiger counters operating at a pressure so low that the probability of a single ray setting off a counter is very much less than unity. We then utilized the relatively high efficiency of these counters for multiple rays in detecting electron showers originating above them. Such an arrangement differs from the usual counter shower device in that the probability of recording a shower is independent of the angular spread of the shower electrons. This fact simplifies the assignment of an upper limit to the total number of showers arising in a specimen as a result of the passage through it of a known number of single rays.

If we count coincidences between the counter groups A and B (Fig. 1) and if P is the probability that a single ray will set off any one counter in A or B, then P^2 is the probability that a single ray in passing through A and B will be recorded as a coincidence. However if n rays pass through A and B simultaneously, the probability of their being recorded is $\{1-(1-P)^n\}^2$. If we take the coincidence counting rate of A and B at high pressure, where the counters are practically 100 percent efficient, we obtain the total number of rays passing through the counter surfaces. The same measurement taken at reduced pressure gives a determination of P for that pressure, and the corresponding efficiency of the coincidence set for a shower of any size. These measurements were taken in open air and multiple rays passing through A and B in the absence of lead, or single rays which pass through more than one counter of A or B, are not sufficiently numerous to affect seriously the calculation of P.

The results shown in the curve were taken with 2 cm of hydrogen in the counters. At this pressure the coincident efficiency of A and B is 6.3 percent for single rays, hence 19 percent for two rays, 34 percent for three rays, 46 percent for four rays, and so on. Employing a relation obtained by C. G. Montgomery and D. D. Montgomery[2] for the frequency of occurrence of showers as a function of shower size we conclude that the average number of rays in a shower from 1.5 cm of lead is four. Assuming this figure for n, and utilizing the maximum increase indicated in our curve it follows that not more than 6 percent of all the ionizing rays passing through A and B produce a shower in lead of this thickness. If we take $n=2$ we obtain an absolute maximum of 15 percent. This figure is obviously too high as $n=2$ corresponds to the smallest shower that can arise in the lead.

If the incoming rays are electrons, having the energy distribution given by Blackett,[3] and producing showers according to the Bethe-Heitler theory, we should have obtained an increase in counting rate with lead not less than ten times that actually observed. If, as seems to be the case, the theory is correct for electrons we are led to conclude that the bulk of those rays which record themselves in counter sets at sea level is not electrons. Rossi,[4] J. C. Street, R. W. Woodward and E. C. Stevenson[5] have concluded that the penetrating component of the radiation is not an electron. Since the penetrating component is dominant at sea level our results are in agreement with this conclusion.

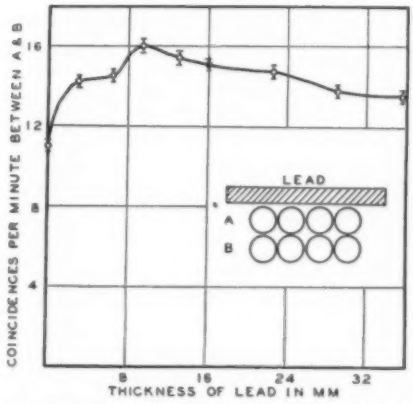

FIG. 1. Arrangement of counters and number of coincident counts per minute with hydrogen at 2 cm pressure in the counters.

W. E. RAMSEY
W. E. DANFORTH

Bartol Research Foundation of the Franklin Institute,
Swarthmore, Pennsylvania,
May 20, 1937.

[1] C. D. Anderson and S. H. Neddermeyer, Phys. Rev. **50**, 263 (1936).
[2] C. G. Montgomery and D. D. Montgomery, Phys. Rev. **50**, 490 (1936).
[3] P. M. S. Blackett, Proc. Roy. Soc. **159**, 1 (1937).
[4] B. Rossi, Zeits. f. Physik **82**, 151 (1933).
[5] J. C. Street, R. H. Woodward, and E. C. Stevenson, Phys. Rev. **47**, 891 (1935). Also J. C. Street, E. C. Stevenson, Phys. Rev. **51**, 1005 (1937).

Neutron Refraction

In a recent letter[1] we suggested the possibility of focusing a neutron beam by means of a paraffin lens, and stated that preliminary experiments indicated the existence of such focusing. This statement must now be withdrawn. Experiments were conducted inside a box which was completely lined with cadmium in order to eliminate scattered neutrons from the furniture and walls of the laboratory. Above a source of slow neutrons a paraffin lens was placed and at varied distances above the lens a dysprosium target. The activity of this target was found to have a maximum at 40 to 50 cm above the lens. However, in order to eliminate the possibility of all spurious effects, such as scattering from the cadmium walls, the experiments were finally continued out of doors, the apparatus being well protected from the ground by cadmium sheets. In these experiments no sign of a maximum was found.

GILBERT N. LEWIS
PHILIP W. SCHUTZ

Department of Chemistry,
University of California,
Berkeley, California,
May 24, 1937.

[1] Lewis and Schutz, Phys. Rev. **51**, 369 (1937).

Conservation of Energy in the Disintegration of Li^8

Some time ago two of us reported an investigation with isotopic targets of the energy balance in the formation of radio-lithium by the process $Li^7+D^2 \rightarrow Li^8+H^1$, and showed that the emission of a beta-particle must be followed by yet another reaction to absorb an excess of energy which amounts to more than 3 Mev, the predicted processes involving the emission of alpha-particles, gamma-rays, or both.[1] The alpha-particles have been found by Lewis, Burcham, and Chang[2] who report that, though most of the alpha-particles have ranges of less than 1.5 cm of air, about 0.3 percent of the total extend to 5 cm. They suggest that the alpha-particles originate in excited Be^8 formed "either in a number of discrete energy states or in a continuous distribution."

We have continued our investigations of the formation and disintegration of radio-lithium with the following results.

(1) The initial reaction, $Li^7+D^2=Li^8+H^1+Q$, seems the only possible one fitting the experimental facts.

(2) The energy balance, Q_1, for the formation of Li^8 must be greater than -360 kv since radio-lithium was formed by deuterons of energies as low as 360 kv.

(3) Q_1 is not greater than $+260$ kv since, using 860-kv deuterons, no proton group of range exceeding 1.7 cm was observed with even a fraction of the intensity necessary for correlation with the amount of radio-lithium produced.

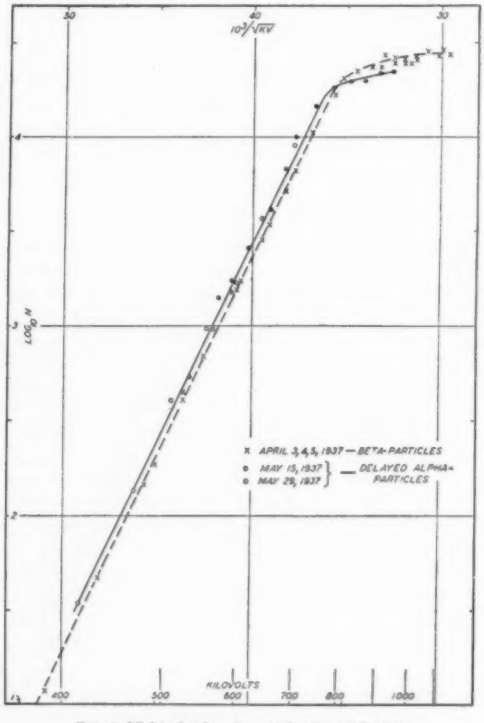

FIG. 1. Yield of delayed particles from Li^7+D^2.

(4) No gamma-radiation was observed in the formation or disintegration of Li^8 although the gamma-radiation from much thinner carbon-targets was readily detected.

(5) The ratio of alpha-particles of ranges exceeding 6 mm to beta-particles counted under the same experimental coaditions is very nearly unity. However, corrections for alpha-particles of shorter range and for the geometry of the beta-particle counter would tend to increase this ratio.

(6) The excitation curves for the delayed alpha- and beta-particles as shown in Fig. 1 are identical and markedly different from eight other carefully measured lithium excitation curves.

(7) The disintegration of Li^8 produces alpha-particles with a half-period of 0.85 ± 0.1 sec. and beta-particles with a half-period of 0.90 ± 0.1 sec., indicating that the decay periods are identical.

(8) We have been unable to observe the instantaneous emission of low energy alpha-particles which might be produced by bombardment of Li^6 with deuterons or Li^7 with protons. These might be expected if the delayed alpha-particles arise from excited states of Be^8.

(9) The number range curve for the delayed alpha-particles shows a smooth continuous distribution falling rapidly with increasing range, and decreasing by a factor of 800 between 0.6 and 5.2 cm.

In view of the experimental results (4), (5), (6), (7), and (8) above, it is highly probable that Li^8 always disintegrates into two alpha-particles and a beta-particle. Combining this fact with (9) and the known form of the energy-distribution curve for beta-rays, it follows that, for any given energy interval, both conservation of energy and of electric charge cannot be satisfied simultaneously by considering charged particles alone.

This difficulty is avoided by including an uncharged body (neutrino hypothesis) in the four-body disintegration

$$_3Li^8 \rightarrow {}_2He^4+{}_2He^4+{}_{-1}\epsilon+{}_0\nu+Q_2.$$

The disintegration energy Q_2 is divided between Q_L, the energy of the light particles, and Q_H, the energy of the heavy particles. From conservation of momentum Q_H is very nearly equal to $2Q_\alpha$, twice the energy of a single alpha-particle. Using the Bainbridge-Jordan[3] mass scale and

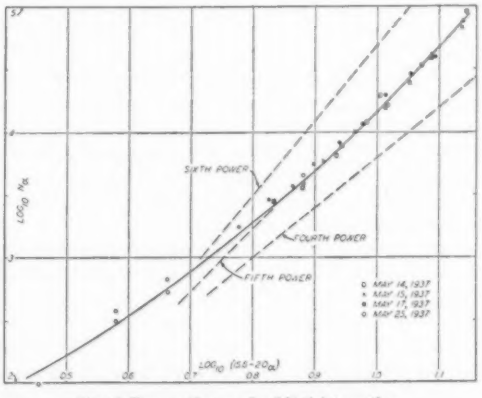

FIG. 2. Energy diagram for Li^8 disintegration.

$Q_1 \sim 0.2$ Mev, according to (2) and (3) above, $Q_2 \sim 15.6$ Mev, whence

$$Q_L = (15.6 - 2Q_\alpha).$$

Since, by conservation of charge, the transition probability for a beta-neutrino energy, Q_L, will be proportional to the number of alpha-particles, N_α, observed with energies Q_α, the relation between this transition probability and Q_L may be obtained by plotting N_α against Q_L as in Fig. 2.

It is interesting to note that *the application of the neutrino hypothesis, conservation of energy, and charge to our alpha-particle data results in a Sargent diagram.* In fact, this diagram is essentially an idealized Sargent diagram because it represents a *continuum* in Q_L for which initial and final nuclei are identical.

We are greatly indebted to Professors Gamow and Teller for discussion of the theory of this disintegration. They have pointed out that considerations based on the Fermi theory predict a number of alpha-particles proportional to $(Q-2E_\alpha)^5(E_\alpha)^n$ where n is $\frac{1}{2}$ or $\frac{3}{2}$ depending on the angular momentum of the alpha-particles. Our observations agree satisfactorily with the fifth power (Fig. 2), although further study of the low energy alpha-particles will be necessary to decide whether n should be $\frac{1}{2}$ or $\frac{3}{2}$. The Konopinsky-Uhlenbeck theory predicts a seventh power dependence which clearly is not in agreement with our observations.

The above interpretation at once suggests additional experiments to establish whether or not tne conservation of momentum is also satisfied by the neutrino hypothesis in the disintegration of Li^8. Preparations for such observations have been undertaken.

L. H. Rumbaugh
R. B. Roberts
L. R. Hafstad

Bartol Research Foundation of the Franklin Institute (LHR), Swarthmore, Pennsylvania.
Department of Terrestrial Magnetism, Carnegie Institution of Washington (RBR, LRH), Washington, D. C.
June 3, 1937.

[1] Rumbaugh and Hafstad, Phys. Rev. **50**, 681 (1936).
[2] Lewis, Burcham, and Chang, Nature **139**, 24 (1937).
[3] Bainbridge and Jordan, Phys. Rev. **51**, 384 (1937).

The Radioactivity of K^{38}

Rocksalt bombarded with 0.05 microamperes of 7 Mev alpha-particles accelerated in a cyclotron displays a strong activity of 7.5 ± 0.1 minutes half-life (Fig. 1). $NiCl_2$ bombarded with alpha-particles gives rise to activity of the same period, while Na_2CO_3 does not, so that the 7.5 minute radioelement must be produced from chlorine. Magnetic deflection of the particles emitted shows them to be positrons. The activity has been shown chemically to be due to an isotope of potassium, by precipitating it with sodium cobaltinitrite. These data make it seem extremely likely that the radioelement is the potassium isotope of mass number 38, formed in the reaction Cl^{35} (α, n) K^{38}.

The absorption of the positrons in aluminium has been measured (Fig. 2); the half-value thickness is about 0.23 g/cm², indicating that the maximum energy of the continuous spectrum is of the order of 3 Mev.

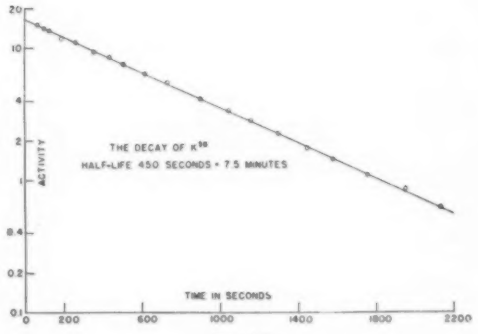

FIG. 1.

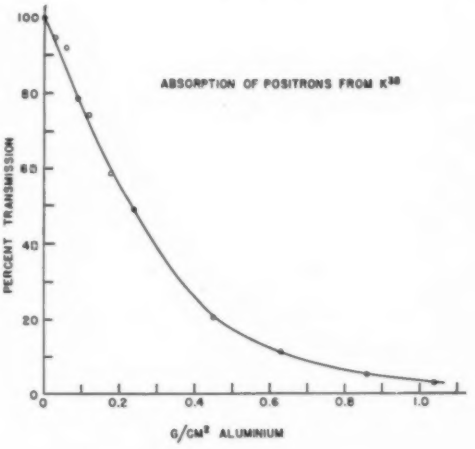

FIG. 2.

Walke[1] has attributed to K^{38} a weak activity of 10.5 hours half-life found by him in the potassium precipitate of a sample of Ca bombarded by deuterons. The present result suggests that this may be a wrong assignment; possibly the observed activity was due to K^{42}, formed by the reaction Ca^{44} (D, α) K^{42}. The half-life of K^{42} is 12.2 hours.

Pollard, Schultz, and Brubaker[2] have observed the emission of neutrons from Cl bombarded with alpha-particles, and have attributed them to the reaction Cl^{37} (α, n) K^{40}. The strength of the activity here reported makes it seem likely that many of the neutrons arise from the reaction Cl^{35} (α, n) K^{38}. The abundance ratio of the chlorine isotopes $(Cl^{35}/Cl^{37} = 76/24)$ slightly favors the second reaction.

W. J. Henderson
L. N. Ridenour
M. G. White
M. C. Henderson

Palmer Physical Laboratory,
Princeton University,
Princeton, New Jersey,
May 17, 1937.

[1] H. Walke, Phys. Rev. **51**, 439 (1937).
[2] E. Pollard, H. L. Schultz and G. Brubaker, Am. Phys. Soc. Meeting, Washington, April 30, 1937.

A Decrease in the Electrical Resistance of Gold with a Magnetic Field at Low Temperatures

In connection with another investigation we have made measurements on the resistance of a sample of gold wire to which 0.1 percent of silver had been added. At about 8°K the resistance passes through a minimum and at 2°K it has increased about 3 percent above the minimum value. This effect has been observed previously by de Haas, de Boer and van den Berg[1] and the present observations are in agreement with their results. The minimum resistance is 0.0957 of the value at the ice point.

We have also made measurements in the presence of a magnetic field at liquid helium temperatures. At 4.23° the resistance increased with a magnetic field; however, at 1.63°K the resistance decreased by over 1 percent when a field of 8000 gauss was applied. The data are shown in Table I. A more complete study is in progress. The sample consisted of number 40 wire wound on a spool, the axis of which was parallel to the magnetic field.

TABLE I. *Change of resistance of gold with a magnetic field.*

$T=1.63$°K		$T=4.23$°K	
H_{Gauss}	$(\Delta R/R)\times 10^4$	H_{Gauss}	$(\Delta R/R)\times 10^4$
1630	−5.1	1630	+2.8
2450	−10.5	2450	4.8
3300	−18.7	3230	6.4
6110	−62.2	6040	15.7
8490	−112.3	8490	26.8

The above reversal in sign and the minimum in resistance are presumably related. A decreasing resistance with magnetic field has previously been observed only in the case of ferromagnetic metals and has been ascribed to effects related to ferromagnetism. A series of gold-silver alloys covering the range 10 to 90 mole percent was also investigated. These materials have no appreciable temperature coefficient of resistance below 10°K and their resistance is practically independent of magnetic field to 8000 gauss.

W. F. GIAUQUE
J. W. STOUT
C. W. CLARK

Department of Chemistry,
University of California,
Berkeley, California,
May 19, 1937.

[1] de Haas, de Boer and van den Berg, Physica **1**, 1115 (1934); de Haas and van den Berg, Physica **3**, 440 (1936).

Connection Between the Second Virial Coefficient and the Phases of Collision Theory

In a recent paper on "Quantum Theory of the Equation of State at Low Temperatures"[1] the writer derived the exact quantum formulae for the second virial coefficient for gases obeying the various statistics, the one for the Einstein-Bose statistics, for example, being, in the absence of any discrete state,

$$B=-\frac{N\pi^{\frac{1}{2}}\lambda^3}{2}+2\sum_{\text{even } l}(l+\tfrac{1}{2})B_l \qquad (1)$$

with the same notation as in the paper cited.

For high temperatures, it was there shown how the quantum formulae for all statistics go over to the classical. Up till now, however, no satisfactory formula has been developed for the low temperature region. And it is just this region which is the most interesting, for at low enough temperatures, it should be possible to verify experimentally, at least for helium, the difference between the statistics theoretically predicted. This ought to be possible since at the lowest temperatures the virial coefficient for the Einstein-Bose statistics is theoretically twice as large as for the Boltzman statistics. And even though the Slater-Margenau potential may be quite inaccurate, there is a margin of a hundred percent difference between the two statistics, which leaves room enough to decide from the experimental data—all the more so, since, as we shall show in a later paper, the virial coefficient is relatively not so sensitive to the potential at the lower temperatures.

In the attempt to find an expression for the virial coefficient valid at low temperatures, the writer was led to derive an *exact* expression for B_l. The result is simply

$$B_l=-8\pi^{\frac{1}{2}}\lambda^3 N\int_0^\infty dk e^{-\lambda^2 k^2}d\eta/dk, \qquad (2)$$

where η is the phase shift in the wave function for two radially interacting molecules. *This expression is valid over the whole temperature region.* The proof will be left to a later paper. We will only show here, that for the case of rigid spheres (2) reduces to the formula given by Uhlenbeck and Beth.[2] For, with rigid spheres,

$$\eta=-\tan^{-1}\left(\frac{J_{l+\frac{1}{2}}(k\sigma)}{J_{-l-\frac{1}{2}}(k\sigma)}(-1)^l\right),$$

so that

$$\frac{d\eta}{dk}=-\frac{2}{\pi k}\frac{1}{J^2_{l+\frac{1}{2}}(k\sigma)+J^2_{-l-\frac{1}{2}}(k\sigma)}.$$

Substitution in (2) gives the Uhlenbeck and Beth result.

This work will be developed more fully when the calculation for the phases is completed.

LEON GROPPER

New York University,
Washington Square College,
May 18, 1937.

[1] L. Gropper, Phys. Rev. **50**, 963 (1936).
[2] G. E. Uhlenbeck and E. Beth, Physica **3**, 729 (1936).

On the Effects in Cosmic-Ray Intensity Observed During the Recent Magnetic Storm

The purpose of this letter is to indicate some effects in cosmic-ray intensity which were observed simultaneously at two stations during the magnetic storm of April 25 to 30, 1937. The data were obtained with Compton-Bennett meters, one at the Cheltenham (Maryland) Magnetic Observatory of the United States Coast and Geodetic Survey and the other at the Huancayo (Peru) Magnetic Observatory of the Department of Terrestrial Magnetism of the Carnegie Institution of Washington. The accompanying figure summarizes the observed effects. On it are plotted for the two stations, in Greenwich mean time, the departures, in percent of the absolute value, of each bi-hourly

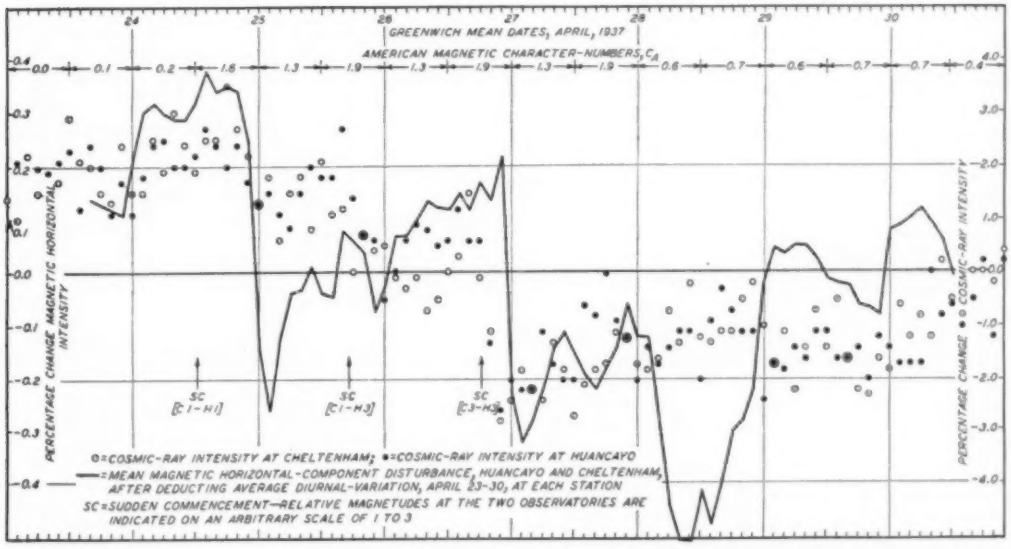
GREENWICH MEAN DATES, APRIL, 1937
AMERICAN MAGNETIC CHARACTER-NUMBERS, C_A
PERCENTAGE CHANGE MAGNETIC HORIZONTAL INTENSITY
PERCENTAGE CHANGE COSMIC-RAY INTENSITY
SC [C1-H1]
SC [C1-H3]
SC [C3-H3]
○=COSMIC-RAY INTENSITY AT CHELTENHAM; ●=COSMIC-RAY INTENSITY AT HUANCAYO
—=MEAN MAGNETIC HORIZONTAL-COMPONENT DISTURBANCE, HUANCAYO AND CHELTENHAM, AFTER DEDUCTING AVERAGE DIURNAL-VARIATION, APRIL 23-30, AT EACH STATION
SC=SUDDEN COMMENCEMENT—RELATIVE MAGNETUDES AT THE TWO OBSERVATORIES ARE INDICATED ON AN ARBITRARY SCALE OF 1 TO 3

FIG. 1. Bi-hourly departures expressed in percentage of absolute values for cosmic-ray intensity and for disturbance of horizontal magnetic component April 23–30, 1937, Huancayo and Cheltenham magnetic observatories.

mean of cosmic-ray intensity, after eliminating bursts, reduced to constant barometric pressure.

The striking similarity of the simultaneous changes in *the bi-hourly means* of cosmic-ray intensity at the two stations is obvious. The separation of the stations excludes the possibility that this is due to barometric changes.

The decrease of nearly four percent in cosmic-ray intensity from April 23 and 24 to April 27 is much greater than the largest changes which have been observed heretofore at either station over a similar period. The intensity of the magnetic storm was also the greatest since these meters have been operating.

The solid curve in the figure indicates the departures in percent of absolute value of bi-hourly means of the horizontal component of the earth's field derived from the magnetograms recorded at the two stations. It shows several storms following the usual course of a magnetic disturbance, namely, an increase in the horizontal component, which often begins abruptly with a "sudden commencement" (SC); this increase usually continues for an hour or more and is followed by a rapid decrease and a slow recovery to normal after a day or two.

The primary field of a magnetic storm is known to arise from external causes and the major changes of that field can be ascribed to an external current-system.[1, 2] This current system is such that, at great distances external to it, the changes are approximately those which would arise from a change in the earth's moment of the same sign as the observed change in horizontal intensity. Thus the decrease in cosmic-ray intensity which appears to follow the decrease in the horizontal component is to be expected on the basis of the theory of Lemaitre and Vallarta. The storm effect—if substantiated by future observations—when considered in the light of the theory of the allowed cones of Lemaitre and Vallarta, may provide further information on the energy distribution of cosmic rays.

Rigorous analysis based on the theory of Lemaitre and Vallarta has not yet been attempted pending receipt of additional magnetic data to determine the uniform part of its external field of the storm. Some discrepancies between the changes in cosmic-ray intensity and the horizontal component of the earth's field may be expected since cosmic rays are probably affected mostly by the equivalent dipole changes in the earth's field. Some discrepancy may be expected also when one considers the effects of the induced current system.

It may be remarked that there is a noticeable similarity between changes in the daily means of cosmic-ray intensity at these two stations. This would seem a necessary but not sufficient condition for the existence of the 27-day variation in cosmic-ray intensity noted by Hess.[3]

While the evidence here presented cannot be regarded in itself as conclusive proof that the observed changes in cosmic-ray intensity are due to the external field of the magnetic storm, this hypothesis seems to be the most reasonable one.

We are under obligation (1) to the staff of the United States Coast and Geodetic Survey at Cheltenham—in particular G. A. Hartnell who is in charge of the meter—and (2) to the staff at the Huancayo Magnetic Observatory.

S. E. FORBUSH

Department of Terrestrial Magnetism,
Carnegie Institution of Washington,
Washington, D. C.

[1] S. Chapman, Terr. Mag. **40**, 349–370 (1935).
[2] L. Slaucitajs and A. G. McNish, Rep. and Comm., Edinburgh Assembly, Internat. Union Geod. Geophys., Ass. Terr. Mag. Electr., Sept. 1936, 7 pp. (July 31, 1936).
[3] V. Hess, Terr. Mag. **41**, 345–350 (1936).

On the Absorption of Cosmic-Ray Electrons in the Atmosphere

The satisfactory description of shower phenomena[1, 2] obtained under the assumption of the validity of radiation theory up to very high energies reopens the question of the effects due to primary electrons in the atmosphere itself. Qualitatively this problem can be treated very simply by the method of Carlson and Oppenheimer.[1] Their diffusion Eq. (12) admits for the distribution $P(E, t)$ as function of energy E and traveled distance t (unit length for air 0.4 m water equivalent) the solution[3]

$$P(E, t)dE = e^{-k_n t}E^{-n}dE, \quad (1)$$

$$k_n = 4/3 - 1/n + \{(2/3 - 1/n)^2 + 4/3(n-1)n\}^{\frac{1}{2}}. \quad (2)$$

An initial distribution of form E^{-n} is therefore preserved as such and absorbed exponentially. At the limit of divergence of the incident energy, i.e., $n=2$, k would be 0 (no apparent absorption) and any apparent coefficient of absorption can thus be accounted for by a suitable exponent n.

In case the primary distribution can be approximated by a sum of falling powers in E its change in the atmosphere can be worked out easily. At large t the terms with smaller n will be the most important. To the $k=0.2$ (0.5/m water equivalent) for the soft component alone of the cosmic radiation near sea level there corresponds an $n=2.3$. Since the maximum near the top of the atmosphere observed by Regener and Pfotzer[4] and Millikan[5] can be well explained by the preponderance of primaries just above the minimum energy for penetration of the earth magnetic field at our latitudes (about 3×10^9 ev) and since the change in the distribution (1) due to the absence of primaries below this energy can be estimated to be negligible for $t>12$ (about half the atmosphere) it is evident that any absorption curve of the type found by Pfotzer can be represented as due to a suitable primary distribution.[6]

A distribution $P(E, 0)=E^{-n(E)}$ with $n(E)$ decreasing smoothly from 2.8 at 3×10^9 ev to 2.3 at about 10^{12} ev has been found to give the entire Pfotzer curve within an error smaller than 20 percent at every point.

The consequences of such a primary distribution seem to be quite compatible with our other knowledge. The distribution in energy at a definite depth would be nearly independent of t from sea level ($t=25$) to $t=15$ and would approximate an $E^{-2.3}$ law. This means that the probability of showers should be nearly proportional to the intensity of the soft component in latitude as well as in altitude. The same should hold for the relative probability of showers of different size. Also the optimal thickness of shower generating lead screens should be independent of altitude for moderate altitudes. All this seems to be approximately correct except possibly in the case of large showers or bursts which show a more rapid increase with altitude than the soft component alone. This could be interpreted as due to a stronger falling off than $E^{-2.3}$ of $P(E, 0)$ at extremely high energies (over 10^{12} ev). For the geomagnetic effect it would follow that the latitude effect at sea level must be entirely due to the hard component. At pressures of about 50 cm Hg a considerable effect (about 25 percent) already would exist for the soft component and near the top of the atmosphere (8 cm Hg) the intensity at the equator should be only a few percent of the intensity at 50° latitude.

It seems therefore to be quite possible to retain the assumption of the unlimited validity of the radiation theory for electrons and photons provided a rather slow falling off of the primary distribution and its extension to at least 10^{12} ev is admitted.[7] A small change in the radiative probabilities at these energies would, however, affect this analysis appreciably.

L. W. NORDHEIM

Purdue University,
Lafayette, Indiana,
May 18, 1937.

[1] J. F. Carlson and J. R. Oppenheimer, Phys. Rev. **51**, 220 (1937).
[2] H. J. Bhabha and W. Heitler, Proc. Roy. Soc. **159**, 432 (1937).
[3] This solution holds only for electrons of energies above 1.5×10^8 ev where the ionization losses become preponderant over the radiation losses. The effect of the ionization and the number of low energy electrons can be estimated by a method analogous to Eqs. (27) to (30) (reference 1) and their inclusion will not modify the absorption coefficient (2).
[4] G. Pfotzer, Zeits. f. Physik **102**, 23, 41 (1936).
[5] R. A. Millikan, H. V. Neher and S. K. Haynes, Phys. Rev. **50**, 992 (1936).
[6] Prior to an analysis in terms of an electron distribution an allowance for the hard component has to be made. We assumed its contribution at sea level to be 70 percent of the total and extrapolated to other altitudes with an absorption coefficient of 0.16/m water. The analysis is not very sensitive against a change in these assumptions.
[7] A somewhat similar analysis of the absorption curve has been given by W. F. G. Swann, Phys. Rev. **50**, 1103 (1936), and C. G. Montgomery and D. D. Montgomery, Phys. Rev. **51**, 217 (1937). The difference in our treatment is that we use the actual theoretical formulae for the radiative effects and identify the electrons with the soft component of the cosmic radiation.

Theory of Recombination of Ions Over an Extended Pressure Range

Recent work by M. E. Gardner[1] in this department has strongly indicated the correctness of the J. J. Thomson[2] theory of ion recombination below one atmosphere pressure. Recent work of Mächler[3] and earlier results indicate that above 5 to 15 atmospheres the recombination occurs according to the classical Langevin[4] theory. As suspected by Thomson[2] these two results are not inconsistent. If a sphere of radius d defined by $e^2/d=3kT/2$ is drawn about an ion in a gas, ions of opposite sign will undergo random diffusion in general away from the ion if outside d and will be actively attracted[2] to it if inside d. Here e is the electron, k the Boltzmann constant and T the absolute temperature. If the electron attaches outside of d to form an ion the recombination will follow Thomson's theory giving a coefficient $\alpha_T=\pi(c_+^2+c_-^2)^{\frac{1}{2}}(2\omega-\omega^2)$.[5] c_+ and c_- are velocities of agitation of the ions and ω is the chance of energy loss by one ion by molecular impact in d. If it attaches inside d it will recombine according to the classical Langevin equation $\alpha_L=4\pi e(k_++k_-)$ (preferential recombination) where k_+ and k_- are the mobilities of the two ions.[4] The fraction f of the electrons diffusing to a distance d or more before attaching can be determined. The fraction $1-f$ attach within d. Hence the true value of the coefficient α is $\alpha=\alpha_T f+(1-f)\alpha_L$. In the absence of the ionic field an electron diffuses a distance d in a time t given by $d=(12Dt/\pi)^{\frac{1}{2}}$.[6] Here D is the coefficient of diffusion roughly given by $D=\frac{1}{3}c\lambda$, where λ is the electron free path. The field reduces diffusion *away* from the parent molecule[7] and thus D should be diminished by a numerical factor η, whose

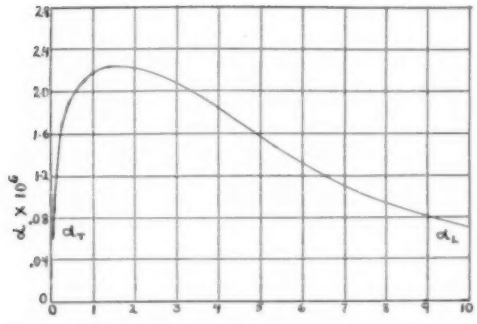

FIG. 1. Coefficient of recombination of ions in oxygen, the function of pressure. The abscissae give the pressure in atmospheres. At 1 atmos. $\alpha_T = 2\times10^{-6}$, $\alpha_L = 6.8\times10^{-6}$, $\eta = 2\times10^6$.

theoretical evaluation is very difficult and which may be quite large, so that $d=(12Dt/\pi\eta)^{\frac{1}{2}}$. Let n be the number of electrons so that in a time dt the number of electrons attaching will be given by $dn=nh\bar{c}dt/\lambda$, where h is the probability of attachment and $\bar{c}/\lambda$ is the collision frequency. If n is the number of electrons after a time t and n_0 is the number at $t=0$, then $f=(n/n_0)e^{-h\bar{c}t/\lambda}$.[6] Hence $f=e^{-\pi h\bar{c}\eta/4\lambda^2}$, which neglecting the variation of λ and h with electron energy can be written $f=e^{-a(p/760)^2}$. Since again $4\pi e(k_+ + k_-)=b(760/p)$ the equation for α becomes

$$\alpha=\alpha_T e^{-a(p/760)^2}+[1-e^{-a(p/760)^2}]b(760/p),$$

where p is the pressure in mm of Hg. There are at present no reliable extensive data to check this theory and our experience indicates that they will be very difficult to obtain. Insertion of the values of the constants into the equation indicates from the unsatisfactory data on hand that η will have to be of the order of 10^6. The shape of the curve for O_2 is indicated below. The 1902 data of Langevin[9] strongly indicate a behavior of this sort and in the limits of high and low p it is naturally in agreement with the character of the results of Gardner and Mächler.

LEONARD B. LOEB

University of California,
Berkeley, California,
May 8, 1937.

[1] M. E. Gardner, Phys. Rev. **51**, 144 (1937).
[2] J. J. Thomson, *Cond. Elect. Through Gases*, Vol. 1, third edition p. 44. L. B. Loeb, *Kinetic Theory of Gases*, second edition p. 586.
[3] W. Mächler, Zeits. f. Physik **104**, 1 (1936).
[4] P. Langevin, Ann. Chim. Phys. **28**, 287, 433 (1903). L. B. Loeb, *Kinetic Theory*, first edition p. 480.
[5] L. B. Loeb, *Kinetic Theory*, second edition p. 595.
[6] A. Einstein, Ann. d. Physik **17**, 558 (1905).
[7] Loeb and Marshall, J. Frank. Inst. **208**, 371 (1929). Loeb, *Kinetic Theory*, second edition p. 590.
[8] Loeb, *Kinetic Theory*, second edition p. 617. N. E. Bradbury, Phys. Rev. **44**, 883 (1933). J. Chem. Phys. **2**, 827 (1934).
[9] P. Langevin, Comptes rendus **137**, 177 (1902).

Thin Film Field Emission

Recently, Malter[1] reported the existence of anomalous secondary electron emission from specially treated electrolytic aluminum oxide. The same type of phenomenon has been produced by evaporating $BaOB_2O_3$ or quartz on to a metal plate and treating the film with caesium and oxygen; the treatment is similar to that used in the case of aluminum oxide. Films showing first and second order

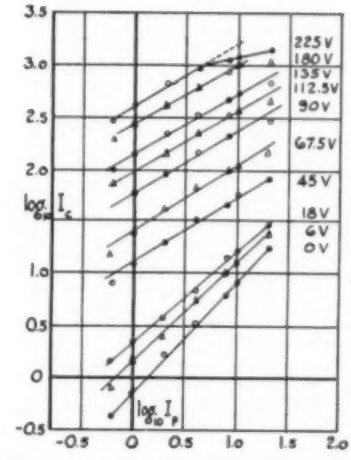

FIG. 1. $\log_{10} I_c$ plotted against $\log_{10} I_p$ for various collector voltages. Currents are expressed in μa.

interference colors, roughly from 600A to 6000A thick, are best in the production of this effect.

A summary of measurements made on treated barium borate films in a tube similar in structure to that used by Malter[1] is presented in the accompanying figures. They

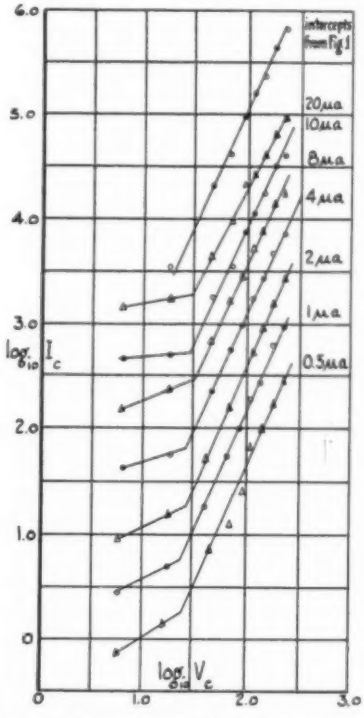

FIG. 2. $\log_{10} I_c$ plotted against $\log_{10} V_c$ for various primary currents. I_c is in μa, V_c in volts. The zero of the ordinate for each successive line is moved up 0.3 units.

are in general agreement with his data. Fig. 1 gives a logarithmic plot of the current to the collector, I_c, as a function of the incident bombarding current, I_p, for constant voltage on the collector, V_c. Fig. 2 gives a similar family with I_c and V_c as variables, and I_p as the parameter. The points were taken with 650 volt primary electron beam covering an area of 0.3 cm² on the target.

Fig. 1 clearly indicates that the collector current, provided it is less than 1.2 ma, is proportional to some power of the primary current; the exponent decreases from, roughly, unity at zero collector voltage, to the constant value of 0.59 above 25 volts. With similar restrictions on collector current and voltage, the family of curves in Fig. 2 is also a group of parallel straight lines. Within these regions the data can thus be expressed by the relations:

$$I_c = aI_p^n V_c^m,$$

where a, n, and m are constants for a given energy and area of the bombarding beam and activation of the surface. For the data presented, $a=2.5\times10^{-3}$, $n=0.59$, and $m=2.23$. The consistency of the relations can be further checked by the fact that the intercepts of the curves in Fig. 1, plotted in Fig. 2, belong to the family of latter curves and *vice versa*. The intercept curve is shown in Fig. 2; the ordinate scale is shifted up 2.4 units for this curve.

As in the case of aluminum oxide, the treated borate surfaces exhibit a time lag between the incident current and the current to the collector, both when the primary current is turned on and off, and when the collector potential is turned on. All the points were taken at the maximum value of I_c with time.

Barium borate, without any treatment, exhibits anomalous emission but to a lesser extent than treated surfaces. Without treatment the current to the collector is much smaller, the build up is much slower and decay very rapid. The collector voltage must be raised to 200 volts or more to observe the anomalous character of the collector current.

E. R. PIORE

Electronic Research Laboratory,
RCA Manufacturing Company, Inc.,
Camden, New Jersey,
May 14, 1937.

L. Malter, Phys. Rev. **50**, 48 (1936).

Experiments on the Magnetic Moment of the Neutron

In order to perform experiments in which polarized beams of neutrons are used, such as determining the sign and magnitude of the magnetic moment of the neutron, it is desirable to have as large a polarization as possible. Various types of single magnet experiments have been performed in an effort to obtain larger effects. As pointed out before,[1] these experiments with a single magnet eliminate difficulties due to adiabatic transitions when the neutrons pass through regions where angular velocity of the changing magnetic field is of the same order of magnitude as the Larmor frequency, $g\mu H/h$, of the neutron.

The experiments[1] involving the transmission of neutrons through three 0.65 cm iron plates magnetized to saturation and then demagnetized have been repeated using neutrons which were emitted from an "howitzer" cooled to approximately the temperature of liquid air. Both experiments were then performed using two plates instead of three. The experimental set-up was identical in the two sets of measurements. The results of these four experiments are compared graphically in Fig. 1. It is seen that with three plates the magnitude of the effect (percentage increase in transmission of slow neutrons with the plates magnetized[1]) increases from 3.6 percent ± 0.6 percent to 5.3 percent ±1.0 percent. With the two plates the effects are smaller, being 1.9 percent ± 0.7 percent and 2.9 percent ± 0.7 percent, respectively.

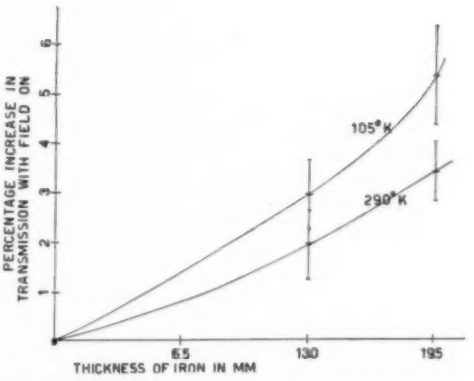

FIG. 1. Change in magnetic scattering with velocity of neutrons.

From these data it is seen that using slower neutrons increases the effect. Also greater thicknesses of iron increase the effect if multiple scattering within the iron is not excessive. However, thicknesses much beyond that corresponding to the three plates reduce the slow neutron intensity to very small values compared to the fast neutron background.

These results are consistent with theory[2-4] in that the change in scattering cross section is proportional to the form factor, $\int \exp(i(\mathbf{k}_0-\mathbf{k})\cdot\mathbf{r})m(\mathbf{r})d\tau$, where $\mathbf{k}_0$ and $\mathbf{k}$ are the propagation vectors of the incident and scattered neutrons, respectively; and $m(\mathbf{r})$ is the magnetization density. For slower neutrons this expression becomes larger and the percentage increase in transmission with the plates magnetized should be greater. Furthermore, within the limits of experimental error the effect varies with the square of the thickness in agreement with the theoretical prediction.[1-4]

Several attempts were made to increase the effect through collimating the neutron beam as completely as possible by various methods. No improvement in the effect was found by this method.

Several types of experiments have been performed with a single magnet in which the scattered neutrons rather than the transmitted neutrons were detected. In one, the same three plates were used; but the central portion of the beam was blocked out with cadmium. Thus the majority of the neutrons detected were scattered neutrons. As is to be expected in this case, the number of neutrons counted was less with the plates magnetized. The percentage change was 1.1 percent ± 0.5 percent. Since it was possible for a small

fraction of unscattered neutrons to be detected, the effect is necessarily small.

In another scattering experiment only one plate was used and the detector was placed out of the direct beam at an angle of about twenty-five degrees so that the only neutrons counted were scattered neutrons. Again the number counted was greatest with the plate demagnetized. The percentage change was 4.1 percent ±1.4 percent. The probable error is rather large because of the high background of fast neutrons in a scattering experiment.

P. N. Powers
H. Carroll
J. R. Dunning

Pupin Physics Laboratories,
Columbia University,
New York, N. Y.,
May 18, 1937.

[1] Powers, Beyer and Dunning, Phys. Rev. **51**, 371 (1937).
[2] Schwinger, Phys. Rev. **51**, 544 (1937).
[3] Bloch, Phys. Rev. **50**, 259 (1936).
[4] Hoffman, Livingston and Bethe, Phys. Rev. **51**, 214 (1937).

Note on the Nature of Cosmic-Ray Particles

The results of Neddermeyer and Anderson,[1] and those of Street and Stevenson,[2] seem quite clearly to indicate the presence, in the penetrating component of cosmic rays, of positive and negative particles of electronic charge, which do not radiate and make showers as do electrons, and which are not protons. Since the probability of radiation can depend essentially only on the charge and the mass of the particle, these authors suggest that we have here to do with particles of mass intermediate between that of the electron and that of the proton. If this mass μ is unique, it introduces a new constant $l=\hbar/\mu c$ into physics; and one would hope to bring this into connection with the length which plays so fundamental a part in the structure of nuclei: the "size" of the proton and neutron: the range of nuclear forces.[3] The value of some 50–100 Mev which this argument suggests for the mass of the particle seems consistent with the cloud chamber observations. These observations themselves, however, could be equally well interpreted if the particles had a quite wide variation in mass; nor do they exclude values considerably lower than 50 Mev.

In fact, it has been suggested by Yukawa[4] that the possibility of exchanging such particles of intermediate mass would offer a more natural explanation of the range and magnitude of the exchange forces between proton and neutron than the Fermi theory of the electron-neutrino field. Thus a straightforward application to this problem of the quantum theory of fields, developed for such particles by Pauli and Weisskopf, gives a Heisenberg exchange force approximately derivable from a potential of the form $-\hbar c e^{-r/l}/4\pi r$. Yet in trying to account in detail along these lines for the characteristics of nuclear forces, one meets with difficulties hardly less troublesome than in the various forms of electron-neutrino theory which have been proposed. In particular, the reconciliation of the approximate saturation character of nuclear forces with the apparent equality of like and unlike particle forces and with the magnetic moments of neutron and proton could here too be achieved only by an extreme artificiality. These considerations therefore cannot be regarded as the elements of a correct theory, nor serve as any argument whatever for the existence of the particles; their valid content can at most be this: that these particles may be emitted from nuclei when sufficient energy ($>\mu c^2$) is available, and that they will ultimately prove relevant to an understanding of nuclear forces. Since even with an energy up to 15 Mev available for the disintegration, nuclei exhibit normal β-decay, the mass of the particles must surely on this view exceed 15 Mev. These particles need not then be primary cosmic rays, but may be ejected from nuclei by γ-rays (and formed by pair production) in the upper atmosphere, and thus complicate the degradation of the primary electrons and greatly increase the effective penetration of the radiation.

The incidence near sea level of multiplicative showers may then be understood in a simple way. For on the one hand we may expect some degraded shower radiation from incident electronic primaries of high initial energy;[5] on the other hand the penetrating particles will produce electronic secondaries by extranuclear impacts; from the curvature distribution of the particles, and with any acceptably low value for their mass, one can see that impacts in which the secondary has energy enough to initiate a small shower should occur about once in 10 m water equivalent. At great elevations (>3 km from sea level) the degraded shower radiation should play the predominant part; under considerable thicknesses of heavy absorber, at sea level, this radiation will be absorbed, and only the secondaries will contribute to the multiplicative showers. Near sea level the two contributions may be comparable in importance.

J. R. Oppenheimer
R. Serber

California Institute of Technology,
Pasadena, California,
June 1, 1937.

[1] S. Neddermeyer and C. D. Anderson, Phys. Rev. **51**, 884 (1937).
[2] J. C. Street and E. C. Stevenson, Bull. Am. Phys. Soc. **12**, 2, 13 (1937).
[3] It is true that the range of nuclear forces is roughly equal to e^2/mc^2; but the fact that it has not been possible to find in electron theory itself any satisfactory physical interpretation of this "electron radius" makes it seem likely that the interpretation of even this quantity must essentially involve the heavy particles and their structure.
[4] H. Yukawa, Proc. Phys. Math. Soc., Japan **17**, 48 (1935).
[5] The number of electrons surviving at sea level depends critically on the energy of the incident particles. For vertical incidence the number surviving per primary of energy E is

$$3\cdot 10^{-12}\times\exp\{x-\tfrac{1}{4}\ln(50x)+9x^{\frac{1}{2}}\},$$

where $x=\frac{1}{3}\ln E/l$, and $l=75$ Mev. This is the asymptotic form for $t=27$ of Eq. (36), in Phys. Rev. **51**, 227 (1937).

Author Index to Volume 51

References with (A) are to abstracts of papers presented at meetings of the Physical Society. References with (L) are to Letters to the Editor.

Abramson, Harold A. Electrophoresis and electroosmosis of drugs through the skin—1025(A)

Adams, J. B., J. C. Hubbard and R. T. K. Murray. Field current emission from metals into gases at high pressures —63(A)

Aebersold, Paul C. Physical measurements concerning the biological action of neutrons—375(A)

Ahlberg, J. E., W. O. Lundberg and I. Estermann. Production of liquid hydrogen without the use of a compressor—1028(A)

Albers, V. M. (see Knorr, H. V.)—1016(A)

——— **and H. V. Knorr.** Visible absorption spectra of porphin and its isomer—1017(A)

Allen, James S. Disintegration of beryllium by protons—59(A), 182

Allison, Samuel K., Graham T. Hatch and Lester S. Skaggs. Construction of a voltage multiplying circuit to yield 700 kv—58(A)

Almy, G. M. (see Challacombe, C. N.)—63(A), 930

——— (see Rassweiller, M. P.)—1019(A)

——— **and R. B. Horsfall, Jr.** Spectra of neutral and ionized boron hydride—491

——— **and H. A. Schultz.** Two new band systems of diatomic antimony—62(A)

Alvarez, Luis W., Edwin McMillan and Arthur H. Snell. Removal of the ion beam of the cyclotron from the magnet field—148(A)

Amaldi, E., L. R. Hafstad and M. A. Tuve. Neutron yields from artificial sources—896

Anderson, Carl D. (see Neddermeyer, Seth H.)—884

Anderson, John A. Some problems connected with the 200-inch telescope—142 (title only)

Anderson, Wilmer C. Measurement of the velocity of light —596(A)

Andrews, D. H., J. A. Sanderson and E. O. Hulburt. Optical properties of evaporated films—1017(A)

Babcock, Harold D. New band of atmospheric oxygen—148(A)

Bacher, R. F. (see Tomboulian, D. H.)—1020(A)

Bainbridge, Kenneth T. (see Jordan, Edward B.)—385(A)

——— **and Edward B. Jordan.** Atomic masses of hydrogen, helium, carbon and nitrogen isotopes—384(A)

——— **and Edward B. Jordan.** Mass-spectrographic measurement of the C^+ band resulting from the dissociation of CO^+—595(A)

Baker, C. P. and M. Stanley Livingston. Discharge tube ion source for the cyclotron—1011(A)

Baker, Edward B. and Howard A. Boltz. Thermionic emission into dielectric liquids—275, 989(L)

Bardeen, John. On the density of energy levels of heavy nuclei—384(A), 799

Barnes, S. W. (see DuBridge, L. A.)—995(L), 1012(A)

———, **L. A. DuBridge, E. O. Wiig, J. H. Buck and C. V. Strain.** Proton-induced radioactivity of elements of atomic number greater than eleven—1012(A)

———, **L. A. DuBridge, E. O. Wiig, J. H. Buck and C. V. Strain.** Proton-induced radioactivity in heavy nuclei—775(L)

Barr, E. S. An infrared study of alcohol-acetate mixtures—685(A)

——— (see Plyler, E. K.)—1017(A)

Bartlett, J. H., Jr. Helium wave equation—661

——— Neutron-proton interactions—889(L)

Barton, Henry A. (see Lampson, Curtis W.)—1021(A)

Baudisch, Oskar (see Welo, Lars A.)—1016(A)

Bayley, D. S. and H. R. Crane. Experiments on Li^8 and B^{12} —1012(A)

Bazzoni, Charles B. (see Weber, Alfred H.)—378(A)

Beams, J. W. (see Hoxton, L. G.)—690(A)

——— (see Snoddy, L. B.)—1008(A)

——— **and F. W. Linke.** An inverted ultracentrifuge—689(A)

——— **and A. Victor Masket.** Concentration of chlorine isotopes by centrifuging—384(A)

Bearden, J. A. Charge on the electron—378(A)

Beck, F. J., Jr. (see Ingerson, W. E.)—1010(A)

Beese, N. C. Focusing of electrons in an x-ray tube—998(A)

Bender, David. Refractive index of air in the infrared—144(A)

Bethe, H. A. Disintegrations of very heavy nuclei by deuterons—1004(A)

——— (see Hoffman, J. G.)—214, 1021(A)

——— (see Konopinski, E. J.)—1004(A)

——— (see Rose, M. E.)—205, 993(L)

——— **and G. Placzek.** Resonance effects in nuclear processes—450

——— **and M. E. Rose.** Kinetic energy of nuclei in the Hartree model—283

Beyer, H. G. (see Dunning, J. R.)—51(L), 382(A)

——— (see Powers, P. N.)—371(L)

Bitter, F. Theory of the ferromagnetism of alloys—383(A)

Black, J. G. An arrangement for simplifying the analysis of a spectrum plate—380(A)

Blake, F. C. Posnjak and Barth's principle of "variate atom equipoints," superlattices and "mixed crystals."—1000(A)

Bless, A. A. Effect on an electric field on the diffraction pattern of liquids—688(A)

Bloch, F. On the magnetic scattering of neutrons. II—994(L)

Blodgett, Katharine B. and Irving Langmuir. Built-up films of barium stearate and their optical properties—964

Bockstahler, Lester and Herman Ritow. Potentials in the intermittent glow discharge—1009(A)

Bollman, Vernon (see DuMond, Jesse W. M.)—400

——— **and Jesse W. M. DuMond.** Precision determination of h/e from the short wave-length limit of the continuous x-ray spectrum—145(A)

Boltz, Howard A. (see Baker, Edward B.)—275, 989(L)

Bonner, Lyman G. and Robert Hofstadter. Infrared absorption spectrum of formic acid vapor—1017(A)

Bowen, I. S. and Everett F. Cox. Ionization of air by γ-rays as a function of pressure and collecting field II—232
——, **R. A. Millikan and H. V. Neher.** Influence of the earth's magnetic field on cosmic-ray intensities up to the top of the atmosphere—1005(A)
Bowls, Woodford E. Effect of mercury vapor on the Townsend coefficient, α, in pure nitrogen—147(A)
Bozorth, R. M. (see Cioffi, P. P.)—1009(A)
—— **and L. W. McKeehan.** An explanation for directions of easy magnetization in ferromagnetic cubic crystals—216(A)
Bradbury, Norris E. (see Nielsen, Russell A.)—69, 143(A)
Bramley, Arthur. Nuclear disintegrations accompanying cosmic-ray showers—385(A)
—— Range of high speed electrons—682(A)
—— Stopping of fast electrons—387(A)
Brammer, Forest E. and Arthur E. Ruark. Improved scale-of-eight recording circuits—688(A)
Brasefield, Charles J. (see Pollard, Ernest)—8
Braun, Milton L. Response of synthetic rubber to temperature changes—684(A)
Breit, G. Approximately relativistic equations for nuclear particles—248
—— Approximately relativistic equations for nuclear particles. Addendum. Proof of approximate invariance—778(L)
——, **J. R. Stehn and E. U. Condon.** Correction to the photoelectric effect of the deuteron—56(L)
—— **and E. Wigner.** Disintegration of Li^6—593(L)
Brenner, W. L. Distribution in a horizontal plane of light from a point source—686(A)
Brice, R. T. Method for sealing β-magnesia windows into steel spectroscopic absorption furnaces and a needle valve for controlling the evacuation of such furnaces—142(A)
Brickwedde, F. G. (see Scott, R. B.)—684(A)
Broch, E. K. Note on the density of eigenfunctions for an electron obeying Dirac's equation—586
Brode, Robert B. and Merle A. Starr. Cosmic-ray showers from lead plates—1006(A)
Brubaker, Gordon (see Pollard, Ernest)—140(L), 1014(A)
—— **and Ernest Pollard.** Maximum energy of the protons emitted by boron under alpha-particle bombardment—1013(A)
Bruce, W. A. (see Foster, E. S., Jr.)—61(A)
—— (see Jauncey, G. E. M.)—60(A), 999(A), 1062, 1067
—— **and E. M. McNatt.** Atomic structure and vibrations in zinc crystals V. Diffuse scattering of x-rays at various scattering angles—1065.
Bruch-Willstätter, M. (see Sponer, H.)—1002(A)
Buck, J. H. (see Barnes, S. W.)—775(L), 1012(A)
—— (see DuBridge, L. A.)—995(L), 1012(A)
——, **C. V. Strain and G. Valley.** Resonance transmutation of Se (34) by protons—1012(A)
Buechner, W. W. (see Lamar, E. S.)—936

Cady, Walter G. Longitudinal effect in Rochelle salt—596(A)
Caldwell, W. I. and K. Lark-Horovitz. X-ray investigations of the structure of wood—998(A)
Camp, Glen D. Heavy particle interaction from β-decay theory—1046
Carlson, J. F. and J. R. Oppenheimer. On multiplicative showers—220
Carroll, H. (see Powers, P. N.)—1022(A), 1112(L)
Carwile, Preston B. Reciprocals to Ampere's law—1016(A)
Challacombe, C. N. Λ-type doubling in the $^3\Pi$ state of OH^+—1001(A)
—— **and G. M. Almy.** Constants of $^3\Pi$ states of AlH, OH^+, BH—63(A)
—— **and G. M. Almy.** On the analysis of molecular $^3\Pi$ states with application to AlH, OH^+, and BH—930
Chapman, Seville. Carrier mobility spectra in the electrification by spraying and bubbling of liquids—145(A)
Chase, C. T. (see Cox, R. T.)—140(L)
Ch'en, Shang-Yi (see Ny Tsi-Zé)—567
Chou, P. Y. (see Compton, Arthur H.)—1104(L)
Christian, Schuyler M. Electrolytic polarization with alternating current—685(A)
Cioffari, Bernard. Structure of the x-ray *K* absorption limits of bromine, iodine, and some of their compounds—630
Cioffi, P. P., H. J. Williams and R. M. Bozorth. Single crystals with exceptionally high magnetic permeabilities—1009(A)
Clark, C. W. (see Giauque, W. F.)—1108(L)
Clark, H. T. and K. Lark-Horovitz. Faraday effect in the x-ray region—61(A)
Clark, O. (see Halpern, O.)—1020(A)
Cobine, J. D. (see Power, R. B.)—594(A)
Cohen, Victor W. (see Ellett, Alexander)—64(A)
—— **and Alexander Ellett.** Velocity analysis of K atoms scattered by a MgO crystal—65(A)
Cohn, Willi M. Polarization of the solar corona—148(A)
Collins, G. B., R. Schager and A. L. Vitter. Electrostatic generator for the production of positrons—58(A)
Colwell, R. C. and A. W. Friend. Reflection of radio waves in the troposphere—1005(A)
—— **and A. W. Friend.** Velocity of radio waves over long distances—990(L)
——, **A. W. Friend and H. C. Hardy.** Frequencies and nodal lines on circular metallic plates—1025(A)
Compton, Arthur H. An energy distribution analysis of primary cosmic rays—59(A)
—— **and P. Y. Chou.** On the origin of cosmic rays—1104(L)
—— **and R. N. Turner.** Variations of cosmic rays with latitude on the Pacific Ocean—1005(A)
Compton, K. T. (see Lamar, E. S.)—936
Comstock, George C. Photoelectric investigation of the "Allison magneto-optic effect"—776(L)
Condon, E. U. (see Breit, G.)—56(L)
—— (see Phillips, M.)—382(A)
Cookson, John W. (see Osterberg, Harold)—1096
Coolidge, Albert Sprague (see James, Hubert M.)—860, 1001(A)
—— **and Hubert M. James.** On the convergence of the Hylleraas variational method—855
Coomes, Edward. Secondary emission from clean tungsten—1008(A)
Cork, J. M. (see Darling, B. T.)—1010(A)

Cork, J. M. (see Kraus, J. D.)—383(A)
——— (see Pool, M. L.)—383(A), 890(L), 1010(A)
——— (see Thornton, R. L.)—383(A)
——— **and R. L. Thornton.** Bombardment of gold with deuterons—59(A)
——— **and R. L. Thornton.** Disintegration of cadmium with deuterons—608
Cornell, S. D. Pressure effect in bands of several dipole molecules—595(A), 739
Cox, Everett F. Current difference in gamma-ray ionization measurements—55(L)
——— (see Bowen, I. S.)—232
Cox, R. T. and C. T. Chase. Scattering of electrons by atomic nuclei—140(L)
Cram, Winston. Influence of temperature of uranin solution on the fluorescence decay time—62(A)
Crane, H. R. High potential apparatus for nuclear studies—58(A)
——— Is the momentum a sufficient description of a photon or an electron?—50(L)
——— (see Bayley, D. S.)—1012(A)
——— (see Gaerttner, E. R.)—49(L), 58(A)
——— (see Turin, J. J.)—1012(A)
Curtis, B. R. (see Darling, B. T.)—1010(A)
Curtis, C. W. First spark spectrum of manganese—1018(A)

Danforth, W. E. (see Swann, W. F. G.)—389
——— (see Ramsey, W. E.)—1105(L)
Darling, B. T., B. R. Curtis and J. M. Cork. Radioactivity in iron by deuteron bombardment—1010(A)
Davey, Wheeler P. (see McLachlan, D., Jr.)—60(A)
——— (see Smith, Sidney D.)—1010(A)
——— **and R. J. Pfister.** Combined still and diffusion pump—1028(A)
Dawson, L. H. and E. O. Hulburt. Scattering of light by water—1017(A)
Delsasso, L. A., W. A. Fowler and C. C. Lauritsen. Energy and absorption of the gamma-radiation from Li^7+H^1—391
———, **W. A. Fowler and C. C. Lauritsen.** Energy and absorption of the gamma-radiation from lithium bombarded by protons—143(A)
———, **W. A. Fowler and C. C. Lauritsen.** Gamma-radiation from fluorine bombarded with protons—527(L)
Dempster, A. J. Electric and magnetic focusing in mass spectroscopy—67
——— Isotopic constitution of neodymium—289(L)
Derieux, John B. New values of the change of resiliency with the velocity of impact—686(A)
d'Eustachio, Dominic. Isotope shifts in Li I—780(L)
DeVoe, Charles F. (see Mendenhall, C. E.)—346
Devol, Lee and Arthur Ruark. Distribution in time of counts due to a constant source and its daughter in equilibrium—710
DeVore, Lloyd T. On the calculation of errors—349
Dicus, A. W. Diffraction patterns by polarized light—686(A)
Dietrich, J. R. (see Snoddy, L. B.)—1008(A)
Downsbrough, G. A. Damping of torsional oscillations in quartz fibers—877, 1014(A)
Driscoll, Raymond L. and Arthur E. Ruark. Fluctuations in the counts of Geiger counters—688(A)
DuBridge, L. A. (see Barnes, S. W.)—775(L), 1012(A)
——— (see Mann, Marvin W., Jr.)—120
———, **S. W. Barnes and J. H. Buck.** Capture of protons by oxygen—1012(A)
———, **S. W. Barnes and J. H. Buck.** Proton induced radioactivity in oxygen—995(L)
Duffendack, O. S. (see Lifschutz, Harold)—1027(A)
——— **and W. H. Gran.** Regularity along a series in the variation of the action cross section with energy discrepancy in impacts of the second kind—804
———, **M. M. Slawsky and Harold Lifschutz.** Discharge mechanism and characteristics of Geiger-Müller counter tubes—1027(A)
Duffin, Richard J. On the behavior of a certain superconducting circuit—575
DuMond, Jesse W. M. (see Bollman, Vernon L.)—145(A)
——— (see Kirkpatrick, Harry A.)—147(A)
——— (see Marlow, Douglas)—145(A)
——— (see Youtz, J. Paul)—144(A)
——— **and Vernon Bollman.** Determination of h/e from the short wave-length limit of the continuous x-ray spectrum—400
Dunning, J. R. (see Powers, P. N.)—371(L), 1022(A), 1112(L)
———, **P. N. Powers and H. G. Beyer.** Experiments on the magnetic properties of the neutron—51(L), 382(A)
Durkee, A. L. Concerning the probable magnitude of the next sunspot maximum—589(L)
Dwight, C. H. (see Kersten, H.)—380(A)

Eckart, Carl. Correction of continuous spectra for the finite resolution of the spectrometer—735
Edwards, Charles W. First courses in physics in American colleges—687(A)
Einarsson, A. W. (see Loeb, Leonard B.)—142(A)
Eisenbud, L. (see Phillips, M.)—382(A)
Ellett, Alexander (see Cohen, Victor W.)—65(A)
——— **and Victor W. Cohen.** A Stern-Gerlach magnetic field as a velocity analyzer for atomic beams—64(A)
Elliott, D. S. Laboratory demonstration experiments in modern physics—687(A)
Ellis, J. W. (see Kinsey, E. L.)—381(A), 1074
Ellwood, W. B. Magnetic hysteresis in 35 permalloy sheet at low flux densities—1009(A)
Elmore, W. C. Properties of the surface magnetization in ferromagnetic crystals—982
Elsasser, W. M. Relations between the self-consistent field and Bohr's nuclear model—144(A)
——— Self-consistent field and Bohr's nuclear model—55(L)
Emo, Lorenzo (see Richardson, J. Reginald)—1014(A)
Estermann, I. (see Ahlberg, J. E.)—1028(A)
———, **O. C. Simpson and O. Stern.** Magnetic deflection of HD molecules—64(A)
———, **O. C. Simpson and O. Stern.** Magnetic moment of the proton—1004(A)

Evans, Robley D. and Clark Goodman. Application of the direct-fusion furnace to the helium method of determining the geologic ages of rocks—595(A)
Ewing, Douglas H. On the electronic constitution of diamond—1002(A)
Eyster, Eugene. Structure of the α and β band systems of SiF—1078

Fano, Ugo. On the anomalous diffraction gratings. II—288(L)
Farnsworth, H. E. Contact potential difference between different faces of silver single crystals—378(A)
Fay, C. H. Scattering of fast neutrons—995(L)
Feenberg, Eugene. On the saturation property of nuclear forces—777(L)
——— **and M. Phillips.** On the structure of light nuclei—597, 683(A)
——— **and E. Wigner.** On the structure of the nuclei between helium and oxygen—95
Ference, Michael, Jr. Auger effect in germanium—720
Field, J. E. and George A. Lindsay. Index of refraction of cerussite for x-rays—165
Fisher, Russell A. Hyperfine structure in the resonance lines of Mg I and Mg II—381(A)
——— Note on the sign of the magnetic moment of the K^{39} nucleus—887(L)
Fisk, J. B. On the cross sections of Cl_2 and N_2 for slow neutrons—25
——— (see Morse, Philip M.)—706
——— **and Philip M. Morse.** Elastic scattering of neutrons by protons—54(L)
Flodin, George E. (see Hoag, J. Barton)—60(A)
Folsom, T. R. Production of very thin beryllium flakes for a Po-Be neutron source—375(A)
Forbush, S. E. On diurnal variation in cosmic-ray intensity—1005(A)
——— On the effects in cosmic-ray intensity observed during the recent magnetic storms—1108(L)
Foster, E. S., Jr., G. E. M. Jauncey and W. A. Bruce. Dependence of diffuse scattering of x-rays from quartz upon the crystal orientation II—61(A)
Foster, J. S. (see Panter, F.)—1028(A)
——— **and C. A. Horton.** Quantitative spectrographic analysis of biological material. II—1028(A)
——— **and C. A. Horton.** Stark effect in argon and krypton—1007(A)
———, **D. C. Jones and S. M. Neamtan.** Stark effect in the HD and D_2 spectra—1029(A)
——— **and E. R. Pounder.** Effect of crossed electric and magnetic fields on the helium spectrum—1029(A)
Fountain, C. R. Present tendencies and status of physics in the high schools of the south—687(A)
Fowler, W. A. (see Delsasso, L. A.)—143(A), 391, 527(L)
——— **and C. C. Lauritsen.** Radioactive alpha-particles from Li^7+H^2—1103(L)
Frank, N. H. Note on the Hartree and Hartree-Fock methods—577
Frevel, Ludo K. Simplified method for indexing Debye-Scherrer-Hull patterns—997(A)
Fricke, Hugo and Homer P. Smith. Chemical activity of x-ray activated water molecules—376(A)
Friend, A. W. (see Colwell, R. C.)—990(L), 1005(A), 1025(A)
Fry, A. S. Four forms of the copper arc in air—63(A)
Frye, Royal M. (see Kent, Norton A.)—990(L)
Furry, W. H. Application of the theory of neutron absorption in aqueous solutions—592(L)
——— Fluctuations in radiative energy loss and range of fast particles—1004(A)
——— Symmetry theorem in the positron theory—125
——— Theory of neutron velocity distributions in aqueous solutions—382(A)
Fussell, L., Jr. Production and absorption of cosmic-ray showers—1005(A)

Gabel, J. W. (see Zumstein, R. V.)—238
Gaerttner, E. R. and H. R. Crane. An improved method for the measurements of high energy gamma-rays—58(A)
——— **and H. R. Crane.** Gamma-radiation from lithium bombarded with protons—49(L)
Gamow, G. and E. Teller. Some generalizations of the β-transformation theory—289(L)
Gardner, M. E. Coefficient of recombination of pure oxygen as a function of pressure and temperature—144(A)
Genevese, Frank (see Livingston, M. Stanley)—835
Germer, L. H. Structure of organic crystals—596 (title only)
Getting, I. A. (see Stevenson, E. C.)—1027(A)
Giauque, W. F., J. W. Stout and C. W. Clark. Decrease in the electrical resistance of gold with a magnetic field at low temperatures—1108(L)
Gibson, G. E. (see Grahame, D. C.)—590(L)
———, **G. T. Seaborg and D. C. Grahame.** On the interaction of fast neutrons with lead—370(L)
Gilliland, T. R. (see Kirby, S. S.)—992(L)
Githens, Sherwood, Jr. Striking potential of the high frequency discharge in hydrogen as conditioned by frequency—688(A)
Glasser, Otto. Dosage determinations on ten different 400 kv roentgen ray generators—375(A)
Glockler, George and F. T. Wall. Raman effect of gaseous methyl- and dimethylacetylenes—529(L)
Goetz, A. (see Jackson, O. B.)—142(A)
——— (see Jacobs, Robert B.)—147(A), 159
——— (see Rinehart, J.)—147(A)
——— **and Robert B. Jacobs.** Intensities of x-ray reflections from Bi crystals between 25° and 530° Abs.—147(A), 151
Goldsmith, H. H. (see Manley, J. H.)—1022(A)
——— **and J. H. Manley.** Absorption of resonance neutrons—382(A), 1022(A)
Goldsmith, Thomas T., Jr. Refractive index of water for electromagnetic waves eight to twenty-four centimeters in length—245
Goodman, Clark. (see Evans, Robley D.)—595(A)
Gordy, Walter. Effects of certain liquids on the OH vibrational band of alcohol—564
——— Infrared absorption of various solutions of acetic acid—685(A)
——— (see Williams, Dudley)—685(A)

Gorter, C. J. Paramagnetism at radiofrequencies—778(L)
Goudsmit, S. Density of excited levels in heavy nuclei—64(A)
Grahame, D. C. (see Gibson, G. E.)—370(L)
———, **G. T. Seaborg and G. E. Gibson.** Inelastic scattering of fast neutrons—590(L)
Gran, W. H. (see Duffendack, O. S.)—804
Green, G. K. (see Kruger, P. Gerald)—57(A), 291(L), 699
——— **and P. Gerald Kruger.** Radiofrequency source and transmission line for the cyclotron—57(A)
Green, J. B. and R. A. Loring. Zeeman effect of tellurium—62(A)
——— **and H. N. Maxwell.** Zeeman effect of N II—243
——— **and J. A. Peoples, Jr.** Zeeman effect in neon—1020(A)
Gronwall, T. H. Helium wave equation—655
Gropper, Leon. Quantum theory of the second virial coefficient—50(L)
——— Connection between the second virial coefficient and the phases of collision theory—1108(L)
Gunn, Ross. Quantitative study of mountain building on an unsymmetrical earth—1027(A)
——— (see Hall, Wayne C.)—1027(A)

Haas, Arthur. An elementary constant of energy—65(A)
——— Interpretation of the red shift of extra-galactic nebulae—1000(A)
Hafstad, L. R. (see Amaldi, E.)—896
——— (see Rumbaugh, L. H.)—1013(A), 1106(L)
———, **N. P. Heydenburg and M. A. Tuve.** Scattering of protons by protons—1023(A)
——— **and M. A. Tuve.** Neutron-yield curves for light elements—376(A)
Hall, Wayne C. and Ross Gunn. An improved electrical telegauge—1027(A)
Halpern, O. Effect of similarity of particles on gas kinetic quantities—596 (title only)
———, **and M. H. Johnson, Jr.** On the theory of neutron scattering by magnetic substances—992(L)
———, **R. Lueneburg and O. Clark.** Diffuse reflection of neutrons from a plane surface—1020(A)
Ham, W. R. (see Post, C. B.)—1016(A)
——— (see Rast, W. L.)—1015(A)
Hanson, Elmo E. Study of kinetic energies of atomic ions formed by electron impact in nitric oxide and hydrogen chloride—86
Hardy, H. C. (see Colwell, R. C.)—1025(A)
Harkins, W. D. Intermediate nucleus and atomic disintegration in steps—52(L)
Harris, W. T. (see Turner, Louis A.)—1019(A)
Harvey, G. G. Fourier analysis of liquid methyl alcohol—998(A)
——— (see Wollan, E. O.)—1054
Hatch, Graham T. (see Allison, Samuel K.)—58(A)
Haworth, L. J. and L. D. P. King. Alpha-particle yield from protons on lithium—59(A)
Haxby, R. O. (see Williams, J. H.)—888(L), 1011(A)
Hayner, Lucy J. (see Kurrelmeyer, Bernhard)—1007(A)
Hebb, M. H. and E. M. Purcell. Entropy and magnetic susceptibility of paramagnetic salts below 1°K—384(A)
Heck, Charles M. Sensitiveness of paraffin crystal formation to the physical and chemical conditions under which they crystalize—690(A)
——— Spirals in paraffin crystals—686(A)
Hemingway, Allan. Biophysical methods in studies of mammalian temperature regulation—377(A)
Hemmendinger, A. and W. R. Smythe. Radioactive isotopes of rubidium—1052
——— (see Smythe, W. R.)—146(A), 178
Henderson, M. C. (see Ridenour, L. N.)—1013(A)
——— (see White, M. G.)—1012(A)
——— (see Henderson, W. J.)—1107(L)
Henderson, W. J. (see Ridenour, L. N.)—1013(A); 1102(L)
——— (see White, M. G.)—1012(A)
———, **L. N. Ridenour, M. G. White and M. C. Henderson.** Radioactivity of K^{38}—1107(L)
Hendricks, S. B. (see Maxwell, L. R.)—1000(A)
Herb, R. G. (see Rodine, M. T.)—508
———, **D. W. Kerst and J. L. McKibben.** Gamma-ray yield from light elements due to proton bombardment—59(A), 691
———, **D. B. Parkinson and D. W. Kerst.** Development and performance of an electrostatic generator operating under high air pressure—58(A), 75
Herod, Newton S. Quizzes and examinations in physics—687(A)
Hershey, Allen V. Positive ion mobilities in H_2 by the Townsend deflection method—146(A)
Heydenburg, N. P. (see Hafstad, L. R.)—1023(A)
Hibben, James H. Common ion effect in some aqueous solutions as shown by means of the Raman effect—593(L)
——— Reemission of visible light and the coloration by ultraviolet light of certain crystals—530(L)
Hill, E. L. Calculation of phase shifts in scattering problems—1023(A)
——— Virial theorem in nuclear problems—370(L)
——— (see Williams, J. H.)—434
Hirschfelder, Joseph O. and John F. Kincaid. Application of the virial theorem to approximate eigenfunctions—1002(A)
Hirsh, F. R., Jr. Note on the search for element 87—584
——— Shape of the density-exposure time curve for x-rays—998(A)
Ho, I-djen and R. A. Sawyer. An extension of the Yt I and Yt II spectra—1020(A)
Hoag, J. Barton (see Murray, F. H.)—60(A), 333
——— **and George E. Flodin.** Electron beam oscillators—60(A)
Hoffman, J. G. (see Livingston, M. Stanley)—1021(A)
——— **and H. A. Bethe.** Neutron absorption limit of cadmium—1021(A)
———, **M. Stanley Livington and H. A. Bethe.** Some direct evidence on the magnetic moment of the neutron—214
Hoffmann, B. and L. Infeld. On the choice of the action function in the new field theory—383(A), 765
Hofstadter, Robert (see Bonner, Lyman G.)—1017(A)
Holland, D. O. and G. W. Stewart. Orientation of liquid crystals by heat conduction—62(A)

Holley, Clifford. X-ray and optical measurements of multimolecular films—1000(A)
Holmes, F. T. An axial magnetic suspension—689(A)
Holton, W. G. (see Koppius, O. T.)—684(A)
Holzer, R. E. (see Workman, E. J.)—149(A)
Horsfall, R. B., Jr. (see Almy, G. M.)—491
Horton, C. A. (see Foster, J. S.)—1007(A), 1028(A)
Houston, William V. Fine structure of Hα and Dα—148(A)
——— New method of analysis of the structure of Hα and Dα—446
Howard, J. B. Rotation-vibration spectrum of C_2H_6 and the question of internal rotation—53(L)
Howe, J. D. and K. Lark-Horovitz. Electron diffraction patterns of sulphur and selenium molecules—380(A)
Howey, J. H. An elementary laboratory experiment dealing with the relationship $I = Q/t$—687(A)
Hoxton, L. G. and J. W. Beams. Steam-driven ultracentrifuge—690(A)
Hubbard, J. C. (see Adams, J. B.)—63(A)
Huggins, Maurice L. Calculation of intermolecular forces and energies—379(A)
Hulburt, E. O. Theory of the three regions of the ionosphere 689(A)
——— (see Andrews, D. N.)—1017(A)
——— (see Dawson, L. H.)—1017(A)
Hull, Gordon F., Jr. Temperature shift of the potassium resonance lines—572, 595(A)
Hume, O. F. (see Hummell, A. D.)—60(A)
Hummell, A. D. and O. F. Hume. New method of determining the relative location of points within a body by x-ray photography—60(A)
Humphreys, C. J. Interference measurements in the spectra of the noble gases in the ultraviolet—1018(A)
Hurst, D. G. and H. Walke. Induced radioactivity of potassium—1033
Hustrulid, A. (see Kusch, P.)—1007(A)
Huxford, W. S. Photoelectric method for tracing current wave forms—1010(A)

Infeld, L. (see Hoffmann, B.)—383(A), 765
Ingerson, W. E. and F. J. Beck, Jr. Magnetic anisotropy in silicon steel—1010(A)
Inglis, D. R. Perturbation theory and heavy-particle interactions—387(A)
——— Perturbation theory of light nuclei: He^4 and Li^6—531
——— (see Kroeger, W. J.)—1003(A)
——— **and L. A. Young.** Stable isobars—525
Iskenderian, Haig P. Rankine magnetic balance and the magnetic susceptibility of H_2O, HDO and D_2O—1092

Jackson, O. B. and A. Goetz. Recording apparatus for the measurement of integrated intensities of x-ray reflections —142(A)
Jacobs, Robert B. X-ray diffraction patterns from crystalline substancesat very high hydro static pressures—999(A)
——— (see Goetz, Alexander)—147(A), 151
——— **and Alexander Goetz.** Thermal expansion of the Bi lattice between 25° and 530° Abs.—147(A), 159
Jacyna, Witold. Note on the mathematical foundation of the thermodynamical equation of state—677(L)
Jaffe, Hans von R. Polymorphism of Rochelle salt—43
James, Hubert M. (see Coolidge, Albert Sprague)—855
——— **and Albert Sprague Coolidge.** Criteria of goodness for approximate wave functions—860
——— **and Albert Sprague Coolidge.** Theoretical test of the Franck-Condon approximation—1001(A)
Jauncey, G. E. M. (see Foster, E. S., Jr.)—61(A)
——— **and W. A. Bruce.** Atomic vibrations of zinc crystals at liquid air temperature—60(A)
——— **and W. A. Bruce.** X-ray measurement of the effect of temperature on the atomic vibrations in single crystals of zinc—999(A)
——— **and W. A. Bruce.** Atomic structure and vibrations in zinc crystals. IV. Diffuse scattering of x-rays at different temperatures—1062
——— **and W. A. Bruce.** Atomic structure and vibrations in zinc crystals. VI. Determination of electron asymmetry and two principal characteristic temperatures —1067
Jesse, William P. Variation of the atomic structure factor of nickel with wave-length in the region of the nickel K absorption limit—999(A)
Johnson, M. H., Jr. Note on the reaction of deuterium on deuterium—779(L)
——— (see Halpern, O.)—992(L)
——— **and H. Primakoff.** Relations between the second and higher order processes in the neutrino-electron field theory—612
Johnson, Thomas H. Radio-transmitted coincidence counter measurements of cosmic-ray intensities in the stratosphere—385(A)
——— (see Read, D. N.)—386(A)
——— **and Donald N. Read.** Unidirectional measurements of the cosmic-ray latitude effect—557
Johnson, Vivian A. and L. W. Nordheim. Distortion of a closed shell due to crystallic fields—1002(A)
Jones, Creighton C. Time delay circuits for operating Wilson cloud chambers—689(A)
Jones, D. C. (see Foster, J. S.)—1029(A)
Jordan, Edward B. (see Bainbridge, Kenneth T.)—384(A), 595(A)
——— **and Kenneth T. Bainbrdige.** Atomic masses of beryllium, boron, neon and argon—385(A)

Kabakjian, D. H. Dependence of luminescence on physical structure in zinc borate compounds—365
Kaiser, Herman F. Estimation of intergranular surfaces and volumes in metals—1015(A)
Kanne, W. R. Transmutation of aluminum by polonium alpha-particles—1013(A)
Kanner, Morton H. (see Ladenburg, Rudolf)—1022(A)
Kaplan, Joseph. Are there metastable molecules in the Lewis-Rayleigh glow?—143(A)
Keen, C. D. High altitude test of a radio-equipped cosmic-ray meter—60(A)
Kennon, W. L. Description of the physical and astronomical equipment at the University of Mississippi prior to 1860—687(A)
Kent, Norton A., Royal M. Frye and William H. Robinson. Structure of Hα of hydrogen—990(L)

Kent, Norton A. and Reginald G. Lacount. Interferometer wave-lengths of certain lines in the secondary spectrum of D_2 and HD—241
Kenty, Carl. Convection currents in mercury arcs—1025(A)
Kerst, D. W. (see Herb. R. G.)—58(A), 59(A), 75, 691
Kersten, H. and C. H. Dwight. Viscosity of sols made from x-irradiated agar—380(A)
Kincaid, John F. (see Hirschfelder, Joseph O.)—1002(A)
King, Allen and W. M. Rayton. Ranges and straggling coefficients of alpha-particles—826
King, Arthur S. (see King, Robert B.)—1020(A)
King, L. D. P. (see Haworth, L. J.)—59(A)
King, Robert B. and Arthur S. King. Multiplet intensities from electric furnace absorption spectra of Fe I and Ti I. —1020(A)
Kinsey, E. L. and J. W. Ellis. Rotation of water molecules in nonpolar solvents—381(A)
——— **and J. W. Ellis.** Rotation of water molecules in carbon disulfide solution—1074
Kip, A. F. (see Loeb, Leonard B.)—142(A)
Kirby, S. S. (see Smith, N.)—890(L)
———, **N. Smith, T. R. Gilliland and S. E. Reymer.** Ionosphere and magnetic storms—992(L)
Kirkpatrick, Harry A. and Jesse W. M. DuMond. Modified scattered spectrum of characteristic molybdenum *K* radiation at large scattering angle with helium gas as the scattering substances using a curved quartz crystal spectrograph—147(A)
Kirkpatrick, Paul and P. A. Ross. Quantum limit of the continuous spectrum—529(L)
Knerr, Henry W. Electric spectrum of liquid water from five to twenty centimeters—1007(A)
Knorr, H. V. (see Albers, V. M.)—1017(A)
——— **and V. M. Albers.** New recording microphotometer —1016(A)
Knipp, Charles T. Cold cathode rectifier—377(A)
Knipp, Julian K. Remark on the creation of pairs by nuclear electrons—381(A)
Konopinski, E. J. (see Livingston, M. Stanley)—835
——— **and H. A. Bethe.** Evaporation model of nuclear disintegrations—1004(A)
Koppius, O. T. and W. G. Holton. Measurement of permeability of porous media by a radial flow method— 684(A)
Kornfeld, Gertrud. Influence of temperature on the reaction of hydrogen atoms with the wall—689(A)
Kraus, J. D. and J. M. Cork. Bombardment of palladium with deuterons—383(A)
Krishnan, K. S. and Asutosh Mookherji. Magnetic anisotropy of $Cs_2[CoCl_4]$—528(L)
——— **and Asutosh Mookherji.** Magnetic anisotropy of four-coordinated CO^{++} ions in crystals—774(L)
Kroeger, W. J. and D. R. Inglis. Perturbation theory of light nuclei: O^{16}—1003(A)
Kruger, P. Gerald. (see Green, G. K.)—57(A)
——— (see Pattin, H. S.)—1019(A)
——— (see Phillips, L. W.)—1019(A)
——— **and G. K. Green.** Construction and operation of a cyclotron to produce one million volt deuterons—699
——— **and G. K. Green.** Million volt cyclotron—57(A)
——— **and L. W. Phillips.** Spectra of K III, Ca IV and Sc V and their relations to the spectra of other ions in the isoelectronic sequence Cl I to Mn IX—1087
———, **G. K. Green and F. W. Stallmann.** Cyclotron operation without filaments—291(L)
———, **W. E. Shoupp and F. W. Stallmann.** Scattering of neutrons of homogeneous energy by protons—1021(A)
———, **S. G. Weissberg and L. W. Phillips.** Spectra of Sc IV, Ti V, Mn VIII and Fe IX in the isoelectronic sequence A I to Fe IX—1090
Krutter, Harry M. (see Manning, Millard F.)—761
Kuper, J. B. H. Small angle scattering of fast electrons —1024(A)
Kurrelmeyer, Bernhard and Lucy J. Hayner. Shot effect of secondary electron currents from nickel and beryllium— 1007(A)
Kusch, P., J. T. Tate and A. Hustrulid. Products of dissociation of benzene vapor by electron impact— 1007(A)

Lacount, Reginald G. (see Kent, Norton A.)—241
Ladenburg, Rudolf and Morton H. Kanner. Yield of protons and neutrons from the deuteron-deuteron reaction—1022(A)
——— **and R. B. Roberts.** Erratum: Investigations of the deuteron-deuteron reaction—141(L)
Lageman, R. T. (see Slack, F. G.)—685(A)
Lamar, E. S., W. W. Buechner and K. T. Compton. Low voltage proton sources—936
Lamb, Willis E., Jr. Note on the capture of slow neutrons in hydrogenous substances—187
——— On the continuous β-ray spectrum of P^{32}—145(A)
Lampson, Curtis W., Donald W. Mueller and Henry A. Barton. Experimental study of neutron-proton interaction—1021(A)
Landahl, H. and G. S. Monk. Interferometer measurements of wave-lengths in H_2 bands—993(L)
Lane, C. T. Magnetic analysis of evaporated Bi deposits —863
Langer, Lawrence M. and Martin D. Whitaker. Shape of the beta-ray distribution curve of radium E at high energies—713, 1023(A)
Langer, Rudolph E. On the connection formulas and the solutions of the wave equation—669
Langer, R. M. Table of observable interstellar lines— 145(A)
Langmuir, Irving (see Blodgett, Katharine B.)—964
——— (see Taylor, John Bradshaw)—753
Langsdorf, Alexander, Jr. Continuously sensitive cloud chamber—1026(A)
Laporte, O. (see Mack, J. E.)—291(L)
Lark-Horovitz, K. (see Caldwell, W. I.)—998(A)
——— (see Clark, H. T.)—61(A)
——— (see Howe, J. D.)—380(A)
——— (see Madigan, S. E.)—61(A)
——— (see Miller, E. P.)—61(A)
——— **and E. P. Miller.** Structure of glasseous selenium —380(A)
Laslett, L. Jackson. Magnetic scattering of slow neutrons— 22, 148(A)

Latimer, Wendell M. Explanation of the relative stabilities of isotopes of the lighter elements—141(L)
Laurence, G. C. Measurement of very hard x-rays in roentgens—374(A)
Lauritsen, C. C. (see Delsasso, L. A.)—143(A), 391, 527(L)
——— (see Fowler, W. A.)—1103(L)
Leberknight, C. E. and John A. Ord. Infrared absorption of dilute solutions of HCl and HBr—430
Legg, V. E. Low flux density a.c. losses in 35 permalloy sheet—1009(A)
Leigh, W. (see Loeb, Leonard B.)—149(A)
Lewis, Gilbert N. Neutron optics—371(L)
——— **and Philip W. Schutz.** Refraction of neutrons—369(L)
——— **and Philip W. Schutz.** Neutron refraction—1105(L)
Libby, W. F. (see Ruben, Samuel)—774(L)
Liben, Israel. Energy distribution of photoelectrons emitted by calcium and calcium oxide—642
Lifschutz, Harold (see Duffendack, O. S.)—1027(A)
———, **O. S. Duffendack and M. M. Slawsky.** Determination of the counting losses in thyratron recording circuits—1027(A)
Linder, Ernest G. Electron scattering and the action of a collector electrode in an electron swarm—1024(A)
Lindsay, George A. (see Field, J. E.)—165
Linke, F. W. (see Beams, J. W.)—689(A)
Livingston, M. Stanley (see Baker, C. P.)—1011(A)
——— (see Hoffman, J. G.)—214
———, **Frank Genevese and E. J. Konopinski.** Excitation of characteristic x-rays by protons—835
——— **and J. G. Hoffman.** Neutron absorption limit in cadmium—1021(A)
Locher, Gordon L. Cosmic-ray bursts photographed with a cloud machine controlled by noncollinear counters—386(A)
——— Photoelectric Geiger-Müller counters for visible and ultraviolet light—386(A)
——— (see Swann, W. F. G.)—389
Loeb, Leonard B. Theory of recombination of ions over an extended pressure range—1110(L)
———, **A. F. Kip and A. W. Einarsson.** Further studies of the C. T. R. Wilson condensation on charged carriers using various liquids—142(A)
——— **and W. Leigh.** Positive needle point corona studies at atmospheric pressure—149(A)
London, F. On the nature of the superconducting state—678(L)
Loring, R. A. (see Green, J. B.)—62(A)
Lowen, Irving S. Effect of nuclear motion in the Dirac equation—190
Lueneburg, R. (see Halpern, O.)—1020(A)
Luhr, Overton and Frank J. Studer. Spectroscopic study of the magnetron discharge—306
Lundberg. W. O. (see Ahlberg, J. E.)—1028(A)
Lyman, Ernest M. Beta-ray spectra of radium E and radioactive phosphorus—1

Mack, J. E. and O. Laporte. Asymmetric Zeeman effect patterns in a complex spectrum—291(L)
Madigan, S. E. and K. Lark-Horovitz. Crystallization of polymorphous substances from the vapor phase II—61(A)
Manley, J. H. (see Goldsmith, H. H.)—382(A), 1022(A)
———, **H. H. Goldsmith and J. S. Schwinger.** Neutron energy levels—1022(A)
——— **and S. Millman.** Nuclear spin and magnetic moment of Li^6—19
Mann, Marvin W., Jr. and Lee A. DuBridge. Absolute photoelectric yields of Mg, Be and Na—120
Manning, Millard F. and Harry M. Krutter. Electronic energy bands in metallic calcium—761
Margenau, H. (see Watson, W. W.)—48(L)
——— **and Dana T. Warren.** Long range interactions between dipole molecules—748
——— **and Dana T. Warren.** Variational calculations on the nuclear three and four body problem—1003(A)
Marinelli, L. D. Study of the secondary radiations emitted by filters used in roentgen therapy—375(A)
Marlow, Douglas and Jesse W. M. DuMond. Method of removing the errors of tooth spacing to produce high precision worm gear wheels by lapping—145(A)
Masket, A. Victor. (see Beams, J. W.)—384(A)
Mason, R. C. Probe measurements of high pressure arcs—28
Maxwell, H. N. (see Green, J. B.)—243
Maxwell, Louis R. Mechanism of delayed killing of maize seedlings with x-radiation—375(A)
———, **S. B. Hendricks and V. M. Mosley.** Interatomic distances of the akali halides—1000(A)
——— **and V. M. Mosley.** Nuclear separation of the Te_2 molecule by electron diffraction—684(A)
McAllister, L. E. Recording machines as a means of teaching and advertising physics—687(A)
McKay, R. E. (see Zumstein, R. V.)—238
McKeehan, L. W. Ferromagnetic anisotropy in nickel-cobalt-iron crystals at various temperatures—136
——— Relation of ferromagnetic anisotropy to atomic structure—1010(A)
——— (see Bozorth, R. M.)—216(A)
McKibben, J. L. (see Herb, R. G.)—59(A), 691
McLachlan, D., Jr. and Wheeler P. Davey. Preferred orientation produced in pure iron-nickel alloys by cold-rolling—60(A)
McMillan, Edwin (see Alvarez, Luis W.)—148(A)
McNatt, E. M. (see Bruce, W. A.)—1065
Mendelssohn, Kurt. Superconductivity—781(L)
Mendenhall, C. E. and Charles F. DeVoe. Photoelectric work functions of the 211 and 310 planes of tungsten—346
Meschter, Emery. Mechanism of electron emission from coated cathodes—377(A)
Miller, E. P. (see Lark-Horovitz, K.)—380(A)
——— **and K. Lark-Horovitz.** Structure of molten salts 61(A)
Miller, L. F. Pyrheliometer having a spherical absorber is used to follow sunspot activities—1018(A)
Miller, R. D. Geiger-Müller counter measurements of reflected Mo $K\alpha$ x-rays from powdered zinc—959, 999(A)
Millikan, R. A. (see Bowen, I. S.)—1005(A)
Millman, S. (see Manley, J. H.)—19

Millman, S., I. I. Rabi and J. R. Zacharias. An attempt at direct measurement of the magnetic moment of the Rb^{81} nucleus—379(A)
——— **and J. R. Zacharias.** Signs of the nuclear magnetic moments of Li^7, Rb^{85}, Rb^{87} and Cs^{133}—380(A), 1049
Mitchell, Allan C. G. Long period activity in cadmium irradiated with neutrons—995(L)
——— **and R. N. Varney.** Scattering of neutrons absorbed by iodine—1021(A)
Mohler, Fred L. Recombination in the afterglow of a discharge—1008(A)
Mohler, Nora M. Photographic penetration of haze—1017(A)
Møller, C. On the capture of orbital electrons by nuclei—84
Monk, G. S. (see Landahl, H.)—993(L)
Montgomery, C. G. and D. D. Montgomery. Nature of the soft component of the cosmic-radiation—217
Montgomery, D. C. (see Montgomery, C. G.)—217
Mookherji, Asutosh. (see Krishnan, K. S.)—528(L), 774(L)
Mooney, R. C. L. Crystal structure of potassium tetrachloriodide—998(A)
More, Kenneth R. Band spectra of NiCl and CoCl—1017(A)
Morgan, Karl Z. (see Nielsen, Walter M.)—689(A)
——— **and W. M. Nielsen.** Cosmic-ray shower production in large thicknesses of lead and iron—689(A)
Morse, Philip M. Analytic wave functions for nuclear and atomic collision problems—1003(A)
——— (see Fisk, J. B.)—54(L)
———, **J. B. Fisk and L. I. Schiff.** Collisions of neutron and proton. II—706
Mosley, V. M. (see Maxwell, Louis R.)—684(A), 1000(A)
Motz, Lloyd (see Rosenthal, Jenny E.)—378(A)
Mouzon, J. C. Simple demonstration in sound—686(A)
Mueller, Donald W. (see Lampson, Curtis W.)—1021(A)
Mulliken, Robert S. Low electronic states of simple heteropolar diatomic molecules: III. Hydrogen and univalent metal halides—310
Murnaghan, F. D. Theory of elasticity—593(L)
Murray, F. H. Erratum: Heights of reflection of radio waves in the ionosphere—779(L)
——— **and J. Barton Hoag.** Heights of reflection of radio waves in the ionosphere—60(A), 333
Murray, R. T. K. (see Adams, J. B.)—63(A)

Neamtan, S. M. (see Foster, J. S.)—1029(A)
Neddermeyer, Seth H. and Carl D. Anderson. Note on the nature of cosmic-ray particles—884
Neher, H. V. (see Bowen, I. S.)—1005(A)
Newson, Henry W. Radioactivity induced in silicon and phosphorus by deuteron bombardment—624
——— Transmutation functions at high bombarding energies—620
Nielsen, A. H. and H. H. Nielsen. Optically active CD_4 fundamental bands—62(A)
Nielsen, H. H. (see Nielsen, A. H.)—62(A)
Nielsen, Russell A. and Norris E. Bradbury. Electron and negative ion mobilities in oxygen, air, nitrous oxide and ammonia—69, 143(A)
Nielsen, W. M. (see Morgan, Karl Z.)—689(A)
——— **and Karl Z. Morgan.** Cosmic-ray shower production in lead of various thicknesses—689(A)
Nier, Alfred O. Isotopic constitution of mercury and lead—1007(A)
Nishida, Sotohiko. On hard gamma-rays from Ra(C+C'+C''+D)—996(L)
Nonaka, I. (see Tanaka, M.)—781
Nordheim, G. (see Nordheim, L. W.)—379(A)
———, **L. W. Nordheim, J. R. Oppenheimer and R. Serber.** Disintegration of high energy protons—1037
Nordheim, L. W. Absorption of cosmic rays in the atmosphere—1006(A)
——— On the matrix element in the Fermi theory of β-decay—64(A)
——— On the absorption of cosmic-ray electrons in the atmosphere—1110(L)
——— (see Johnson, Vivian A.)—1002(A)
——— (see Peterson, E. L.)—355
——— **and G. Nordheim.** On the interaction of heavy and light particles at very high energies—379(A)
——— (see Nordheim, G.)—1037
——— **and F. L. Yost.** On the matrix element in Fermi's theory of β-decay—942
Northrup, D. L. and L. C. Van Atta. Generating voltmeter measurements at Round Hill—1014(A)
Nottingham, W. B. Electrical and luminescence properties of willemite screen material—1008(A)
——— Potential and luminescence of insulated willemite cathode-ray screens—591(L)
Ny, Tsi-Zé and Ch'en, Shang-Yi. Displacement of principal series lines of rubidium by the addition of rare gases—567

O'Bryan, H. M. (see Schneider, E. G.)—293
O'Connor, J. S., S. J. Beta-ray spectrum of radium E.—1023(A)
Oldenberg, O. and F. F. Rieke. Absorption spectrum as a quantitative test for free hydroxyl radicals—381(A)
Oppenheimer, J. R. (see Carlson, J. F.)—220
——— (see Nordheim G.)—1037
——— **and R. Serber.** Note on the nature of cosmic-ray particles—1113(L)
Ord, John A. (see Leberknight, C. E.)—430
Osterberg, Harold and John W. Cookson. Piezo dielectric effect and electrostrictions in anisotropic or isotropic media—1096

Page, Chester H. Van der Waals forces between helium atoms—1002(A)
Panter, F. and J. S. Foster. Stark effect in iron, and the contrast with the pole effect—1028(A)
Parker, Herman. Stable states of two deuterons—682(A)
Parkinson, D. B. (see Herb, R. G.)—58(A), 75
Parratt, Lyman G. Widths of *L*-series lines and of energy levels of Ag(47)—999(A)
Pattin, H. S. and P. Gerald Kruger. Spectra of scandium VI and scandium VII and their relation to the isoelectronic sequences starting with sulphur and phosphorus—1019(A)
Paul, Fred W. Preliminary observations of absorption spectra in the Schumann region—594(A)

Paxton, Hugh C. Radiations emitted from artificially produced radioactive substances. III. Details of the beta-ray spectrum of P^{32}—170
Pearson, G. L. Formation of metallic bridges in separated contacts—1015(A)
Peebles, J. B. (see Sledd, Marvin)—684(A)
Peoples, J. A., Jr. (see Green, J. B.)—1020(A)
Peterson, E. L. and L. W. Nordheim. Resistance of monovalent metals—355
Pfister, R. J. (see Davey, Wheeler P.)—1028(A)
Phillips, L. W. and P. Gerald Kruger. Spectra of scandium IV and scandium V and their relation to the spectra of the isoelectronic sequences starting with argon and chlorine—1019(A)
Phillips, M., L. Eisenbud and E. U. Condon. Interaction between light nuclei—382(A)
——— (see Feenberg, E.)—597, 683(A)
——— (see Kruger, P. Gerald)—1087, 1090
Pickering, William H. Secondary particles from the penetrating component of the cosmic radiation—628
Piore, E. R. Thin film field emission—1111(L)
Placzek, G. (see Bethe, H. A.)—450
Plyler, E. K. Infrared absorption of strong and weak acid solutions—685(A)
——— **and E. S. Barr.** Infrared absorption of aqueous solutions of the halogen salts—1017(A)
Pollard, Ernest. Emergence of low energy protons from nuclei—290(L)
——— (see Brubaker, Gordon)—1013(A)
——— **and Charles J. Brasefield.** Alpha-particle bombardment of neon, calcium and argon and masses of light nuclei—8
———, **H. L. Schultz and Gordon Brubaker.** Emission of neutrons from chlorine and argon under alpha-particle bombardment—140(L)
———, **H. L. Schultz and Gordon Brubaker.** Transmutation of argon and chlorine by alpha-particles—1014(A)
Pollard, W. G. Calculations on beta-ray spectra—682(A)
Pool, M. L. and J. M. Cork. Deuteron bombardment of barium, lanthanum and cerium—1010(A)
——— **and J. M. Cork.** Radioactive isotopes from aluminum—383(A)
———, **J. M. Cork and R. L. Thornton.** Radioactivity due to neutron ejection produced by fast neutrons—890(L)
Post, C. B. and W. R. Ham. Diffusion of hydrogen through carbonyl iron at temperatures from 900° to 1125° centigrade—1016(A)
Potter, J. G. (see Waterman, A. T.)—63(A)
Pounder, E. R. (see Foster, J. S.)—1029(A)
Power, R. B. and J. D. Cobine. Application of Paschen's law to the reignition of an arc—594(A)
Powers, P. N. (see Dunning, J. R.)—51(L), 382(A)
———, **H. G. Beyer and J. R. Dunning.** Experiments on the magnetic moment of the neutron—371(L)
———, **H. Carroll and J. R. Dunning.** Experiments on the magnetic moment of the neutron—1022(A), 1112(L)
Present, R. D. (see Rarita, William)—788
——— **and W. Rarita.** On the nuclear three-body problem —382(A)
Preston, William M. Modification of spectral lines by very close collisons—298
Primakoff, H. Additional interaction of protons with an electromagnetic field, due to the presence of the electron-neutrino field—990(L)
——— (see Johnson, M. H., Jr.)—612
Purcell, E. M. (see Hebb, M. H.)—384(A)
Quimby, Edith H. Measurement of backward scattered x-radiation—374(A)
Rabi, I. I. Space quantization in a gyrating magnetic field —652
——— Transitions between states of space quantization in a rotating magnetic field—683(A)
——— Nuclear moments—596 (title only)
——— (see Millman, S.)—379(A)
——— (see Schwinger, Julian)—1003(A)
——— (see Torrey, H. C.)—379(A)
Ramberg, E. G. (see Richtmyer. F. K.)—925
——— **and F. K. Richtmyer.** Radiation probabilities, auger effect and energy level widths for Au(79)—913
Ramsey, Willis E. Type of high potential battery which combines extreme lightness with long shelf life—1028(A)
——— **and W. E. Danforth.** Determination of the shower producing efficiency of cosmic-ray particles—1105(L)
Rarita, W. (see Present, R. D.)—382(A)
——— **and R. D. Present.** On the nuclear two-, three-and four-body problems—788
Rassweiler, M. P. and G. M. Almy. Spectrum of caesium hydride—1019(A)
Rast, W. L. and W. R. Ham. Diffusion of hydrogen through iron at temperatures between 780° and 90°C—1015(A)
Rayton, W. M. (see King, Allen)—826
——— **and T. R. Wilkins.** Wilson cloud chamber investigation of the alpha-particles from uranium—818
Razor, C. T. Spark timer actuated by thermionic tubes—684(A)
Read, Donald N. (see Johnson, Thomas H.)—557
——— **and Thomas H. Johnson.** Automatically recorded coincidence counter measurements of the cosmic-ray latitude effect—386(A)
Reiss, Karl Hans. Remarks on the paper by E. B. Baker and H. A. Boltz "Thermionic emission into dielectric liquids"—781(L)
Reymer, S. E. (see Kirby, S. S.)—992(L)
Richardson, J. Reginald and Lorenzo Emo. Photodisintegration of the deuteron—1014(A)
Richtmyer, F. K. Absorption of ultra-short x-rays—376(A)
——— (see Ramberg, E. G.)—913
——— **and E. G. Ramberg.** Satellite structure of $L\alpha$ and $L\beta_2$ of Au(79)—925
———, **C. H. Shaw and R. E. Shrader.** L-satellites in the atomic number range $73<Z<79$—380(A)
Ridenour, L. N. (see Henderson, W. J.)—1107(L)
——— (see White, M. G.)—1012(A)
——— **and W. J. Henderson.** Artificial radioactivity produced by alpha-particles—1102(L)
———, **W. J. Henderson, M. C. Henderson and M. G. White.** Radioactivity induced by alpha-particles—1013(A)

Rieke, F. F. (see Oldenberg, O.)—381(A)
Riffolt, N. (see Thompson, L.)—377(A)
Rinehart, J. and A. Goetz. Method for the production of metal single crystals between 20μ and 0.2μ—147(A)
Risser, J. R. Long-period radioactivity in cobalt induced by slow neutrons—1013(A)
Ritow, Herman (see Bockstahler, Lester)—1009(A)
Roberts, Richard B. Investigation of the deuteron-deuteron reaction—810
——— (see Ladenburg, R.)—141(L)
——— (see Rumbaugh, L. H.)—1013(A), 1106(L)
Robertson, H. P. Dynamical effects of radiation in the solar system—1000(A)
Robinson, Howard A. Helium I like spectra—14, 65(A)
——— Lithium I like spectrum of phosphorus P XIII—381(A)
——— Spectra of phosphorus. Part II: The spectra of doubly, triply and quadruply ionized phosphorus (P III, P IV, PV). Additions and corrections to P II—726
——— **and G. H. Shortley.** Coupling of the normal p-electron configurations—1018(A)
Robinson, William H. (see Kent, Norton A.)—990(L)
Rochester, George D. Band spectra of BiF, BiCl, SbF, and SbCl—146(A)
——— Band spectra of SbF and BiF—486
Rodine, M. T. and R. G. Herb. Effect of CCl_4 vapor on the dielectric strength of air—508
Rogers, F. T., Jr. Erratum: The precise measurement of three radium B beta-particle energies—588
——— On the ionization of gases by high energy beta-particles—528(L)
Rose, Morris E. Multiple scattering and stopping of electrons—1024(A)
——— Relativistic wave functions in the continuous spectrum for the coulomb field—484
——— (see Bethe, H. A.)—283
——— **and H. A. Bethe.** Nuclear spins and magnetic moments in the Hartree model—205; Erratum—993(L)
Rosenthal, Jenny E. and Lloyd Motz. Application of a new mathematical method to vibration-rotation interaction—378(A)
Ross, P. A. (see Kirkpatrick)—529(L)
Ruark, Arthur E. (see Brammer, Forest E.)—688(A)
——— (see Devol, Lee)—710
——— (see Driscoll, Raymond L.)—688(A)
Ruben, Samuel and W. F. Libby. Width of iodine resonance neutron band—774(L)
Rumbaugh, L. H., R. B. Roberts and L. R. Hafstad. Transmutation-processes of Li^6 and Li^7—1013(A)
———, **R. B. Roberts and L. R. Hafstad.** Conservation of energy in the disintegration of Li^8—1108(L)

St. Helens, H. J. (see Wilkins, T. R.)—1026(A)
Sakata, Shoichi. (see Yukawa, Hideki)—677(L)
Sampson, J. B. Energy levels in neon and argon—1017(A)
Sanderson, J. A. (see Andrews, D. N.)—1017(A)
Sawyer, R. A. (see Ho, I-djen)—1020(A)
Saxl, Irving J. Elastic hysteresis in wires, sheets and yarns—596(A)
Schager, R. (see Collins, G. B.)—58(A)
Schiff, L. I. Inelastic collision of deuteron and deuteron—595(A), 783
——— Low energy collision of neutron and deuteron—1003(A)
——— (see Morse, Philip M.)—706
Schlapp, Robert. Fine structure in the $^3\Sigma$ ground state of the oxygen molecule, and the rotational intensity distribution in the atmospheric oxygen band—342
Schneider, E. G. and H. M. O'Bryan. Absorption of ionic crystals in the ultraviolet—293
Schremp, E. J. Shadow effect of cosmic radiation and some associated general dynamical theorems—1006(A)
Schultz, H. A. (see Almy, G. M.)—62(A)
Schultz, H. L. Disintegration of the deuteron under fast alpha-particle bombardment—1023(A)
——— (see Pollard, Ernest)—140(L), 1014(A)
Schutz, Philip W. (see Lewis, Gilbert N.)—369(L); 1105(L)
Schwinger, Julian. On nonadiabatic processes in inhomogeneous fields—648
——— On the magnetic scattering of neutrons—544
——— (see Manley, J. H.)—1022(A)
——— **and I. I. Rabi.** Depolarization by neutron proton scattering—1003(A)
——— **and E. Teller.** Scattering of neutrons by ortho- and parahydrogen—775(L)
Scott, George W., Jr. (see Smith, Lloyd P.)—1025 (A)
Scott, R. B. and F. G. Brickwedde. Molecular volumes and lattice forces of liquid normal- and parahydrogen—684(A)
Seaborg, G. T. (see Gibson, G. E.)—370(L)
——— (see Grahame, D. C.)—590(L)
Seemann, Herman E. Secondary radiation intensity as a function of certain geometrical variables—376(A)
Serber, R. (see Nordheim, G.)—1037
——— (see Oppenheimer, J. R.)—1113(L)
Shankland, Robert S. Compton effect with gamma-rays—1024(A)
Shaw, A. E. Focusing criteria for electrons in superimposed electric and magnetic fields—58(A)
——— New precision determination of e/m for electrons—887(L)
Shaw, C. H. (see Richtmyer, F. K.)—380(A)
Shaw, R. William. Optical absorption of fused germanium dioxide from 0.185μ to 8.5μ—146(A)
——— Vibrational analysis of the emission bands of germanous oxide—12
Shearin, Paul E. Observation of spectra—an experiment for the elementary laboratory—687(A)
Shen, S. T., Y. T. Yao and Ta-You Wu. Depolarization of Raman lines and structure of chlorate, bromate and iodate ions—235
Shenstone, A. G. First spark spectrum of platinum—1018(A)
Shepherd, W. G. (see Williams, J. H.)—888(L), 1011(A)
Sherr, Rubby. Separation of isotopes by diffusion—1007(A)
Shinohara, U. (see Toriyama, Y.)—680(L)
Shockley, William. Energy bands for the face-centered lattice—129
——— Test of the cellular method of obtaining lattice functions—379(A)

Shortley, G. H. (see Robinson, H. A.)—1018(A)
Shoupp, W. E. (see Kruger, P. Gerald)—1021(A)
Shrader, R. E. (see Richtmyer, F. K.)—380(A)
Siegel, Sidney. Elastic constants of crystalline sodium at 80°K—1015(A)
Simon, F. Magnetic experiments at very low temperatures—1010(A) (title only)
Simpson, O. C. (see Estermann, I.)—64(A), 1004(A)
Sixtus, K. J. Powder patterns on ferromagnetic crystals—870
——— Remanence in single crystals—780(L)
Skaggs, Lester S. (see Allison, Samuel K.)—58(A)
Skellett, A. M. Time lag in gas-filled photoelectric cells—1026(A)
Slack, F. G., R. T. Lageman and Newton Underwood. Measurements of the verdet constant of crystalline nickelous sulphate—685(A)
Slater, J. C. Damped electron waves in crystals—840
——— Energy levels of fast electrons in a periodic lattice—596 (title only)
——— Nature of the superconducting state—195
——— Wave functions in a periodic potential—846
Slawsky, M. (see Duffendack, O. S.)—1027(A)
——— (see Lifschutz, Harold)—1027(A)
Sledd, Marvin and J. B. Peebles. Study of the thyratron inverter—684(A)
Smith, Homer P. (see Fricke, Hugo)—376(A)
Smith, Lincoln G. Ionization and dissociation of polyatomic molecules by electron impact. I. Methane—263
Smith, Lloyd P. and George W. Scott, Jr. Stable source of focused ions—1025(A)
Smith, N. Quantitative study of the Doppler effect in sound waves—686(A)
——— (see Kirby, S. S.)—992(L)
——— **and S. S. Kirby.** Critical frequencies of low ionosphere layers—890(L)
Smith, Sidney D. and Wheeler P. Davey. An x-ray study of the Ar_3 and Ac_3 points for pure Fe and Fe-Ni alloys—1010(A)
Smythe, W. R. and Hemmendinger, A. Radioactive isotope of potassium—146(A), 178
——— (see Hemmendinger, A.)—1049
Snell, Arthur H. New radioactive isotope of fluorine—143(A)
——— Radioactivities of bromine—1011(A)
——— (see Alvarez, Luis W.)—148(A)
Snoddy, L. B., J. R. Dietrich and J. W. Beams. Propagation of potential in discharge tubes—1008(A)
Sponer, H. and M. Bruch-Willstätter. Lattice energy of solid CO_2—998(A)
Stallmann, F. W. (see Kruger, P. Gerald)—291(L), 1021(A)
Starr, Chauncey. Thermal diffusivity of nickel—376(A)
Starr, Merle A. (see Brode, Robert B.)—1006(A)
Stehn, J. R. (see Breit, G.)—56(L)
Stenstrom, Wilhelm and Irwin Vigness. Effect of irradiation on oil drops—376(A)
Stephenson, R. J. X-ray fluorescence yields—62(A), 637
Stern, O. Molecular ray method for the separation of isotopes—1028(A)
——— New method for the measurement of the Bohr magneton—852, 1004(A)
——— (see Estermann, I.)—64(A), 1004(A)
Stevenson, A. F. Correction due to motion of center of gravity in the Hartree approximation in nuclei—590(L)
——— Spherical symmetry of self-consistent atomic fields—285
Stevenson, E. C. (see Street, J. C.)—1005(A)
——— **and I. A. Getting.** Vacuum tube circuits for scaling down counting rates—1027(A)
Stewart, G. W. (see Holland, D. O.)—62(A)
Stout, J. W. (see Giauque, W. F.)—1108(L)
Strain, C. V. (see Barnes, S. W.)—775(L), 1012(A)
——— (see Buck, J. H.)—1012(A)
Street, J. C. (see Young, R. T., Jr.)—386(A)
——— **and E. C. Stevenson.** Penetrating corpuscular component of the cosmic radiation—1005(A)
Strong, John. Evaporation process and its application to optical surfaces—142 (title only)
Studer, Frank J. (see Luhr, Overton)—306
Stuhlman, Otto, Jr. Physical analysis of the dead beat mechanism of the auditory ossicles—1026(A)
——— Physical constants of the ossicles of the human ear—688(A)
Swann, W. F. G. Effect of galactic rotation upon the intensity of cosmic radiation—718, 1006(A)
——— Nature of cosmic rays—596 (title only)
———, **G. L. Locher and W. E. Danforth.** Geiger-Müller counter measurements of cosmic-ray intensities in the stratosphere—389

Tanaka, M. and I. Nonaka. Production of x-rays by high speed argon ions—781(L)
Taschek, Richard (see Williams, Dudley)—1016(A)
Tate, J. T. (see Kusch, P.)—1007(A)
——— (see Williams, J. H.)—434
Tatel, H. Analysis of the linear amplifier—146(A)
Taub, A. H. Quantum equations in cosmological spaces—512
Taylor, John Bradshaw and Irving Langmuir. Vapor pressure of caesium by the positive ion method—753
Taylor, Lauriston S. Some problems in radiological physics—374(A)
Teller, E. (see Gamow, G.)—289(L)
——— (see Schwinger, Julian)—775(L)
Thompson, L. and N. Riffolt. Characteristics of shock-wave propagation near an explosive source—377(A)
Thornton, R. L. Radioactivity produced in nickel by deuteron bombardment—893
——— (see Cork, J. M.)—59(A), 608
——— (see Pool, M. L.)—890 (L)
——— **and J. M. Cork.** Induced radioactivity in lead—383(A)
Thomas, L. H. Approximation to discrete quantum states by iteration—202
Tomboulian, D. H. and R. F. Bacher. On the measurement of hyperfine structure separations—1020(A)
Tonks, Lewi. Drift of ions and electrons in a magnetic field—744
——— Drift of ions and electrons under the action of concentration gradient, electric and magnetic fields—1025(A)

Toriyama, Y. and U. Shinohara. Electric breakdown field intensity of water and aqueous solutions—680(L)
Torrey, Henry Cutler. Sign of the magnetic moment of the K^{39} nucleus—501
——— **and I. I. Rabi.** Sign of the nuclear magnetic moment of K^{39}—379(A)
Turin, J. J. and H. R. Crane. Stopping of the recoil electrons produced by the $F+H^1$ gamma-rays—1012(A)
Turner, Louis A. and W. T. Harris. Ultraviolet bands of magnesium hydride—1019(A)
Turner, R. N. (see Compton, A. H.)—1005(A)
Tuve, M. A. (see Amaldi, E.)—896
——— (see Hafstad, L. R.)—376(A), 1023(A)

Ufford, C. W. Term values in carbon—1020(A)
Underwood, Newton (see Slack, F. G.)—685(A)

Valasek, Joseph. X-ray emission spectra of sulphides and sulphates—832
Valley, G. (see Buck, J. H.)—1012(A)
Van Atta, C. M. and L. C. Van Atta. High-speed multi-jet oil diffusion pumps of metal construction—377(A)
———, **R. J. Van de Graaff and L. C. Van Atta.** Accelerating tube for the Round Hill electrostatic generator—1013(A)
Van Atta, L. C. (see Northrup, D. L.)—1014 (A)
——— (see Van Atta, C. M.)—377(A), 1014(A)
Van de Graaff, R. J. (see Van Atta, C. M.)—1014(A)
Van Vleck, J. H. Influence of dipole-dipole coupling on electric magnetic susceptibilities—384(A)
Varney, R. N. (see Mitchell, Allan C. G.)—1021(A)
Vigness, Irwin (see Stenstrom, Wilhelm)—376(A)
Vitter, A. L. (see Collins, G. B.)—58(A)

Wait, G. R. Coefficient of combination between small ions and large ions—1025(A)
Walke, Harold. Induced radioactivity of calcium—439
——— Induced radioactivity of titanium—1011(A)
——— Radioactivity induced in calcium under deuteron bombardment—143(A)
——— (see Hurst, D. G.)—1033
Wall, F. T. (see Glockler, George)—529(L)
Wannier, Gregory H. On electron excitation in crystals—1001(A)
Warren, Dana T. (see Margenau, Henry)—748, 1003(A)
Waterman, A. T. Note on quantum absorption probability in the case of the photoelectric effect—378(A)
——— **and J. G. Potter.** Contact potential between filaments in vacuum by Kelvin method—63(A)
Watson, W. W. and H. Margenau. Pressure broadening in bands of dipole molecules—48(L)
Way, Katharine. Photoelectric cross section of the deuteron—552
——— **and John A. Wheeler.** Photoelectric cross section of the deuteron—683(A)
Weber, Alfred H. and Charles B. Bazzoni. Shenstone effect in bismuth—378(A)
Weber, Ernst. Critique of the quantum theory of metallic conduction—378(A)
Weissberg, S. G. (see Kruger, P. G.)—1090
Wells, W. H. (see Williams, J. H.)—434
Welo, Lars A. and Oskar Baudisch. Change from γ-FeOOH and γ-Fe_2O_3 to γ-Fe_2O_3 at lower temperatures and the irreversible transition: γ-FeOOH to α-FeOOH—1016(A)
Wheeler, John A. Resonating group structure in the nucleus—683(A)
——— (see Way, Katharine)—683(A)
Whitaker, Martin D. (see Langer, Lawrence M.)—713, 1023(A)
White, M. G. (see Ridenour, L. N.)—1013(A)
———, **M. C. Henderson, W. J. Henderson and L. N. Ridenour.** Production of high energy alpha-particles by the Princeton cyclotron—1012(A)
——— (see Henderson, W. J.)—1107(L)
Wigner, E. On the consequences of the symmetry of the nuclear Hamiltonian on the spectroscopy of nuclei—106
——— On the structure of nuclei beyond oxygen—947
——— (see Breit, G.)—593(L)
——— (see Feenberg, E.)—95
Wiig, E. O. (see Barnes, S. W.)—775(L), 1012(A)
Wilkins, T. R. (see Rayton, W. M.)—818
——— **and H. J. St. Helens.** Grain spacing of alpha-ray, proton and deuteron tracks in a photographic emulsion—1026(A)
Williams, Dudley. Infrared absorption of the hydrogen halides in organic solvents—288(L)
——— **and Walter Gordy.** Infrared spectra of binary mixtures of certain organic liquids—685(A)
——— **and Richard Taschek.** Effects of elastic stretch on the infrared spectrum of rubber—1016(A)
Williams, H. J. Magnetic properties of single crystals of silicon iron—1009(A)
——— (see Cioffi, P. P.)—1009(A)
Williams, J. H., W. G. Shepherd and R. O. Haxby. Disintegration of lithium by deuterons—1011(A)
———, **W. G. Shepherd and R. O. Haxby.** Evidence for the instability of He^5—888(L)
———, **W. H. Wells, J. T. Tate and E. L. Hill.** Resonance process in the disintegration of boron by protons—434
Williams, S. R. Project methods for college students—596 (title only)
Wilsey, R. B. Measurement of scattered radiation in roentgenography of the chest—376(A)
Witmer, Enos E. Energy levels of the asymmetrical rotator and the correspondence principle—1001(A)
——— Magnetic susceptibility of molecular hydrogen calculated by quantum mechanics—383(A)
Wollan, E. O. and G. G. Harvey. Effect of temperature on the intensity of reflection of x-rays from zinc crystals—1054
Workman, E. J. and R. E. Holzer. An anomalous lightning discharge—149(A)
Wu, Ta-You (see Shen, S. T.)—235

Yao, Y. T. (see Shen, S. T.)—235
Yost, F. L. (see Nordheim, L. W.)—942
Young, L. A. (see Inglis, D. R.)—525

Young, R. T., Jr. and J. C. Street. Cosmic-ray ionizations under various thicknesses of lead shield in northern and equatorial latitudes at different altitudes—386(A)

Youtz, J. Paul and Jesse W. M. DuMond. Thirty kilowatt continuous-rating x-ray outfit of the Watters Memorial Research Laboratory at the California Institute of Technology—144(A)

Yukawa, Hideki and Shoichi Sakata. On the nuclear transformation with the absorption of the orbital electron—677(L)

Zacharias, J. R. (see Millman, S.)—379(A), 380(A), 1049

Zener, Clarence. Mechanism of internal friction—1015(A)

——— On the nonassociation of photoconductivity with optical absorption in nonconducting crystals—64(A)

Zirkle, Raymond E. Columnar ion concentration and the biological effectiveness of x-rays, neutrons and alpha-particles—375(A)

Zumstein, R. V., J. W. Gabel and R. E. McKay. $^1\Sigma^+ - ^1\Sigma$ band system of ionized cadmium deuteride—238

Zwicky, F. Fundamental properties of light from distant nebulae—148(A)

——— Nebulae as gravitational lenses—290 (L)

——— On the probability of detecting nebulae which act as gravitational lenses—679(L)

Analytic Subject Index to Volume 51

References with (A) are to abstracts of papers presented at meetings of the Physical Society. References with (L) are to Letters to the Editor.

Absorption phenomena
- Electrons produced by Li+H gamma-rays, energy losses, E. R. Gaerttner, H. R. Crane—49; L. A. Delsasso, W. A. Fowler, C. C. Lauritsen—391
- Electrons produced by F+H¹ gamma-rays; energy losses, J. J. Turin, H. R. Crane—1012(A)
- Ionic crystals in ultraviolet, E. G. Schneider, H. M. O'Bryan—293
- Photographic penetration of haze, N. M. Mohler—1017(A)
- Scattering of light by water, L. H. Dawson, E. O. Hulburt—1017(A)

Absorption and reflection of light (see **Absorption phenomena; Spectra, absorption**)

Accommodation coefficient
- Of K atoms on MgO, V. W. Cohen, A. Ellett—65(A)

Acoustics
- Doppler effect, N. F. Smith—686(A)
- Mechanism; physical constants of the auditory ossicles, O. Stuhlman, Jr.—688(A); 1026(A)
- Recording machines; teaching physics, L. E. McAllister—687(A)
- Shock-wave propagation near explosive source, L. Thompson, N. Riffolt—377 (A)
- Simple demonstration, harmonics, J. C. Mouzon—686(A)

Afterglow
- Metastable molecules in Lewis-Rayleigh glow, J. Kaplan—143(A)

Arcs (see **Discharge of electricity in gases**)

Astrophysics
- Dynamical effects of radiation, H. P. Robertson—1000(A)
- Elementary constant of energy; energy production of the stars, A. Haas—65(A)
- Nebulae as gravitational lenses, F. Zwicky—290(L), 679(L)
- Observable interstellar lines, R. M. Langer—145(A)
- Polarization of solar corona, W. M. Cohn—148(A)
- Properties of light from distant nebulae, F. Zwicky—148(A)
- Quantum equations in cosmological spaces, A. H. Taub—512
- Red shift, interpretation of, A. Haas—1000(A)

Atomic and molecular beams
- Bohr magneton, measurement of, O. Stern—852; 1004(A)

Atomic and molecular radii (see also **Scattering of electrons**)
- Of Cl_2 and N_2 for slow electrons, J. B. Fisk—25

Biophysics
- Absorption of ultra-short x-rays, F. K. Richtmyer—376(A)
- Backward scattered x-radiation, E. H. Quimby—374(A)
- Biological action of neutrons, P. C. Aebersold—375(A)
- Biological effectiveness, columnar ion concentration, R. E. Zirkle—375(A)
- Chemical activity of x-ray activated water molecules, H. Fricke, H. P. Smith—376(A)
- Delayed killing of seedlings with x-radiation, L. R. Maxwell—375(A)
- Dosage determinations, O. Glasser—375(A)
- Irradiation of oil drops, W. Stenstrom, I. Vigness—376(A)
- Measurement of hard x-rays, G. C. Laurence—374(A)
- Po-Be neutron source, T. R. Folsom—375(A)
- Problems in radiological physics, L. S. Taylor—374(A)
- Scattered radiation in roentgenography of the chest, R. B. Wilsey—376(A)
- Secondary radiations emitted by filters, L. D. Marinelli—375(A)
- Secondary radiation, geometrical variables, H. E. Seemann—376(A)
- Shock-wave propagation near explosive source, L. Thompson, N. Riffolt—377(A)
- Temperature regulation; high frequency currents, A. Hemingway—377(A)
- Transport of drugs through the skin, H. A. Abramson—1025(A)
- Viscosity of sols from x-irradiated agar, H. Kersten, C. H. Dwight—380(A)

Chemical reactions
- Reaction of hydrogen atoms with wall, G. Kornfeld—689(A)

Collision diameter (see also **Atomic and molecular radii**)
- Impacts of second kind, O. S. Duffendaek, W. H. Gran—804

Collisions of second kind
- Action cross section, O. S. Duffendack, W. H. Gran—804

Compton effect (see **X-rays, diffraction, scattering**)

Conductivity, electrical (see **Electrical conductivity; Discharge of electricity in gases**)

Constants, physical, standards
- Determination of h/e, short wave-length limit, J. W. M. DuMond, V. Bollman—145(A); 400; P. Kirkpatrick, P. A. Ross—529(L)

Contact potentials
- Between crystal faces, H. E. Farnsworth—378(A)
- Between filaments in vacuum, A. T. Waterman, J. G. Potter—63(A)

Cosmic radiation
- Absorption in atmosphere, L. W. Nordheim—1006(A); —1110(L)
- Altitude test of radio-equipped meter, C. D. Keen—60(A)
- Analysis of primary rays, A. H. Compton—59(A)
- Bursts; noncollinear counters, G. L. Locher—386(A)
- Diurnal variation, S. E. Forbush—1005(A)
- Earth's magnetic field, top of atmosphere, I. S. Bowen, R. A. Millikan, H. V. Neher—1005(A)

Cosmic radiation (continued)
Effect of galactic rotation, W. F. G. Swann—1006(A)
Galactic rotation and intensity, W. F. G. Swann—718
Grain spacing of tracks in photographic emulsion, T. R. Wilkins, H. J. St. Helens—1026(A)
High energy electrons, stopping of, A. Bramley—387(A), 682(A)
Intensities in stratosphere, W. F. G. Swann, G. L. Locher, W. E. Danforth—389
Ionization of air by γ-rays, pressure and collecting field, I. S. Bowen, E. F. Cox—232
Ionization by high energy beta-particles, F. T. Rogers, Jr.—528(L)
Ionization under various thicknesses of Pb, R. T. Young, Jr., J. C. Street—386(A)
Latitude effect; coincidence counter, D. N. Read, T. H. Johnson—396(A); 557
Multiplicative showers, J. F. Carlson, J. R. Oppenheimer—220
Nature of particles, energy losses, H. R. Crane—50(L); J. R. Oppenheimer, R. Serber—1113(L); S. H. Neddermeyer, C. D. Anderson—884; J. C. Street, E. C. Stevenson—1005(A)
Nature of rays producing showers, W. E. Ramsey, W. E. Danforth—1105(L)
Nuclear disintegrations, A. Bramley—385(A)
Origin of rays, A. H. Compton, P. Y. Chou—1104(L)
Radio-transmitted measurements of intensities, T. H. Johnson—385(A)
Secondary particles from penetrating component, W. H. Pickering—628
Shadow effect, E. J. Schremp—1006(A)
Shower mechanism, M. H. Johnson, Jr., H. Primakoff—612
Shower production in Pb, W. M. Nielsen, K. Z. Morgan—689(A); R. B. Brode, M. A. Starr—1006(A)
Shower production in Pb and Fe, K. Z. Morgan, W. M. Nielsen—689(A)
Showers, production and absorption of, L. Fussell, Jr.—1005(A)
Soft component, nature of, C. G. Montgomery, D. D. Montgomery—217
Variations with latitude on Pacific Ocean, A. H. Compton, R. M. Turner—1005(A)

Crystal structure
Debye-Scherrer-Hull patterns, indexing of, L. K. Frevel—997(A)
Patterns at high hydrostatic pressures, R. B. Jacobs—997(A)
Of potassium tetrachloriodide, R. C. L. Mooney—999(A)
Structure of wood, W. I. Caldwell, K. Lark-Horovitz—998(A)
Superlattices and "mixed crystals," F. C. Blake—1000(A)

Crystalline state
Anisotropy in unstrained ferromagnetic crystals, L. W. McKeehan—1010(A)
Ar_3 and Ac_3 points for pure Fe and Fe-Ni alloys, S. D. Smith, W. P. Davey—1000(A)
Contact potential between crystal faces, H. E. Farnsworth—378(A)
Counter measurements of reflected x-rays, R. D. Miller—959, 999(A)
Crystallic fields, effect on closed shell, V. A. Johnson, L. W. Nordheim—1002(A)
Crystallization from vapor phase, S. E. Madigan, K. Lark-Horovitz—61(A)
Electron asymmetry atomic vibration, characteristic temperature in Zn, G. E. M. Jauncey, W. A. Bruce—60(A), 999(A), 1062, 1067; E. O. Wollan, G. G. Harvey—1054
Electron excitation in crystals, G. H. Wannier—1001(A)
Electronic constitution of diamond, D. H. Ewing—1002(A)
Electronic energy bands, Ca, M. F. Manning, H. M. Krutter—761
Electron waves in crystals, J. C. Slater—840
Energy bands for face-centered lattice, W. Shockley—129
Glasseous selenium, structure of, K. Lark-Horovitz, E. P. Miller—380(A)
Intergranular surfaces in metals, H. F. Kaiser—1015(A)
Lattice energy of CO_2, H. Sponer, M. Bruch-Willstätter—998(A)
Magnetic analysis of Bi deposits, C. T. Lane—863
Mechanism of internal friction, C. Zener—1015(A)
Paraffin crystal formation; conditions, C. M. Heck—686(A); 690(A)
Photoconductivity and optical absorption, C. Zener—64(A)
Piezodielectric effect and electrostriction, H. Osterberg, J. W. Cookson—1096
Polymorphism of Rochelle salt, H. von R. Jaffe—43
Preferred orientation in cold rolled alloys, D. McLachlan, Jr., W. P. Davey—60(A)
Production of metal single crystals between 20μ and 0.2μ, J. Rinehart, A. Goetz—147(A)
Coloration by ultraviolet light of MgO, reemission of light, J. H. Hibben—530(L)
Remanence in single crystals, K. J. Sixtus—780(L)
Resistance of monovalent metals; calculation, E. L. Peterson, L. W. Nordheim—355
Scattering of x-rays from Zn, G. E. M. Jauncey, W. A. Bruce—1062; W. A. Bruce, E. M. McNatt—1065
Single crystals with high magnetic permeabilities, P. P. Cioffi, H. J. Williams, R. M. Bozorth—1009(A)
Single crystals of silicon iron; magnetic properties, H. J. Williams—1009(A)
Surface magnetization in crystals, W. C. Elmore—982
Transition of γ-FeOOH, L. A. Welo, Oskar Baudisch—1016(A)

Diffusion
Of H_2 through Fe, C. B. Post, W. R. Ham—1016(A); W. L. Rast, W. R. Ham—1015(A)

Discharge of electricity in gases
Coefficient of combination, G. R. Wait—1025(A)
Convection currents in H_2 arcs, C. Kenty—1025(A)
Drift of ions in magnetic field, L. Tonks—744; 1025(A)
Effect of Hg vapor on Townsend coefficient, W. E. Bowls—147(A)

Discharge of electricity in gases (continued)
Forms of the Cu arc in air, A. S. Fry—63(A)
Gases at high pressures, J. B. Adams, J. C. Hubbard, R. T. K. Murray—63(A)
High frequency discharge, striking potential, S. Githens, Jr.—688(A)
Glow discharge, potentials in. L. Bockstahler, H. Ritow —1009(A)
Ionization of air by γ-rays, pressure and collecting field, I. S. Bowen, E. F. Cox—232
Magnetron discharge, O. Luhr, F. J. Studer—306
Needle point corona studies, L. B. Loeb, W. Leigh—149(A)
Probe measurements on high pressure arcs, R. C. Mason —28
Propagation of potential in tubes, L. B. Snoddy, J. R. Dietrich, J. W. Beams—1008(A)
Recombination in afterglow, F. L. Mohler—1008(A)
Recombination in O_2, M. E. Gardner—144(A)
Reignition of an arc, R. B. Power, J. D. Cobine—594(A)
Theory of recombination of ions over an extended pressure range, L. B. Loeb—1110(L)
Disintegration of nucleus (see also **Radioactivity**)
Accompanying cosmic-ray showers, A. Bramley—385(A)
Of Al by alpha-particles, W. R. Kanne—1013(A)
Of A and Cl by $_2He^4$, E. Pollard, H. L. Schultz, G. Brubaker—1014(A)
Of Be by $_1H^1$, J. S. Allen—59(A); 182
Of B, $_1H^1$ emitted, G. Brubaker, E. Pollard—1013(A)
Of B, resonance process, J. H. Williams, W. H. Wells, J. T. Tate, E. L. Hill—434
Of Cd by $_1H^2$, J. M. Cork, R. L. Thornton—608
Of Cl and A, neutron emitted, E. Pollard, H. L. Schultz, G. Brubaker—140(L)
Creation of pairs, J. K. Knipp—381(A)
Evaporation model, E. J. Konopinski, H. A. Bethe—1004(A)
γ-radiation from $F+H^1$, L. A. Delsasso, W. A. Fowler, C. C. Lauritsen—527(L)
γ-radiation from Li^7+H^1, L. A. Delsasso, W. A. Fowler, C. C. Lauritsen—143(A); 391
γ-rays from light elements, R. G. Herb, D. W. Kerst, J. L. McKibben—691
Of Au, by $_1H^2$, J. M. Cork, R. L. Thornton—59(A)
Of heavy nuclei by $_1H^2$, H. A. Bethe—1004(A)
Of high energy protons, G. Nordheim, L. W. Nordheim, J. R. Oppenheimer, R. Serber—1037; L. W. Nordheim, G. Nordheim—379(A)
$_1H^2-{}_1H^2$ forces, R. Ladenburg, R. B. Roberts—141(L); M. H. Johnson, Jr.—779(L); L. I. Schiff—595(A); 783; R. B. Roberts—810; R. Ladenburg, M. H. Kanner—1022(A)
Of $_1H^2$ under $_2He^4$ bombardment, H. L. Schultz—1023(A)
Instability of He^5, J. H. Williams, W. G. Shepherd, R. C. Haxby—888(L)
Interaction of proton with field, H. Primakoff—990(L)
Intermediate steps, W. D. Harkins—52(L)
I resonance neutron band, S. Ruben, W. F. Libby—774(L)
Of light elements, by $_1H^1$, γ-ray yield, R. G. Herb, D. W. Kerst, J. L. McKibben—59(A)
Of Li, α-particle radioactivity, W. A. Fowler, C. C. Lauritsen—1103(L)
Of Li, α-particle yield, L. J. Haworth, L. D. P. King—59(A)
Of Li by $_1H^2$, efficiency, J. H. Williams, W. G. Shepherd, R. O. Haxby—1011(A)
Of Li^6 and Li^7, transmutation-processes, L. H. Rumbaugh, R. B. Roberts, L. R. Hafstad—1013(A)
Of Li^7, γ-rays, E. R. Gaerttner, H. R. Crane—49(L)
Of Li^8, G. Breit, E. Wigner—593(L)
Of Li^8 and B^{12}, D. S. Bayley, H. R. Crane—1012(A)
Low energy protons from nuclei, E. Pollard—290(L)
Of Ne, Ca and A, E. Pollard, C. J. Brasefield—8
Neutron-yields from artificial sources, E. Amaldi, L. R. Hafstad, M. A. Tuve—896
Nuclear transformation, absorption of orbital electron, C. Møller—84; J. A. Knipp—381(A); Hideki Yukawa, Shoichi Sakata—677(L)
Photodisintegration of deuteron, J. Richardson, L. Emo—1014(A)
Transmutation functions; C^{12}, N^{14}, O^{16}, and H^2, H. W. Newson—620
Dissociation
Of benzene vapor by electron impact, P. Kusch, J. T. Tate, A. Hustrulid—1007(A)
Kinetic energies of atomic ions: electron impact in NO and HCl, E. E. Hanson—86
Of methane by electron impact, L. G. Smith—263
Dynamics
Frequencies and nodal lines on circular plates, R. C. Colwell, A. W. Friend, H. C. Hardy—1025(A)

Elasticity
Change of resiliency with velocity, J. B. Derieux—686(A)
Of crystalline Na at 80° K, S. Siegel—1015(A)
Damping in quartz fibers, G. A. Downsbrough—877, 1014(A)
Hysteresis in wires, sheets and yarns, I. J. Saxl—596(A)
Response of synthetic rubber, M. L. Braun—684(A)
Theory of large strains, F. D. Murnaghan—593(L)
Electrical circuits
Cold cathode rectifier, C. T. Knipp—377(A)
Electron beam oscillators, J. B. Hoag, G. E. Flodin—60(A)
Electrical conductivity and resistance
Of air at low temperatures, W. F. Giauque, J. W. Stout, C. W. Clark—1108(L)
Electric breakdown, water and aqueous solutions, Y. Toriyama, U. Shinohara—680(L)
Formation of metallic bridges in contacts, G. L. Pearson —1015(A)
Of monovalent metals, calculation, E. L. Peterson, L. W. Nordheim—355
Photoconductivity and optical absorption, C. Zener —64(A)
Polarization with alternating current, S. M. Christian —685(A)
Superconducting state, J. C. Slater—195; F. Landon—678(L); K. Mendelssohn—781(L)

Electrical conductivity and resistance (continued)
Supraconducting circuit, R. J. Duffin—575
Theory of metallic conduction, E. Weber—378(A)
Electrical oscillations and waves
Five to twenty centimeter waves in water, H. W. Knerr—1007(A)
Electromagnetic theory
Action function in field theory, B. Hoffmann, L. Infeld—383(A); 765
Ampere's law, reciprocals to, P. B. Carwile—1016(A)
Electron diffraction (see also **Electrons, scattering of**)
In S and Se molecules, J. D. Howe, K. Lark-Horovitz—380(A)
Electrons (see also **Positive electron**)
Charge, J. A. Bearden—378(A)
Energy loss of particles, S. H. Neddermeyer, C. D. Anderson—884
Electrons, secondary
From clean W, E. Coomes—1008(A)
Secondary electron from Ni and Be, B. Kurrelmeyer, L. J. Hayner—1007(A)
Willemite screen material, W. B. Nottingham—1008(A)
Elements
Search for element 87, F. R. Hirsh, Jr.—584
E/m
Deflection measurements, A. E. Shaw—58(A); 887(L)
Entropy
Of paramagnetic salts below 1°K, M. H. Hebb, E. M. Purcell—384(A)
Errata
Heights of reflection of radio waves in the ionosphere, F. H. Murray—779(L)
Investigations of the deuteron-deuteron reaction, R. Ladenburg, R. B. Roberts—141(L)
Nuclear spins and magnetic moments in the Hartree model, M. E. Rose, H. A. Bethe—993(L)
Photoelectric effect of the deuteron, G. Breit, E. U. Condon, J. R. Stehn—56(L)
The precise measurement of three Ra B β-particle energies, F. T. Rogers, Jr.—588
Reflection of radio waves, F. H. Murray—779(L)
Errors of measurements
Calculation of errors, L. T. DeVore—349

Faraday effect (see **Magneto-optical effects**)
Ferromagnetism (see **Magnetic properties**)
Field currents
Formation of metallic bridges, G. L. Pearson—1015(A)
From coated cathodes, E. Meschter—377(A)
Into gases at high pressures, J. B. Adams, J. C. Hubbard, R. T. K. Murray—63(A)
In thin films, E. R. Piore—1111(L)
Field theory
Action function, B. Hoffmann, L. Infeld—383(A), 765
Fine structures (see also **Spectra, etc. and Hyperfine structure**)
In O_2, ground state, R. Schlapp—342
Fluorescence
Decay time, influence of temperature, W. Cram—62(A)
X-ray fluorescence yields, R. J. Stephenson—62(A)

Geophysics
He method, ages of rocks, R. D. Evans, C. Goodman—595(A)
Mountain building, quantitative study, R. Gunn—1027(A)

High voltage tubes and machines
CCl_4 vapor and dielectric strength of air, M. T. Rodine, R. G. Herb—508
Cyclotron, at Ill., P. G. Kruger, G. K. Green—57(A), 699
Cyclotron without filament, P. G. Kruger, G. K. Green, F. W. Stallmann—291(L)
Electrostatic generator for positrons, G. B. Collins, R. Schager, A. L. Vitter—58(A)
Electrostatic generator under high air pressure, R. G. Herb, D. B. Parkinson, D. W. Kerst—58(A), 75
Ion source for cyclotron, C. P. Baker, M. S. Livingston—1011(A)
Production of 9 MV alpha-particles, M. G. White, M. C. Henderson, W. J. Henderson, L. N. Ridenour—1012(A)
Propagation of potential in tubes, L. B. Snoddy, J. R. Dietrich, J. W. Beams—1008(A)
Radiofrequency source and transmission line for cyclotron, G. K. Green, P. G. Kruger—57(A)
Removal of ion beam of cyclotron from field, L. W. Alvarez, E. McMillan, A. H. Snell—148(A)
Transformer apparatus 10^6 volts, H. R. Crane—58(A)
Tube for Round Hill generator, C. M. Van Atta, R. J. Van de Graaff, L. C. Van Atta—1013(A)
Voltage multiplying circuit, S. K. Allison, G. T. Hatch, L. S. Skaggs—58(A)
Voltmeter measurements at Round Hill, D. L. Northrup, L. C. Van Atta—1014(A)
Hydrodynamics
Flow in porous media, O. T. Koppius, W. G. Holton—684(A)
Hyperfine structure (see also **Nuclear spin**)
Measurement separations, D. H. Tomboulian, R. F. Bacher—1020(A)
Resonance lines of Mg I and Mg II, R. A. Fisher—381(A)

Instruments (see **Methods and instruments**)
Ionization by particles (see also **Ionization potentials**)
Ionization by high energy beta-particles, F. T. Rogers, Jr.—528(L)
Ionization potentials
Of methane by electron impact, L. G. Smith—263
Of P, H. A. Robinson—726
Ionization by radiation (see **Photoionization**)
Ionosphere
Critical frequencies of low layers, N. Smith, S. S. Kirby—890(L)
Heights of reflection of radio waves, F. H. Murray, J. B. Hoag—60(A)
Magnetic storms, S. S. Kirby, N. Smith, T. R. Gilliland, S. E. Reymer—992(L)
Three regions, theory, E. O. Hulburt—689(A)

Ions, mobility
Ions produced by spraying and bubbling of liquids, S. Chapman—145(A)
In O_2, air, N_2O and NH_3, R. A. Nielsen, N. E. Bradbury —69; 143(A)
Positive ion in H_2, A. V. Hershey—146(A)
Isotopes
C^+ band from dissociation of CO^+, K. T. Bainbridge, E. B. Jordan—595(A)
Concentration of Cl isotopes, J. W. Beams, A. V. Masket—384(A)
Masses of Be, B, N and A isotopes, E. B. Jordan, K. T. Bainbridge—385(A)
Masses of H, He, C, and N isotopes, K. T. Bainbridge, E. B. Jordan—384(A)
Of Hg and Pb, A. O. Nier—1007(A)
Of Nd, A. J. Dempster—289(L)
Separation by diffusion, R. Sherr—1007(A)
Separation of isotopes; method of, O. Stern—1028(A)

Liquids (see also **Hydrodynamics**)
Analysis of liquid methyl alcohol, x-ray, G. G. Harvey—998(A)
Normal- and parahydrogen molecular volumes and lattice forces, R. B. Scott, F. G. Brickwedde—684(A)
Orientation of crystals by heat conduction, D. O. Holland, G. W. Stewart—62(A)
Structure of molten salts, E. P. Miller, K. Lark-Horovitz —61(A)
Luminescence
In ZnB_2O_4 compounds, D. H. Kabakjian—365

Magnetic properties
Analysis of Bi deposits, evaporated, C. T. Lane—863
Anisotropy of Cs_2, $CoCl_4$, K. S. Krishnan, A. Mookherji —528(L)
Anisotropy in Ni-Co-Fe crystals, L. W. McKeehan—136
Anisotropy of CO^{++} ions in crystals, K. S. Krishnan, A. Mookherji—774(L)
Anisotropy in silicon steel, W. E. Ingerson, F. J. Beck, Jr.—1010(A)
Of crystals of silicon iron, H. J. Williams—1009(A)
Dipole-dipole coupling; susceptibilities, J. H. Van Vleck —384(A)
Directions of easy magnetization in cubic crystals, R. M. Bozorth, L. W. McKeehan—216(A)
Ferromagnetic anisotropy and atomic structure, L. W. McKeehan—1010(A)
Ferromagnetism of alloys; theory, F. Bitter—383(A)
Hysteresis in 35 permalloy, W. B. Ellwood—1009(A)
Losses in 35 permalloy, V. E. Legg—1009(A)
Paramagnetism at radiofrequencies, C. J. Gorter—778(L)
Permeabilities, high, of single crystals, P. P. Cioffi, H. J. Williams, R. M. Bozorth—1009(A)
Powder patterns, ferromagnetic crystals, K. J. Sixtus —870
Susceptibility of H_2O, HDO and D_2O, H. P. Iskenderian —1092
Remanence in single crystals, K. J. Sixtus—780(L)
Surface magnetization in crystals, W. C. Elmore—982
Susceptibility of H_2; calculated, E. E. Witmer—383(A)
Magneto-optical effects
Allison magneto-optic effect, G. C. Comstock—776(L)
Faraday effect in x-ray region, H. T. Clark, K. Lark-Horovitz—61(A)
Verdet constant of nickelous sulphate, F. G. Slack, R. T. Lageman, N. Underwood—685(A)
Mechanics, quantum; atomic structure and spectra
Function for He; Hylleraas variational method, A. S. Coolidge, H. M. James—855
He wave equation, T. H. Gronwall—655; J. H. Bartlett, Jr.—661
Nuclear motion and the Dirac equation, I. S. Lowen—190
Symmetry of self-consistent fields, A. F. Stevenson—285
Mechanics, quantum; general
Approximate wave functions, H. M. James, A. S. Coolidge—860
Approximation to quantum states by iteration, L. H. Thomas—202
Collision of neutron and deuteron, L. I. Schiff—1003(A)
Density of eigenfunctions for Dirac electron, E. K. Broch—586
Hartree-Fock methods, N. H. Frank—577
Lattice energy of CO_2, H. Sponer, M. Bruch-Willstätter —998(A)
Nonadiabatic processes in inhomogeneous fields, J. Schwinger—648
Phase shifts in scattering problems, E. L. Hill—1023(A)
Quantum equations in cosmological spaces, A. H. Taub—512
Relativistic wave functions for coulomb field, M. E. Rose—484
Solutions of wave equation, connection formulas, R. E. Langer—669
Virial theorem and approximate eigenfunctions, J. O. Hirschfelder, J. F. Kincaid—1002(A)
Wave functions for nuclear collisions, P. M. Morse—1003(A)
Mechanics, quantum—molecular structure and spectra
Levels of asymmetrical rotator, E. E. Witmer—1001(A)
Test of Franck-Condon approximation, H. M. James, A. S. Coolidge—1001(A)
Vibration-rotation interaction, calculation, J. E. Rosenthal, L. Motz—378(A)
Mechanics, quantum—of solid bodies
Cellular method of obtaining lattice functions, W. Shockley—379(A)
Crystallic fields; effect on closed shell, V. A. Johnson, L. W. Nordheim—1002(A)
Electron excitation in crystals, G. H. Wannier—1001(A)
Electron waves in crystals, J. C. Slater—840
Electronic energy bands in Ca, M. F. Manning, H. M. Krutter—761
Functions in a periodic potential, J. C. Slater—846
Theory of metallic conduction, E. Weber—378(A)
Metals (see **Crystalline state**)

Meteorology
Anomalous lightning discharge, E. J. Workman, R. E. Holzer—149(A)
Penetration of haze, N. M. Mohler—1017(A)
Pyrheliometer having a spherical absorber; sunspot activities, L. F. Miller—1018(A)
Reflection of radio waves, F. H. Murray, J. B. Hoag—333, 779(L); R. C. Colwell, A. W. Friend—1005(A)
Sunspot maximum, A. L. Durkee—589(L)
Three regions in ionosphere, E. O. Hulbert—689(A)
Velocity of radio waves, R. C. Colwell, A. W. Friend—990(L)
Methods and instruments
Analysis of structure of Hα and Dα, W. V. Houston—446
Arrangement for analysis of spectrum plate, J. G. Black—380(A)
Axial magnetic suspension, F. T. Holmes—689(A)
β-magnesia windows in absorption furnaces: needle valve, R. T. Brice—142(A)
Bohr magneton; measurement of, O. Stern—852; 1004(A)
Built-up films of barium stearate, K. B. Blodgett, I. Langmuir—964
Calculation of errors, L. T. DeVore—349
Calibration of galvanometer, J. H. Howey—687(A)
CCl_4 vapor and dielectric strength of air, M. T. Rodine, R. G. Herb—508
Characteristics of counters, O. S. Duffendack, M. M. Slawsky, H. Lifschutz—1027(A)
Circuits for scaling down counting rates, E. C. Stevenson, L. A. Getting—1027(A)
Cloud chamber, continuously sensitive, A. Langsdorf, Jr.—1026(A)
Cold cathode rectifier, C. T. Knipp—377(A)
Condensation on charged carriers, L. B. Loeb, A. F. Kip, A. W. Einarsson—142(A)
Counter measurements of reflected x-rays, R. D. Miller—959
Current wave forms, photoelectric method, W. S. Huxford—1010(A)
Debye-Scherrer-Hull patterns, indexing of, L. K. Frevel—997(A)
Diffraction patterns by polarized light, A. W. Dicus—686(A)
Distribution of counts, constant source and daughter in equilibrium, L. Devol, A. Ruark—710
Distribution of light, W. L. Brenner—686(A)
Doppler effect in sound, N. F. Smith—686(A)
Electrical telegauge, W. C. Hall, R. Gunn—1027(A)
Electron beam oscillators, J. B. Hoag, G. E. Flodin—60(A)
Electrostatic generator for positrons, G. P. Collins, R. Schager, A. L. Vitter—58(A)
Electrostatic generator under high air pressure, R. G. Herb, D. B. Parkinson, D. W. Kerst—58(A), 75.
Equipment at the U. of Miss., W. L. Kennon—687(A)
Experiments in modern physics, D. S. Elliott—687(A)
First courses in physics, C. W. Edwards—687(A)
Fluctuations in G-M counters, R. L. Driscoll, A. E. Ruark—688(A)
Focusing in mass spectroscopy, A. J. Dempster—67
Focusing of electrons in superimposed fields, A. E. Shaw—58(A)
G-M counters for visible and ultraviolet light, G. L. Locher—386(A)
Grain spacing of tracks in photographic emulsion, T. R. Wilkins, H. J. St. Helens—1026(A)
High potential battery; extreme lightness and long shelf life, W. E. Ramsey—1028(A)
High precision worm gear wheels, D. Marlow, J. W. M. DuMond—145(A)
Integrated intensities of x-rays; recording apparatus, O. B. Jackson, A. Goetz—142(A)
Ion source for cyclotron, C. P. Baker, M. S. Livingston—1011(A); P. G. Kruger, G. K. Green, F. W. Stallman—291(L)
Ion sources, E. S. Lamar, W. W. Buechner, K. T. Compton—936
Linear amplifier; analysis of, H. Tatel—146(A)
Location of points by x-ray photography, A. D. Hummell, O. F. Hume—60(A)
Losses in thyratron recording circuits, H. Lifschutz, O. S. Duffendack, M. M. Slawsky—1027(A)
Measurement of velocity of light, W. C. Anderson—596(A)
Measurements of high energy γ-rays, E. R. Gaerttner, H. R. Crane—58(A)
Metal diffusion pump, C. M. Van Atta, L. C. Van Atta—377(A)
Production of metal single crystals between 20μ and 0.2μ, J. Rinehart, A. Goetz—147(A)
Pyrheliometer having a spherical absorber, L. F. Miller—1018(A)
Recording machines; teaching physics, L. E. McAllister—687(A)
Microphotometer, recording, H. V. Knorr, V. M. Albers—1016(A)
Observation of spectra, P. E. Shearin—687(A)
Production of liquid hydrogen, J. E. Ahlberg, W. O. Lundberg, I. Estermann—1028(A)
Quizzes and examinations in physics, N. S. Herod—687(A)
Radiofrequency source and transmission line for cyclotron, G. K. Green, P. G. Kruger—57(A)
Removal of ion beam of cyclotron from field, L. W. Alvarez, E. McMillan, A. H. Snell—148(A)
Resolution of spectrometer, C. Eckart—735
Scale-of-eight recording circuits, F. E. Brammer, A. E. Ruark—688(A)
Separation of isotopes, O. Stern—1028(A)
Sound, simple demonstration, J. C. Mouzon—686(A)
Source of focused ions, L. P. Smith, G. W. Scott, Jr.—1025(A)
Spark timer, C. T. Razor—684(A)
Status of physics in high schools of the south, C. R. Fountain—687(A)
Still and diffusion pump, W. P. Davey, R. J. Pfister—1028(A)
30 kw continuous-rating x-ray outfit, J. P. Youtz, J. W. M. DuMond—144(A)

Methods and instruments (continued)
Thyratron inverter, M. Sledd, J. B. Peebles—684(A)
Time delay circuits for cloud chambers, C. C. Jones—689(A)
Ultracentrifuge, inverted, J. W. Beams, F. W. Linke—689(A)
Ultracentrifuge, steam-driven, L. G. Hoxton, J. W. Beams—690(A)
Velocity analyzer for atomic beams, A. Ellett, V. W. Cohen—64(A)
Voltage multiplying circuit, S. K. Allison, G. T. Hatch, L. S. Skaggs—58(A)
Willemite screen material, W. B. Nottingham—591(L) 1008(A)
Mobility of ions (see **Ions, mobility**)
Molecular beams (see **Atomic and molecular beams**)
Molecular structure and constants (see also **Spectra, molecular; Raman spectra**)
Depolarization of Raman lines; structure of chlorate, bromate and iodate ions, S. T. Shen, Y. T. Yao, Ta-You Wu—235
Interactions between dipole molecules, H. Margenau, D. T. Warren—748
Interatomic distances in alkali halides, L. R. Maxwell, S. B. Hendricks, V. M. Mosley—1000(A)
Intermolecular forces and energies, M. L. Huggins—379(A)
Levels of asymmetrical rotator, E. E. Witmer—1001(A)
Nuclear separation of Te_2; electron diffraction, L. R. Maxwell, V. M. Mosley—684(A)
Spectrum of C_2H_6 and internal rotation, J. B. Howard—53(L)
Vibration-rotation interaction, J. E. Rosenthal, L. Motz—378(A)

Neutrons (see also **Scattering of electrons, neutrons, and ions**)
Absorption in aqueous solutions, W. H. Furry—592(L)
Absorption limit of Cd, J. G. Hoffman, H. A. Bethe—1021(A); M. S. Livingston, J. G. Hoffman—1021(A)
Absorption of resonance neutrons, H. H. Goldsmith, J. H. Manley—382(A), 1022(A)
Biological action of neutrons, P. C. Aebersold—375(A)
Capture of slow neutrons, W. E. Lamb, Jr.—187
Energy levels, J. H. Manley, H. H. Goldsmith, J. S. Schwinger—1022(A)
Inelastic scattering, D. C. Grahame, G. T. Seaborg, G. E. Gibson—590(L)
Interaction with Pb, G. E. Gibson, G. T. Seaborg, D. C. Grahame—370(L)
Magnetic moment; J. R. Dunning, P. N. Powers, H. G. Beyer—51(L); 382(A); J. G. Hoffman, M. S. Livingston, H. A. Bethe—214; P. N. Powers, H. G. Beyer, J. R. Dunning—371(L); P. N. Powers, H. Carroll, J. R. Dunning—1022(A)
Magnetic scattering, J. S. Schwinger—544; O. Halpern, M. H. Johnson, Jr.—992(L); F. Bloch—994(L); P. N. Powers, H. Carroll and J. R. Dunning—1112(L)
Neutron optics, G. N. Lewis—371(L); G. N. Lewis, P. W. Schutz—369(L); 1105(L)
Po-Be neutron source, T. R. Folsom—375(A)
Scattering, L. Jackson Laslett—22, 148(A); J. Schwinger 544; J. Schwinger, E. Teller—775(L); C. H. Fay—995(L)
Velocity distributions in aqueous solutions, W. H. Furry—382(A)
Yield curves for light elements, L. R. Hafstad, M. A. Tuve—376(A)
Yield from artificial sources, E. Amaldi, L. R. Hafstad, M. A. Tuve—896
Nuclear moments and spin (see also **Hyperfine structure**)
In Hartree model, M. E. Rose, H. A. Bethe—205; Erratum—993(L)
Of Li^7, Rb^{85}, Rb^{87}, and Cs^{133}, S. Millman, J. R. Zacharias—380(A); 1049
Magnetic deflection of HD molecules, I. Estermann, O. C. Simpson, O. Stern—64(A)
Nonadiabatic processes in inhomogeneous fields, J. Schwinger—648
Of K^{39}, sign, H. C. Torrey—501; H. C. Torrey, I. I. Rabi—379(A); R. A. Fisher—887(L)
Of proton, magnetic, I. Estermann, O. C. Simpson, O. Stern—1004(A)
Of Rb^{85}, S. Millman, I. I. Rabi, J. R. Zacharias—379(A)
Space quantization in gyrating field, I. I. Rabi—652; 683(A)
Spin and magnetic moment of Li^6, J. H. Manley, S. Millman—19
Nucleus (see also **Disintegration of nucleus**)
Collisions of neutron and proton, P. M. Morse, J. B. Fisk, L. I. Schiff—706
Density of energy levels, J. Bardeen—384(A); 799; S. Goudsmit—64(A)
Hartree approximation, motion of center of gravity, A. F. Stevenson—590(L)
Hartree-Fock methods, N. H. Frank—577
Interaction between light nuclei, M. Phillips, L. Eisenbud, E. U. Condon—382(A)
Kinetic energy; Hartree model, H. A. Bethe, M. E. Rose—283
Neutrino-electron field theory; range of forces, M. H. Johnson, Jr., H. Primakoff—612; H. Primakoff—990(L)
Neutron-proton interactions, J. H. Bartlett, Jr.—889(L)
O^{16}, perturbation theory, W. J. Kroeger, D. R. Inglis—1003(A)
Perturbation theory, He^4 and Li^6, D. R. Inglis—387(A); 531
Photoelectric cross section of deuteron, K. Way—552
Relativistic equations, G. Breit—248; 778(L)
Resonance effects, H. A. Bethe, G. Placzek—450
Resonating group, J. A. Wheeler—683(A)
Saturation property of forces, E. Feenberg—777(L)
Self-consistent field and Bohr's model, W. M. Elsasser—55(L); 144(A)
Stable states of two deuterons, H. Parker—682(A)
Stabilities of isotopes of lighter elements, W. M. Latimer—141(L)
Stable isobars, E. Wigner—106; D. R. Inglis, L. A. Young—525

Nucleus (continued)
Structure of heavy nuclei, E. Wigner—946
Structure of light nuclei, E. Feenberg, M. Phillips—597; 683(A)
Structure; He to O, E. Feenberg, E. Wigner—95
Symmetry of nuclear Hamiltonian, E. Wigner—106
Three and four body problem, H. Margenau, D. T. Warren—1003(A)
Two-, three- and four-body problems, W. Rarita, R. D. Present—382(A); 788
Virial theorem, E. L. Hill—370(L)

Optical constants and properties
Of built-up films of barium stearate, K. B. Blodgett, I. Langmuir—964
Of evaporated films, D. H. Andrews, J. A. Sanderson, E. O. Hulburt—1017(A)
Five to twenty centimeter waves in water, H. W. Knerr —1007(A)
Measurement of velocity of light, W. C. Anderson— —596(A)
Refractive index of air in infrared, D. Bender—144(A)
Refractive index of water; 8 to 24 cm waves, T. T. Goldsmith, Jr.—245
Optical theory
Anomalous diffraction gratings; theory of, U. Fano— 288(L)
Resolution of spectrometer, C. Eckart—735
Oscillators (see **Electrical circuits**)

Permeability (see **Magnetic properties**)
Photoelectric effect and properties; cells
Absolute yields of Mg, Be and Na, M. W. Mann, Jr., L. A. DuBridge—120
Auger effect and energy level widths for Au(79), E. G. Ramberg, F. K. Richtmyer—913
Auger effect in Ge, M. Ference, Jr.—720
Cross section of deuteron, K. Way, J. A. Wheeler— 683(A); K. Way—552; G. Breit, E. U. Condon, J. R. Stehn—56(L)
Disintegration of deuteron, J. R. Richardson, L. Emo— 1014(A)
Effect of current through Bi, A. H. Weber, C. B. Bazzoni —378(A)
Energy distribution electrons from Ca and CaO, I. Liben—642
Quantum absorption probability, A. T. Waterman— —378(A)
Time lag in gas-filled cells, A. M. Skellett—1026(A)
Work functions of 211 and 310 planes of W, C. E. Mendenhall, C. F. DeVoe—346
Photography
Density-exposure time curve for x-rays, F. R. Hirsh, Jr. —998(A)
Photoionization
Ionization measurements, positive and negative currents, E. F. Cox—55(L)
Photons
Sufficient description of, H. R. Crane—50(L)

Piezoelectric effect
Longitudinal effect in Rochelle salt, W. G. Cady— 596(A)
Piezodielectric effect and electrostriction, H. Osterberg, J. W. Cookson—1096
Polarization of radiation
Depolarization of Raman lines, structure of chlorate, bromate and iodate ions, S. T. Shen, Y. T. Yao, Ta-You Wu—235
Positive electron
Symmetry theorem, W. H. Furry—125

Radio
Heights of reflection of radio waves in the ionosphere, F. H. Murray, J. B. Hoag—333; F. H. Murray— 779(L)
Ionosphere and magnetic storms, S. S. Kirby, N. Smith, T. K. Gilliland, S. E. Reymer—992(L)
Reflection of waves in troposphere, R. C. Colwell, A. W. Friend—1005(A)
Velocity of radio waves, R. C. Colwell, A. W. Friend— 990(L)
Radioactivity (see also **Disintegration of nucleus**)
α-particles from U, W. M. Rayton, T. R. Wilkins—818
Of Al, by $_1H^2$, M. L. Pool, J. M. Cork—383(A)
Of Ba, La and Ce; by $_2H^4$, M. L. Pool, J. M. Cork— 1010(A)
β-decay, Fermi's theory, L. W. Nordheim, F. L. Yost —942
β-decay theory, heavy particle interactions, G. D. Camp —1046
β-ray spectra, calculations, W. G. Pollard—682(A)
β-ray spectrum of P^{32}, H. C. Paxton—170; W. E. Lamb, Jr.—145(A)
β-ray spectra of RaE and P^{32}, E. M. Lyman—1
β-ray spectrum of RaE, L. M. Langer, M. D. Whitaker— 713; 1023(A); J. S. O'Conor—1023(A)
β-transformation theory, G. Gamow, E. Teller—289(L)
Of Be^8, W. A. Fowler, C. C. Lauritsen—1103(L)
Of B, N, Al by $_2He^4$, L. N. Ridenour, W. J. Henderson, M. C. Henderson, M. G. White—1013(A)
Of Br by $_1H^2$, A. H. Snell—1011(A)
Of Ca, by $_1H^2$, H. Walke—143(A); 439
Of Cd by neutrons, long period, A. C. G. Mitchell— 995(L)
Of Co, by slow neutrons, J. R. Risser—1013(A)
Of Co, Cu and Ni by $_2He^4$, L. H. Ridenour, W. J. Henderson—1102(L)
Capture of orbital electrons, C. Møller—84; J. A. Knipp —381(A); Hideki Yukawa Shoichi Sakata—677(L)
Of elements Mg to Sb, S. W. Barnes, L. A. DuBridge, E. O. Wiig, J. H. Buck, C. V. Strain—1012(A)
Fermi theory of β-decay, L. W. Nordheim—64(A)
Of F^{18}; ($Ne^{20}+{}_1H^2$), A. H. Snell—143(A)
γ-rays from Ra (C+C′+C″+D), Sotohiko Nishida— 996(L)
In heavy nuclei by $_1H^1$, S. W. Barnes, L. A. DuBridge, E. W. Wiig, J. H. Buck, C. V. Strain—775(L)
Of Fe; by $_1H^2$, B. T. Darling, B. R. Curtis, J. M. Cork— 1010(A)

Radioactivity (continued)
Of Pb by $_1H^2$, R. L. Thornton, J. M. Cork—383(A)
Neutron ejection produced by fast neutrons, M. L. Pool, J. M. Cork, R. L. Thornton—890(L)
Of Ni by $_1H^2$, R. L. Thornton—893
Of O by $_1H^1$, L. A. DuBridge, S. W. Barnes, J. H. Buck—995(L); 1012(A)
Of Pd by $_1H^2$, J. D. Kraus, J. M. Cork—383(A)
Of K^{38}, W. J. Henderson, L. N. Ridenour, M. G. White, M. C. Henderson—1107(L)
Of K^{40}, W. R. Smythe, A. Hemmendinger—178: 146(A); E. Pollard, H. L. Schultz, G. Brubaker—1014(A)
Of K, induced, D. G. Hurst, H. Walke—1033
RaB β-energies, erratum, F. T. Rogers, Jr.—588
Relativistic equations for nuclear particles, G. Breit—248; 778(L)
Of Rb, natural, A. Hemmendinger, W. R. Smythe—1052
Of Se by $_1H^1$, resonance, J. H. Buck, C. V. Strain, G. Valley—1012(A)
Of Si and P by $_1H^2$, H. W. Newson—624
Straggling of α-particles, A. King, W. M. Rayton—826
Of Ti, by $_1H^2$, H. Walke—1011(A)
Raman spectra
Common ion effect shown, J. H. Hibben—593(L)
Depolarization of Raman lines, structure of chlorate, bromate and iodate ions, S. T. Shen, Y. T. Yao, Ta-You Wu—235
Of gaseous methyl- and dimethylacetylenes, G. Glockler, F. T. Wall—529(L)
Relativity
Nebulae as gravitational lenses, F. Zwicky—290(L); 679(L)
Relativistic equations for nuclear particles, G. Breit—248; 778(L)
Relativistic wave functions for coulomb field, M. E. Rose—484
Resistance, electrical (see **Electrical conductivity and resistance**)

Scattering of atoms and molecules (see also **Atomic and molecular beams**)
K atoms scattered by MgO, V. W. Cohen, A. Ellett—65(A)
Scattering of electrons, neutrons, and ions (see also **Electrons, scattering of; Electron diffraction**)
Collision of neutron and $_1H^2$, L. I. Schiff—1003(A)
Collisions of neutron and $_1H^1$, P. M. Morse, J. B. Fisk, L. I. Schiff—706
Diffuse reflection of neutrons, O. Halpern, R. Lueneburg, O. Clark—1028(A)
Electron scattering and action of collector, E. G. Linder—1024(A)
Of electrons by atomic nuclei, R. T. Cox, C. T. Chase—140(L)
Of fast electrons, small angle, J. B. H. Kuper—1024(A)
Fluctuations in radiative energy loss, W. H. Furry—1004(A)
High energy electrons, stopping of, A. Bramley—387(A), 682(A)
Inelastic collisions of $_1H^2$, L. I. Schiff—783
Inelastic scattering of fast neutrons, D. C. Grahame, G. T. Seaborg, G. E. Gibson—590(L)
Magnetic scattering of neutrons, L. J. Laslett—22; 148(A); J. S. Schwinger—544; O. Halpern, M. H. Johnson, Jr.—992(L); F. Bloch—994(L); P. N. Powers, H. Carroll, J. R. Dunning—1112(L)
Of neutrons by ortho- and parahydrogen, J. Schwinger, E. Teller—775(L)
Of neutrons by $_1H^1$, J. B. Fisk, P. M. Morse—54(L)
Neutron-proton interaction, P. G. Kruger, W. E. Shoupp, F. W. Stallmann—1021(A); C. W. Lampson, D. W. Mueller, H. A. Barton—1021(A)
Neutron proton scattering; depolarization, J. Schwinger, I. I. Rabi—1043(A)
Of neutrons absorbed by I, A. C. G. Mitchell, R. N. Varney—1021(A)
Phase shifts in scattering problems, E. L. Hill—1023(A)
Of $_1H^1$ by $_1H^1$, L. R. Hafstad, N. P. Heydenburg, M. A. Tuve—1023(A)
Scattering and stopping of electrons, M. E. Rose—1024(A)
Secondary electrons (see **Electrons, secondary**)
Solid state (see **Crystalline state**)
Solutions
Common ion effect, J. H. Hibben—593(L)
Electric breakdown, Y. Toriyama, U. Shinohara—680(L)
Sound (see **Acoustics**)
Spectra, absorption (see also **Absorption of light**)
Of acetic acid; infrared, W. Gordy—685(A)
Of acid solutions; infrared, E. K. Plyler—685(A)
Of alcohol-acetate mixtures; infrared, E. S. Barr—685(A)
Of Sb_2, G. M. Almy, H. A. Schultz—62(A)
Of aqueous solutions of halogen salts, E. K. Plyler, E. S. Barr—1017(A)
Of binary mixtures of organic liquids; infrared, D. Williams, W. Gordy—685(A)
Of CsH, M. P. Rassweiler, G. M. Almy—1019(A)
Of formic acid vapor, L. G. Bonner, R. Hofstadter—1017(A)
Of GeO_2, R. W. Shaw—146(A)
Of HCl and HBr; infrared, C. E. Leberknight, J. A. Ord—430
Of hydrogen halides in organic solvents, D. Williams—288(L)
Of Fe I and Ti I, R. B. King, A. S. King—1020(A)
Of MgH, L. A. Turner, W. T. Harris—1019(A)
Of NiCl and CoCl, K. R. More—1017(A)
OH vibrational band of alcohol, W. Gordy—564
Of porphin and its isomer, V. M. Albers, H. V. Knorr—1017(A)
Pressure effect, dipole molecules, S. D. Cornell—739
Rotation of water molecules, E. L. Kinsey, J. W. Ellis—381(A)
In Schumann region; Ag, F. W. Paul—594(A)
Of stretched rubber, D. Williams, R. Taschek—1016(A)
Of water in CS_2, E. L. Kinsey, J. W. Ellis—1074

Spectra, atomic
Energy levels in N and A, J. P. Sampson—1017(A)
Of He, effect of electric and magnetic fields, J. S. Foster, E. R. Pounder—1029(A)
He I like spectra, H. A. Robinson—14; 65(A)
Structure of Hα and Dα, W. V. Houston—148(A)
Structure of Hα, N. A. Kent, R. M. Frye, W. H. Robinson—990(L)
Of Li I; isotope shifts, D. d'Eustachio—780(L)
Of Mn II, C. W. Curtis—1018(A)
Of noble gases in ultraviolet, C. J. Humphreys—1018(A)
Normal p electron configurations; coupling, H. A. Robinson, G. H. Shortley—1018(A)
Of K III, Ca IV, and Sc V, P. G. Kruger, L. W. Phillips—1082
Of P XIII, H. A. Robinson—381(A)
Of Pt II, A. G. Shenstone—1018(A)
Of P III, P IV, P V, H. A. Robinson—726
Of K_1; temperature shift, G. F. Hull, Jr.—572, 595(A)
Of Rb; addition of rare gases, Ny Tsi-Zé, Ch'en Shang-Yi—567
Of Sc IV, Ti V, Mn VIII and Fe IX, P. G. Kruger, S. G. Weissberg, L. W. Phillips—1090
Of Sc IV, V, L. W. Phillips, P. G. Kruger—1019(A)
Of Sc VI, VII, H. S. Pattin, P. G. Kruger—1019(A)
Term values in C, C. W. Ufford—1020(A)
Of Yt I, II, I-djen Ho, R. A. Sawyer—1020(A)
Spectra, general
Absorption spectrum, test for hydroxyl radicals, O. Oldenberg, F. F. Rieke—381(A)
Analysis of biological material, J. S. Foster, C. A. Horton—1006(A)
Arrangement for analysis of spectrum plate, J. G. Black—380(A)
Continuous bands near metal lines, W. M. Preston—298
Fine structure in O_2, R. Schlapp—342
Interferometer wave-lengths of D_2 and HD, N. A. Kent, R. G. Lacount—241
Magnetron discharge; spectra in, O. Luhr, F. J. Studer—306
Pressure broadening in bands, W. W. Watson, H. Margenau—48(L); S. D. Cornell—595(A)
Observable interstellar lines, R. M. Langer—145(A)
Spectra, molecular (see also **Molecular structure and constants**)
Of SbF and BiF, G. D. Rochester—486
Of AlH, OH^+, BH, C. N. Challacombe, G. M. Almy—63(A); 930
Of atmospheric oxygen, H. D. Babcock—148(A)
Of BiF, BiCl, SbF, and SbCl, G. D. Rochester—146(A)
Of BH and BH^+, G. M. Almy, R. B. Horsfall, Jr.—491
Of Cd^+ D, R. V. Zumstein, J. W. Gabel, R. E. McKay—238
Of C_2H_2, internal rotation, J. B. Howard—53(L)
Of GeO, R. W. Shaw—12
H_2 and univalent metal halides, R. S. Mulliken—310
H_2 bands precision measurements, H. D. Landahl, G. S. Monk—993(L)
Levels of asymmetrical rotator, E. E. Witmer—1001(A)
Λ-type doubling in $^2\Pi$ state, C. N. Challacombe—1001(A)
Metastable molecules in Lewis-Rayleigh glow, J. Kaplan—143(A)
Of CD_4; optically active bands, H. H. Nielsen, A. H. Nielsen—62(A)
Of SiF; α and β bands, E. H. Eyster—1078
Test of Franck-Condon approximation, H. M. James, A. S. Coolidge—1001(A)
Spectra, Raman (see **Raman spectra**)
Stark effect
In A and Kr, J. S. Foster, C. A. Horton—1007(A)
In HD and D_2, J. S. Foster, D. C. Jones, S. M. Neamtan—1029(A)
In Fe; pole effect, F. Panter, J. S. Foster—1028(A)
Structure factor
Of Ni, W. P. Jesse—999(A)
Superconductivity (see **Electrical conductivity and resistance**)

Thermal diffusivity
Of Ni, C. Starr—376(A)
Thermal expansion
Of Bi lattice between 25° and 530° absolute, R. B. Jacobs, A. Goetz—147(A), 159
Thermionic emission of electrons; Emitting surfaces (see also **Vacuum tubes**)
Into dielectric liquids, E. B. Baker, H. A. Boltz—275; 989(L); K. H. Reiss—781(L)
Of W, change with temperature, A. T. Waterman, J. G. Potter—63(A)
Thermodynamics
Equation of state, W. Jacyna—677(L)
Transmutation (see **Disintegration of nucleus**)

Vacuum tubes
Electron scattering and action of collector, E. G. Linder—1024(A)
van der Waals forces
Between He atoms, C. H. Page—1002(A)
Interactions between dipole molecules, H. Margenau, D. T. Warren—748
Vapor pressure
Of Cs by positive ion method, J. B. Taylor, I. Langmuir—753
Virial coefficient
Quantum theory of, L. Gropper—50(L)
Virial theorem in nuclear problems, E. L. Hill—370(L)

Work function (see **Thermionic emission; Photoelectric effect**)

X-rays, absorption
Measurement of hard x-rays, G. C. Laurence—374(A)
K limits of Br I, and compounds, B. Cioffari—630
Of ultra-short rays, F. K. Richtmyer—376(A)
X-rays, diffraction, scattering, reflection, refraction and polarization
Analysis of liquid methyl alcohol, G. G. Harvey—998(A)
Backward scattered x-radiation, E. H. Quimby—374(A)

X-rays, diffraction, scattering, reflection, refraction and polarization (continued)
Coincidences in Compton effect, R. S. Shankland—1024(A)
Compton scattering in He gas, H. A. Kirkpatrick, J. W. M. DuMond—147(A)
Counter measurements of reflected rays, R. D. Miller—999(A)
Debye-Scherrer-Hull patterns, indexing of, L. K. Frevel—997(A)
Diffraction pattern of liquids; effect of electric field, A. A. Bless—688(A)
Diffuse scattering from quartz, E. S. Foster, Jr., G. E. M. Jauncey, W. A. Bruce—61(A)
Index of refraction of cerussite, J. E. Field, G. A. Lindsay—165
Multi-molecular films; thickness, C. Holley—1000(A)
Scattering from Zn, G. E. M. Jauncey, W. A. Bruce—999(A), 1062, 1067; E. O. Wollan, G. G. Harvey—1054; W. A. Bruce, E. M. McNatt—1065
Patterns at high hydrostatic pressures, R. B. Jacobs—999(A)
Reflections from Bi crystals between 25° and 530° Abs., A. Goetz, R. B. Jacobs—147(A)
Structure of molten salts, E. P. Miller, K. Lark-Horovitz—61(A)
Structure of wood, W. I. Caldwell, K. Lark-Horovitz—998(A)
Superlattices and "mixed crystals," F. C. Blake—1000(A)
X-rays, emission (see also **X-rays, spectra and spectroscopy, etc.**)
Energy level widths for Au(79), E. G. Ramberg, F. K. Richtmyer—913
Excitation by protons, M. S. Livingston, F. Genevese, E. J. Konopinski—835
Fluorescence yields, R. J. Stephenson—62(A), 637
L-satellites, $73<Z<79$, F. K. Richtmyer, C. H. Shaw, R. E. Shrader—380(A)
L-lines of Ag; width, L. G. Parratt—999(A)
Production by A ions, M. Tanaka, I. Nonaka—781(L)
Satellites of $L\alpha$ and $L\beta_2$ of Au(79), F. K. Richtmyer, E. G. Ramberg—925
Search for element 87, F. R. Hirsh, Jr.—584
Secondary radiation; geometrical variables, H. E. Seemann—376(A)
Secondary radiations emitted by filters, L. D. Marinelli—375(A)
Of sulphides and sulphates, J. Valasek—832
X-rays, spectra and spectroscopy, wave-length measurements (see also **X-rays, emission**)
Density-exposure time curve, F. R. Hirsh, Jr.—998(A)
Precision determination; short wave-length limit, V. L. Bollman, J. W. M. DuMond—145(A); P. Kirkpatrick, P. A. Ross—529(L)
Integrated intensities of x-rays; recording apparatus, O. B. Jackson, A. Goetz—142(A)
X-rays, tubes, apparatus
30 kw, continuous rating x-ray outfit, J. P. Youtz, J. W. M. DuMond—144(A)
Focusing of electrons, N. C. Beese—998(A)
Location of points by x-ray photography, A. D. Hummell, O. F. Hume—60(A)

Zeeman effect
Asymmetric patterns in complex spectrum, J. E. Mack, O. Laporte—291(L)
In Ne, J. B. Green, J. A. Peoples, Jr.—1020(A)
Of N II, J. B. Green, H. N. Maxwell—243
Of Te, J. B. Green, R. A. Loring—62(A)

THE JOHN CRERAR
JUN 21 1937
LIBRARY

THE PHYSICAL REVIEW

VOLUME 51 *Second Series* NUMBER 12

JUNE 15, 1937

Published for the

AMERICAN PHYSICAL SOCIETY

by the

AMERICAN INSTITUTE OF PHYSICS
Incorporated

LANCASTER, PA., AND NEW YORK, N. Y.

CONTENTS

PHYS. REV. 51 (1937) JUNE 15

Induced Radioactivity of Potassium. . . . . D. G. HURST AND H. WALKE 1033

Disintegration of High Energy Protons. . . . . G. NORDHEIM, L. W. NORDHEIM, J. R. OPPENHEIMER AND R. SERBER 1037

Heavy Particle Interactions from β-Decay Theory. . . . . GLEN D. CAMP 1046

Signs of the Nuclear Magnetic Moments of Li^7, Rb^{85}, Rb^{87} and Cs^{133}. . . . . S. MILLMAN AND J. R. ZACHARIAS 1049

Radioactive Isotope of Rubidium. . . . . A. HEMMENDINGER AND W. R. SMYTHE 1052

Effect of Temperature on the Intensity of Reflection of X-Rays from Zinc Crystals. . . . . E. O. WOLLAN AND G. G. HARVEY 1054

Atomic Structure and Vibrations in Zinc Crystals. IV. Diffuse Scattering of X-Rays at Different Temperatures. . . . . G. E. M. JAUNCEY AND W. A. BRUCE 1062

Atomic Structure and Vibrations in Zinc Crystals. V. The Diffuse Scattering of X-Rays at Various Scattering Angles. . . . . W. A. BRUCE AND E. M. MCNATT 1065

Atomic Structure and Vibrations in Zinc Crystals. VI. Determination of Electron Asymmetry and Two Principal Characteristic Temperatures . G. E. M. JAUNCEY AND W. A. BRUCE 1067

Rotation of Water Molecules in Carbon Disulfide Solution. . E. L. KINSEY AND J. W. ELLIS 1074

Structure of the α and β Band Systems of SiF . . . . . EUGENE H. EYSTER 1078

Spectra of K III, Ca IV, and Sc V, and their Relation to the Spectra of Other Ions in the Isoelectronic Sequence Cl I to Mn IX. . . . . P. GERALD KRUGER AND L. W. PHILLIPS 1087

Spectra of Sc IV, Ti V, Mn VIII and Fe IX in the Isoelectronic Sequence A I to Fe IX. . . . . P. GERALD KRUGER, S. G. WEISSBERG AND L. W. PHILLIPS 1090

Rankine Magnetic Balance and the Magnetic Susceptibility of H_2O, HDO and D_2O. . . . . HAIG P. ISKENDERIAN 1092

Piezodielectric Effect and Electrostriction in Anisotropic or Isotropic Media . . . . . HAROLD OSTERBERG AND JOHN W. COOKSON 1096

Letters to the Editor:

Artificial Radioactivity Produced by Alpha-Particles . LOUIS N. RIDENOUR AND W. J. HENDERSON 1102

Radioactive Alpha-Particles from Li^7+H^2 . . . . . W. A. FOWLER AND C. C. LAURITSEN 1103

On the Origin of Cosmic Rays . . . . . A. H. COMPTON AND P. Y. CHOU 1104

Determination of the Shower Producing Efficiency of Cosmic-Ray Particles . . . . . W. E. RAMSEY AND W. E. DANFORTH 1105

Neutron Refraction . . . . . GILBERT N. LEWIS AND PHILIP W. SCHUTZ 1105

Conservation of Energy in the Disintegration of Li^3 . . . . . L. H. RUMBAUGH, R. B. ROBERTS AND L. R. HAFSTAD 1106

Radioactivity of K^{38} . W. J. HENDERSON, L. N. RIDENOUR, M. G. WHITE AND M. C. HENDERSON 1107

Decrease in the Electrical Resistance of Gold with a Magnetic Field at Low Temperatures. . . . . W. F. GIAUQUE, J. W. STOUT AND C. W. CLARK 1108

Connection Between the Second Virial Coefficient and the Phases of Collision Theory . . . . . LEON GROPPER 1108

On the Effects in Cosmic-Ray Intensity Observed During the Recent Magnetic Storm . . . . . S. E. FORBUSH 1108

On the Absorption of Cosmic-Ray Electrons in the Atmosphere. . . . . L. W. NORDHEIM 1110

Theory of Recombination of Ions Over an Extended Pressure Range. . . . LEONARD B. LOEB 1110

Thin Film Field Emission . . . . . E. R. PIORE 1111

Experiments on the Magnetic Moment of the Neutron. . . . . P. N. POWERS, H. CARROLL AND J. R. DUNNING 1112

Note on the Nature of Cosmic-Ray Particles . . . . . J. R. OPPENHEIMER AND R. SERBER 1113

Author Index to Volume 51 1114

Analytic Subject Index to Volume 51 1128

LANCASTER PRESS, INC., LANCASTER, PA.